



McGettrick, Michael (2024) *Novel imaging approaches in the assessment of chronic thromboembolic pulmonary vascular disease and pre-capillary pulmonary hypertension*. MD thesis.

<http://theses.gla.ac.uk/84238/>

Copyright and moral rights for this work are retained by the author

A copy can be downloaded for personal non-commercial research or study, without prior permission or charge

This work cannot be reproduced or quoted extensively from without first obtaining permission in writing from the author

The content must not be changed in any way or sold commercially in any format or medium without the formal permission of the author

When referring to this work, full bibliographic details including the author, title, awarding institution and date of the thesis must be given

Enlighten: Theses

<https://theses.gla.ac.uk/>
research-enlighten@glasgow.ac.uk

**Novel imaging approaches in the assessment
of chronic thromboembolic pulmonary
vascular disease and pre-capillary pulmonary
hypertension.**

Student: Michael McGettrick

University ID:

Supervisors: Dr Colin Church & Prof Ninian Lang

Declaration

I certify that the thesis presented here for examination for Doctor of Medicine degree of the University of Glasgow is solely my own work other than where I have clearly indicated that it is the work of others (in which case the extent of any work carried out jointly by me and any other person is clearly identified in it) and that the thesis has not been edited by a third party beyond what is permitted by the University's PGR Code of Practice. The copyright of this thesis rests with the author.

No quotation from it is permitted without full acknowledgement.

I declare that the thesis does not include work forming part of a thesis presented successfully for another degree [unless explicitly identified and as noted below].

I declare that this thesis has been produced in accordance with the University of Glasgow's Code of Good Practice in Research.

Acknowledgments

I would like to thank my clinical supervisor, Dr Colin Church, for his continued backing in the completion of this thesis. I would also like to thank my academic supervisor, Professor Ninian Lang, for his constant source of support and regular contact that have maintained momentum such that this has been completed. The Covid-19 pandemic interrupted the original research plans for this thesis and was a testing time for us all. Thanks to their encouragement, I was able to refocus my research plans and complete several projects that have led to this thesis. Both supervisors have helped me improve my work, without which this, and the several published manuscripts, would not have been possible.

To all of the team at the Scottish Pulmonary Vascular unit, I would like to thank them for their support during my research time there, for allowing me to successfully complete research projects and allowing me to develop my clinical and research skills. In particular, Dr Helen Dormand who was the second reviewer for imaging and a significant help in my learning of interpreting CMR. I'd like to thank my good friends and research colleagues, Paul McCaughey and Sandy MacLellan, for the good humour and support that allowed me to enjoy my time in research and encouraged me to complete this thesis.

I would like to extend the greatest thanks to my wife, Jasmine, who has been incredibly patient and who encouraged me to persist with my research interests during difficult Covid-19 lockdowns when I felt completing a thesis would be impossible, and who has sacrificed her own time in her support of this completion.

Contents

Publications	14
List of Figures	16
List of Tables	18
Preface	20
1 General Introduction.....	22
1.1 1.1 The Normal Pulmonary Vasculature	25
1.1.1 Structure and Function of the Normal Pulmonary Circulation	25
1.1.2 The Pulmonary Macrocirculation	25
1.1.3 The Bronchial Circulation	27
1.1.4 The Pulmonary Microcirculation	28
1.1.5 Alveolar and Extra-alveolar vessels	30
1.1.6 The Pulmonary Vascular Endothelium	30
1.1.7 Maintenance of Pulmonary Haemodynamics	32
1.1.8 Influences on Pulmonary Haemodynamics	33
1.1.9 The Structure of the Right Ventricle	33
1.1.10 Location and shape of RV	35
1.1.11 The Right Ventricular Architecture.....	35
1.1.12 Function of the Right Ventricle	36

1.1.13	Blood Supply of the Right Ventricle	39
1.1.14	Left Ventricular Architecture	39
1.1.15	Left Ventricular Displacement	39
1.1.16	Ventricular Interdependence.....	40
1.2	The pulmonary circulation and right ventricle in pulmonary hypertension	41
1.2.1	The aetiology of Pulmonary Hypertension.	41
1.2.2	The classification of Pulmonary Hypertension.....	41
1.2.3	The pathophysiology of pulmonary hypertension	43
1.2.4	The pathophysiology of chronic thromboembolic pulmonary hypertension 45	
1.2.5	Remodelling of the Right Ventricle.....	46
1.3	Assessment of the RV.....	48
1.3.1	Echocardiography	48
1.3.2	Cardiac Magnetic Resonance Imaging	50
1.3.3	Right Heart Catheterisation	52
1.3.4	The Six Minute Walk Test	56
1.3.5	Cardiopulmonary Exercise Testing.....	57
1.3.6	Natriuretic Peptides	60
1.4	Cardiovascular Magnetic Resonance Imaging	62
1.4.1	Theory of Magnetic Resonance Imaging	62

1.4.2	Right Ventricular Volumes, Function and Mass	63
1.4.3	Flow Mapping	64
1.4.4	Tissue Tracking	65
1.5	Covid PTE	67
1.5.1	Coronaviruses	67
1.5.2	Covid-19 syndrome.....	68
1.6	Aims and Objectives	69
1.7	Hypothesis	69
2	Materials and Methods	70
2.1	Effect of exercise rehabilitation on cardiac function in pre-capillary pulmonary hypertension.....	70
2.1.1	Patient recruitment.....	70
2.1.2	Methods.....	70
2.1.3	Routine Diagnostic Assessment.....	72
2.1.4	Non-Invasive Assessment	73
2.1.5	Right Heart Catheterisation	75
2.1.6	Echocardiography	76
2.1.7	Common problems	78
2.1.8	Cardiovascular Magnetic Resonance Imaging	79
2.1.9	Data Storage	80

2.1.10	Common Problems Encountered During Image Acquisition	80
2.1.11	Analysis of Cardiovascular imaging	81
2.1.12	T1 Mapping	83
2.1.13	Tissue Tracking	86
2.1.14	Common Problems Encountered with Image analysis	86
2.1.15	Statistical Analysis	87
2.2	The use of Cardiac Geometry in the Diagnosis of Thrombotic Pulmonary Vascular Disease.....	88
2.2.1	Patient Recruitment	89
2.2.2	Echocardiogram	90
2.2.3	Cardiopulmonary Exercise Testing.....	90
2.2.4	Cardiac Magnetic Resonance Imaging	92
2.2.5	Right Heart Catheterisation	93
2.2.6	Data management and Statistical Analysis.....	93
2.2.7	Problems Encountered in assessing the Cardiac Geometry.....	94
2.3	Pulmonary Thromboembolism in Hospitalised Patients with COVID-19.....	95
2.3.1	Patient Recruitment	95
2.3.2	Inclusion Criteria	96
2.3.3	Calculating the incidence of Disease.....	97
2.3.4	Control Group.....	97

2.3.5	Statistical analysis	98
2.3.6	Problems Encountered with these methods.....	98
3	Assessing Cardiac Geometry with Echocardiography in the Diagnosis of Chronic Thromboembolic Pulmonary Vascular Disease	100
3.1	Introduction	100
3.1.1	Background.....	100
3.1.2	Aims	106
3.2	Methods	108
3.2.1	Echocardiography	108
3.2.2	Cardiopulmonary Exercise Testing.....	109
3.2.3	Right Heart Catheterisation	109
3.2.4	Data management and Statistical Analysis.....	109
3.3	Results.....	110
3.3.1	Assessing those with Pulmonary Hypertension.....	111
3.3.2	Subgroups of Chronic Thromboembolic Pulmonary Vascular Disease	116
3.3.3	Correlation between Invasive and Non-invasive Assessment	120
3.4	Discussion.....	122
3.4.1	Detection of pulmonary hypertension	122
3.4.2	Subgroup Analysis	124
3.4.3	Correlations	125

3.4.4	Comparison to other studies.....	126
3.4.5	Strengths and weaknesses	127
3.5	Conclusions	127
4	Assessing Cardiac Geometry, using cardiac Magnetic Resonance Imaging, in the Diagnosis of Chronic Thromboembolic Pulmonary Vascular Disease .	129
4.1	Introduction	129
4.1.1	Background.....	129
4.1.2	Aims	133
4.2	Methods	135
4.2.1	Cardiopulmonary exercise testing	135
4.2.2	Cardiac magnetic resonance imaging	135
4.2.3	Right heart catheterisation.....	136
4.2.4	Statistical analysis	136
4.3	Results.....	137
4.3.1	Assessing those with pulmonary hypertension.....	138
4.3.2	Subgroups of chronic thromboembolic pulmonary vascular disease	143
4.3.3	Normal pulmonary vasculature versus CTEPD	148
4.3.4	Correlations between CMR Indices and established markers of pulmonary hypertension severity	150
4.3.5	Comparing cardiac magnetic resonance imaging with echocardiography	152

4.4	Discussion	154
4.4.1	Analysis of pulmonary hypertension compared to controls.....	154
4.4.2	Comparing the subgroups of pulmonary vascular disease.....	157
4.4.3	Correlating CMR findings with echocardiogram and CPET	159
4.4.4	Strengths and weaknesses	160
4.4.5	Implications for current practice	161
4.5	Conclusions	162
5	The Effect of Exercise Rehabilitation on Cardiac Function in Precapillary Pulmonary Hypertension, as Measured by Cardiac Magnetic Resonance Imaging	163
5.1	Background	163
5.1.1	Precapillary pulmonary hypertension	163
5.1.2	Treatment of Precapillary pulmonary hypertension	163
5.1.3	Exercise Rehabilitation in Cardiorespiratory Disease.....	165
5.1.4	Exercise rehabilitation in Pulmonary Hypertension.....	166
5.1.5	Aims	167
5.2	Methods	168
5.2.1	Study Design	168
5.2.2	Inclusion Criteria	169
5.2.3	Imaging Technique	170
5.2.4	Tissue Tracking	171

5.2.5	Quality of Life Assessment.....	171
5.2.6	Data Analysis.....	172
5.3	Results.....	173
5.3.1	Baseline Characteristics.....	173
5.3.2	Effect of Training on Cardiac Function	176
5.3.3	Cardiac Strain.....	179
5.3.4	T1 Mapping.....	180
5.4	Discussion.....	181
5.5	Study Limitations.....	184
5.6	Conclusions.....	184
6	Pulmonary Thromboembolism in Hospitalised Patients with COVID-19	186
6.1	Introduction	186
6.1.1	Coronaviruses.....	186
6.1.2	COVID-19 clinical syndrome	188
6.1.3	Thrombosis.....	189
6.1.4	Treatments.....	190
6.1.5	Assessment in Covid-19.....	191
6.1.6	Aims	192
6.2	Methods	193
6.2.1	Patient recruitment.....	193

6.2.2	Control Cohort	195
6.2.3	Statistical analysis	196
6.3	Results.....	197
6.3.1	Incidence of PTE in Patients Admitted to Hospital with COVID-19	197
6.3.2	The effects of comorbidities on the risk of death or likelihood of requiring critical care	198
6.3.3	Survival with pulmonary thromboembolism.....	201
6.3.4	Differences in biomarkers between COVID-19 and historical control patients	202
6.4	Discussion.....	204
6.5	Limitations.....	209
6.6	Conclusions.....	209
7	Conclusions	210
8	Future Directions	213
9	Appendix	215
9.1	Study Design - Using Iodine Mapping in the diagnosis and assessment of function limitation in patients with chronic thromboembolic disease.....	215
9.2	Background	215
9.3	Study.....	223
9.3.1	Aims and Objectives	223
9.3.2	Study design.....	223

9.3.3	Inclusion Criteria	223
9.3.4	Exclusion Criteria	224
9.4	Methodology.....	225
9.4.1	Iodine Mapping	225
9.4.2	Postprocessing	226
9.4.3	Interpretation.....	227
9.5	Follow-up	227
9.6	Data Management	229
9.7	Expected Outcomes.....	229
9.8	Power of Study	229
9.9	Ethical Approval	229

Publications

The following publications have been published, which form part of this thesis:

McGettrick M, et al. Pulmonary Thromboembolism in hospitalized patients with Covid-19: a retrospective national study of patients managed in critical care and ward environments in Scotland. *BMJ Open* 2021;11:e050281

McGettrick M, Lang NN, Church AC. Contemporary Imaging in Chronic Pulmonary Thromboembolic Disease. *Hypertens* 2021;7(3): 142-148.

McGettrick M, Dormand H, Brewis M, Johnson MK, Lang NN and Church AC (2022) Cardiac geometry, as assessed by cardiac magnetic resonance, can differentiate subtypes of chronic thromboembolic pulmonary vascular disease. *Front. Cardiovasc. Med.* 9:1004169.

The following publications were performed as part of my research and have been published but do not form part of this thesis:

McGettrick M, Peacock A. Group III Pulmonary Hypertension: Challenges and Opportunities. *Glob Cardiol Sci Pract.* 2020 Apr 30; 2020(1): e202006.

McGettrick M, et al. Social deprivation in Scottish populations with pulmonary hypertension secondary to connective tissue disease and chronic thromboembolic disease. *ERJ Open Research* 2020 6: 00297-2019

Presentations

These presentations formed part of my research during my tenure at the Scottish Pulmonary Vascular Unit.

M McGettrick, AC Church et al. Cardiac Geometry in the diagnosis of Chronic Thromboembolic Pulmonary Vascular Disease. Oral presentation at the British Thoracic Society Winter Meeting, November 2021

M McGettrick, A MacLellan et al. Pulmonary Thromboembolism in Hospitalised Patients with Covid-19: *A National Study of Patients Managed in Critical Care and Ward Environments*. Presented at the Presented at the Scottish Thoracic Society August 2021

M McGettrick, A MacLellan et al. Pulmonary Thromboembolism in Hospitalised Patients with Covid-19: *A National Study of Patients Managed in Critical Care and Ward Environments*. Presented at the Presented at the National Pulmonary Hypertension Forum, London, UK. November 2020

M McGettrick, G Jayasekera, M Brewis, C Church, M Johnson, A Mackenzie. The Effect of exercise rehabilitation on cardiac function, measured by cardiac MRI, in patients with pre-capillary pulmonary hypertension. Presented at European Respiratory Society Congress, Madrid October 2019.

M McGettrick, P McCaughey, A MacLellan. Social deprivation and prognosis in Scottish patients with connective tissue disease associated pulmonary hypertension. Presented at the International Pulmonary Hypertension Forum, Berlin, Germany March 2019

M McGettrick. Social Deprivation Pre-capillary Pulmonary Hypertension. Presented at the National Pulmonary Hypertension Forum, London, UK, December 2018

List of Figures

Figure 1. Central divisions of the main pulmonary artery	27
Figure 2. The top images are of an endocast of the normal heart, dissected specimens by Prof Damian Sanchez-Quintana.	35
Figure 3. Right Ventricular Pressure Flow Loop.	38
Figure 4. Circle Cardiovascular imaging of short axis demonstrating the endocardial contours used to calculate chamber volume	52
Figure 5. Summary of patient recruitment.....	71
Figure 6. Diagnostic admission pathway.....	73
Figure 7. Short axis view of echocardiogram demonstrating dilated Right ventricle seen in pulmonary hypertension	74
Figure 8. Ventilation perfusion scan	75
Figure 9. Assessment of right atrial pressure using the size of the inferior vena cava.	78
Figure 10. Short axis view of cardiac ventricles demonstrating epi and endocardial bordering	82
Figure 11. T1 Mapping of short axis in healthy volunteer (A) and the T1 Mapping reference scale (B).....	85
Figure 12. Short axis view of cardiac ventricles with epi- and endocardial borders with the analysis of the LV eccentricity index	92
Figure 14. Diagram Describing Balloon Pulmonary Angioplasty	103
Figure 15. Pictorial description of how to measure the eccentricity index in diastole and systole.....	105
Figure 16. Patient recruitment to study.....	111

Figure 17. Pictorial description of how to measure the eccentricity index in diastole and systole.....	133
Figure 18. Patient recruitment to study.....	137
Figure 19. Receiver Operator Curves for thresholds of novel MRI indices.....	142
Figure 20. Sensitivity of pulmonary hypertension detection using combined systolic and diastolic LVEI with pulmonary artery distensibility.....	143
Figure 21. Novel MRI indices in no pulmonary vascular obstruction, CTEPD, proximal and distal CTEPH.....	147
Figure 22. Bland-Altman Comparison of Echocardiogram and CMR when measuring Systolic (A) and Diastolic (B) LV Eccentricity Index.	153
Figure 23. European Society of Cardiology Risk Stratification of Pulmonary Arterial Hypertension.....	164
Figure 24. Exercise Trial Recruitment	169
Figure 25. Emphasis 10 Questionnaire	172
Figure 26. Changes in Left ventricular ejection function (LVEF) between responders to training and non-responders.....	180
Figure 27. Electron Microscopy of Coronavirus	187
Figure 28. Consort diagram of patients included in study	194
Figure 29. Kaplan Meier curve of 90-day survival in those with right heart strain.	202
Figure 30. Comparison in biomarkers between those with COVID-19 and control group.	203
Figure 31. Images of Chronic and Acute Thrombus	220
Figure 32. Comparison of standard CT angiography with image subtraction iodine mapping in detecting pulmonary embolus.	222

List of Tables

Table 1 Classification of Pulmonary Hypertension	41
Table 2. Normal values of indices measured during right heart catheterization	54
Table 3. Baseline Variables between those with and without pulmonary hypertension..	112
Table 4. Parameters measured by echocardiogram in patients with chronic thromboembolic pulmonary hypertension versus those without.....	114
Table 5. Baseline Cardiopulmonary exercise tests between those with and without resting pulmonary hypertension	115
Table 6. Haemodynamic values of across all groups (ANOVA)	117
Table 7. Differences in echocardiographic measurements between all sub-groups	118
Table 8. Unpaired t-test of the differences in echocardiographic measurements between those with CTEPH and proximal CTEPH	119
Table 9. Baseline Cardiopulmonary exercise testing between subgroups of thrombotic pulmonary vascular disease.....	120
Table 10. Correlation between Invasive Haemodynamic Indices, exercise capacity and biomarker levels and Echocardiogram Measurements	121
Table 11. Baseline Variables between those with and without pulmonary hypertension.	139
Table 12. Baseline Cardiopulmonary exercise tests between those with and without resting pulmonary hypertension	140
Table 13. CMR indices in patients with chronic thromboembolic pulmonary hypertension versus those without	141
Table 14. ANOVA of the haemodynamic values of across all groups	144

Table 15. Baseline Cardiopulmonary exercise testing between subgroups of thrombotic pulmonary vascular disease	145
Table 16. Baseline CMR indices between subgroups of thrombotic pulmonary vascular disease	146
Table 17. Differences between patients with normal pulmonary vasculature and CTEPD group	149
Table 18. Correlation of prognostic indices with novel geometric cardiac MRI indices.	151
Table 19. Baseline characteristics, treatment, and pulmonary hypertension subtype.	175
Table 20. Change in primary outcome measures in control phase versus exercise training phase.	176
Table 21. Changes to cardiac indices before and after training (n=26).	177
Table 22. Comparison of change in cardiac indices between responders and non responders to training.....	179
Table 23. T1 Value Comparison Pre versus Post exercise in all patients, those who responded to rehabilitation as determined by 6-minute walk test and those who did not	181
Table 24 Demographics of Population	198
Table 25. The Effects of Comorbidities on the Likelihood of admission to Critical Care or Mortality	199
Table 26. Univariate analysis of comorbidities in those with COVID-19	200
Table 27 Comorbidities of Critical Care patients and those in Level 1 Care....	200
Table 28. 30-day Survival from admission with Pulmonary Thromboembolism	201

Preface

Knowledge of chronic thromboembolic disease and the post-pulmonary embolism syndrome has been evolving over recent years. However much remains unknown about which patients are most likely to have symptoms, why they develop symptoms and the long-term effects of chronic pulmonary vascular occlusion in those without resting pulmonary hypertension. This was my main area of interest when starting out in research at the Scottish Pulmonary Vascular Unit. I planned to assess the functional impact of chronic pulmonary vascular occlusion using CT pulmonary angiogram iodine mapping and, on 7th April 2020, we were granted ethical approval to assess 50 patients who were symptomatic following at least 3 months of treatment following acute pulmonary embolus. In addition, I had approval to look at blood flow within the pulmonary artery using 4D cardiac magnetic resonance imaging (CMR). This was with the aim to devise non-invasive methods of assessing the pulmonary vasculature in patients with chronic thromboembolic disease and chronic thromboembolic pulmonary hypertension. The use of CMR for the measurement of vascular pressures is not yet robust measuring pressure and I wanted to assess flow patterns within the pulmonary vasculature to understand whether these could be useful indicators of pressure within the pulmonary vasculature.

However, during this time, the UK was put under national lockdown because of the increasing number of cases of Covid-19, the syndrome caused by the novel Coronavirus, known as Severe Acute Respiratory Syndrome Coronavirus 2 (SARS Cov-2). Understandably, all elective research was halted whilst the health service faced unprecedented demand in the acute services. I returned to working in respiratory medicine to provide support to clinical colleagues in Glasgow. Research efforts rightly focused on trying to establish effective therapy for Covid-19, for which there were no known effective treatment strategies besides supportive care. I was part of a team enrolling patients on a variety of national clinical trials, which provided some insight into how quickly a common goal can be reached with a collective effort.

It became apparent soon after the start of the pandemic that patients with Covid-19 seemed to have an increased risk of pulmonary thromboembolism. As there were no active prospective research studies ongoing, I took the opportunity to look nationally at the incidence of pulmonary thromboembolism in patients with Covid-19, to help guide effective prophylaxis and improve patient safety in Scotland. This project has been included as part of this thesis.

As the pandemic progressed over months, I was not able to embark on the trial to assess the impact of chronic pulmonary vascular occlusion or on the 4D flow in patients with CTEPD and CTEPH to allow results for this thesis. Instead, I refocused my research time in evaluating other novel indices in imaging patients with thrombotic pulmonary vascular disease. As the incidence of acute pulmonary embolus increases, so does that of chronic thromboembolic pulmonary disease, including those with pulmonary hypertension. As such, there is a need for more non-invasive tools that can be used to detect the presence of thrombotic pulmonary vascular diseases. I assessed the value of changes in cardiac geometry using both echocardiogram and cardiac magnetic resonance imaging in the detection of pulmonary vascular disease, and these projects form part of this thesis.

1 General Introduction

Pulmonary hypertension reflects a raised pressure within the pulmonary circulation and is the result of many underlying disease processes. These processes result in a rise in pulmonary vascular resistance (PVR) because of narrowing or rarefaction of the microvasculature. This leads to an increase in the main pulmonary artery pressure, leading to a greater strain on the right ventricle. Over time, as the disease progresses, there is dilatation and dysfunction of the right ventricle, leading to ventricular failure and premature death. The prognosis of pulmonary hypertension, despite medical therapy, remains poor. The prognosis is dependent on the subtype of pulmonary hypertension but the overall 1-, 2- and 3-year survival for pulmonary arterial hypertension in the early 2000s was 82.9%, 67.1% and 58.2% respectively(1). This prognosis is dependent on the risk status at time of presentation, with low, medium, and high-risk patients having a mortality rate of 2.8%, 9.9% and 21.2% respectively(2). As a result of these poor survival figures, there has been significant research efforts and international collaboration with the aims of understanding the disease processes and establishing effective treatments. Over the last 50 years, the World Symposium on Pulmonary Hypertension, consisting of a group of world experts in pulmonary hypertension, have met six times to summarise the scientific progress over recent years and identify the areas where further research should be directed. The world symposia, divided into task forces, focus on different aspects of pulmonary hypertension, ranging from pathophysiology, to diagnostic techniques and management of the disease(3). The aetiology of pulmonary hypertension have been divided into 5 groups, based on their pathophysiology, their presentations and their response to therapy(4). Pulmonary vasoconstriction is an important mediator of this rise in pulmonary pressure. However, it is now understood, and accepted, that one of the key pathological processes underpinning the pulmonary vascular remodelling process is increased proliferation of the endothelial cells, rather than being solely attributable to hypoxic vasoconstriction(5). However, anti-proliferative treatments in clinical practice remain elusive in the management of pulmonary hypertension. Instead, most therapies available for clinical use are predominantly pulmonary

vasodilators (Phosphodiesterase-5 Inhibitors, endothelin receptor antagonists and the prostacyclin groups) for idiopathic pulmonary arterial hypertension and, interestingly, pulmonary hypertension caused by other diseases.

Pulmonary hypertension secondary to chronic thromboembolic disease, group IV in the WHO classification, has been increasing in incidence over the last decade, and is projected to continue to increase over the coming years as there is enhanced awareness of the condition and improving management options(6). In a similar way to IPAH, chronic thrombus leads to obstruction and remodelling of the small pulmonary arterioles, pulmonary veins, and venules. This leads to increased pulmonary vascular resistance, pulmonary hypertension, right ventricular failure, and premature death. This is classified into central and peripheral disease, depending on the position of the thromboembolic disease and the treatment options vary dependent on the type.

With the increasing incidence of pulmonary hypertension and success of existing medical and surgical therapies, and the potential of even more successful evolving therapy, it is now more important than ever before to identify patients early and initiate appropriate therapies. Echocardiography is the recommended first line investigation when pulmonary hypertension is suspected. It is inexpensive, widely available, and non-invasive. The tricuspid regurgitation pressure gradient (TRPG) can be used to estimate pulmonary artery pressure, in addition to the evaluation of the size and function of the atria and ventricles. However, despite this utility, there are limitations with echocardiography. This has led to the increasing use of cardiac magnetic resonance imaging in recent years due to increased availability, improved acquisition times and ease of use(7). Cardiac Magnetic Resonance Imaging (CMR) has several advantages over echocardiography, including improved assessment of ventricular mass, volume and ejection fraction, and is the gold standard for assessment of the RV(8). CMR measurements are also more reproducible than echocardiography (8).

Although CMR has been shown to be effective at measuring chamber volumes there is, as yet no reliable way of measuring pressure. However, there are a number of ways that a CMR may indicate the presence of increased RV and pulmonary artery pressure. *Johns et al* have assessed computational models assessing the use of black blood models and septal angle in order to estimate pressure with some positive results(9). In addition, *Whitfield et al.* have demonstrated the value of septal angle and ventricular mass in a regression model to detect the presence of pulmonary hypertension, using the most up to date definition(10). In order to minimise interobserver variability and analysis time, the use of artificial intelligence has been employed by *Alabed et al (11)* with favourable results in correlating MRI values to invasive measurements.

1.1 1.1 The Normal Pulmonary Vasculature

1.1.1 Structure and Function of the Normal Pulmonary Circulation

The circulation of the lung is unique in its volume and function. It receives two blood supplies, via the bronchial and pulmonary circulations. The bronchial arteries provide a small amount of blood from the systemic circulation and supply oxygenated blood to the lungs. The pulmonary arterial circulation constitutes the whole of the cardiac output from the right ventricle (RV), supplying mixed venous blood drained from all tissues in the body. As such, the RV must deliver high blood flow at low pressure to the lungs. The structure of the pulmonary arteries varies depending on the function required of the vessels, from the high capacitance main pulmonary arteries to the thin-walled endothelium in the capillaries, required for gas exchange. The pulmonary arteries are named in 'order' as they divide from the main pulmonary artery, generation 17, to the subdivisions creating further orders down to pulmonary arterioles with no muscular wall. As the pulmonary arteries divide to each order, there is a 9-fold increase in surface area of the endothelium. This blood, in the pulmonary capillaries, then takes part in gas exchange within the lung alveoli. The pulmonary blood flow is equal to the cardiac output, an average of 3.5L/min. Whilst the bronchial arteries have systemic pressure within them, the pulmonary circulation is low pressure, with a normal pressure being 8-20mmHg(12).

1.1.2 The Pulmonary Macrocirculation

With the pulmonary circulation having to accommodate the entire cardiac output, the resistance within the lung is much lower than systemic vascular resistance with higher compliance. Pulmonary vascular resistance (PVR) is approximately one tenth of the systemic circulation and is defined using Ohm's law ($PVR = (\text{mean pulmonary artery pressure} - \text{pulmonary artery wedge pressure}) / \text{cardiac output}$). The resistance is mainly due to the small distal muscular arteries and branching of the pulmonary arteries with very good accommodation of the blood vessels(13). The pulmonary vasculature comprises a heterogenous group of vessel types, which are adapted to perform specific functions. There is some overlap of the features seen in the blood vessels as the vessels decrease in size.

- Elastic arteries, orders 17-13 have intimal, muscular, and adventitial layers. These larger vessels have more elastic lamina, allowing them to accommodate a higher volume when needed.
- Muscular arteries, orders 13 - 3, have a thicker muscular layer and contain an internal and external laminal layer.
- Partially muscular arteries, orders 5-3, the spiral muscular layer surrounding the vessels tapers, leaving an incomplete muscular layer.
- Non-Muscular arteries, orders 5-1, where there is absence of elastic laminae. The smooth muscle cells are replaced by pericytes, which have a basement membrane that fuses with the endothelial cells. These can then control the permeability of the endothelial membrane.
- The pulmonary veins follow a similar path to the pulmonary arteries but have only 15 orders because four pulmonary veins enter the left atrium and do not form the final two orders.

Blood flow through the pulmonary arteries is pulsatile due to cardiac contraction. However, during systole, a small volume of blood is stored in the compliant pulmonary artery. This blood is released during diastole and dampens the pulsatile delivery of blood, reducing the work of the right ventricle and ejection pressure(14). During exercise, there is a rise in cardiac output but a reduction in pulmonary vascular resistance. This is facilitated by a combination of the distensibility of the capacitance vessels and recruitment of the pulmonary microvasculature. It is diseases of the microvasculature that often causes the PVR to increase.

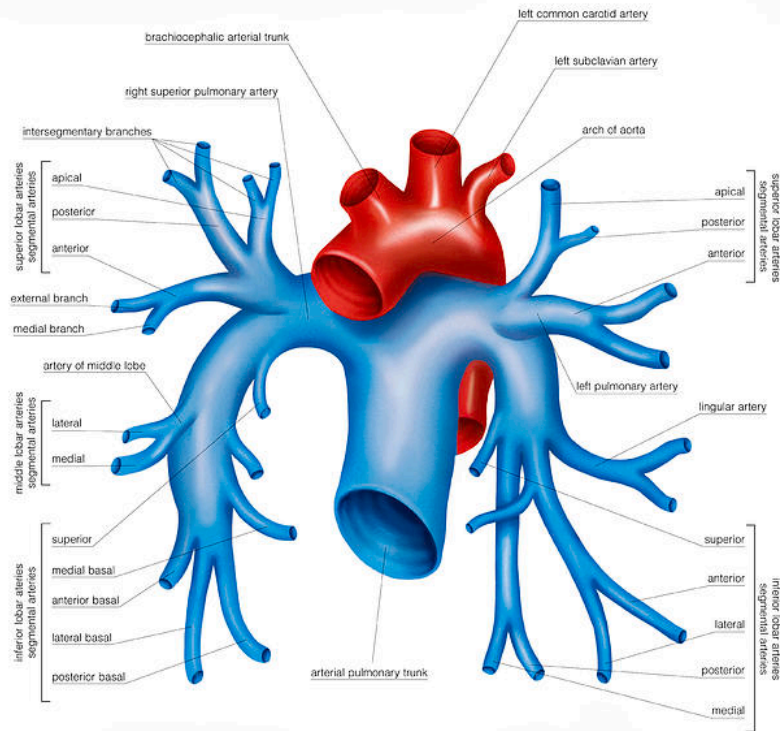


Figure 1. Central divisions of the main pulmonary artery (15)

1.1.3 The Bronchial Circulation

The bronchial arteries arise from the aortic arch and thoracic aorta, supplying oxygenated blood to the structures of the lung at systemic pressure, roughly six-times that of pulmonary arterial pressure. This accounts for approximately 1% of the left ventricular cardiac output(16). Within the bronchial tree, the respiratory bronchioles, pulmonary nerves, lymphatics, and parenchymal tissue are all supplied by the bronchial arteries(17, 18). The blood from the bronchial tree as far as the second order bronchi then drain via the bronchial veins directly into the right atrium. The remaining blood from the distal bronchial tree then drains via the bronchopulmonary veins, which merge with the pulmonary veins and into the left atrium(19). The normal size of the bronchial arteries are between 0.5-2mm(20). With this smaller diameter, they provide low capacitance, high-resistance flow of blood. In response to hypoxia, the bronchial arteries dilate in to supply oxygen to the affected areas of lung. In response to pulmonary arterial

obstruction or chronic obstruction, they hypertrophy to ensure that oxygenated blood is supplied to the lung through systemic-pulmonary anastomoses beyond any obstruction. Bronchial arteries above 2mm are deemed to be enlarged(21). For reasons that are not fully understood, bronchial artery hypertrophy is not commonly seen in patients with pulmonary arterial hypertension, but this is a more common finding of patients with chronic pulmonary vascular obstruction, such as those with chronic thromboembolic pulmonary hypertension(22). In these cases, the vessels may accommodate up to 30% of left ventricular cardiac output(22).

1.1.4 The Pulmonary Microcirculation

The vessels are divided into the vessels surround the acinus, and alveoli and those distal to the capillary bed. With the need for a low vascular resistance, the muscular component of the vessels is very low. The size of vessels is between 100µm and 300µm, with the media only contributing 2-3% of this diameter (23). There is minimal autonomic innervation. As a result of the low muscle content and absent intravascular valves, the distensibility of the vessels is high and, as such, the resistance and pressure are low. The pressure in a healthy lung is only just sufficient to perfuse the apices in the upright lung. The function of the microcirculation is to facilitate effective gas exchange, and this is enabled by the slow flow but large surface area of the endothelium. The total blood volume at any given time is around 52mls/m², but can be increased during times of exercise when blood vessels are recruited to accommodate the higher cardiac output, and can be reduced by disease states, such as pulmonary hypertension(24).

Within the microvasculature, there are several forces at play that maintain the blood within the vascular lumen and prevent it passing through the vessel into the lung parenchyma. This can be explained using the Starling Equation(25):

$$J_v = L_p S ([P_c - P_i - \sigma (\pi_p - \pi_i)])$$

J_v is the trans endothelial solvent filtration volume per second (SI units of m^3/s^{-1}).

$[P_c - P_i - \sigma (\pi_p - \pi_i)]$ is the net driving force, (SI units of $P_a = \text{kg}\cdot\text{m}^{-1}\cdot\text{s}^{-2}$, expressed as mmHg)

P_c = the capillary hydrostatic pressure. This is the pressure exerted by a fluid at equilibrium due to the force of gravity. Hydrostatic pressure increases with the depth of the fluid because of the fluid above it exerting pressure downwards.

P_i = the interstitial hydrostatic pressure

π_p = the plasma protein oncotic pressure. This is a form of osmotic pressure exerted by proteins, which displace water molecules, creating a relative deficit of water, which draws water back into the relative low pressure of the venous capillaries.

π_i = the interstitial oncotic pressure.

L_p = the hydraulic conductivity of the membrane. This is a product of the membrane's permeability to water and the surface area of the membrane ($\text{ml}/\text{min}/\text{mmHg}$).

S = the surface area for filtration (m^2)

σ = the Staverman's reflection coefficient. This reflects the integrity of the glycocalyx ultrafilter, which surrounds the extracellular matrix and regulates the flow of small molecules across the membrane, keeping larger molecules such as albumin in the vascular lumen. When the glycocalyx is intact, this is close to 1.

Overall, the balance of Starling's forces in the healthy lung favour fluid to remain within the vascular lumen and prevent fluid leaking into the alveoli, which would impede effective gas exchange. Several acute and chronic disease states, such as left heart disease can result in these forces becoming unbalanced and favour fluid passing into the alveolus - this results in clinical appearance of pulmonary oedema.

1.1.5 Alveolar and Extra-alveolar vessels

The alveolar vessels are the thin-walled capillaries that supply the alveolar septum. These vessels are exposed to the pressure changes that occur within the alveoli during respiration. The extra-alveolar vessels are a collection of the pulmonary arteries, pulmonary veins, lymphatics and are held in a loose connective tissue sheath, termed the bronchovascular bundle. The vessels in this bundle are affected by the pressures of the connective tissue surrounding them, which are similar to pleural pressures rather than alveolar pressures(26). The alveolar and extra-alveolar vessels are exposed to opposite pressures. High lung volumes lead to increased pulmonary vascular resistance within the alveolar vessels. However, the connective tissue around the bronchovascular bundle is subject to radial traction and negative pleural pressures so there is reduction in pulmonary vascular resistance.

1.1.6 The Pulmonary Vascular Endothelium

The pulmonary vascular endothelium has two main functions due to its location as the interface between the blood and the lung: it is responsible for optimising gas exchange of oxygen between the blood vessels and the lung and in regulating pulmonary vascular tone. The latter is maintained through four main pathways: the nitric oxide, the prostacyclin and endothelin pathways(27). The vascular endothelium is a continuous, uninterrupted surface of cells joined by complex junctional mechanisms, namely adherens junctions, tight junctions, and gap junctions. Adherens junctions initiate cell to cell contact and maintain the contact with other cells(28). Tight junctions allow the movement of fluid, proteins and cells across the endothelial barrier(29). The cells are highly metabolically active, and their homeostatic mechanism respond to chemical, mechanical and physical stimuli, which encourage maintenance of blood flow within the pulmonary circulation. The interaction of the cells in the blood vessels, and their responses to circulating hormones and other cells leads to maintenance of the thrombosis free surface and competent vascular wall(30).

The cytoplasm of the endothelial cells and the smooth muscle cells are connected via connexins, which are two intracellular channels that allow the transport of water-soluble molecules, known as gap junctions. These junctions are closed in the rested state but are easily opened when exposed to low extracellular calcium, mechanical stresses, for example shear stress(31) and metabolic imbalance(32), for example ischemia. The mechanism by which they open has been proposed to be the result of dephosphorylation as the connexins are inhibited by certain kinases(33). These signalling pathways play a central role in regulating vascular tone and vascular resistance, and disruption of these mechanisms can lead to vascular remodelling and increased pulmonary vascular resistance (Myoendothelial gap junctional signalling induces differentiation of pulmonary arterial smooth muscle cells). Whilst there has been shown to be an increase in the gap junctions, Cx 43, in the development of systemic hypertension(34), the extent to which gap junctions play a role in the development of pulmonary hypertension remains to be fully understood, partly because of the varying aetiology of the different types of pulmonary hypertension, such as hypoxic lung disease and thrombotic disease. Animal models have been used to assess this further. Functional connexins are seen in both hypoxic and monochrotaline-treated rat models of pulmonary hypertension, but they vary between sub-type of connexin and rat model. As such, further study is required to evaluate if they play a role in the disease state and if they could be a therapeutic target.

Imbalances to this process can lead to the development of pulmonary diseases. Increased permeability of the endothelium in response to acute lung injury, seen in infection or high-altitude pulmonary oedema, leads to vascular leakage and pulmonary oedema. The change in harmony between vasodilation and vasoconstriction mechanisms, along with increase in proliferative mechanisms can lead to vascular narrowing rarefaction of the pulmonary vasculature(35) can lead to pulmonary hypertension; increased pro-thrombotic mediators can lead to thrombosis in situ.

Whilst traditionally the pulmonary endothelium was thought to be a homogenous collection of cells throughout the lung, it has now been demonstrated that the cells are heterogenous. Two cell phenotypes have been identified, the tip cells and the stalk cells. These have been identified when assessing the lung's response to injury, such as infection with influenza. In response to injury, the endothelium must establish oxygenation to the damaged tissues through regeneration of the blood supply via angiogenesis. Tip cells lead the regeneration process by initiation new vessel growth and migration through the tissue and coordinate the multiple process ongoing during angiogenesis(36). Stalk cells then follow, with the aid of filopodia, the tip cells elongate and proliferate and form the endothelial surface(37).

1.1.7 Maintenance of Pulmonary Haemodynamics

Whilst the systemic circulation is required to accommodate blood flow across the whole body, it requires a high-pressure gradient and can autoregulate the pressure to ensure blood is appropriately distributed. However, the pulmonary circulation must adapt to the whole cardiac output and has no mechanism by which to adjust blood flow. The blood flow in the lung is dependent on the calibre of the vessel, and changes with exercise, where more vessels are recruited to meet demand of increased cardiac output. Throughout the lung, there is heterogeneity in the flow of blood. There are several influences at play, which lead to varied flow throughout the lung. Extrapulmonary vessels are subject to the pleural pressures, which change throughout the respiration cycle. Intra-pulmonary blood vessels are divided into extra-alveolar and alveolar vessels, and are both affected by alveolar pressures and pressures from the surrounding lung tissues(38). The pressure is increased by inspiration of the lung. Posture can also influence the distribution of blood throughout the lung. Gravity exerts increased blood flow to the lung bases in the healthy lung, with flow increasing by 11% to the base of the lung for every centimetre of descent in an upright human(39). Ventilation is affected by several factors: firstly, the right lung is larger than the left so receives a larger proportion of total ventilation. Gravity causes the lower parts of the lung to be compressed by the upper zones, meaning that the apices are proportionately ventilated more in the upright position. Finally, airway distribution has an influence on ventilation with central areas of lung more ventilated than peripheral areas(40).

1.1.8 Influences on Pulmonary Haemodynamics

The main contribution to pulmonary artery pressure in the healthy lung is from the pulmonary vascular resistance, which is controlled by passive and active forces. The passive forces are associated with respiration and vascular architecture. During inspiration, as the lung volume increases, there is extramural pressure on the vascular walls, and this can cause the vessel to become narrowed and collapse. If the lung volume is reduced, it can cause some of the blood vessels to be tortuous. In both situations, PVR will be increased. The branching of blood vessels may also contribute to the heterogenous perfusion of the lung and the gravitational difference in flow. Bifurcation of blood vessels into two different size vessels has a significant impact on the flow in both vessels. The number of blood vessels is greater than the number of corresponding airways. As such, the branching of the vessels at right angles will impact the perfusion in different parts of the lungs.

The active forces are mediated by vasoactive substances in such a way that the pulmonary vasculature is maintained in a state of vasodilation. Some of the vasodilators, vasoactive intestinal peptide, and prostaglandins, have a direct effect on smooth muscle. Nitric oxide is the common product of several pathways and is found in two forms, constitutive and inducible. The inducible form is produced in response to inflammatory mediators. The constitutive form exists in most cells, including the pulmonary endothelium, and is released in response to changes in intracellular calcium. The nitric oxide activate guanylate cyclase to produce cyclic guanosine monophosphate (cGMP), which then activates protein kinase G, leading to relaxation of the blood vessel(41).

1.1.9 The Structure of the Right Ventricle

The right ventricle is the most anterior of the four heart chambers, extending from the right atrium to the apex. It sits immediately posterior to the sternum, between the 3rd and 6th ribs. Blood flows out of the pulmonary valve as it enters the pulmonary artery in the right ventricular outflow tract (RVOT). The RV mass is approximately one sixth of the left ventricle, but has the same cardiac output into a lower pressure system(42). The tricuspid valve is the border with the right

atrium, where blood flows into the right ventricle. Although, anatomically, it is usually found anteriorly, the RV is defined by its structures rather than its anatomical position. The structures that define it include the prominent trabeculations, presence of a moderator band, presence of three or more papillary muscles, trileaflet configuration of the tricuspid valve with septal papillary attachments and the apical hinge line of the septal tricuspid valve leaflet relative to the mitral valve anterior leaflet(43).

Internally, the ventricle can be divided into three areas: the inlet, the apex, and the infundibulum. At the inlet, the ventricle contains the annulus, chordae tendinae and papillary muscles for the tricuspid valve(44). The ventricle is lined by trabeculae and towards the apex becomes increasingly trabeculated. The trabeculae are irregular ridges of intersecting myocardium that help to direct the blood from the inflow to the outflow tract. The supraventricular crest separates the trabecular from the smooth walled right ventricular outflow tract. The ventricle narrows into a funnel shape towards the outflow tract, known as the infundibulum. This is smooth walled and is separated from the main pulmonary trunk by the pulmonary valve. This is comprised of 3 semilunar shaped leaflets, joined by commissures. Unlike the tricuspid valve, it is not attached by papillary muscles or chordae, but instead its closure is dependent on shifts in pressure gradient across the valve. During systole, it should open to allow deoxygenated blood to be delivered from the RV to the pulmonary trunk and during diastole should close to prevent regurgitant flow (43).

There are three muscular bands in the RV: the moderator band, the parietal band and the septomarginal band(45). The moderator band is a continuation inferiorly of the septomarginal band and enters the anterior papillary muscle. If this becomes thickened, it can divide the RV into two chambers. The parietal band and the infundibular septum make up the crista supraventricularis. The ventriculoinfundibular fold separates the tricuspid and pulmonary valves(45).

1.1.10 Location and shape of RV

The right ventricle is positioned immediately posterior to the sternum. The RV is more triangular, compared to the conical shape of the LV. It wraps around the left ventricle, with the interventricular septum being the common boundary. In the healthy heart, the interventricular septum bows towards the low-pressure right ventricle. The ventricle extends from the atrioventricular junction leftwards towards the apex. The annuli of the tricuspid valves and the pulmonary valves delineate the ventricle from the atrium and pulmonary trunk respectively. Figure 2 shows the position of the right and left ventricles and how they are joined at the interventricular septum(43).

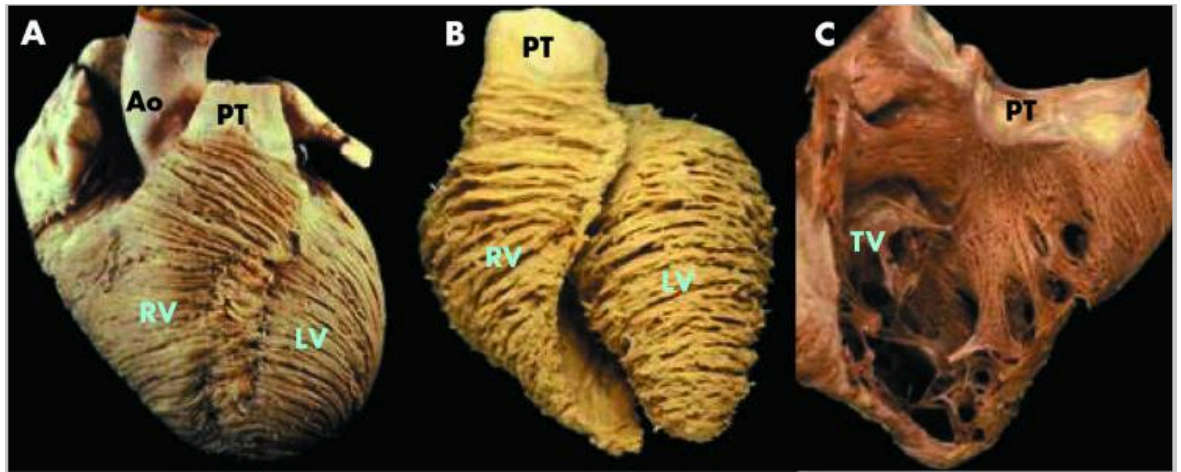


Figure 2. The top images are of an endocast of the normal heart, dissected specimens by Prof Damian Sanchez-Quintana(43).

(A) The heart is viewed from the anterior aspect and demonstrates the orientation of the myofibres of the subendocardium. (B) The subepicardial myofibres are demonstrating the circumferential arrangement in the right ventricle but change from oblique to circumferential in the LV. (C) A longitudinal section of the subendocardial myofibres. Ao- Aorta; PT - Pulmonary Trunk; RV - right ventricle; LV - Left Ventricle; TV - Tricuspid Valve.

1.1.11 The Right Ventricular Architecture

The RV is composed of two muscular layers(46), the superficial and the deep layers. In the superficial layer, the muscle fibres are orientated circumferentially, parallel to the atrioventricular groove(43). These fibres continue into the superficial layers of the left ventricle and bind the two ventricles together. Despite the different muscle mass and chamber geometry, the superficial muscle layer contributes to the ventricular interdependence, along with the interventricular septum and the pericardium. Towards the apex this layer spirals

deep into the subendocardial layer of the RV. The deep muscle layer fibres are orientated longitudinally, perpendicular to the superficial layer and span from the base to the apex(42). During contraction, the subepicardial layer of the inflow tract generates pressure initially, leading to circumferential contraction. Subendocardial fibres then contract leading the longitudinal shortening during the ejection phase. The interventricular septum bowing from the high pressure LV to the lower pressure RV also aids in the ejection of blood from the RV(47). This is termed interventricular dependence.

1.1.12 Function of the Right Ventricle

The main functions of the right ventricle are:

- to maintain adequate pulmonary perfusion to deliver deoxygenated blood to the membranes which facilitate gas exchange and
- to maintain a low systemic venous pressure to prevent tissue and organ congestion(48).

In addition, it contributes to the normal overall function of the heart. It pumps the same stroke volume as the left ventricle but at lower pressure and as a result the ventricle is more thin-walled and distensible than the left(49).

Preload, afterload, and contractility all determine the RV function but can be impacted by several other factors. Heart rate and rhythm, the synchrony of contraction, valve dysfunction and ventricular interdependence can all influence cardiac function(42, 50). Preload is the load present in the RV prior to contraction. Within limits, the higher the preload, the more effective the contractility is, as is demonstrated by the Frank-Starling mechanism(51). However, beyond the physiological range, with over-stretching of the RV sarcomeres by a very high preload, there is reduced LV filling and LV function. Functions that affect the preload include fluid status, ventricular relaxation and compliance, heart rate and the passive and active filling from the atria and pericardial limitation. The afterload represents the pressure the RV must overcome during systole. The RV is more sensitive to changes in afterload than the LV(52). Clinically, the pulmonary vascular resistance is used to assess the afterload of the RV, and a high PVR is one

of the key diagnostic criteria used to diagnosis pulmonary hypertension(53). The contractility of the RV is best measured using the ventricular elastance. This is the relationship between end-systolic pressure and volume and can be seen using flow loops of the RV, as seen in Figure 3(54). The slope connecting the end-diastolic volume and pressure points is the end-systolic pressure volume-relationship and is a measure of the RV function(55).

Ventriculo-arterial coupling refers to the concept that the heart and the arterial vasculature are and interdependent connected system, where the function of one is dependent on the function of the other, rather than distinct structure. Thus, considering them together, provides a greater comprehension of their overall function in health and helps to better understand the pathological basis in disease. This is seen in both the left ventricle, where there is systemic vascular thickening in response to age, and in the right ventricle, where the pulmonary vasculature is thickened in disease states such as idiopathic pulmonary hypertension, or chronic thromboembolic pulmonary disease(56).

The contractile function of the ventricles is dependent on the elastance of the arteries, which is defined as a change in pressure for a given volume. Traditionally represented by the Frank-Starling curve, the ventricular function is perhaps more accurately measured by the ventricular pressure-volume loop, which simultaneously measures intraventricular pressure (cardiac end-systolic elastance, (E_{es})) and stroke volume within the pulmonary artery (Arterial elastance, (E_a)) during multiple cardiac cycles. Having measurements in both the left and right ventricle helps to identify the similarities and the differences between these two ventricles. The differences in afterload and lower pressures within the ventricles lead to different shapes of the pressure volume curves. With the low afterload, the RV ejection occurs after the pressure reaches systolic pressure, and therefore it looks less rectangular than seen in the left side. A ratio of E_{es}/E_a between 1.5 and 2 is considered within normal physiological limits(57).

Where the pressure increases in the pulmonary vasculature, the main pulmonary artery becomes dilated. This reduces its ability to dilate and accommodate the cardiac output, and as such the pressure increases. This is reflected in reduced pulmonary artery distensibility and leads to un-coupling of the ventriculo-arterial uncoupling, and may only become apparent when the patient exercises, or becomes more unwell, leading to increased stress and rise in cardiac output. This uncoupling process reflects a reduced contractile reserve and is a poor prognostic indicator in those with pulmonary hypertension(57).

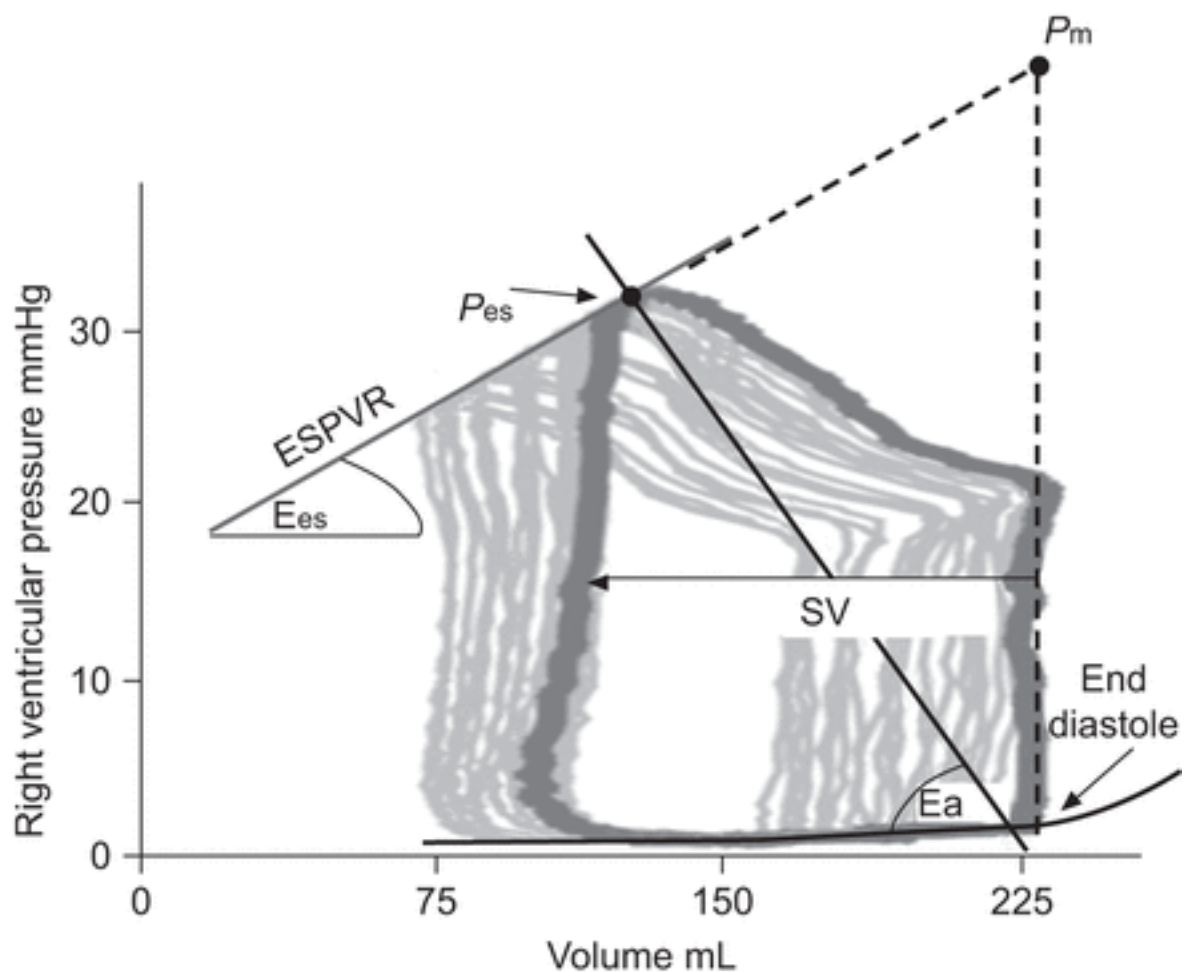


Figure 3. Right Ventricular Pressure Flow Loop(54).

This contains four phases, which begin at End Diastole when ventricular volume is at its highest and pressure is lowest. The phases are isovolumic contraction, ejection, isovolumic relaxation, and the filling phase. In early diastole there is a large increase in volume with little changes in pressure. Diastolic filling is decreased by vena caval occlusion, there is a rise in pressure (grey lines) without a rise in volume. The end systolic pressure volume relationship (ESPVR) links the end-systole pressure volume points. The slope of this line, E_{es} , is a measure of RV contractility. The slope of the line connecting end diastolic volume and end systolic pressure, E_a , is called arterial elastance and is a measure of ventriculo-arterial coupling. Stroke Volume (SV) measured by the change in volume between end diastole and end systole.

1.1.13 Blood Supply of the Right Ventricle

The blood supply to the RV is very similar to that of the LV, as would be expected from the heart's embryological development. The vessels are less conspicuous in the RV because of the lower muscle bulk in the healthy heart(58). The blood supply is dependent on the dominant coronary artery system. Approximately 80% of the population has a right dominant system and the right coronary artery supplies the right ventricle. The posterior descending artery, which runs along the moderator band, supplies the posterior wall and the inferioseptal region and the lateral wall is perfused from the marginal branches of the RCA. The left anterior descending artery supplies the anterior and anterioseptal areas(42, 58).

1.1.14 Left Ventricular Architecture

The left ventricle has a prolate ellipsoid shape, with the long axis reaching from the base to the apex. The inflow of blood, through the mitral valve, separated by the anterior mitral valve leaflet is at 30 degrees to the outflow tract, the aortic valve. As such, the blood flows in and out through valves that are very close together. Therefore, blood flow is bi-directional: into the ventricle and out of the ventricle. The ellipsoid shape of the ventricle is an evolution in bi-pedal man to generate adequate blood pressure to supply the systemic circulation.

The LV comprises two continuous helical fibres. These are counter-directional helix - the right handed helix, angled at +60degrees, in the subendocardium and the left handed helix, angled at -60 degrees, in the subepicardium(59). This is an energetically efficient orientation and allows effective redistribution of stress. This change in the angles is due to the 3-dimensional-myofibril architecture. In the cardiac base, the fibres are orientated circumferentially and towards the base run obliquely(60). Subendocardial region consisted of longitudinally directed fibres forming the trabeculae and papillary muscles(60).

1.1.15 Left Ventricular Displacement

The orientation of muscle fibres leads to efficient muscle contraction in three planes, radial, circumferential, and longitudinal, which is measurable using

cardiac magnetic resonance imaging. Radial displacement is directed inwards throughout the LV. The maximal strain occurs at the apex, moving axially to the base leading to downward motion of the mitral annulus. The circumferential deformation leads to rotation of the myocardium, the greatest of which is seen at the base. Longitudinal deformation leads to shortening along the long axis of the heart by descent of the base towards the apex. The greatest magnitude is seen at the base, progressing to the apex(61).

1.1.16 Ventricular Interdependence

Ventricular interdependence refers to the theory that the size, shape, and function of one ventricle has effects on the other through mechanical interaction at the interventricular septum. The interdependence is most apparent when there is an increased load in one ventricle, which then clearly affects the function of the other. This is central to the pathophysiology of pulmonary hypertension where the RV is usually both pressure and volume overloaded.

Systolic interdependence is largely reliant on the interventricular septum. Approximately 20-40% of the RV outflow is a result of the LV contraction(62). Should the RV suffer an insult resulting in an area of poor or absent contraction, the interventricular septal contraction is usually able to compensate for this if the RV is not dilated(63).

Diastolic ventricular interdependence is reliant on the interventricular septum and the pericardium. In the overloaded state, it is seen that LV and RV diastole can occur at different times, with RV diastole occurring later than the LV. This results in a period when RV pressure is greater than the LV, leading to septal shift towards the left side. This alters the geometry of contraction and can lead to strain on the pericardium. The septal bowing to the left leads to decreased LV distensibility, increased end-diastolic pressure and reduced LV preload. As is demonstrated by the Frank-Starling mechanism, this then leads to a low cardiac output state(42, 62).

1.2 The pulmonary circulation and right ventricle in pulmonary hypertension

1.2.1 The aetiology of Pulmonary Hypertension.

The term pulmonary hypertension describes the clinical syndrome of raised blood pressure within the pulmonary vasculature. The 6th World Symposium of Pulmonary Hypertension recently proposed threshold of >20mmHg in the main pulmonary artery and a pulmonary vascular resistance of >3 Wood Units, associated with increased breathlessness and functional limitation(3). The European Guidelines include a lower threshold of >2 Wood Units in order to detect disease early(3). However, there are several conditions that will result in pulmonary hypertension, which vary greatly in their response to treatment. As such, the term alone is not a sufficient diagnosis, and it is imperative to define pulmonary hypertension subtype in order to provide details of its aetiology and likely response to therapy.

As of 2003 there Pulmonary Hypertension has been sub-classified into five groups, updated at the World Symposium on Pulmonary Hypertension, most recently held in Nice, France in 2018(64). These have been grouped according to their pathophysiological phenotype, with the aim of focussing research efforts towards development of therapeutic targets. Indeed, over recent years there has been an increasing number of treatment options developed that have been proven to improve the quality of life and exercise capacity of patients. The most recent classification of pulmonary hypertension is outlined in Table 1.

1.2.2 The classification of Pulmonary Hypertension

Table 1 Classification of Pulmonary Hypertension

i. Pulmonary Arterial Hypertension
a. Idiopathic PAH
b. Heritable PAH
c. Drug- and toxin-induced PAH
d. PAH associated with
i. Connective tissue disease
ii. HIV infection
iii. Portal Hypertension
iv. Congenital heart disease
v. Schistosomiasis
e. PAH - Long term responders to calcium channel blockers
f. PAH with overt features of venous/capillaries (PVOD/PVH)
g. Persistent PH of the new-born
ii. Pulmonary Hypertension Secondary to left heart disease
a. PH due to heart failure with preserved LVEF
b. PH due to heart failure with reduced LVEF
c. Valvular heart disease
d. Congenital/acquired cardiovascular conditions leading to post capillary PH
iii. Pulmonary Hypertension due to lung diseases and/or hypoxia
a. Obstructive Lung Disease
b. Restrictive lung disease

	c. Other lung disease with mixed obstruction/restriction
	d. Hypoxia without lung disease
	e. Developmental lung disorders
iv.	Pulmonary Hypertension secondary to Pulmonary Artery Obstructions
	a. Chronic thromboembolic PH
	b. Other pulmonary artery obstruction, e.g., pulmonary vascular sarcoma
v.	Pulmonary Hypertension with unclear and/or multifactorial mechanisms
	a. Haematological disorders
	b. Systemic and metabolic disorders
	c. Others
	d. Complex congenital heart disease

1.2.3 The pathophysiology of pulmonary hypertension

Pathological findings in pulmonary arterial hypertension are similar, irrespective of whether it is idiopathic or associated with a secondary cause. These changes include increased pulmonary arteriole contractility, remodelling and proliferation of smooth muscle and endothelial cells, endothelial dysfunction and increased in-situ thrombosis. These changes result in narrowing and occlusion of the small pulmonary arteries, leading to increased pulmonary vascular resistance. Over time, the increased resistance leads to clinically significant increases in pulmonary artery pressure, right ventricular dysfunction, and premature death(65).

There have been three cell signalling pathways identified that lead to the pulmonary vascular dysfunction: the nitric oxide pathways, the prostaglandin and thromboxane, and endothelin-1 (ET-1) pathways. There is decreased vasodilation from reduced prostacyclin and nitric oxide synthase production, with additional vasoconstrictive and mitogenic effects of the increased endothelin-1 pathway(66, 67).

In the healthy pulmonary vasculature, nitric oxide is produced by endothelial nitric oxide synthase (eNOS). Once exposed to oxygen and other co-enzymes, this catalyses L-arginine to L-citrulline. Nitric oxide diffuses into the pulmonary vascular endothelium and binds to soluble guanylate cyclases (sGC), which converts guanosine triphosphate (GTP) to cyclic guanosine monophosphate (cGMP). This then activates dependent proteins, leading to vasodilatation. Nitric oxide also inhibits smooth muscle cell proliferation, platelet aggregation and thrombosis. In PAH, there is a reduction in the availability of nitric oxide, leading to vasoconstriction, smooth muscle cell proliferation, platelet aggregation and in situ thrombosis development. There are therapeutic agents now available that target this pathway. Phosphodiesterase-5 inhibitors prevent the degradation of existing cGMP, increasing the concentration of this and promoting vasodilatation and inhibiting smooth muscle cell proliferation(68).

Prostacyclins are produced by healthy endothelial cells from arachidonic acid from cyclooxygenase and prostacyclin synthase. Prostacyclin activates adenylate cyclase by binding to prostanoid receptors in smooth muscle cells. Adenylate cyclase converts adenosine triphosphate to cyclic adenosine monophosphate (cAMP), leading to relaxation of the smooth muscles and vasodilatation. In a similar way to nitric oxide, prostacyclin leads to a reduction in platelet aggregation, smooth muscle cell proliferation and exhibits antithrombotic effects. In patients with PAH, the pathway is altered such that cAMP is not the product of the pathway but is, instead, thromboxane A₂, which leads to vasoconstriction, smooth muscle proliferation and platelet aggregation(69). There is reduced production of prostacyclins and reduced expression of the receptors(70). The therapeutics used for PAH are prostacyclin analogues and receptor agonists.

ET-1 is produced on endothelial cell membranes from big-endothelin-1 by endothelin converting enzymes. There are 2 different receptor subtypes- ET_A and ET_B. Vascular smooth muscle cells contain ET_A and promotes vasoconstriction, proliferation, cell migration and fibrosis. ET_B is found on both vascular smooth muscle and endothelial cell surfaces. Activation of ET_B leads to vasoconstriction on endothelial cell surfaces. However, on vascular smooth muscle, it activates NO and prostacyclin production, causing vasodilation and exhibits anti-proliferation properties. In PAH, there is increased ET_A and endothelial ET_B expression(71). There is also increased ET-1 concentrations in plasma and pulmonary vascular endothelial cells(72). Endothelin receptor antagonists have been developed as a further therapeutic option, which are ET_A selective or act on both ET_A and ET_B.

1.2.4 The pathophysiology of chronic thromboembolic pulmonary hypertension

The majority of pulmonary embolism is the result of thrombosis formation within a deep vein of the body, the most common of which is in the lower limb. This forms as the result of venous stasis, trauma and hypercoagulability, known as Virchow's triad (73).

Acute pulmonary embolism is a common and potentially fatal condition. It affects 0.06% of the population annually (74), with the risk substantially increasing with age, and has a high incidence of recurrence. There is an in-hospital rate of death ranging from 6-15%. The presence of acute thrombus induces an acute inflammatory response within the lumen. This process organises the thrombus, before spontaneously lysing it. In the majority of cases there is full resolution of thrombus but, in some cases, the inflammatory and lysing process can lead to damage of the vascular endothelium (75). The spontaneous process of thrombus resolution with the endogenous fibrinolytic system, allows the lumen of the vessel to become patent and the normal pattern of venous flow to be re-established. With follow up imaging of patients treated for acute pulmonary embolus, there is approximately 50% reduction in thrombus burden by 4 weeks (76).

Despite treatment, however, approximately half of patients have chronic pulmonary vascular abnormalities at follow up and the underlying cause of incomplete thrombus resolution is unknown. Larger, central thrombi are least likely to fully resolve. Pathology studies from patients who have had pulmonary endarterectomy for chronic thromboembolic pulmonary hypertension (CTEPH) have yielded a heterogeneous collection of thrombus material, consisting of fibrous plaques with signs of angiogenesis or atherosclerotic lesions containing cholesterol, macrophages, and T-lymphocytes(77, 78). The clinical significance of incomplete thrombus resolution is unknown as is not clear how many of these patients have resulting functional limitation(79).

CTEPH is the result of thrombus-related persistent perfusion defects within the pulmonary vasculature, which leads to increased pulmonary vascular resistance and increased pulmonary arterial pressure. It is defined by a mean pulmonary arterial pressure above 20mmHg and a pulmonary capillary wedge pressure of less than 15mmg, as measured by right heart catheterisation along with at least one persistent perfusion defect seen on imaging (V/Q scanning or pulmonary angiography) after 3 months of anticoagulation. CTEPH can cause remodelling of the small pulmonary vasculature, in addition to chronic stenosis of larger vessels. Clinically, it leads to impaired exercise capacity and can progress to right heart failure and premature death. The diagnosis and management of CTEPH is well validated(80, 81). It has been shown to affect 2.3% of patients after acute PE after 2 years in a prospective study by the FOCUS Investigators(82) and 1.9% of patients in a retrospective analysis of patients after acute pulmonary embolus over the same time(83).

1.2.5 Remodelling of the Right Ventricle

There are thought to be two phases of right ventricular remodelling in pulmonary hypertension: adaptive and maladaptive. In the early stage of pulmonary hypertension, there is remodelling in response to the increased afterload. There is concentric hypertrophy, associated with preserved systolic and diastolic function and patients are often asymptomatic during this phase. However, in most patients, these adaptive mechanisms are insufficient to maintain an adequate cardiac output and progress through the maladaptive process, leading to right heart failure, characterised by exercise intolerance and fluid retention, and ultimately to premature death(84).

The maladaptive remodelling process is complex and depends on the level of pulmonary hypertension, along with the right ventricular perfusion, the metabolic activity of the RV and neurohormonal activation. It is characterised by eccentric remodelling and is associated with systolic and diastolic dysfunction. In addition, with the volume and pressure overload, there is dilatation of the right ventricle, which leads to broadening of the annulus causing tricuspid incompetence. This further exacerbates the volume overload status in the RV leading to progressive dysfunction(85). This has been further evaluated when comparing the RV mass and volume ratio. *Badalaghiacca et al* have shown that the mass to volume ratio and reduced cardiac index can suggest moving to a maladaptive phase of function and predicts clinical deterioration(86). This is supported by a retrospective analysis by *Goh et al* who demonstrated that patients with a high RV volume: low RV mass ratio are entering into maladaptive phase and has an impact in prognosis(87). Reduced RV perfusion via the coronary arteries also leads to the maladaptive pathway. Insufficient perfusion from the capillary network also impairs vascular endothelial growth signalling and the hypertrophic response. As such, increased myocardial fibrosis can reduce the compliance of the RV. Furthermore, a change in the metabolic activity of the myocardium is another feature of right heart failure. There is a switch from fatty acid oxidation to glycolytic metabolism as this requires less oxygen(88). Decreased mitochondrial activity leading to a change from aerobic to anaerobic metabolism may also play a part in the RV adaptive mechanisms changing the pathophysiology to maladaptive(88).

RV dyssynchrony is a further maladaptive mechanism, which contributes to the dysfunction. In PAH, there is continued RV free wall contraction during early diastole of the LV. Myocytes under mechanical stress prolong their contraction and action potential. This leads to interventricular septal shift towards the LV. As such, with progressive disease and worsening free wall stress, there is further dyssynchrony(89).

1.3 Assessment of the RV Function

The structure and function of the right ventricle is an important determinant for the outcome of patients with pulmonary hypertension(90). In early pulmonary hypertension, the right ventricle is usually able to remain well functioning in response to the increased afterload with little or no increase in the dimensions of the chamber. As the disease progresses, there is maladaptation of the ventricle during times of stress, such as during exercise, where the heart is unable increase cardiac output to meet demand. In more advanced PH, there is systolic dysfunction and dilation of the ventricle, and it cannot match the

afterload of the increased pulmonary vascular resistance(91). These changes are associated with fibrosis of the myocardium and stiffening of the ventricle, leading to both systolic and diastolic dysfunction. This collection of changes leads to limitation of RV function, with increased filling pressures, under filling of the RV, poor systolic function and reduced cardiac output.

Complete evaluation of the right ventricle requires a multimodal approach to accurately measure the function. This involves both invasive and non-invasive techniques. Assessing the right ventricle is not only essential to the diagnosis of pulmonary hypertension in all its forms but, particularly in pulmonary arterial hypertension, it is essential to help assess patients' risk of deterioration and risk of death in the coming year. This then has implications for prognosis but also on the treatment strategy for the individual(53).

1.3.1 Echocardiography

Echocardiography is usually the first investigation that alerts the clinician to the presence of pulmonary hypertension. It is a widely available, inexpensive, and non-invasive technique that is the first line investigation for assessment of the RV size and function. In the parasternal long axis and apical four chamber view, the RV is approximately two thirds the size of the LV. The RV should also be evaluated using subcostal views. If it appears larger in length or diameter, there is likely to be RV dilatation. The LV should have a circular shape and, as it contracts concentrically during the cardiac cycle, should remain circular in the normal heart(92). The echocardiogram can accurately assess LV size, function, and ejection fraction, in addition to evaluating valve function in the left and right sided chambers.

On the other hand, assessing the RV during the cardiac cycle is more difficult. The change in size during the cardiac cycle makes assessing function more labour intensive and has a higher interobserver variability(93). There have been methods developed to reduce the variability, including RV tracing techniques using radionuclide injections. However, these techniques are not always possible to execute because of difficulties in tracing the thin-walled RV. Tricuspid annular plane systolic excursion (TAPSE) is another, more reproducible, technique used to assess RV function(94). This estimates systolic function by measuring the level of systolic excursion of the lateral tricuspid valve annulus towards the cardiac apex when using the four-chamber view. This has been shown to correlate well with RV ejection fraction(94).

In addition to assessment of RV size and function, echocardiography has utility for the estimation of pressure within the pulmonary artery. Traditionally, the pulmonary artery systolic pressure is estimated using the modified Bernoulli equation from the peak tricuspid regurgitant velocity and adding this to estimated right atrial pressure (RAP). It has been shown there is a good correlation across populations in estimating the pulmonary artery systolic pressure, however, there has only been moderate precision of the absolute pressure(95). This can lead to incorrect treatment options for the individual so should be interpreted in conjunction with clinical history and other clinical investigations.

There are several reasons why there is poor level of agreement between pressure estimations measured using echocardiogram and those invasively measured. Firstly, small inaccuracies in measuring the tricuspid regurgitant velocity (TRV) will be magnified using the simplified Bernoulli equation, $P=4[TR_{max}]^2$. Secondly, to accurately measure the pulmonary artery systolic pressure, the right ventricular systolic pressure (RVSP) is added to the RAP. To calculate the RAP, inferior vena cava dimensions are measured in response to inspiration. This often cannot be obtained in patients and, even when measured, has a low correlation with invasively measured values(96). Thirdly, if there is primary tricuspid valve dysfunction, there is poor correlation between TRV and RVSP. Moreover, it can be difficult to attain satisfactory windows using echocardiography to adequately measure pressure values in those with a high body mass index and in those with pulmonary hyperinflation, for example in chronic obstructive pulmonary disease. Although, *Bax et al* have demonstrated that a composite score using echocardiogram can be used to detect the presence of severe pulmonary hypertension in patients with interstitial lung disease(97). Finally, up to 30% of patients do not have tricuspid regurgitation and therefore this cannot be used to measure pulmonary artery pressure(53). As such, echocardiography cannot be used independently in the diagnosis of pulmonary hypertension. However, when measured correctly, this has shown to have good correlation with pressures measured using right heart catheterisation(98).

1.3.2 Cardiac Magnetic Resonance Imaging

Despite echocardiography being a valuable first line investigation, weaknesses outlined above mean that more comprehensive evaluation is required when there is diagnostic uncertainty. Cardiac magnetic resonance imaging (CMR) is currently recognised as the gold standard imaging modality for assessing right ventricular size and function. As pulmonary hypertension progresses and the pulmonary artery is unable to accommodate the full cardiac output, the right ventricle begins to adapt to the pressure changes. CMR can characterise these morphological and functional changes over time. As pressure increases, the interventricular septum shifts towards the left ventricle during late systole and, in severe cases, the septum bows towards the LV as PA pressures exceed systemic pressure(99). Computational models assessing the use of black blood models and septal angle in order to estimate pressure with some positive results(9). Furthermore, the value of septal angle and ventricular mass in a regression model to detect the presence of pulmonary hypertension, using the most up to date definition(10).

Cine MRI images are obtained by repeatedly imaging an area of interest over a period of time. In CMR, this is achieved by acquisition of images at multiple time points during the cardiac cycle once it has been synchronised with the ECG. These images can be arranged such that the blood flow within the heart can be seen during a cardiac cycle. From this, both RV and LV end-diastolic and end-systolic volumes can be measured. Ejection fraction and stroke volume can then be calculated(8)(Figure 4). Not only can this be helpful in the diagnosis of pulmonary hypertension but can also be used in order to risk stratify patients. *Alabed et al* showed that with every 1% reduction in RV ejection fraction, there is a 4.9% risk of clinical worsening over the subsequent 22 months(100). Ventricular dimensions and muscle masses can also be measured. In pulmonary hypertension these are both seen to increase. When the RV:LV >1, this is suggestive of PH and having a RV wall thickness of >4mm also suggests PH(101). Furthermore, *Lewis et al* have demonstrated the use of high right ventricular end systolic volume and low end diastolic left ventricular volume in the prediction of mortality(102). In addition, the high tissue characterization and multi-planar images make CMR well suited to assess for and quantify intracardiac shunts.

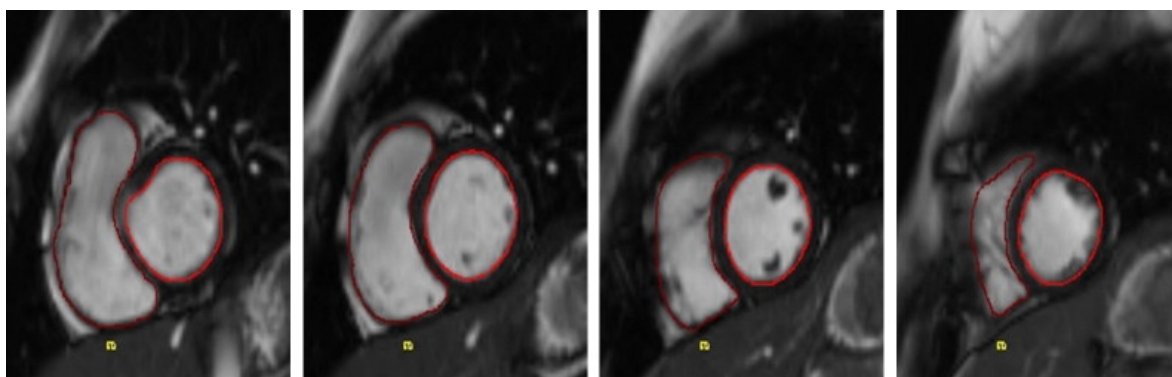


Figure 4. Circle Cardiovascular imaging of short axis demonstrating the endocardial contours used to calculate chamber volume

Not only is CMR used in the diagnosis of PH but is also useful in risk stratifying patients in terms of their likelihood of deterioration. Increased RV volume and reduced RV ejection fraction is predictive of a worse outcome(103).

Phase contrast imaging is an MRI technique that can be used to visualise moving fluid. Proton spins moving in the same direction as the magnetic field gradient develop a phase shift that is proportional to the spin velocities. In a pulse sequence, bipolar gradients are used to encode spin velocities. Moving spins in fluid will experience a different magnitude of the second gradients compared to the first because of the spatial position. This information can be used to determine the velocity of the fluid. This technique can be applied to the pulmonary artery to assess cardiac output(104). Blood velocity can be calculated, which has been shown to strongly correlate with pulmonary artery pressures and pulmonary vascular resistance.

However, despite the strengths of cardiac MRI in the evaluation of the RV, there is yet no reliable way of measuring pulmonary artery pressure. The ‘gold standard’ investigation remains the right heart catheterisation. This is the most accurate way of measuring pressure and is indirectly able to assess RV function by the assessment of the RAP, which is a measure of preload, pulmonary artery pressure, pulmonary vascular resistance, and stroke volume, to measure contractility.

1.3.3 Right Heart Catheterisation

Right heart Catheterisation (RHC) is the definitive investigation in the diagnosis of pulmonary hypertension; it remains the most accurate investigation in assessment of pressure within the pulmonary artery. It is performed using the Swan-Ganz balloon floatation catheter and allows the measurement of systolic and diastolic pressure, to facilitate the calculation of mean pressure within the vessel. The RHC also helps to further classify the diagnosis of pulmonary hypertension into precapillary (Groups 1, 3, 4, 5) and post-capillary PH by measuring the pulmonary artery wedge pressure (PAWP). A PAWP threshold of 15mmHg is set as being normal, and above it, PH is thought to reflect post-capillary in origin. Precapillary pulmonary hypertension is characterised by a PAWP of <15mmHg in addition to mean PAP of >20mmHg and a pulmonary vascular resistance (PVR) of >2 wood units(53).

In diagnostic work up, it is recommended that during the RHC, there is a comprehensive haemodynamic assessment by measuring the right atrial pressure, pulmonary artery pressure, cardiac output, and the mixed venous oxygen saturation (Table 2). From these measurements, transpulmonary gradient, diastolic pressure gradient, PVR and cardiac index can all be calculated. These indices not only facilitate an accurate diagnosis but allow the clinician to stratify disease severity and risk of deterioration over the coming year(53). This then helps to determine the treatment strategy for the patient(105).

Measurement	Normal Range
Right Atrial Pressure	0-5mmHg
Right Ventricular Pressure, systolic	15-25mmHg
Right Ventricular Pressure, diastolic	0-10mmHg
Pulmonary Artery Pressure, systolic	15-25mmHg
Pulmonary Artery Pressure, diastolic	6-12mmHg
Mean Pulmonary Artery Pressure	<20mmHg
Pulmonary Capillary Wedge Pressure	<15mmHg
Cardiac Output	>5L/min
Cardiac Index	>2.4L/min/m ²
Transpulmonary Gradient	>12mmHg
Pulmonary Vascular Resistance	<3Wu

*Table 2. Normal values of indices measured during right heart catheterization
mmHg - millimetres of mercury; L/min - Litres per minute; L/min/m² - litres per minute per metre squared of body surface area; Wu - Wood units*

Inhaled nitric oxide is used during RHC to identify those who have vasoreactivity. This, again, helps to risk stratify patients and aid treatment decisions. Those who are 'vaso-responders' are in a better prognostic group and respond well to the use of calcium channel blocker therapy(53). Those who are deemed to have vasoreactivity have a reduction in mean PAP to below 40mmHg and have a reduction by at least 10mmHg, with no reduction in cardiac output, in response to inhaled Nitric oxide delivered at a concentration of 40ppb (parts per billion) for 5 minutes.

Despite RHC being the 'gold standard' investigation in the diagnosis of PH, errors in data acquisition may result in erroneous treatment decisions. Distinguishing between PAH and post-capillary PH presents a common challenge. Identifying those with heart failure with preserved ejection fraction (HFpEF) can be complex and a normal PAWP does not exclude HFpEF, since the volume status of the patient is key(106). In those who are volume-deplete, those with HFpEF or pulmonary venous hypertension, a normal PAWP may lead to erroneous management decisions. Where this is found to be the case, or HFpEF is suspected due to the clinical history or the presence of enlarged left atrium on imaging modalities, patients can be challenged with fluid, usually 500ml of 0.9% sodium chloride administered over 5-10minutes. This has been shown to differentiate occult pulmonary venous hypertension (PVH) from PAH, increasing the PAWP to >15mmHg(107). Another option to try and distinguish PVH from PAH, involves an exercise challenge, while the patient is on the catheter table. This additional stress on the table may unmask LV dysfunction, leading to an increase in PAWP >15mmHg.

Although RHC remains the definitive investigation for the diagnosis of pulmonary hypertension, using a multi-modal approach allows a reliable and accurate assessment of the right ventricular function. Using this approach minimises the chance of erroneous diagnosis and, therefore, maximises the chance of initiating the optimal management plan. In addition, multi-modal assessment allows patients to have their disease severity categorised and aggressive therapy can be started at the time of diagnosis if they have a high mortality risk in the year after diagnosis.

1.3.4 The Six Minute Walk Test

Exercise intolerance is usually one of the first symptoms of PH. Determining a patient's exercise capacity is an important part of patient evaluation. Depending on the symptom burden of the patient, six-minute walk distance (6MWD) or cardiopulmonary exercise testing (CPET), or both, can be performed to assess the level of functional impairment. 6MWD has been shown to correlate with survival(1) and changes in 6MWD have been used as a primary endpoint in many trials of pulmonary vasodilator therapies(108).

6MWD is a submaximal measure of exercise capacity. It is a simple, repeatable, and inexpensive test to perform that can be done in the outpatient clinic setting. It better reflects the functional abilities of patients in day-to-day life than laboratory-based assessments. However, its efficacy as an assessment tool is influenced by gender, height, weight, patient effort and musculoskeletal pathology, poor balance, and medical comorbidities, such as ischaemic heart disease. The environment in which the test takes place can also influence results: the length of the corridor, encouragement from bystanders and learning effect can all alter the distance walked. There are limitations of the 6MWD, and it may not detect mild disease in those with limited symptoms and a longer walk distance at baseline, which is more commonly seen in younger patients. The ceiling effect is seen above 450 metres(108). The ceiling effect is seen in those with low symptom burden and high baseline walk distances but in the setting of significant cardio-respiratory impairment, may be able to compensate by other mechanisms, for example peripheral muscle function(109). Thus, improvements in response to therapy or deteriorations in cardio-respiratory function are less likely to be identified using the 6MWD.

The American Thoracic Society have released guidelines on how best to perform the test(110). Heart rate, blood pressure and oxygen saturations are assessed, along with a subjective score on symptoms of breathlessness using the Borg Scale(111). According to the ESC/ERS guidelines, this should be performed at baseline and 3-4 months following treatment change, or change in symptoms, to assess for change in disease status.

Whilst the 6MWD is very useful, and commonly performed in the evaluation of functional limitation with PAH, its limitations should be borne in mind and if further, more detailed, assessment of functional limitation is required, then a cardiopulmonary exercise test should be considered.

1.3.5 Cardiopulmonary Exercise Testing

The cardiopulmonary exercise test (CPET) is a further non-invasive method of assessing functional limitation. This can provide a far more detailed evaluation of cardiovascular, respiratory, and muscular responses to exercise. It can be used to help determine the cause of breathlessness in a patient where there is diagnostic uncertainty, and quantify functional limitation where the diagnosis is clear, such as in patients with PAH.

To maximise the use of CPET in PAH, it is useful to understand the pathophysiology of exercise intolerance in the disease. In the healthy subject, cardiac output (CO) should rise during exercise to meet the increased oxygen demand of peripheral muscles. In PAH, there is an inability to increase the stroke volume to meet this demand due to increased pulmonary artery pressure and RV dysfunction. As such, there is early anaerobic respiration of peripheral muscles and early lactic acidosis. Invasive studies assessing haemodynamic response to exercise have shown that in PAH there is no significant increase in stroke volume and the increase in cardiac output is attributed to the increase in heart rate(112).

Furthermore, low alveolar-arterial diffusion, high physiological dead spaces, and intra-cardiac shunting, for example, through patent foramen ovale, all can lead to hypoxaemia. This worsens the early lactic acidosis and increases the minute ventilation (V'_E). In turn, this worsens the perfusion to the areas of well-ventilated alveoli, as it does in any situation. However, in CTEPH there is a greater effect as it increases the existing ventilation-perfusion mismatch, leading to inefficient ventilation, which is seen in the raised V_E/V_{CO_2} . The inefficient ventilation is further exacerbated by an increase in dead space ventilation, leading to a reduction in end-tidal carbon dioxide tension (P_{ETCO_2}), which is the most sensitive marker for the prediction of CTEPH(113). This decrease is the result of inefficient ventilation that causes the dilution of P_{ETCO_2} relative to P_{aCO_2} . The difference between arterial and end-tidal CO_2 (P_{a-ETCO_2}) is the result of ventilation-perfusion mismatch and is usually positive at rest, increasing with exercise in PAH patients but decreases in healthy individuals and is negative at peak exertion. *Held* et al have also demonstrated that using CPET there is a 23.5% relative increase in the diagnosis of CTEPH in patients with a diagnosis of with CTEPD, further increasing its use as a non-invasive diagnostic tool(114).

An increase in chemosensitivity of the carotid bodies also plays a role in PAH, leading to hyperventilation. Increased sympathetic tone, as a result of low CO has been described in severe PAH, which can lead to heightened chemosensitivity. Progressive lactic acidosis, catecholamine release, RV dilatation and high pulmonary artery pressures can all increase chemosensitivity during exertion(115). There has been shown to be an increase in chemosensitivity for oxygen and carbon dioxide in PAH. In addition, there is a direct correlation between chemoreceptor activity and minute ventilation(116). Given that central chemoreceptors have a functional sensitivity for hypercapnoea of ten times that of peripheral chemoreceptors, it suggests that the minute ventilation is mediated by central receptors(117).

Finally, muscular impairment also contributes to exercise intolerance. Patients with PAH are often largely sedentary have an element of deconditioning due to distressing symptoms when exercising. However, it has been shown that PAH patients also have reduced skeletal muscle microcirculation(118).The metabolic products resulting from dysfunctional muscle increase hyperventilation.

1.3.5.1 CPET in the diagnosis of PAH

CPET results become progressively more abnormal as the pulmonary artery pressure rises. Peak V'_{O_2} indicates the presence of a functional impairment and correlates with functional class in PAH. It represents the oxygen delivery and uptake of the peripheral muscles. Although not enough to diagnose PAH, when used with increased V'_E/V'_{CO_2} and reduced (P_{ETCO_2}), it suggests the presence of a pulmonary vasculopathy. There is a reduction in peak V'_{O_2} and work rate (WR). There is a decrease in oxygen pulse, anaerobic threshold and the V'_{O_2}/WR ratio. There is a marked increase in the V'_E/V'_{CO_2} and V_D/V_T . To calculate the V_D/V_T a blood gas must be performed to have an accurate oxygen saturation. An increase of >30% in the V_D/V_T indicates a pulmonary vascular limitation. This is usually associated with an increase in alveolar-arterial gradient to >45mmHg caused by the ventilation perfusion mismatch and the low alveolar capillary diffusion of oxygen. Moreover, PAH patients experience oxygen desaturation during exertion. It is seen across the spectrum of disease in PAH the level of desaturation correlates with severity of disease(119).

1.3.5.2 CPET in guiding prognosis in PAH

CPET is useful in evaluating functional limitation at the time of diagnosis of PAH but is not a replacement for right heart catheterisation. CPET is also useful in the prognosis of PAH. Most of the patient's symptoms initially are during exertion, and a CPET can evaluate the changes during exercise, where right heart catheterisation is generally only able to provide evaluation at rest. V'_{O_2} remains the most widely used value for risk stratifying patients and guiding therapeutic decisions(120). Decrease in the oxygen pulse, which is dependent on stroke volume(121), has also been seen to correlate with survival in PAH(122).

Whilst there is existing evidence for the use of CPET in the diagnosis and in risk stratifying patients with PAH, it remains underused across centres investigating patients for PAH. Further work is required to identify novel indices that will correlate with survival and help to guide clinicians with therapeutic decisions.

1.3.6 Natriuretic Peptides

B-natriuretic peptide (BNP) and the functionally inert N-terminal prohormone of BNP (NT-proBNP) are well established biomarkers used in cardiovascular disease and are a surrogate of cardiac function(53). Natriuretic peptides are hormones that are secreted from the heart, kidneys, and brain, which lead to vasodilatation and natriuresis. There are several peptides in the family, of which BNP is perhaps the most recognised and clinically useful one. They generally have a short half-life, but BNP has a half-life of around 22 minutes, which makes it an attractive option as a biomarker(123). NT-proBNP has a longer half-life of 70 minutes and is more stable when stored, and has a better correlation with prognosis in PAH so is now most commonly used in this setting(124). They are secreted by the myocardium of the ventricles and is released in response to increased pressure, volume overload and hypoxia and levels peaking in the serum around one hour after stimulation(125).

NT-proBNP correlates with pulmonary haemodynamics in PAH, including RAP, Cardiac index and mPAP, and is an independent predictor of survival(126). Similarly, it has been shown to correlate with indices measured with echocardiogram. It correlates with TAPSE, RAP and PAP. Furthermore, NT-proBNP correlates with CMR measure of RV structure and function(127).

Given its correlations with invasive and non-invasive assessments in pulmonary hypertension, NT-proBNP is part of the multimodal assessment used in risk stratifying patients as part of the ERS/ESC guidelines in the investigation and management of PAH(53). It should be performed at baseline and at routine follow up, treatment changes and changes in symptoms. The guidelines provide clear cut off values of NT-proBNP to help guide when treatment should be escalated.

1.4 Cardiovascular Magnetic Resonance Imaging

1.4.1 Theory of Magnetic Resonance Imaging

Magnetic resonance imaging was discovered by Paul Lauterbur and Peter Mansfield in the 1940s. It uses the natural magnetic properties of the body to produce images. The human body is composed of cells which all contain water, which is principally made from the hydrogen ion (H_2O). The magnet in the MRI scanner can act upon the positively charged hydrogen ions and can cause them to spin. The frequency of atomic nuclei rotation, is dependent on the strength of the magnetic field they are in. The Larmor precession frequency is the rate of oscillation of a collection of protons spinning in the same direction.

Under normal circumstances, the hydrogen ions have two poles, north and south, and spin on their axes, which are randomly aligned. When exposed to a magnetic field, in an MRI scanner, the protons axes then align. The uniform position then creates a magnetic vector along the axis of the MRI scanner. The vector is created by an electromagnetic wave and represents the instantaneous magnetic field strength and direction at any point in which the wave is propagating.

When radio waves are added to the magnetic field, frequency of rotation of the protons can be increased, changing the vector. The vector can be altered in magnitude and direction. The radio wave frequency that causes the protons to reverberate is dependent on the strength of the magnetic field. The strength of the magnetic field can be changed using a series of electric coils. This can be done for different parts of the body with different sections of the body resonating as different frequencies are applied.

As the radiofrequency is turned off, the vector returns to its resting state with proton axes randomly aligned, this in itself causes a radio wave to be emitted. This is the signal used to create the MRI images. There are coils used around the region of the body that is being imaged to optimise the detection of that emitted signal. These signals are plotted and with multiple signals, images are developed(128).

Multiple radio wave pulses can be used to highlight particular tissues or abnormalities. Tissue differentiation is seen as different tissues, such as water and fat, have different relaxation times once the radio waves are turned off. This relaxation time can be measured. T1 relaxation is the time taken for the vector to return to its normal resting state and T2 is the time taken for the axial spin to return to baseline.

Most diseases lead to an increase in the water content of tissues, so MRI is sensitive in detecting pathology. However, differentiating between pathologies is more difficult, with infection and malignancy often having similar appearances(129).

1.4.2 Right Ventricular Volumes, Function and Mass

CMR allows the 3-dimensional visualisation of the right ventricle, superior to that of other methods because it overcomes the challenges of body size, restrictions of acoustic windows, avoids scar tissue around the heart and does not have the complications associated with iodising radiation. From the images, CMR allows visualisation and quantification of blood flow and blood volumes within the heart and measurement of valve regurgitation. In addition, there is no requirement for a contrast agent to assess the function accurately.

Steady State Free Precession (SSFP) is the pulse sequence used for the cine-MRI, which allows volumetric quantification. With this sequence, there is excellent definition of the endocardial borders and blood pool. With the ventricular volumes at systole and diastole being measured, the ejection fraction can then be calculated which gives an indication of the heart function. CMR phase velocity encoded imaging can also be used to quantify the flow over the valves, which also allows measurement of the stroke volumes, cardiac output, and regurgitation fractions. Shunt fractions can also be assessed in the presence of structural heart disease. The measurement of the RV areas has traditionally been done manually, but is more commonly now done by fully automated segmentation frameworks(130).

Whilst the blood volumes can be used to assess the cardiac function, the excellent tissue characterisation can be used to quantify the right ventricular mass and allows the clinician to identify any intracardiac structural abnormality that may lead to a shunt.

Whilst this is a useful assessment to perform as a diagnostic examination in patient with unknown medical conditions, this is also a useful follow-up investigation to assess response to therapy and can give an indication of prognosis. In pulmonary hypertension, the CMR can be grossly abnormal at time of diagnosis, with both enlarged ventricular volumes but also increased myocardial mass. After a period of therapy with pulmonary vasodilators, the CMR can be repeated to look for changes in the volume and mass, which indicates and improvement in pulmonary haemodynamics. This can reduce the requirement for invasive right heart catheterisation and can be used in conjunction with clinical assessment help guide prognosis(53).

1.4.3 Flow Mapping

Phase contrast measurements of blood flow through the great vessels can be used to calculate the cardiac output, shunt fractions and regurgitant flow over the valves. It is a phase-sensitive method that can calculate velocity of blood flow from the detected signals in vessel lumen. The flow is measured by obtaining thin, cross-sectional images of the vessels that are sensitised to through-plane velocity during a single cardiac cycle, usually 3mm or less. An oblique slice is obtained to intersect the vessel. The lumen is covered by a set of pixels by drawing a region of interest around blood pool. If a region of interest is drawn around each slice in the cardiac cycle, the cardiac output can be calculated. The flow through each pixel is calculated and multiplied by the number of pixels covering the area of the vessel(131).

Flow velocity can also be measured. This is done by applying a flow-encoding gradient along the direction of the imaging pulse sequence after the excitation. This generates a flow curve and can be used to determine if there is significant valve regurgitation and allows quantification of intracardiac shunts. In addition, vessel compliance can also be evaluated using this technique. Measuring the

change in vessel area in cross section during the cardiac cycle can be used to calculate the distensibility, which is reduced when there is high pressure in the vessel(131).

Although the phase contrast measurements are the most accurate way of measuring the cardiac outputs on CMR, there are some issues that may introduce inaccuracies to the measurements. The regions of interest around the vessel lumen needs to be accurately drawn, otherwise the signals will only partially be from flowing magnetisation. This results in the signal strength of tissue being compared to that of blood, which is increased by the inflow enhancement. If the magnitude of the blood is brighter, this will lead to an overestimation of blood flow. Misalignment of the velocity-encoded gradient can also lead to underestimation of the blood flow. Changes in the flow velocity using a 2-dimensional acquisition can lead to ghosting artifacts. This can occur during respiration. As such, there can be replication of blood vessels along the direction of the phase-encoded signal. Using signal averaging during non-breath-hold can reduce the risk of these flow variables(132).

1.4.4 Tissue Tracking

Regional wall abnormalities can impact ventricular function and influence clinical outcomes, in addition to contributing to increased symptom burden for patients. Regional ventricular function can be measured using both CMR and echocardiogram. However, the latter can be complicated by poor image quality using subcostal views. CMR provides higher quality images and can provide biventricular imaging. This imaging can be done using several techniques, including myocardial tagging, phase contrast velocity imaging, displacement encoding, strain encoding and feature tracking. The technique used for the analysis in this these was CMR feature tracking (CMR-FT).The exact methods are dependent on the software packages used for analysis(133).

CMR-FT is a useful technique as, unlike the other techniques, can be applied to the short axis stack acquired during standard CMR protocols, whereas the other techniques often require specific tissue tracking image acquisition in addition to the standard protocol. Tracking methods identify a small window on one image

and search for a comparable image on the subsequent frame. The displacement detected on serial images represents the local tissue displacement. In cardiac tissue tracking, the window is required to be at least 8 x 8 pixels. Much larger images leads to degradation of the quality and any smaller may mean that the tissue displacement is beyond the limits of some of the images, and therefore not detect the tissue movement. The resolution of the images is important. If this is too low, the larger displacement led to larger search areas and images become less comparable. If too high, the frame-to-frame displacements are too small, such that the pixels are difficult to identify. The sequences detect movement inward and outward, during systole and diastole. It is easier to track tissues moving apart, and, as such, the sequence begins near end-systole and tracks the tissue during diastole. Initially, tracking was designed for 2-dimensional images, but has now been developed for 3-dimensional volumetric regions, such that radial, longitudinal and circumferential tracking can be performed(133).

Although a useful tool, tissue tracking does have some flaws which must be borne in mind when using this technique to evaluate cardiac function. It is assumed that the changes in greyscale represents displacement of tissue, but this may not be the case. Other structures may be misidentified as tissue displacement, leading to erroneous results. It is assumed that myocardium is a coherent, deformable tissue. However, the myocardium is heterogeneous, especially around the trabeculae, making tissue tracking more difficult in different ventricular regions. In these areas, good spatial resolution and image quality is essential to identify the ventricular boundaries. Using CMR, special care must be taken to ensure that blood is not mistakenly identified as ventricular tissue, as they move in opposite directions, and can lead to erroneous interpretation. In addition, tissues tracking has poor reproducibility. This is partially related to post-processing techniques, but it has been shown to have poor correlations between different studies and between different observers. Finally, the tissue displacement measurements are based on estimates and, as such, small errors are unavoidable(133).

Tissue tracking is a novel and potentially useful tool that will help clinicians detect early changes in disease processes. However, its flaws need to be kept in mind. As such, it should be used in conjunction with other indices to make clinical diagnoses and treatment decisions.

1.5 Covid PTE

1.5.1 Coronaviruses

Viruses are inert packages of DNA or, in the case of coronaviruses, RNA, that are only able to reproduce once inside living cells that are vulnerable to viral infection. These cells must have the ability to replicate the nucleic acids into amino acids, which can then build viral proteins. As such, viruses can only survive within a host and can be transmitted between individuals to survive and replicate via a vector. Most viruses affecting humans have occurred due to host-switching from animals to humans. This switching process is affected environmental and biological factors, which offer the environment for interaction between the host and the new species and there must be shared cell receptors that allow viral penetration.

Coronaviruses contain RNA and are found infecting many species. The important coronaviruses found within humans are divided into alpha- and Beta- groups. There are four human coronaviruses (human coronavirus-OC43 (HCoV-OC43), human coronavirus-HKU1 (HCoV-HKU1), human coronavirus-229E (HCoV-229E), and human coronavirus NL63 (HCoV-NL63)) that developed at some time in the past, which mainly lead to self-limiting upper respiratory tract infections.

Given the mild syndrome associated with endemic coronaviruses, little was known about them as research into them was relatively marginal. The emergence of SARS-Cov in the early 2000s changed this. It led to spread throughout 29 countries and lead to the death of over 800 people. In 2012, there was a further coronavirus pandemic, MERS-CoV, which lead to fatalities throughout the Middle East. This had spread from camels, but the transmission of this virus was inefficient between humans and, as such, isolation of cases meant that the spread was limited.

Bat species harbour many coronaviruses, which do not affect humans usually, but mutations have led to the above coronaviruses host-switching, and, indeed, saw the emergence of the novel coronavirus, SARS-COV2(134).

December 2019 saw the rapid spread of a novel coronavirus, SARS-CoV-2, origination from Wuhan City in China. This was named after a related virus, SARS-CoV-1, which caused a pandemic in early 21st century. Prior to 2019, this virus or its genetic sequences had never been before seen in animals or humans(134). However, all previous coronaviruses have had zoonotic origins and its emergence has similarities to previous novel virus pandemics. Epidemiological data suggests that the wet markets in Wuhan were the centre of disease spread. Here, there was trade of thousands of live, wild animals, including civets and racoon dogs, known to be reservoirs of thousands of coronaviruses.

1.5.2 Covid-19 syndrome

The first reported patient in Scotland with SARS-CoV-2 was case in Scotland was in March 2020. COVID-19, the clinical syndrome of SARS-CoV-2 infection, has well described but patients have been presenting with various complaints - including fever, shortness of breath or loss of taste or smell. Around 80% of patients present with mild symptoms. However, 20% of patients have been shown to present with a severe or critical illness, characterised by fever, shock, acute lung injury and coagulopathy. The haematological abnormalities mimic other disorders, such as disseminated intravascular coagulation and thrombotic microangiopathy. There associated with an increased mortality rate(135) COVID-19 also predisposes to thrombotic complications, which has been shown to be up to 30% in those with critical illness(136). Other viral and bacterial pneumonia are known to also cause similar symptoms, but anecdotal evidence suggests that the incidence of thrombosis may be higher(136).

There remain few data available on the incidence of thrombosis and comorbidity potentially associated with the development of thrombosis in hospitalised patients with COVID-19, particularly in patients managed outside the critical care setting. Most reports have been limited to a few hospital centres. We made a retrospective assessment of the incidence of PTE in all patients with COVID-19 admitted to hospitals in Scotland in both critical care and ward environments. In addition, we aimed to assess if right heart strain increased the risk of death or requiring critical care support.

1.6 Aims and Objectives

This thesis encompasses various aspects of thrombotic pulmonary vascular disease. I aim to

- To assess the efficacy of novel imaging indices in detecting the presence of thrombotic pulmonary vascular disease using CMR and echocardiogram, which would reduce the need for repeated right heart catheterization (Chapters 3 and 4).
- Evaluate if rehabilitation affects cardiac function and functional abilities in those with pulmonary hypertension, including chronic thromboembolic pulmonary hypertension (Chapter 5).
- Evaluate the risk that Covid-19 poses to the Scottish population developing thrombotic pulmonary vascular complications in hospital and examine where there are any contributing co-morbidities that make this more likely (Chapter 6).

1.7 Hypothesis

The hypotheses from which this thesis has evolved are below:

- left ventricular eccentricity index would be abnormal in CTEPH and normal in CTEPD and that we could use this investigation to detect those who would benefit from established treatments.
- exercise rehabilitation improves quality of life and exercise tolerance because of its effect on cardiac function.
- Covid-19 posed an increased risk of pulmonary thromboembolism in hospitalised patients.

2 Materials and Methods

This chapter will outline the methods used in the relevant chapters of the thesis. All studies performed in this these have been done so with appropriate ethical consent. The studies include research on human subjects: this has been done in keeping with the ethical principles for medical research listed in the Declaration of Helsinki(137).

2.1 Effect of exercise rehabilitation on cardiac function in pre-capillary pulmonary hypertension.

2.1.1 Patient recruitment

Patients for this study have been prospectively recruited from the Scottish Pulmonary Vascular Unit, based at the Golden Jubilee National Hospital in Glasgow, between February 2016 and July 2018. Since its inception in 1992 it has had the remit as the only centre in Scotland investigating, diagnosing, and managing patients with pulmonary hypertension. All patients investigated at the unit have had their diagnosis agreed by a multidisciplinary team of national experts in pulmonary hypertension, and so the information contained is as accurate as possible. The patients were identified from the electronic database that includes all patients investigated by the unit and invited to participate.

2.1.2 Methods

Ethical approval for the study was granted by the West of Scotland Research Ethics Committee 4 (15/WS/0197), NCT02961023. The active intervention was a training programme developed in Heidelberg specifically designed for patients with pulmonary hypertension, which includes aerobic and resistance training and respiratory muscle training (138). The programme is of high frequency (several daily sessions) but of low intensity (moderate workload targets) and was delivered in two phases. In the first phase, patients underwent three weeks of supervised residential exercise training in small groups or individually. Patients then returned home, where they underwent a further 12 weeks of remotely supervised exercise. Exercise programmes were individualised to the patient, principally by using targets of heart rate achieved and perceived Borg score for breathlessness (111) with exercise intensity increasing if the subject improved.

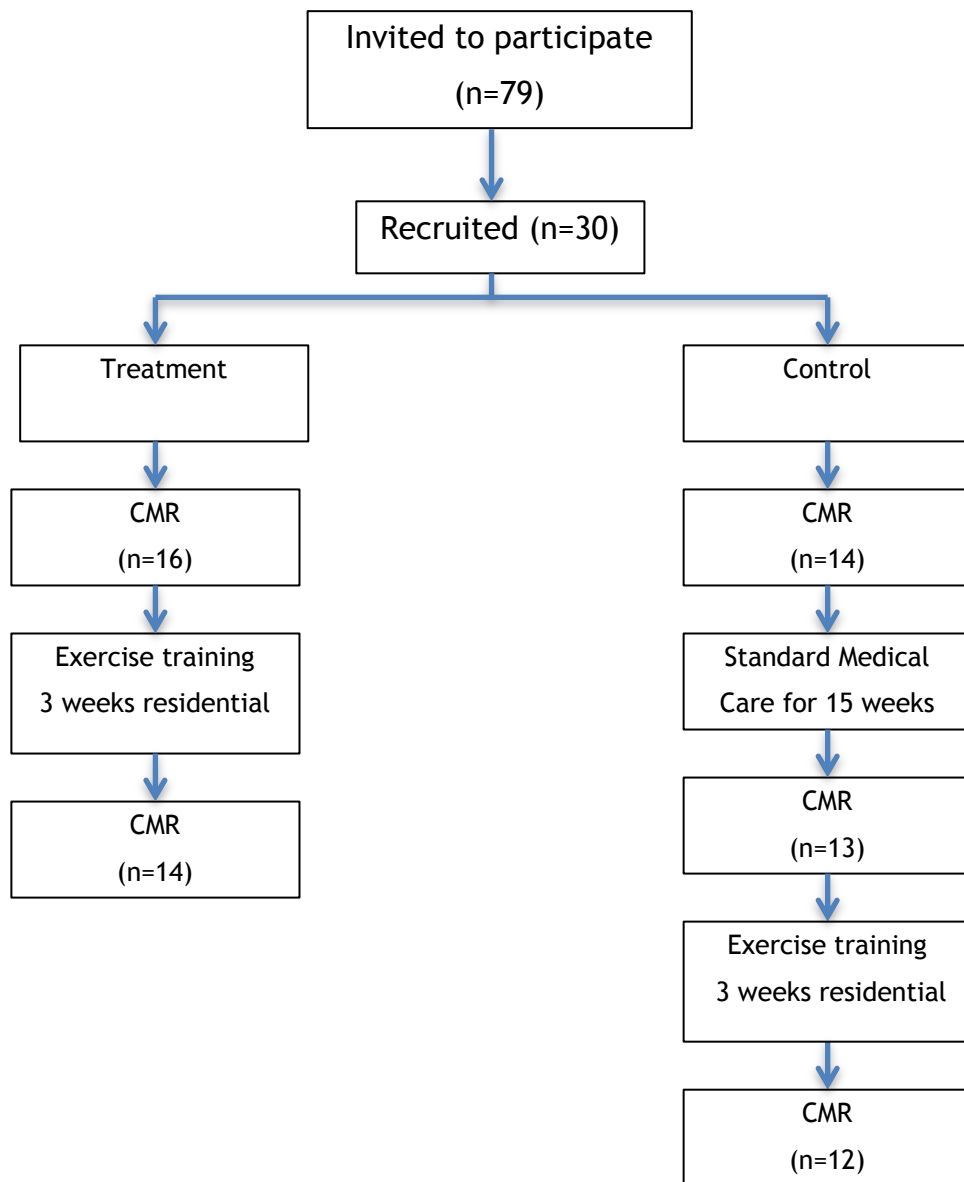


Figure 5. Summary of patient recruitment

As seen in Figure 5, the cohort of patients was divided into two arms, treatment, and control. In the treatment group, patients were entered immediately into the exercise programme, and were assessed before and after the training programme. In the control group, patients received standard medical therapy only for fifteen weeks, before being entered into the exercise programme. These patients were assessed at three time points namely on enrolment, immediately prior to and after exercise training.

The study population included patients who were over the age of 18 classed as World Health Organisation functional class (WHO-FC) II-III and stable on optimal disease targeted therapy for ≥ 3 months. Pregnant patients, those who had features of decompensated pulmonary hypertension, such as exercise induced syncope and those with significant peripheral vascular disease, neurological or musculoskeletal comorbidity were all excluded.

The primary outcomes of the study were multiple: change in 6MWD, change in quality of life measured by the Emphasis 10 questionnaire(139), and change in resting RV ejection fraction measured by CMR at 15 weeks. Detailed CMR analysis was a secondary outcome measure.

For the secondary outcome measures, CMR results were compared pre and post exercise using the paired T-test. Stroke volume and Cardiac outputs presented have been calculated by flow methods. To explore further the variable effect of exercise training amongst patients, the group were split into those who responded to exercise training and those who did not. Response was defined as a $>30\text{m}$ improvement in walk distance(140). We then compared the cardiac function between responders and non-responders using the unpaired T-test.

2.1.3 Routine Diagnostic Assessment

Patients are referred to the Scottish Pulmonary Vascular Unit from around Scotland. Due to the geographical difficulties and the requirement to have contemporaneous investigations to identify the presence of, and cause of, pulmonary hypertension, patients come for a mid-week stay at the Golden Jubilee Hospital in Glasgow and undergo invasive and non-invasive investigations, which can be seen in Figure 6.

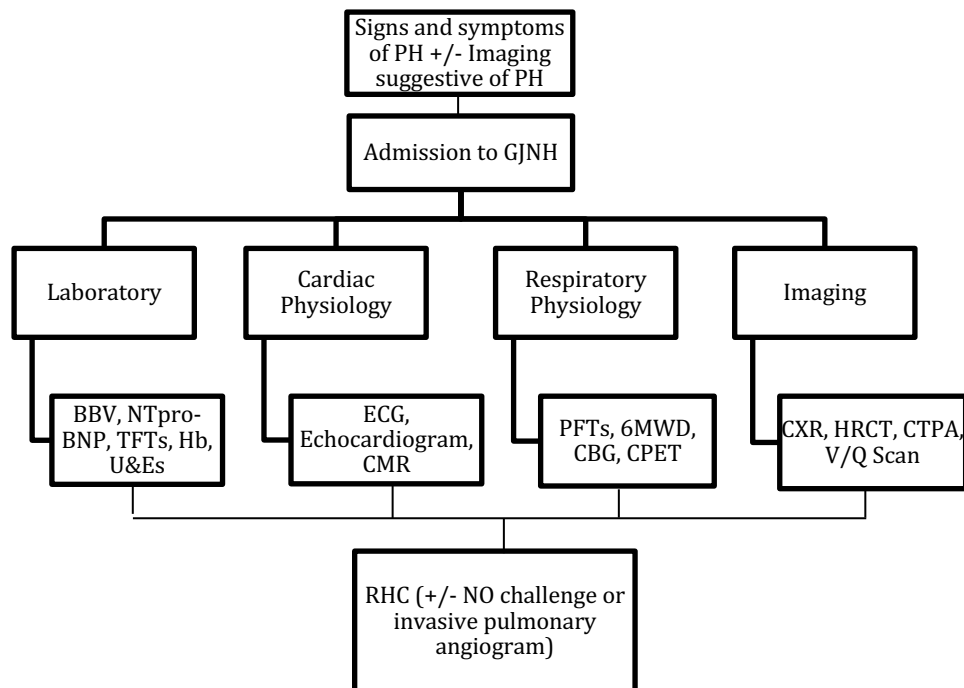


Figure 6. Diagnostic admission pathway

PH - Pulmonary Hypertension; GJNH - Golden Jubilee National Hospital; BBV - Blood born virus screen (Hepatitis B&C, HIV) NTpro-BNP - N-Terminal Proatriuretic Peptide; TFTs- Thyroid Function Tests; Hb - Haemoglobin; U&Es - Urea and Electrolytes; ECG - Electrocardiogram; CMR - Cardiac Magnetic Resonance Imaging;; PFTs - Pulmonary Function Tests; 6MWD - 6-Minute Walk Distance; CBG - Capillary Blood Gas; CPET - Cardiopulmonary Exercise Testing; CXR - Chest X-ray; HRCT - High Resolution Computer Tomography; CTPA - Computer Tomography Pulmonary Angiogram; V/Q - ventilation/perfusion scan; RHC - Right Heart Catheter; NO - Nitric Oxide.

2.1.4 Non-Invasive Assessment

As part of the routine non-invasive work-up, patients undergo several investigations, some of which are included in my study. Firstly, routine blood tests, to assess for haemoglobin, renal and liver function, and biomarkers to assess for the presence of atrial dilatation, which can be a sign of ventricular dysfunction, in the form of N-Terminal pro-natriuretic peptide (NT-proBNP). In addition, autoimmune screen and blood born virus screens are performed to assess for potential causes of group one disease, in the form of connective tissue

disease associated pulmonary hypertension, HIV associated disease or portopulmonary hypertension. Secondly, they undergo cardiac investigations in the form of an echocardiogram and an electrocardiogram.

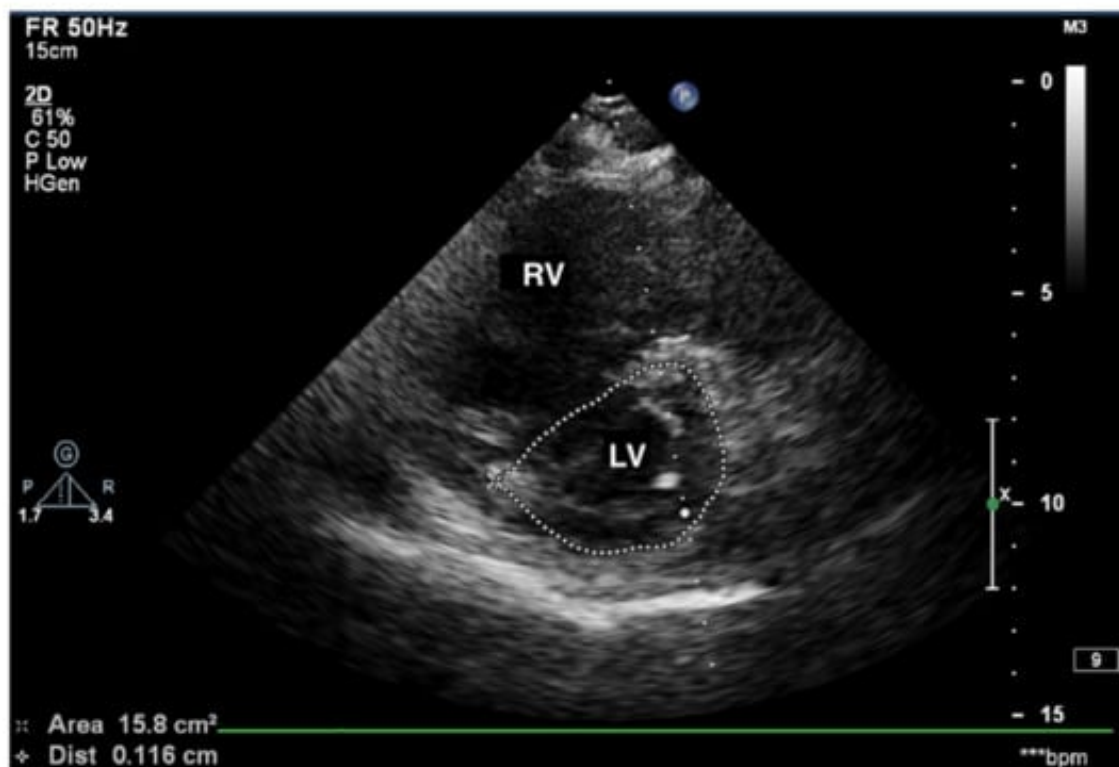


Figure 7. Short axis view of echocardiogram demonstrating dilated Right ventricle seen in pulmonary hypertension

Thirdly, they undergo pulmonary physiology testing, in the form of pulmonary function tests with lung volumes, gas transfer and reversibility testing to bronchodilators, capillary blood gas analysis and 6-minute walk test. Where patients have a good functional capacity, typically with a walk distance above 150metres, they go on to have a cardiopulmonary exercise test. If it is below this, the results from a cardiopulmonary exercise test will be less robust and difficult to interpret. The final non-invasive investigations are radiological imaging, in the form of CT pulmonary angiogram, high resolution CT thorax during inspiration and expiration and a cardiac magnetic resonance imaging scan and nuclear ventilation/perfusion scanning (V/Q), Figure 8.

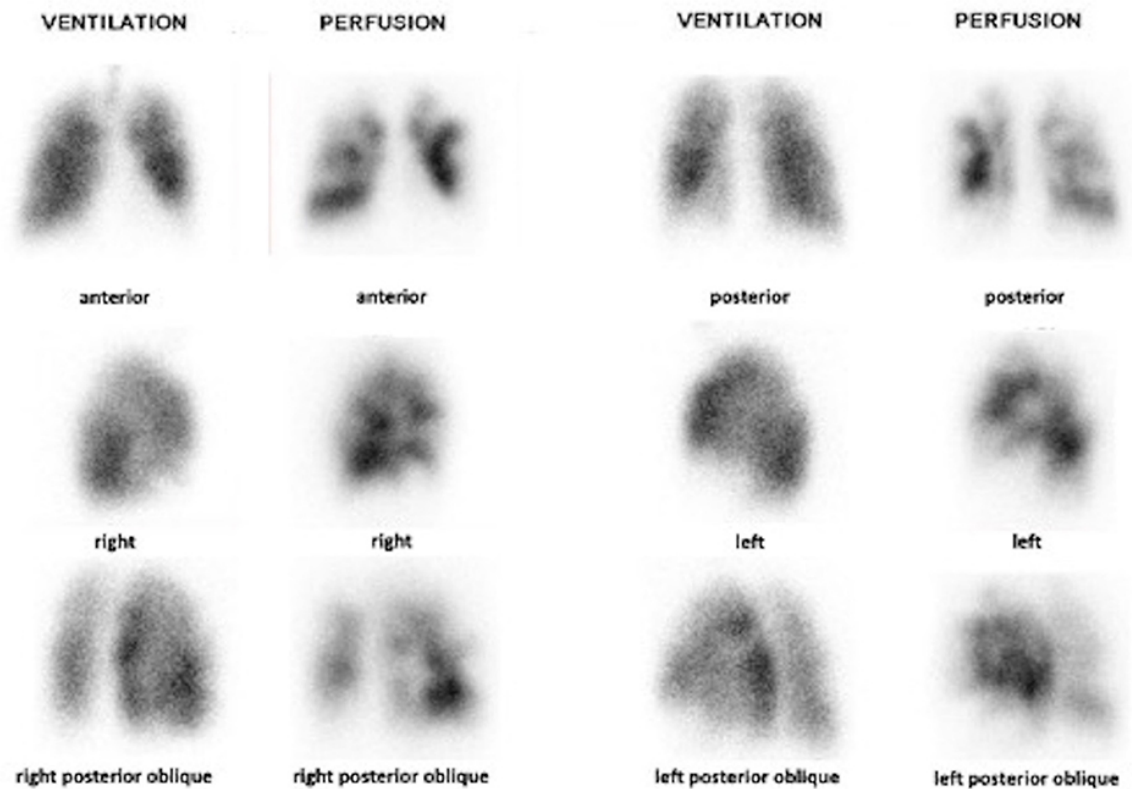


Figure 8. Ventilation perfusion scan

2.1.5 Right Heart Catheterisation

All patients diagnosed with pulmonary hypertension in this study underwent right heart catheterisation at the catheter laboratories in the Golden Jubilee Hospital, which took place after all non-invasive investigations had taken place. Any pulmonary vasodilatory therapy that might have been started prior to this was stopped several days prior to give baseline assessment. The patients were in the supine position, at rest. Local anaesthetic was used to maximise patient comfort and no pre-medication was used. Under sterile conditions, an 8F introducer sheath was inserted into the right internal jugular vein using direct ultrasound guidance. Right heart catheterisation was performed using a 7F triple-channel thermodilution Swan Ganz Catheter. Measurements taken included right atrial pressure (RAP), Right ventricular systolic pressure (RVSP) and end diastolic pressure (RVEDP), systolic, diastolic, and mean pulmonary artery pressures. Pulmonary artery wedge pressure was taken once the catheter is the wedge position, such that there is no flow from behind the catheter and the tip of the catheter measuring only pressure beyond it. As such, it is a surrogate for left atrial pressure. Cardiac output was measured using the

thermodilution method. Using the equation $((\text{mean pulmonary artery pressure} - \text{pulmonary artery wedge pressure}) / \text{cardiac output})$, the pulmonary vascular resistance could then be determined. Cardiac index was calculated using the cardiac output/body surface area. A sample of mixed venous blood was taken from the catheter in the main pulmonary artery to measure mixed venous saturations.

In those considered to have idiopathic pulmonary hypertension, they were given a trial of nitric oxide inhalation for five minutes at 40ppm with high flow oxygen. In those whose mean pulmonary artery pressure dropped below 40mmHg and by 10mmHg, they were deemed to be responders and would qualify for treatment with calcium channel blockers. In those with a V/Q scan or CTPA suggestive of pulmonary vascular occlusion, an invasive pulmonary angiogram was performed in the catheter laboratory.

2.1.6 Echocardiography

2.1.6.1 Patient positioning

The echocardiograms were performed in an area designed specifically for optimal image acquisition, with appropriate space and lighting, and ensuring patient safety and privacy. The patients were positioned in the left lateral decubitus position with their left arm raised or left hand under their heads. The couch on which the patients were positioned has a drop-down segment which better allows access to the left ventricular apex.

2.1.6.2 Standard imaging

The British Society of Echocardiography has produced guidance on the images that should be included in a standard echocardiogram examination(141). The cohort of patients in this study had dedicated right heart study echocardiogram, which involved assessment in three windows using the M-mode examination: parasternal, apical, and subcostal views.

The parasternal view allows visualisation of the changes seen in the right ventricle in pulmonary hypertension, dilatation, and hypertrophy of the myocardium. In addition, the parasternal view allows measurement of the RV function using both long and short axis views. Using the long axis, 2D and Doppler, tricuspid regurgitation velocity can be measured, which is often increased in pulmonary hypertension. The short axis views facilitate assessment of the tricuspid and pulmonary valves and can be used to identify septal abnormalities. Applying colour doppler to these areas facilitated assessment for the identification of intracardiac shunting across the septum. Septal movement in pulmonary hypertension is often abnormal, which is best seen in the short axis views.

The apical four-chamber view is used to identify the presence of RV dilatation, hypertrophy, defined by a thickness of $>5\text{mm}$ (142), and global systolic dysfunction with reduced myocardial tissue velocities being identified using tissue doppler. As the pulmonary artery pressure increases, there is less forceful opening of the tricuspid valves. Care was taken to ensure it was not a structural abnormality in the tricuspid valve itself, but rather dysfunction secondary to raised pulmonary pressures.

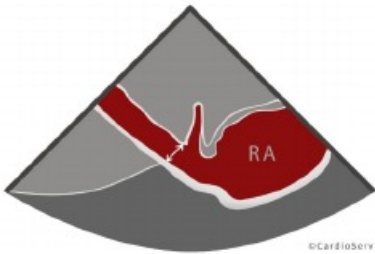
The subcostal views were used to estimate the degree of RV hypertrophy and RV dysfunction. It has many advantages in that there is no bone or lung obstructing the view of the heart. This provides the best view for RV inferior wall thickness measurement and can help detect any atrial septal abnormalities. In this view, the diameter of the inferior vena cava is measured at rest and during sharp inspiration, or sniff testing to estimate right atrial pressure. The diameter of the inferior vena cava should vary with respiration, and collapsible during the sniff test, as reduced intrathoracic pressure will encourage venous return to the right atrium. In the fluid overloaded state, or where there is right ventricular dysfunction, leading to high right atrial pressure, there is little or no variability in the diameter of the vena cava and it does not collapse during sniffing demonstrates the thresholds use to estimate pressure.

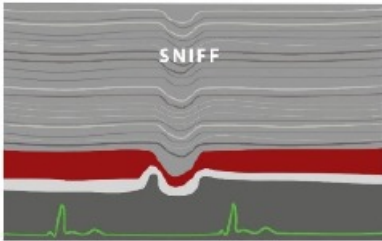
HOW TO CALCULATE RIGHT ATRIAL PRESSURE (RAP)

in echocardiography

MEASURE IVC

- Open IVC to its fullest
- Perpendicular to vessel
- 1-2 cm away from RA
- Inner-to-inner
- Abnormal >2.1 cm





IVC COLLAPSIBILITY

- Patient must sniff
- M-Mode preferred
- Do not measure at RA junction
- Normal > 50%
- Abnormal < 50%

RAP	mmHg	IVC SIZE	COLLAPSE
Normal	3	Normal	Normal
Intermediate	8	Normal	Abnormal
Intermediate	8	Abnormal	Normal
High	15	Abnormal	Abnormal

Figure 9. Assessment of right atrial pressure using the size of the inferior vena cava(143).

Pressure measurements taken during echocardiogram can be used to estimate pulmonary artery pressure. Tricuspid regurgitation velocity reflects the difference in pressure between the RV and the RA and is measured using continuous doppler flow in the apical four-chamber view, or from the parasternal RV inflow view. In the absence of pulmonary valve stenosis, the RV systolic pressure is assumed to be approximately that of the pulmonary artery systolic pressure. This can be calculated using the Bernoulli equation(144).

2.1.7 Common problems

Starting with the patient in the optimal left lateral decubitus position helps to reduce the chance of encountering problems in image acquisition. However, patients who are breathless and unwell may not be able to move into the ideal

position and problems may arise. Bone, air, and limited space are all factors that reduce the access to good cardiac windows with the transducer. Having the patient on their left side reduces the volume of air in the lung between transducer and the heart. The specific areas of interest in the heart may not fall between ribs, despite manipulating the patients' position. The patients' body mass index will also play a part in potentially limiting the good cardiac windows if it is higher than normal.

There is some subjectivity in the assessment of chamber volumes with echocardiograms. Difference in transducer rotation and position can lead to erroneous measurements, meaning that there can be significant interobserver variability, especially where the views of the cardiac chambers is suboptimal.

2.1.8 Cardiovascular Magnetic Resonance Imaging

2.1.8.1 Patient positioning

CMR imaging was performed in the supine position on a 1.5-T magnetic resonance imaging scanner (Sonata Magnetom, Siemens, Erlangen, Germany) using an 8-channel cardiac coil. The table remotely moved out-with the scanner to allow easier access. 3-lead ECG was then attached to the patient using adhesive electrodes. A phased array coil was then placed on the patients' chest and held in place with a loose strap. Ear-defenders were then provided to the patient for comfort, and they were provided with an emergency buzzer should they need it. The centre of the chest coil represented the cardiac position. A laser pointer, attached to the 12 o'clock position of the inner circumference of the magnet, was used to highlight the centre of the coil, and therefore the cardiac position, to facilitate movement of the patient such that the heart was in the centre of the magnetic field. Once the door of the scanning room was closed and sealed, the radiographers checked the functioning of the microphones and headphones prior to image acquisition.

Prior to undergoing the CMR, patients completed the safety questionnaire. If there was a history of injury involving any metal fragments, x-rays were taken to ensure no fragments remained. The movement of the table and safety checks took place prior to the patient entering the room.

2.1.8.2 Image Acquisition

Steady state imaging sequences were used to generate the initial axial scout, which are used to locate the heart within the thorax and generate the cine images. The scout images were also used to then acquire the vertical and horizontal long axis cines. The horizontal long axis images were used to then identify the intersection of the aortic and pulmonary roots, to start the short axis series of images. The series of short axis images then propagates towards the apex with 8-mm slices, with a 2-mm gap between slices. This short axis acquires images of both the structure of left and right ventricles and facilitate the calculation of the ventricular volumes. The standard imaging parameters for the subject in this thesis were TR/TE/flip angle/voxel size/FoV = 3.14ms/1.6ms/60° /2.2 x 1.3 x 8.0 mm/340mm. No gadolinium was used in standard acquisition but was given if a pulmonary angiogram was done after the cardiac images were acquired.

2.1.9 Data Storage

All imaging data is stored on the National Picture Archiving Communications System. This is a National Health Service Secure, encrypted platform that archives all radiological investigations taken for patients in Scotland. All analysis is stored on NHS encrypted IT servers based at the Golden Jubilee National Hospital in Glasgow.

2.1.10 Common Problems Encountered During Image Acquisition

A common challenge with acquiring good quality imaging in CMR is overcoming motion artefact from patients' respiration. Respiratory artefact can be overcome by asking the patient to breath hold. However, this can be difficult in a breathless patient, who is undergoing the investigation for that very reason. Several attempts were made to assess if the patients could breath-hold for the acquisition but if there was ongoing difficulty, then the images were taken during free breathing, accepting the image quality would be poorer.

Artifacts from cardiac contraction can only be overcome by using ECG gating, which acquires images during diastole when the heart is not moving. The ECG-gating in itself can yield problems in that the electromagnetic field can have an effect on the iron-containing haemoglobin cells leading to a change in the

amplitude of the T-wave on the ECG. This change is proportionate to the strength of the magnetic field, meaning that when a radiofrequency pulse is applied to the patient, the scan can be triggered on the R-wave, rather than the T-wave, meaning that images are poorly synced with the cardiac cycle. This can be overcome by adjusting the ECG leads attached to the patients and images acquire with the usual protocol.

2.1.11 Analysis of Cardiovascular imaging

CMR images were analysed using a satellite computer, attached to the MRI scanner, using Circle Cardiovascular Imaging (CVi) analysis software (Calgary, Alberta, Canada). Images were downloaded into the workstation from the National Picture Archiving Communications System (PACs) archive. At the time of analysis, I was blinded to the groups or haemodynamic results of the patient. To obtain the images from the archive, I was not blinded to the name of the patient. The analysis of the images was performed at least a year after their diagnostic right heart catheterisation, and, as such, I was blinded as to what the patients' underlying diagnoses were when analysing the images.

The short axis cine was identified from the images downloaded. CVi automatically identified the images at end-systole and end-diastole. These were manually checked, including the images with smallest left ventricular volumes as end-systole and the largest as end-diastole, Figure 10. The end diastolic image was usually the first image after the R-wave on the ECG. CVi automatically maps the epicardial and endocardial boundaries of the left ventricle. The borders were also automatically determined and manually checked and adjusted as necessary by manual planimetry. The endocardial borders of the RV were also automatically detected and manually adjusted, but the epicardial borders were manually mapped using a trackball cursor to define the borders with manual planimetry. These methods have previously been described as accepted methods of analysis(145). Of note, as part of the analysis, all trabeculations and papillary muscles were deliberately included. CVi was able to calculate the left and right ventricular volumes at end-systole (LVESV and RVESV, respectively) and end-diastole (LVEDV and RVEDV, respectively) using Simpson's calculation; by multiplying the individual slice areas by the thickness of the slice (8mm), adding the inter-slice thickness (2mm).

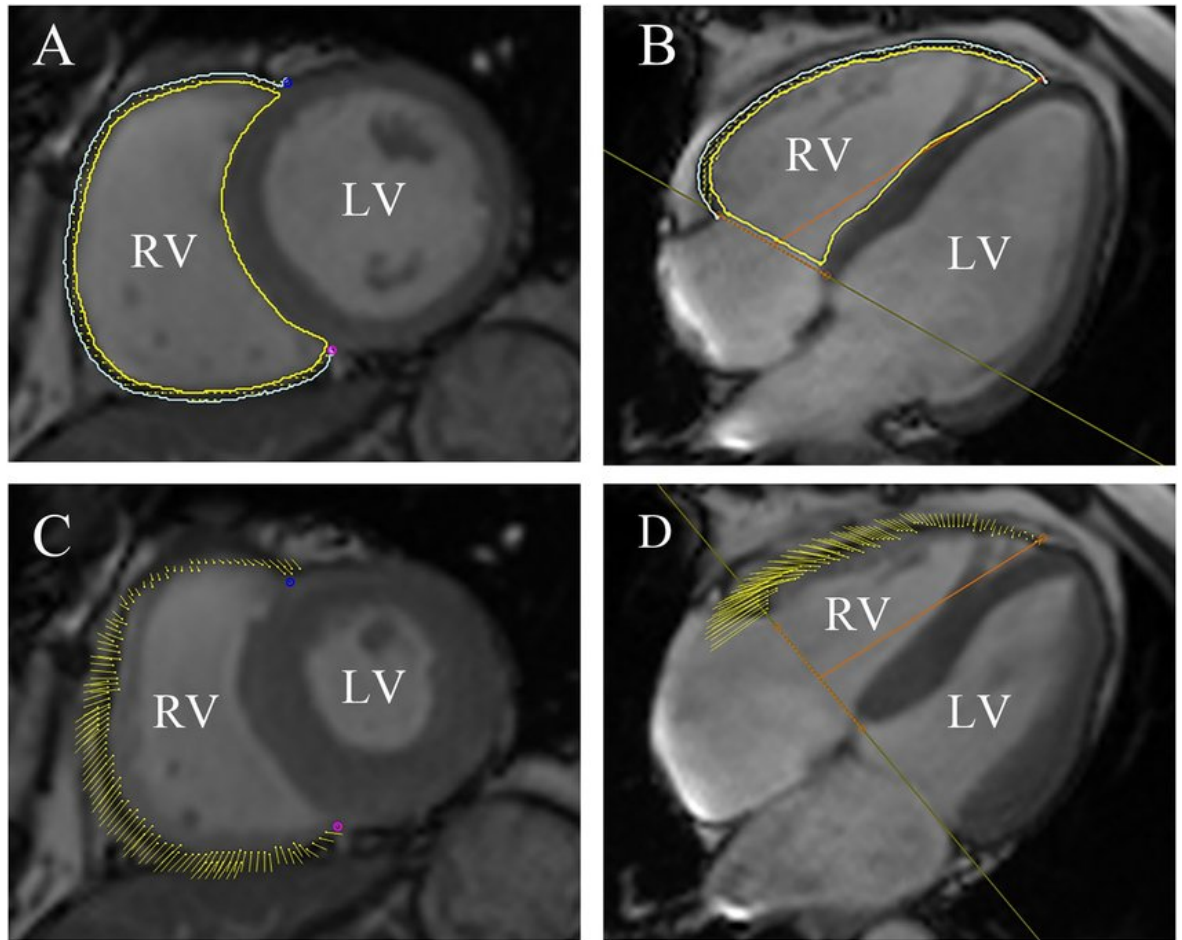


Figure 10. Short axis view of cardiac ventricles demonstrating epi and endocardial bordering

Stroke volume (SV) can then be calculated by subtracting the end-systolic volume from the end-diastolic volume, EDV-ESV. However, in the studies, I used velocity encoded flow mapping forward stroke volumes across the aortic valve, which has shown to be a more accurate method of determining the precise volume(146) as it prevents the measurement error caused by tricuspid regurgitation when using ventricular volume determined stroke volume. Right and Left Ventricular Volume and Ejection Fraction can then be calculated using $(SV/EDV) \times 100$.

Ventricular mass was then determined by the difference between the endocardial and epicardial boundaries mapped in short axis images at end-diastole and end-systole. The LV mass included the LV free wall and the interventricular septum, whereas the RV mass included only the RV free wall. Where the index has been used in the thesis, the values have been adjusted to

the body surface area of the patient.

2.1.11.1 Determining left and right stroke volume and ejection fraction

Stroke volumes stated for both right and left ventricles were all measured using velocity encoded flow maps to reduce the error induced by tricuspid regurgitation when using short axis images. As part of the velocity encoded image series, there are anatomical and velocity encoded images acquired of the aorta and the pulmonary artery, representing left and right ventricular outputs respectively. Anatomical images were used to ensure that the target vessel has been identified and that there is minimal artefact.

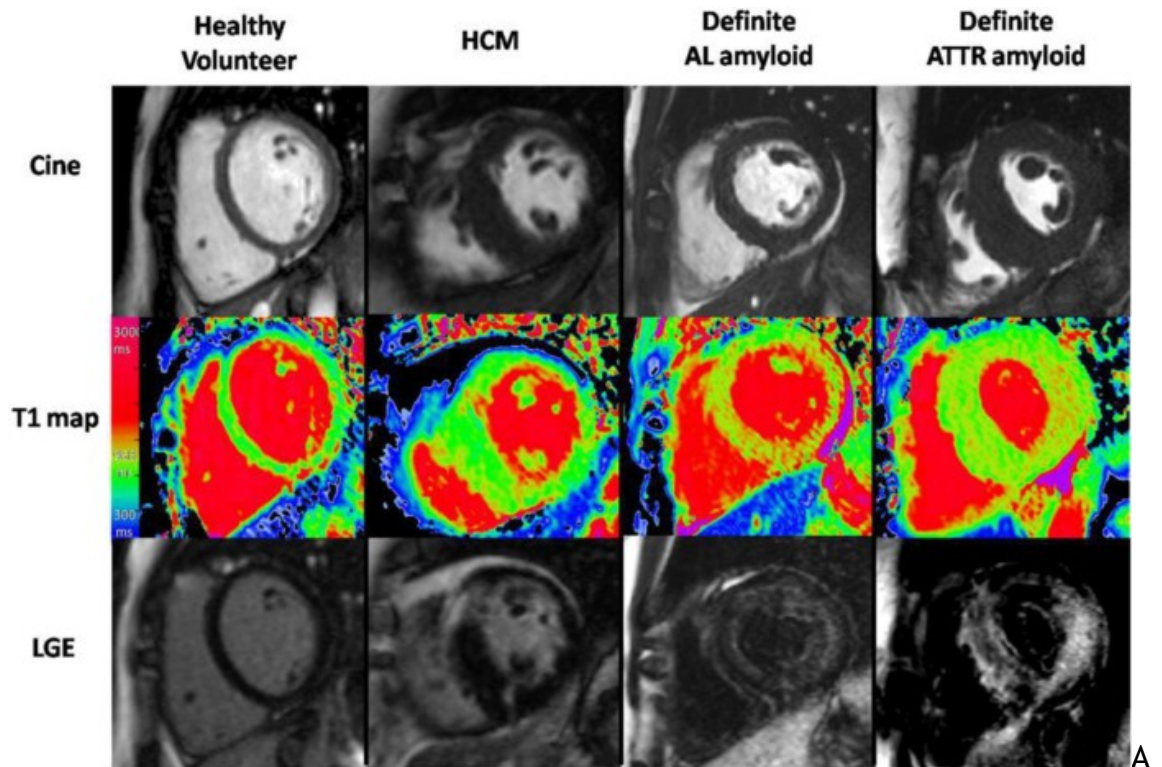
Velocity images were used to then calculate the volume of blood flow. This was performed by drawing a region of interest around the first anatomical image, using a tracker ball cursor with manual planimetry, ensuring to only include the lumen of the vessel. This region of interest was then automatically propagated across the images of the cardiac cycle. The regions of interest were then checked manually and adjusted to include only the vessel lumen. These were then automatically applied to the velocity encoded images.

CVi automatically calculates the forward flow across the region of interest in each point of time. The forward flow from each image were then combined to make the left and right ventricular stroke volumes from the aorta and the pulmonary artery, respectively. Cardiac output was calculated by multiplying the stroke volume with the heart rate at the time of the study. The right and left ventricular ejection fractions, stated as a percentage, were calculated by $((\text{velocity encoded image stroke volume}/\text{end-diastolic volume}) \times 100)$.

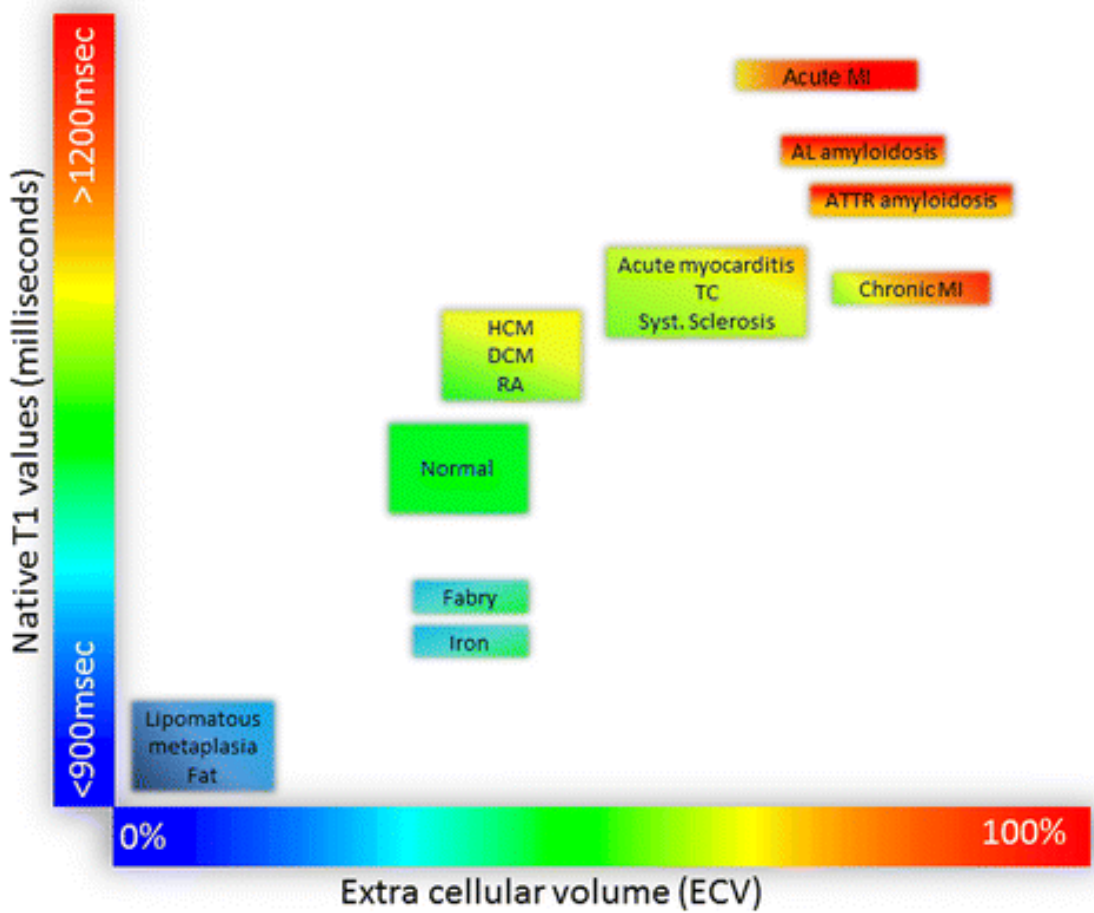
2.1.12 T1 Mapping

Changes in cardiac fibrosis have been seen in patients with left heart disease after exercise rehabilitation(147). T1 maps were used as a marker of response of fibrosis to exercise training. Normal myocardial T1 values were taken as between 900 and 1100milliseconds. Global T1 values were taken

for the whole left ventricle. The ventricle was then divided into six segments, with 3 areas (anterior, middle, and posterior) highlighted in the interventricular septum and 3 areas in the left ventricular free wall. A mean of these three values were taken for the septum and the free wall. These values were compared before and after exercise as a representation of changes in cardiac fibrosis in response to exercise.



T1 Mapping and ECV in clinical practice



B

Figure 11. T1 Mapping of short axis in healthy volunteer (A)(148) and the T1 Mapping reference scale (B)(149)

2.1.13 Tissue Tracking

Furthermore, 3-Dimensional tissue tracking was used to evaluate the myocardial motion and deformation and provide a non-invasive assess the mechanics of the left ventricle. Using this method, global longitudinal, circumferential and radial strain pre and post exercise training, can be assessed, the former of which have been shown to be robust and reproducible measurements in clinical practice(150). This technique can detect early changes in ejection fraction. Strain is a measure of the compressibility of the myocardium. The strain is expressed as a fractional change in the size of the ventricle. Where there is a shortening, the figure is expressed in a negative value and a lengthening expressed as a positive value(151). Longitudinal strain reflects a change in length, so in systole there is shortening, representing a negative change. Circumferential strain reflects a change in length along the circumferential axis of the LV when viewing the heart in the short axis. There is a shortening in systole, representing a negative figure. Radial strain represents a change in thickness of the myocardium, which increases in systole, leading to a positive value(151, 152).

Ten cases were reviewed by a second observer (>10 years' experience), who was blinded to the diagnosis and RHC values, and Pearson's correlation is used to assess for agreement between continuous variables.

2.1.14 Common Problems Encountered with Image analysis

Ensuring the precise capture of the ventricular borders is essential to minimize inaccuracies in ventricular volumes. Errors can arise when areas are included in the RV volume, which are not part of the RV. In particular, areas around the basal aspect of the RV can be challenging to identify what is part of the atrium and what is part of the ventricle. To minimize the risk of inducing these errors, the horizontal long axis views were used to ensure that only the RV areas were included in analysis.

Identifying end-systole and end-diastole can be challenging in pulmonary hypertension. The bowing of the interventricular septum towards the LV can make identification of the cardiac phases difficult for CVi because the RVEDV is

increased, but the volume of the LV is reduced. For all the CMRs in this study, where there was dubiety about the cardiac phases, the ventricular volumes were calculated for each phase and the once with the largest volume was included as end-diastole and the smallest as end-systole.

2.1.15 Statistical Analysis

Data are presented as mean +/- standard deviation. The null hypothesis was that there would be no change improvement in exercise capacity following training. To reject this, power calculation suggested a sample size of 10 patients in each group was required if the means of the distribution with equal SDs of 56m differed by at least 74m(153) with a type I error of 0.05 and 80% power. In order to account for potential dropouts, 30 patients were enrolled. Baseline characteristics were compared by Mann Whitney U testing. For comparison of categorical variables, chi-squared test was performed. Analysis of the primary outcome measures comparing exercise training and control arms was carried out using the Mann-Whitney U test.

2.2 The use of Cardiac Geometry in the Diagnosis of Thrombotic Pulmonary Vascular Disease

The methods described here refer to chapters 4 and 5, assessing cardiac geometry using CMR and echocardiogram in the detection of thrombotic pulmonary vascular disease. Echocardiography is the most commonly used screening tool in the detection of the presence of pulmonary vascular disease as it is readily available, non-invasive and has the added benefit of being able to estimate pulmonary artery pressure using the tricuspid regurgitant pressure gradient (TRPG). However, the use of CMR has been increasing in pulmonary arterial hypertension in recent years due to increased availability, improved acquisition times and ease of use(7). Although CMR has been shown to be effective at measuring chamber volumes, there is, as yet no reliable way of measuring pressure. However, there are several ways that a CMR may indicate the presence of increased RV and pulmonary artery pressure. At end-systole, there is shifting of the septum from the right to the left, signifying pressure overload in the RV compared to the LV. The eccentricity index (EI) quantifies the septal flattening, which has potential to indicate the pressure within the RV(154). This is defined as the ratio of the length of two perpendicular minor-axis diameters, one of which is bisected and was perpendicular to the interventricular septum. The aim of this study is to assess, firstly, if there are differences between the eccentricity index between patients who have pulmonary hypertension at rest and those who do not, firstly using echocardiogram, and using CMR. Furthermore, to assess the use of other novel CMR indices in the detection of pulmonary hypertension using CMR, namely pulmonary artery distensibility and peak pulmonary artery blood flow.

Correlations between these findings from echocardiograph and CMR with right heart catheter indices, exercise capacity using cardiopulmonary exercise testing and six-minute walk distance (6MWD) and the biomarker, N-Terminal pro natriuretic peptide (NT pro BNP) was performed.

I hypothesised that systolic and diastolic eccentricity index predicts the presence of pulmonary hypertension in patients with CTEPH and that these indices are normal in those without resting pulmonary hypertension, even in the

presence of thrombotic pulmonary vascular disease. Furthermore, I hypothesised that the distensibility of the main pulmonary arteries is reduced in CTEPH and CTEPD and that peak blood flow within the pulmonary artery are reduced in CTEPH and CTEPD.

Moreover, I postulated that there is a correlation between CPET findings (low peak $\dot{V}O_2$, high V_E/V_{CO_2}) and EI in thrombotic pulmonary vascular disease.

2.2.1 Patient Recruitment

Patients were identified from the electronic database in the Scottish Pulmonary Vascular Unit, based at the Golden Jubilee National Hospital, Glasgow. A cross-section of 30 patients diagnosed with CTEPH since 2014 were identified (20 with proximal disease and 10 with distal disease), as only patients from this time onwards had CMR available for analysis. Central CTEPH was defined as those who had obstruction in the major vessels, whereas peripheral defined as those who had obstruction in the segmental or subsegmental vessels. Comparison with 20 patients who had no resting pulmonary hypertension was made, 10 of whom have chronic thromboembolic disease. These were a group of patients who have been investigated in the SPVU and found at right heart catheter to have no evidence of pulmonary hypertension. As described earlier in this chapter, the investigations were obtained contemporaneously.

2.2.2 Echocardiogram

A British Society of Echocardiography accredited cardiac physiologist, who was not involved in data analysis, performed the echocardiogram. The image acquisition was performed according to a standard protocol that would be expected for a comprehensive echocardiogram and the standard images were acquired as previously described(155). In addition to these, the left ventricular eccentricity index was measured using the 2D parasternal short axis images between the mid-papillary muscle and the tip of the mitral valve leaflets level at end-systole and end-diastole(141). End-systole is taken as the image with the smallest ventricular cavity size and end-diastole was measured at the peak of the R-wave. The ratio of the minor axis dimensions was measured, $D2/D1$, where $D1$ is ventricular diameter perpendicular to the septum and $D2$ is ventricular diameter parallel to the septum. Left ventricular eccentricity index >1.1 is considered abnormal.

2.2.3 Cardiopulmonary Exercise Testing

Cardiopulmonary exercise testing was performed using an incremental cycle ergometer, which is the safest form of ergometer. It is usable by a greater range of patients that might be limited in their use of a treadmill due to, for example, deconditioning, obesity, and musculoskeletal issues. It also allows more convenient monitoring, such as ECG, blood pressure and blood sampling. Due to the risk of exercise induced complications, they were all supervised by a physiologist and medical staff. The patients were given preparatory advice before the CPET, had taken all regular medications, were free of intercurrent illness and were dressed appropriately. The ramp rate was chosen by the physiologist, based on the participants' self-reported fitness. This allows a short assessment time with low initial work rate, and a brief period of high-intensity workload. The aim was to have the patient exercise for 8-12mins in total. The CPET procedure is divided into four parts:

1. Resting phase (2-3mins): adaptation of patient to the face mask and measurement of resting ventilation, heart rate and opportunity for blood measurements

2. Unloaded phase (2-3mins): Cycling with no resistance applied to the ergometer, aiming to stay at 55-65 rotations per minute. VO_2 often doubles during this period.
3. Incremental exercise phase (8-/- 2mins), aiming 55-65 rotations per minute.
4. Recovery phase (3-5mins): unloaded cycling

Standard examination procedures listed in the European Respiratory Society statement in CPET were performed(156). I used the indices of low peak VO_2 and high VE/VCO_2 to assess the level of functional limitation.

2.2.4 Cardiac Magnetic Resonance Imaging

As described above, CMR imaging was performed in the supine position on a 1.5-T magnetic resonance imaging scanner (Sonata Magnetom, Siemens, Erlangen, Germany) using an 8-channel cardiac coil. Short axis cine images were acquired using electrographic gating multislice balance steady state free precession sequence (20 frames per cardiac cycle, 8mm slice thickness, matrix 256x256; BW, 125kHz/pixel; TR/TE, 3.7/). Main pulmonary artery flow curve is captured using velocity-encoded CMR (VE-CMR), perpendicular to the pulmonary artery and performed during breath hold.

2.2.4.1 CMR Analysis

RV and LV volumes was determined by automatic tracing endocardial borders of short axis stack obtained during breath-hold using. Images were analysed using the Circle Vascular Imaging (version 5.11 Calgary, Canada) with the observer blinded to the patients' clinical information. All borders were manually checked and corrected as needed.

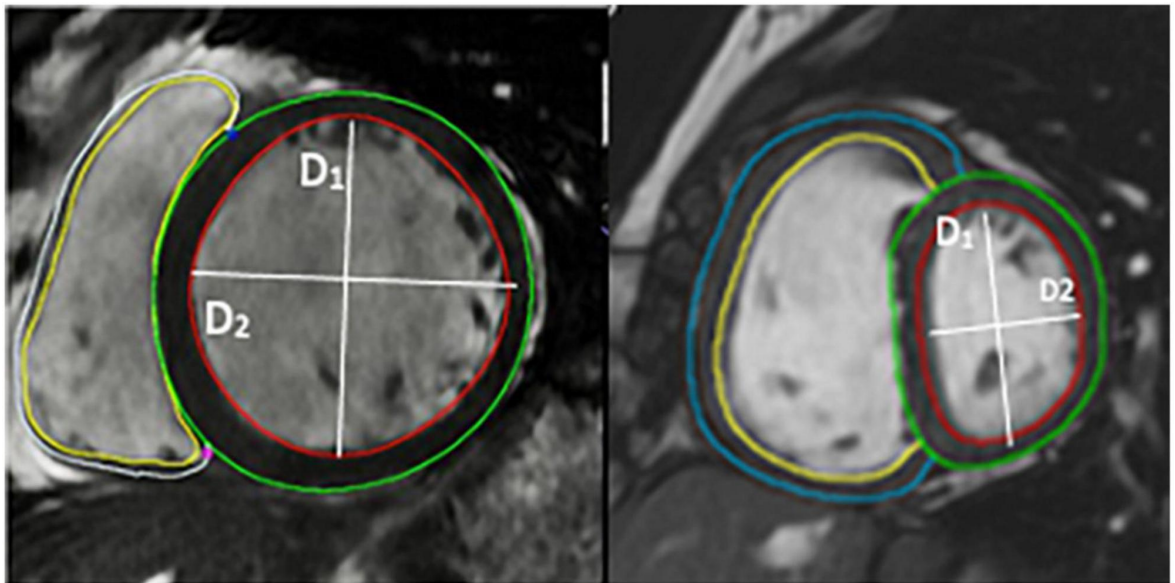


Figure 12. Short axis view of cardiac ventricles with epi- and endocardial borders with the analysis of the LV eccentricity index

I measured the eccentricity index at end systole and end diastole in the left and right ventricles a mid-ventricular level - defined as the level of the papillary muscles, Figure 12. The eccentricity index was defined as the ratio of the length of the two-perpendicular minor-axis diameters, one of which is bisected and was perpendicular to the interventricular septum. As the LV is circular, this was expected to be 1.0(154).

Main pulmonary artery distensibility was determined from lumen area measurements at the moment of maximal flow and the moment of isovolumetric contraction to calculate $(PA \text{ maximum area} - PA \text{ minimum area}) / PA \text{ minimum area}$. Flow curves were developed using the VE-CMR images obtained perpendicular to the pulmonary artery during breath hold.

Ten cases were reviewed by a second observer (>10 years' experience), who was blinded to the diagnosis and RHC values, and Pearson's correlation is used to assess for agreement between continuous variables.

2.2.5 Right Heart Catheterisation

All patients underwent RHC within 4 days of CMR. Right heart catheterisation described earlier in the chapter all took place at the Golden Jubilee National Hospital with an 8F Swan-Ganz, introduced using the Seldinger technique through the internal jugular or femoral vein. Hemodynamic parameters including the right atrial pressure, right ventricular pressure and pulmonary artery pressure and pulmonary artery wedge pressure were all taken at rest. Cardiac output was measured using the thermodilution method and PVR calculated after the procedure.

2.2.6 Data management and Statistical Analysis

Data is stored on NHS password secure encrypted computers and was analysed using Microsoft Excel and Graph Pad Prism version 9 (San Diego, CA, USA)

Students t-test or Mann-Whitney U test were used, depending on the distribution of the data. ANOVA was used to assess for differences between subgroups. Correlation analysis was performed by Spearman analysis. Receiver Operator Curves were used to identify clinically relevant thresholds that can be used to identify the presence of chronic thromboembolic pulmonary vascular disease. Bland Altman plots were used to describe the agreements between investigations.

2.2.7 Problems Encountered in assessing the Cardiac Geometry

These investigations were performed for clinical care, rather than according to trial criteria. However, similar limitations apply to the precise capture of the ventricular borders, which is essential to minimize inaccuracies in ventricular volumes and to minimize the risk of inducing these errors, the horizontal long axis views were used to ensure that only the RV areas were included in analysis.

Identifying end-systole and end-diastole can be challenging in pulmonary hypertension both using echocardiogram and CMR. The bowing of the interventricular septum towards the LV can make identification of the cardiac phases difficult for CVI because the RVEDV is increased, but the volume of the LV is reduced. Where there was doubt about the cardiac phases, the ventricular volumes were calculated for each phase and the one with the largest volume was included as end-diastole and the smallest as end-systole.

Echocardiography by its nature can lead to observer variability, depending on the operator. In addition, the specific areas of interest in the heart may not be well visualised between the ribs fall between ribs. The patients' body habitus will also play a part in potentially limiting the image quality.

There can also be some subjectivity in the assessment of chamber volumes with echocardiograms. Difference in transducer rotation and position can lead to erroneous measurements, meaning that there can be significant interobserver variability, especially where the views of the cardiac chambers is suboptimal. I have used both CMR and echocardiogram in this study to minimise interobserver variability and lend confidence to the reader that the findings are genuine.

2.3 Pulmonary Thromboembolism in Hospitalised Patients with COVID-19

In late 2019, The World Health Organisation was informed of a cluster of patients presenting with a rapidly progressive and fatal pneumonia in Wuhan City, Hubei Province, China. The causative agent was identified from viral genetic sequencing as a novel coronavirus, known as Severe Acute Respiratory Syndrome Coronavirus 2 (SARS-CoV-2). The syndrome caused by SARS-CoV-2, which consists mainly of upper respiratory coryzal symptoms and pneumonitis, was named COVID-19. In addition to the lung parenchymal changes observed in COVID-19, a coagulopathy was also seen. The coagulation abnormalities appeared to mimic other haematological conditions including disseminated intravascular coagulation (DIC) and thrombotic microangiopathy and are linked to higher mortality(135, 157). During this same time period, COVID-19 was noted increase the risk of thrombotic complications in the intensive care unit, with the incidence being as high as 30%(136).

The aims of this study were to establish the incidence of pulmonary thromboembolism in this national Cohort of hospitalized patients with Covid-19 and to determine if the risk of pulmonary thromboembolism remains in patients managed out with critical care. In addition, I planned to assess if right heart strain increased the risk of death or requiring critical care support and to detect if there is any signal towards comorbidities that increase the risk of critical care admission or death.

2.3.1 Patient Recruitment

All patients in Scotland between 23rd March 2020 and 31st May 2020 who underwent a computer tomography pulmonary angiogram (CTPA) were identified using the Scottish National Picture Archiving and Communications System (PACS), which archives all radiological imaging procedures performed in all public hospitals in Scotland. This captured all patients during the ‘first wave’ of the COVID-19 pandemic, where the wild-type virus was the predominant strain in the community. Patients who were diagnosed with pulmonary embolism were

identified and cross-referenced with the Scottish Care Information (Sci-Store) database, which allowed assessment of whether a Covid-19 PCR had been performed, its result and allowed access to biomarkers, including haematological and biochemical investigations.

2.3.2 Inclusion Criteria

Patients included in the study had to have a positive RT-PCR test results for SARS-CoV-2 up to 30 days (mean 9.5 days) before their CTPA or within fourteen days afterwards in order to detect those who presented with pulmonary embolus, but symptoms were brought on by the presence of pulmonary arterial occlusion. If no RT-PCR test had been performed or, if it was negative, patients were deemed to have COVID-19 clinical syndrome if they had classical lung parenchymal changes, as described by the British Society of Thoracic Radiology(158). Establishing a secure diagnosis where there was limited access to testing was challenging. Clinically, a pragmatic approach was taken when evaluating the clinical picture in conjunction with diagnostic investigations. However, to lend confidence to this cohort for the purposes of this study, patients who did not have a RT-PCR positive swab and with ‘probable’ or ‘indeterminate’ radiographic features of COVID-19 were excluded due to potential diagnostic uncertainty.

Demographic data, the level of patient care (level 1 [ward-level] care or critical care) and comorbidities were gathered from the SCI Store database. Biomarker data and risk factors for PTE were also collected.

Right heart strain was considered to be present in patients who had serum troponin greater than the local reference limit or had radiological evidence of right ventricular (RV) dilatation (right ventricular: left ventricular ratio [RV:LV] diameter >1), in agreement with the European Society of Cardiology guidelines(159).

2.3.3 Calculating the incidence of Disease

The Scottish Government published the data on the incidence of COVID-19 in hospitalised patients between 23rd March and 31st May 2020 online(160). These were the denominator for the calculation of the incidence of PTE in hospitalised patients with COVID-19 and used to calculate how many patients from the overall hospitalised COVID-19 population developed pulmonary thromboembolism.

Incidence of pulmonary thromboembolism percentage was calculated using the total number of hospitalized COVID-19 patients during the described time period divided by the number of patients with evidence of COVID-19 and a positive CTPA for pulmonary thromboembolism. I then assessed the comorbidities in the population managed in level 1 care areas and grouping together all those managed in critical care, levels 2 and 3 to identify if the risk of PTE was high both in ward-based environments and in critical care.

2.3.4 Control Group

202 patients diagnosed with pulmonary embolus between 11th July 2011 and 4th December 2018 were used as a control to examine for differences between biomarkers in those with and without COVID-19 disease. These patients were a heterogenous group of hospitalised patients with provoked and unprovoked pulmonary embolus followed up in the outpatient clinic when this facility was in its infancy, and therefore includes only a small proportion of those diagnosed with pulmonary thromboembolism during that time. However, it was felt to be a representative population of hospitalised patients with pulmonary embolism to allow a comparison. Patients in this group with troponin, above the local reference range, or with RV:LV ratio >1 were classified as having right heart strain. In addition, data were gathered from previously published studies on the incidence of pulmonary embolus in hospitalised patients(161) and those with pneumococcal pneumonia from a cohort in Taiwan(162).

2.3.5 Statistical analysis

Incidence of pulmonary thromboembolism percentage was calculated using the total number of hospitalized COVID-19 patients during the described time period divided by the number of patients with evidence of COVID-19 and a positive CTPA for pulmonary thromboembolism. Binary logistic regression was used to establish if the presence of comorbidity, increasing age or sex leads to an increased risk of a composite endpoint of critical care admission or death.

Survival was calculated using Cox Proportionate Hazard Regression in those patients with right heart strain, those in intensive care and in males. I then assessed the comorbidities in the population managed in level 1 care areas and grouping together all those managed in critical care, levels 2 and 3 to identify if the risk of PTE was high both in ward-based environments and in critical care. Chi Squared test was used to look for increased frequency of PTE in the critical care groups compared with the ward-based patients. Mann Whitney U test was used to look for any significant differences between non-parametric data in the biomarker groups. I used multivariate analysis to adjust for age and gender when comparing the presences of right heart strain in the control versus Covid-19 group. Statistical analysis was completed using IBM SPSS Statistics Version 27 and GraphPad Prism version 8. A p-value of <0.05 was taken to be statistically significant.

2.3.6 Problems with these methods

Due to the retrospective nature of the study, there were missing data points for both demographic data, including BMI, and biomarkers. As such, all analysis was performed only for those with available complete data. The investigations were performed as part of clinical care rather than under trial conditions. As such, there will naturally be some variation as to the timing of investigations and not all investigations I assessed were performed for all patients.

Whilst all CTPAs performed across Scotland during this time are included, some patients may have been too unwell to facilitate safe transfer for this to be performed and therefore would have been missed and under reported in the critical care units. In addition, some smaller, rural hospitals will not have had access to CTPA equal to that of urban-based

university hospitals. As such, there may have been some patients not included in my study who did have underlying Covid-19 PTE. Furthermore, I have not included those who had lower limb doppler performed and had venous thromboembolism diagnosed by this measure. Finally, I have acknowledged that those who had a COVID-19 test post CTPA may have contracted Covid-19 whilst in healthcare setting.

3 Assessing Cardiac Geometry with Echocardiography in the Diagnosis of Chronic Thromboembolic Pulmonary Vascular Disease

3.1 Introduction

3.1.1 Background

Chronic Thromboembolic pulmonary hypertension (CTEPH), classified as Group IV in the 2018 Nice classification of pulmonary hypertension(64) is defined by a mean pulmonary arterial pressure above 20mmHg and a pulmonary capillary wedge pressure of less than 15mmg, as measured by right heart catheterization, along with at least one persistent perfusion defect seen on imaging (V/Q scanning or pulmonary angiography) after 3 months of anticoagulation (3).

CTEPH involves both the larger central vessels, along with the smaller distal vessels. It is considered to be a rare and late complication in those who have one or more episodes of acute pulmonary thromboembolism - the exact incidence is unknown but it is estimated from registries of patients that it is between 2-4%(163). Around 75% of those with CTEPH have a reported incidence of acute pulmonary embolism(164).

The presence of acute thrombus triggers the inflammatory cascade within the vessel lumen. In most cases, this cascade will lead to complete lysis restoring vessel patency. However, in a small but significant number of cases, the lysis is incomplete. The acute thrombus, which comprises of red cells and platelets in a fibrin mesh, which is easily detached from the endothelial wall. In chronic disease, the thrombus material changes to a fibrous plaque, containing macrophages and lymphocytes and can occasionally contain areas of calcification(77, 78). This plaque has stronger adherence to the intraluminal surface leading to permanent pulmonary vascular occlusion. Organisation of this material into webs or bands obstructs blood flow, leading to increased pulmonary vascular resistance and increased pulmonary artery pressure(165).

The reasons why patients go on to develop CTEPH is not always clear, but there have been some predisposing factors identified. Large, central acute pulmonary emboli are less likely to fully resolve, potentially because the lytic system lacks the capacity to deal with the size of the clot or because these agents are unable to reach the centre of the thrombus and are thus unable to lyse the central regions. Those with underlying autoimmune disorders, thrombophilia and those who have had a splenectomy, because of increased platelet activation(166), are more likely to present with CTEPH. Those with non-O blood group have a higher incidence of CTEPH compared to those of blood group O (167). People requiring thyroid replacement therapy and those with a history of malignancy are also at higher risk(165). Those with malignancy have increased risk of thromboembolism because of the activation of inflammatory pathways and cytokine production(168). The link here is so strong that it is recommended that CTEPH should be excluded in all those patients with malignancy who develop pulmonary hypertension(167).

There have been some biological and genetic causes for CTEPH identified. Antiphospholipid antibodies and lupus anticoagulant have been found to be more frequent in patients with CTEPH than IPAH(169) but, interestingly, there was no increased frequency of protein C and S deficiency(170). Factor VIII was also noted to be significantly higher in over a third of patients with CTEPH, compared to those with PAH not related to thrombosis(171). Those with CTEPH have also been shown to have abnormal fibrinogen, which leads to modified fibrin. The changes mean that the fibrin chains are less susceptible to endogenous thrombolysis, therefore increasing the risk of chronic thrombus formation(172). In addition to increased prevalence of coagulopathies, platelet function abnormalities have been observed in those with CTEPH. *Remkova et al* observed that those with CTEPH have a lower platelet count, a higher platelet volume compared with controls and increased platelet aggregation(173).

CTEPH can cause remodelling of the small pulmonary vasculature, in addition to chronic stenosis of larger vessels. Pathological specimens obtained during lung biopsy or at autopsy have shown that there are similar findings to those seen in IPAH, such as increased intimal thickening, intimal fibrosis and fibromuscular proliferation and remodelling of the small vessels down to the arterioles and venule levels(174). This has been thought to occur because of the redirected

blood flow into vessels that are not obstructed by thrombus, leading to increased shear stress, endothelial damage, and dysfunction. Given that this is seen in vessels affected by thrombus as well as those unaffected by thrombus, it suggests there are more explanations for this remodelling pattern, leading to the development of pulmonary vascular remodelling. It has been postulated that there are anastomoses between the systemic circulation and the pulmonary circulation via hypertrophic bronchial arteries and the small blood vessels of the pulmonary circulation. Bronchial artery hypertrophy is one of the features of CTEPH(175). It is thought that these anastomoses already exist but are opened in response to the pressure gradient between the bronchial arteries and the post-obstruction vessels. This oxygenated blood from the systemic circulation may help to perfuse the lung parenchyma found after the thrombotic obstruction. However, given it is at systemic pressure, this blood flow may lead to shear stress and vascular remodelling. Endothelial dysfunction may also contribute to the small vessel vasculopathy. There is an increased level of nitric-oxide synthase, which leads to the inhibition of the vasodilator nitric oxide in CTEPH, versus controls. This finding is supported by the clinical improvements seen in patients who are not suitable for surgical intervention and are treated with medications which potentiate the nitric oxide pathway(176).

Clinically, it leads to exercise intolerance and, in advanced cases, can cause right heart failure and premature death(177). Initially, the RV can compensate for the increased afterload by increasing thickness and cell size. This adaptive increase in the thickness can maintain effective function for some time. However, it is not sustained, particularly during times of stress. In addition, the thrombotic process or remodelling process usually progresses with time, further increasing RV afterload. Maladaptive changes then ensue, contributing to the failing of the RV. The ventricle then enters a cycle of decline, with increased wall tension, increased oxygen demand, reduced cardiac output, poor RV perfusion and increase inflammatory infiltrate.

The management of CTEPH is well validated, which has been based on the pre-2018 definition of pre-capillary pulmonary hypertension (mPAP \geq 25mmHg, \geq 3 Wu and pulmonary artery wedge pressure of $<$ 15mmHg) (178): for central disease, where there is occlusion of the main pulmonary artery, its branches down to segmental level, a potential cure is possible with surgery. Pulmonary

thromboendarterectomy, which involves median sternotomy, and opening of both left and right pulmonary arteries with removal of the thrombotic material. This has been shown to restore vessel patency, which leads to a significant clinical improvement and greater survival (178). For those who do not wish to go undertake the surgical risks, or for those in whom the thromboembolism distribution is more distal, meaning that surgery is not possible, there is an alternative mechanical solution in the form of balloon pulmonary angioplasty (BPA). In BPA, a catheter is passed transcutaneously into the pulmonary vasculature. The catheter tip has a balloon, which is inflated in the lumen where there is obstruction, removing the obstruction from the centre of the vessel, allowing blood to flow with less resistance, shown in Figure 13.

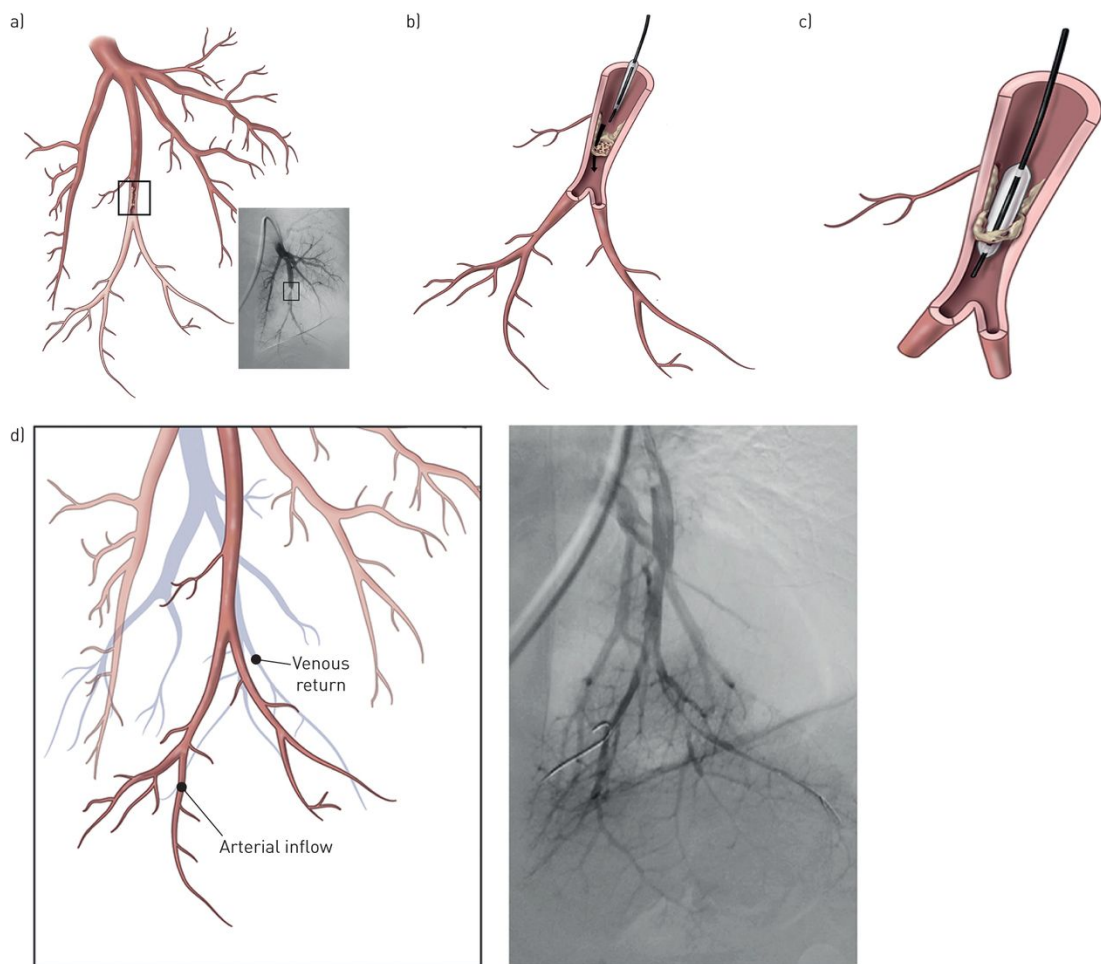


Figure 13. Diagram Describing Balloon Pulmonary Angioplasty(81)

Chronic thromboembolic pulmonary disease (CTEPD) is characterized by chronic vascular obstruction and exercise intolerance, without evidence of pulmonary hypertension at rest. However, in some cases there is a disproportionate rise in pulmonary artery pressure during exercise as the vascular tree does not have the capacity to accommodate the increased cardiac output and, as a result, leads to reduced oxygenation and exercise limitation. The degree of exercise limitation can be accurately quantified using cardiopulmonary exercise testing (CPET) (177, 179) (180) and successful treatment with PEA has been performed(181), however there is no evidence for pharmacotherapy in these patients.

A prompt diagnosis is required for patients to benefit from these well-established treatments. Echocardiography is inexpensive, widely available, and convenient to perform and is the main screening tool used in patients with reported functional limitation following treatment for acute pulmonary embolus. The gold standard diagnostic investigation remains right heart catheterization (RHC)(53), in conjunction with a number of imaging modalities, namely computer tomography (CT) and magnetic resonance imaging of the heart (CMR) and the lung. RHC and pulmonary angiography is an invasive investigation, which carries some associated risks and discomfort for patients. Ideally there would be an accurate non-invasive investigation, which would reliably provide the diagnosis without exposing patients to such risk.

Echocardiography determines the pulmonary vascular pressures via its ability to estimate pulmonary artery pressure using the tricuspid regurgitation pressure gradient. However, tricuspid regurgitation is not present in up to 30% of adults in the general population(182). As such, other indices, such as the pulmonary valve acceleration time has been used in identifying the presence of pulmonary hypertension. However, having more measurements to confirm these findings increases the diagnostic yield. The eccentricity index has been used to identify the presence of pulmonary hypertension. In pulmonary hypertension, there is abnormal movement of the interventricular septum. At end-systole, there is shifting of the septum from the right to the left, signifying pressure overload in the RV compared to the LV. The eccentricity index (EI) quantifies the septal flattening, which has potential to indicate the pressure within the RV(154). This is defined as the ratio of the length of two perpendicular minor-axis diameters, one of which is bisected and was perpendicular to the interventricular septum.

This is explained in diagrammatic form in Figure 14Figure 16. This is obtained at end-systole and end-diastole(154). This has recently been validated for use in paediatric patients with pulmonary hypertension and in adults with IPAH(183). This has not been assessed in patients with CTEPD or CTEPH.

Schematic Drawing of Eccentricity Index

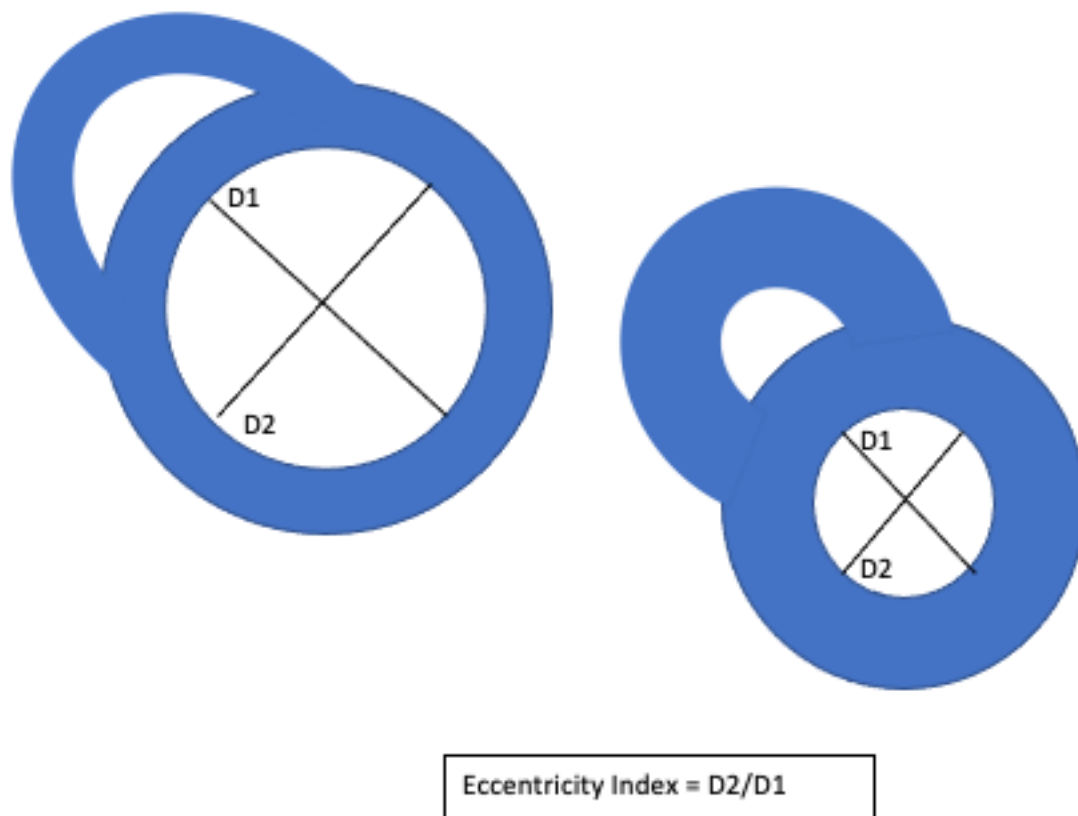


Figure 14. Pictorial description of how to measure the eccentricity index in diastole and systole.

Additional investigation such as cardiopulmonary exercise testing can be effective non-invasive method of assessing functional limitation in pulmonary hypertension. It can assess cardiac, respiratory, and peripheral muscle function, along with metabolic assessment if blood gas analysis is performed. It is useful for those in functional class II-III, although has been shown to be safe in those with severe functional limitation. In those with the most advanced functional limitation, however, the information gleaned from CPET can be limited and sub-maximal assessment, such as 6MWT is more clinically useful. The most effective indices used in the assessment of pulmonary hypertension are peak VO₂, end-tidal CO₂ tensions (PETCO₂) and the minute ventilation (VE)/carbon dioxide production (VCO₂) relationship, which can be measured at the anaerobic threshold, or its slope as seen on graphic form. These are not only of diagnostic value but can also help to guide prognosis(119, 184).

CMR remains a valuable tool that can be employed to detect the presence of pulmonary hypertension, and developments are being made in its use in measuring pressure within the pulmonary artery. *Johns et al* have shown that a model using RV mass, septal angle and pulmonary arterial measurements can accurately measure pressure in a cohort of patients with chronic obstructive pulmonary disease. This model is yet to be evaluated in CTEPH, but the eccentricity index is a similar measurement to the septal angle and may prove useful in the diagnosis of CTEPH(185).

3.1.2 Aims

It is hypothesised that systolic and diastolic eccentricity index predicts the presence of pulmonary hypertension in patients with CTEPH and is normal in those without resting pulmonary hypertension, even in the presence of thrombotic pulmonary vascular disease. Given that validated treatments thus far are based on the pre-2018 definition of pulmonary hypertension, I have used that definition (mPAP \geq 25mmHg, \geq 3 Wu and pulmonary artery wedge pressure of <15mmHg) for the patients in this study.

I aimed to evaluate:

- whether the left ventricular eccentricity index is abnormally high in those with thrombotic pulmonary vascular disease
- discriminating factors between CTEPD and CTEPH using non-invasive investigations.
- correlations between CPET findings (low peak $\dot{V}O_2$, high \dot{V}_E/\dot{V}_{CO_2}) and EI in thrombotic pulmonary vascular disease

3.2 Methods

Subjects were identified for this study from a clinical database from the Scottish Pulmonary Vascular Unit, Glasgow. They were referred between January 2016 and December 2019 for investigation of potential CTEPH or CTEPD and they underwent contemporaneous invasive and non-invasive investigations, including right heart catheterisation, CT and MRI imaging, pulmonary function testing, echocardiography, cardiopulmonary exercise testing, clinical blood testing and biomarker assessment. Patients with significant obstructive lung disease, valvular or congenital heart disease, atrial fibrillation and untreated sleep apnoea were all excluded from the study, as were those who were already treated with pulmonary vasodilator therapy.

Comparison of data from right heart catheter and echocardiography across all subgroups was performed to assess for any differences that might allow prediction of the presence or absence of thrombotic vascular disease using non-invasive methods.

A sub-analysis comparing those with CTEPD with the those who have no resting pulmonary hypertension and have no evidence of chronic thromboembolic obstruction was performed.

Finally, correlation of non-invasive measurements with right heart catheterisation was assessed to measure performance against well-defined diagnostic and prognostic investigations.

3.2.1 Echocardiography

Transthoracic echocardiography was performed as a detailed screening tool to assess for evidence of pulmonary hypertension. This was performed by a British Society of Echocardiography accredited cardiac physiologist, who was not involved in data analysis. Image acquisition was performed according to a standard protocol used for comprehensive echocardiography(155). Left ventricular eccentricity index was measured using the 2D parasternal short axis images between the mid-papillary muscle and the tip of the mitral valve leaflets level at end-systole and end-diastole(141). End-systole was taken as the image with the smallest ventricular cavity size and end-diastole was measured at the peak of the R-wave. The ratio of the minor axis dimensions was measured,

D2/D1, where D1 is ventricular diameter perpendicular to the septum and D2 is ventricular diameter parallel to the septum. Left ventricular eccentricity index >1.1 was considered abnormal(141).

3.2.2 Cardiopulmonary Exercise Testing

Cardiopulmonary exercise testing was performed using an incremental cycle ergometer. The ramp rate was chosen by the physiologist, based on the participants' self-reported fitness, with the aim of exercising for 8-12 minutes. This assesses patients' respiratory and cardiovascular capacity. Low peak VO₂ and high VE/VCO₂ were used to assess the level of functional limitation.

3.2.3 Right Heart Catheterisation

Right heart catheterisation was performed at the Golden Jubilee National Hospital by two physicians with an 8F Swan-Ganz, introduced using the Seldinger technique through the internal jugular or femoral vein. These were performed within four days of the echocardiogram and CPET testing. Hemodynamic parameters including right atrial pressure, right ventricular pressure and pulmonary artery pressure and pulmonary artery wedge pressure were all taken at rest. Cardiac output was measured using the thermodilution method and pulmonary vascular resistance (PVR) calculated after the procedure.

3.2.4 Data management and Statistical Analysis

Data was stored on NHS password secure encrypted computers and was analysed using Microsoft Excel and Graph Pad Prism version 9 (San Diego, CA, USA)

ANOVA was used to assess for differences between subgroups. Students t-test or Mann-Whitney U test were used depending on the distribution of the data.

Correlation analysis was performed using Spearman analysis. Receiver operator curves were used to identify clinically relevant thresholds that could be used to identify the presence of chronic thromboembolic pulmonary vascular disease.

Bland Altman plots were used to describe agreements between investigations.

3.3 Results

Only those patients with complete datasets were included in the study. 71 patients were referred and underwent investigations but did not have pulmonary hypertension at rest. Of these, 23 had CTEPD and 10 of these patients had complete data, including CPET. The main limiting factor in the datasets was access to reliable CPET data. The remaining 48 patients had normal pulmonary vasculature on imaging, and had normal resting pulmonary haemodynamic values, of whom 10 had complete data. 114 patients were diagnosed with CTEPH. 20 of these patients had complete data and were seen to have pulmonary vascular occlusion in the main pulmonary arteries and or segmental pulmonary arteries, classed as “central” disease.

Thus, 50 patients were included in the study: twenty patients with no pulmonary hypertension at rest and thirty with pulmonary hypertension, as shown in Figure 17. In the group with no pulmonary hypertension at rest, ten had normal pulmonary vasculature and ten had CTEPD. In the group with pulmonary hypertension, twenty had central distribution of thromboembolic material and ten with distal distribution, as agreed by the multidisciplinary team at the Scottish Pulmonary Vascular Unity and the UK National Thromboendarterectomy Unit at Papworth Hospital, Cambridge. Those with distal disease were functionally limited to the extent whereby they were unable to perform CPET, so these patients were not included in the CPET data.

A sub-analysis comparing the 10 patients with CTEPD, without resting pulmonary hypertension (CTEPD), with the 20 patients who have resting pulmonary hypertension was performed.

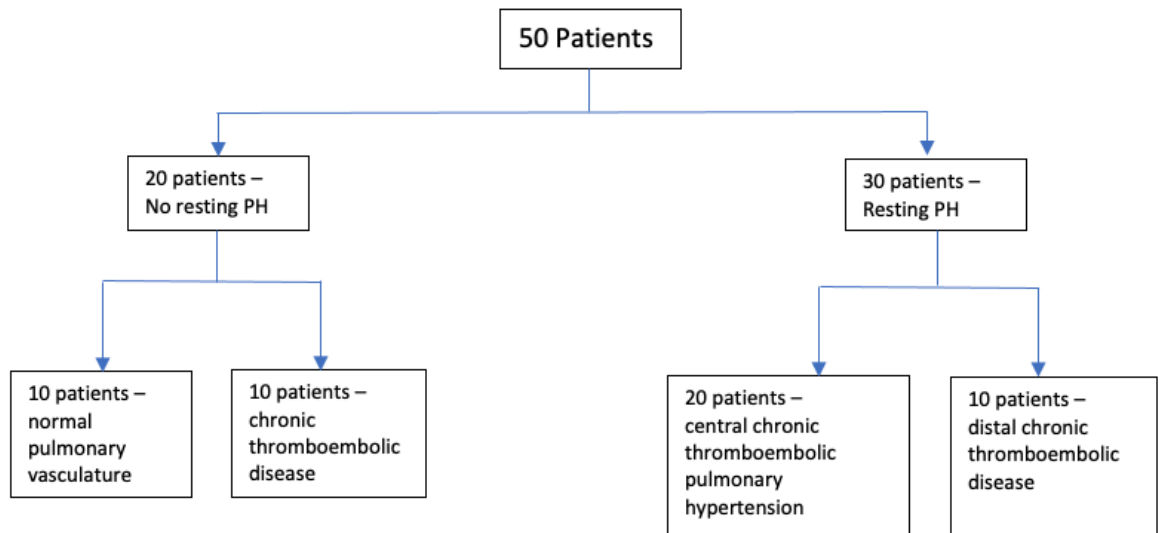


Figure 15. Patient recruitment to study.

3.3.1 Assessing those with Pulmonary Hypertension

The baseline variables between those with and without resting pulmonary hypertension can be seen in Table 11. As expected, there were significant differences in the haemodynamic values between the groups, with no differences in age and sex ($p=0.79$ and $p=0.36$, respectively). There was a significantly higher right atrial pressure (6.0 ± 3.9 mmHg vs 3.2 ± 2.3 mmHg; $p=0.01$), mean pulmonary artery pressure (40.2 ± 11.4 mmHg vs 17 ± 4.4 mmHg; $p<0.01$) and pulmonary vascular resistance (8.5 ± 4.7 Wu vs 1.9 ± 1.2 Wu; $p<0.01$) in the CTEPH group. There was a higher cardiac index (2.5 ± 0.6 L/min/m² vs 2.1 ± 0.4 L/min/m²; $p=0.01$) and mixed venous saturations ($73.1\% \pm 4.2$ vs $63.5\% \pm 6.8$; $p<0.01$) in the non-pulmonary hypertension group.

Index	Non-PH, n=20 Mean (SD)	CTEPH, n=30 Mean (SD)	P-Value ⁺
Age (Years)	53.9 (17.5)	52.2 (15.9)	0.79
Sex (M)	8	16	0.36
BMI (kg/m ²)	32.3 (6.0)	28.4 (5.6)	0.03
RAP (mmHg)	3.2 (2.3)	6.0 (3.9)	0.01
EDP (mmHg)	5.3 (2.6)	8.8 (4.3)	0.01
mPAP (mmHg)	17 (4.4)	40.2 (11.4)	<0.01
PAWP (mmHg)	8.3 (3.4)	7.5 (3.6)	0.41
CO (mmHg)	5.1 (1.1)	4.1 (0.9)	<0.01
CI (L/min/m ²)	2.5 (0.6)	2.1 (0.4)	0.01
PVR (Wu)	1.9 (1.2)	8.5 (4.7)	<0.01
SvO ₂ (%)	73.1 (4.2)	63.5 (6.8)	<0.01
NT-proBNP (pg/ml)	184 (155)	1004 (1291)	0.01
6 MWT (m)	407 (115)	389 (95)	0.55

Table 3. Baseline Variables between those with and without pulmonary hypertension.

⁺Mann Whitney U Test

BMI - Body Mass Index; RAP - Right Atrial Pressure; EDP - End Diastolic Pressure; mPAP - mean Pulmonary Artery Pressure; PAWP - Pulmonary Artery Wedge Pressure; CO - Cardiac Output; CI - Cardiac Index; BSA - Body Surface Area; PVR - Pulmonary Vascular Resistance; SvO₂ - Mixed venous saturations.

3.3.1.1 Echocardiography

I compared echocardiographic parameters between the groups with and without pulmonary hypertension at rest, as shown in Table 4. There were no significant differences between these groups when assessing left ventricular ejection fraction ($62.7\% \pm 5.9$ vs $65.3\% \pm 9$, $p=0.3$), left atrial area ($16.7 \pm 3.9 \text{ cm}^2$ vs $15.3 \pm 4.1 \text{ cm}^2$) or left ventricular internal diameter in diastole ($4.5 \pm 0.5 \text{ cm}$ vs $4.3 \pm 0.6 \text{ cm}$, $p=0.16$) or systole ($2.9 \pm 0.5 \text{ cm}$ vs $2.9 \pm 0.7 \text{ cm}$, $p=0.8$). As expected, there were significant differences between these groups in indices that are already established to identify pulmonary hypertension using echocardiogram, namely higher tricuspid regurgitation pressure gradient (TRPG) ($59 \pm 2 \text{ mmHg}$ vs $27.2 \pm 7.4 \text{ mmHg}$; $p=0.01$) and lower pulmonary valve acceleration time (PVAcCT) ($54.7 \pm 21.4 \text{ m/sec}$ vs $98.9 \pm 31.2 \text{ m/sec}$; $p=0.01$). The right atrial area was also higher in those with pulmonary hypertension ($14.3 \pm 2.8 \text{ cm}^2$ vs $17.1 \pm 4.7 \text{ cm}^2$, $p<0.01$). Eccentricity index using echocardiography was also higher in those with CTEPH compared to those without, both in systole (1.4 ± 0.8 vs 1.1 ± 0.1 ; $p=0.01$) and diastole (1.2 ± 0.1 vs 1.0 ± 0.1 ; $p=0.01$) but with no differences seen in TAPSE (Table 2).

Index	Non-PH, n=20	CTEPH, n=30	P-Value ⁺
	Mean (SD)	Mean (SD)	
Heart rate (bpm)	66 (9)	73 (16)	0.03
LVEF (%)	62.7 (5.9)	65.3 (9)	0.30
LA area (cm ²)	16.7 (3.9)	15.3 (4.1)	0.19
LVIDd (cm)	4.5 (0.5)	4.3 (0.6)	0.16
LVIDs (cm)	2.9 (0.5)	2.9 (0.7)	0.80
RA area (cm ²)	14.3 (2.8)	17.7 (4.7)	<0.01
RV max length (cm)	6.3 (1.6)	7.5 (0.8)	0.03
TRPG (mmHg)	27.4 (7.4)	59 (2.0)	<0.01
Pulmonary Valve AccT (m/sec)	98.9 (31.2)	54.7 (21.4)	<0.01
Systolic LVEI	1.1 (0.1)	1.4 (0.8)	<0.01
Diastolic LVEI	1.0 (0.1)	1.2 (0.1)	<0.01
TAPSE	2.1 (0.4)	1.8 (0.4)	0.11

Table 4. Parameters measured by echocardiogram in patients with chronic thromboembolic pulmonary hypertension versus those without.

⁺Mann Whitney U Test.

SD – standard deviation; BPM – beats per minute; LVEF – Left Ventricular Ejection Fraction; LA – Left Atrium; cm – centimetres; LVIDd – Left Ventricular Internal Diameter in diastole; LVIDs – Left Ventricular Internal Diameter in systole; RA – Right atrium; TRPG – Tricuspid Regurgitant Pressure Gradient; PV AccT – Pulmonary Valve Acceleration Time; LVEI – Left Ventricular Eccentricity Index; TAPSE – Tricuspid Annular Plane Systolic Excursion

3.3.1.2 Cardiopulmonary Exercise Testing

Mean CPET values for the two groups are shown in Table 12. There was no significant difference in the spirometry between the two groups, nor was there any difference noted in the maximum work rate achieved or the maximum heart rate. There was no significant difference in the peak VO_2 but there was a significantly higher V_E/V_{CO_2} (49.6 ± 11.5 vs 34.3 ± 6.9 ; $p < 0.01$) in those with CTEPH. In addition, there was a higher oxygen pulse seen in the group with no resting pulmonary hypertension (10.3 ± 2.5 ml/beat vs 8.3 ± 2.6 ml/beat. $p = 0.01$).

	Non-PH, n=20	CTEPH, n=20	p-value [†]
	Mean (SD)	Mean (SD)	
FEV1 (%)	94 (26)	88 (13)	0.07
FVC (%)	102 (18)	92 (14)	0.11
VE (L/min)	60 (18.7)	66 (21.5)	0.21
Work Rate (W)	107.8 (40)	86.5 (42)	0.06
Respiratory Exchange Rate	1.22 (0.13)	1.12 (0.1)	0.01
Maximum Load Achieved (METS)	5.59 (1.9)	4.7 (1.6)	0.12
Maximum Heart Rate Achieved (bpm)	144 (25)	144 (22)	0.89
Peak VO_2 ml/kg/min	16 (5.1)	13 (3.8)	0.13
V_E/V_{CO_2}	34.3 (6.9)	49.6 (11.5)	<0.01
Oxygen Pulse (ml/beat)	10.3 (2.5)	8.3 (2.6)	0.01

Table 5. Baseline Cardiopulmonary exercise tests between those with and without resting pulmonary hypertension

FEV 1 – % predicted Forced Expiratory Volume in 1 second; FVC – % predicted Forced Vital Capacity; VE – Ventilatory Equivalent for Oxygen; L/min – Litres per minute; METS – Metabolic Equivalent of Task; bpm – Beats per Minute; ml/kg/min – millilitres per kilogram per minute; ml - millilitres [†]Mann Whitney U test

3.3.2 Subgroups of Chronic Thromboembolic Pulmonary Vascular Disease

3.3.2.1 Baseline variables

Table 14 shows the distribution of the variables across all four subgroups.

Between the groups, there was a progressive rise in the mean pulmonary artery pressure ($p < 0.01$) and pulmonary vascular resistance ($p < 0.01$) and a reduction in the cardiac index ($p < 0.01$) and mixed venous saturations ($p < 0.01$).

Interestingly, using the new definition of pulmonary hypertension, a significant number of the CTEPD patients would be labelled as having CTEPH in view of the mean PVR of 2.5 and mPAP of 19.9.

Index	Normal Mean (SD) n=10	CTEPD Mean (SD) n=10	Proximal CTEPH Mean (SD) n=20	Distal CTEPH Mean (SD) n=10	P-Value ⁺
Age (Years)	46 (18.9)	61.8 (12.2)	51.9 (16.2)	65.7 (9.3)	0.01
BMI (kg/m ²)	30.4 (5)	34.1 (6.5)	28.5 (5.7)	29.7 (4.3)	0.08
RAP (mmHg)	3.4 (2.8)	2.9 (1.9)	6.3 (3.9)	5.6 (4.1)	0.04
EDP (mmHg)	6.2 (2.8)	4.3 (2.2)	8.9 (4.4)	8.7 (4.4)	0.01
mPAP (mmHg)	14.1 (3.4)	19.9 (3.1)	41.1 (13.5)	38.3 (4.4)	<0.001
PAWP (mmHg)	7.8 (3.0)	8.7 (3.9)	7.4 (3.4)	7.7 (4.1)	0.82
CO (mmHg)	5.6 (1.1)	4.5 (0.8)	4.3 (0.9)	3.9 (0.8)	<0.001
CI (CO/BSA)	2.9 (0.6)	2.2 (0.2)	2.2 (0.4)	2.0 (0.4)	<0.001
PVR (Wu)	1.2 (0.9)	2.5(1.1)	8.6 (4.5)	8.3 (2.7)	<0.001
SvO ₂ (%)	74.7 (5.1)	71.5 (2.2)	64.45 (6.7)	61.6 (7.0)	<0.001
NT-proBNP (pg/ml)	198 (162)	173 (157)	987 (1296)	1037 (1349)	0.09
6 MWT (m)	431 (129)	383 (101)	416 (100)	310 (127)	0.07

Table 6. Haemodynamic values of across all groups (ANOVA)

SD – Standard Deviation; BMI – Body Mass Index; mmHg – millimetres of mercury; RAP – Right Atrial Pressure; EDP – End Diastolic Pressure; mPAP – mean Pulmonary Artery Pressure; PAWP – Pulmonary Artery Wedge Pressure; CO – Cardiac Output; CI – Cardiac Index; BSA – Body Surface area; PVR – Pulmonary Vascular Resistance; SvO₂ – Mixed venous saturations; NT-proBNP – N-Terminal Pro Natriuretic Peptide; 6MDT – 6-minute walk test distance

⁺ANOVA

3.3.2.2 Echocardiography

To try and identify where a patient may be on the thrombotic pulmonary vascular disease spectrum, the echocardiogram findings in the respective disease groups were compared in Table 7, including those well-established indices and the novel measurements of the eccentricity index. Between groups, there was a progressive decline in the pulmonary valve acceleration time ($p < 0.01$) and a rise in the TRPG ($p < 0.01$), the systolic and diastolic LVEI ($p < 0.01$).

Index	Normal, n=10 <i>Mean (SD)</i>	CTEPD, n=10 <i>Mean (SD)</i>	Proximal CTEPH, n=20 <i>Mean (SD)</i>	Distal CTEPH, n=10 <i>Mean (SD)</i>	P-Value ⁺
TRPG (mmHg)	22.5 (5.5)	32.3 (5.7)	61.8 (17.2)	57.6 (18.7)	<0.01
PV AccT (msec)	115.3 (26.4)	77.2 (23.4)	58.6 (16.2)	54.4 (22.3)	<0.01
Systolic LVEI	1.0 (0.05)	1.09(0.06)	1.3 (0.25)	1.3 (0.2)	<0.01
Diastolic LVEI	1.0 (0.03)	1.0 (0.08)	1.2 (0.14)	1.2 (0.1)	<0.01

Table 7. Differences in echocardiographic measurements between all sub-groups

⁺ANOVA.

SD – standard deviation; *TRPG* – Tricuspid Regurgitant Pressure Gradient; *PV AccT* – Pulmonary Valve Acceleration Time; *msec* – milliseconds; *LVEI* – Left Ventricular Eccentricity Index

Given these differences between the four groups, the differences between CTEPD and proximal CTEPH was further evaluated. These are the groups whereby invasive investigations are often performed to detect the presence of pulmonary hypertension and where treatments have been shown to be of greatest benefit. These differences are shown in Table 8. As expected, there was significant difference between the TRPG (32.3 ± 5.7 mmHg vs 61.8 ± 17.2 , $p < 0.01$) but not in PVAccT ($p = 0.06$). However, in both systolic and diastolic LVEI there were significant differences (1.09 ± 0.1 vs 1.3 ± 0.2 , $p = 0.02$, (1.0 ± 0.1 vs 1.2 ± 0.1 , $p < 0.01$, respectively).

Index	CTEPD, n=10 <i>Mean (SD)</i>	Proximal CTEPH, n=20 <i>Mean (SD)</i>	P-Value ⁺
TRPG (mmHg)	32.3 (5.7)	61.8 (17.2)	<0.01
PV AccT (msec)	77.2 (23.4)	58.6 (16.2)	0.06
Systolic LVEI	1.09(0.1)	1.3 (0.2)	0.02
Diastolic LVEI	1.0 (0.1)	1.2 (0.1)	<0.01

Table 8. Unpaired t-test of the differences in echocardiographic measurements between those with CTEPH and proximal CTEPH

⁺ unpaired t-test

SD – standard deviation; TRPG – Tricuspid Regurgitant Pressure Gradient; PV AccT – Pulmonary Valve Acceleration Time; msec – milliseconds; LVEI – Left Ventricular Eccentricity Index

3.3.2.3 Cardiopulmonary Exercise Testing

Table 9 demonstrates the changes in cardiopulmonary exercise testing. Those with distal CTEPH were unable to perform cardiopulmonary exercise testing due to physical limitations and, therefore, there was no data available for this group. There was a reduction in peak VO_2 between the groups of pulmonary vascular disease as the pulmonary artery pressure increases ($p=0.02$). In addition, between the groups there was a progressive rise in the $\text{V}_E/\text{V}_{\text{CO}_2}$ ($p<0.01$).

	Normal	CTEPD	Proximal CTEPH	p-value ⁺
VO_2 ml/kg/min	17.7 (5.3)	14.4 (4.7)	12.8 (3.8)	0.02
$\text{V}_E/\text{V}_{\text{CO}_2}$	31.7 (5.2)	36.9 (7.7)	49.67 (11.81)	<0.01

Table 9. Baseline Cardiopulmonary exercise testing between subgroups of thrombotic pulmonary vascular disease

CTEPD – chronic thromboembolic pulmonary disease; CTEPH – chronic thromboembolic pulmonary hypertension

⁺Mann Whitney U test

3.3.3 Correlation between Invasive and Non-invasive Assessment

Correlations between echocardiographic measurements and haemodynamic findings were assessed (Table 10). Notably, there were strong correlations between all echocardiogram indices and the pressure indices - end diastolic pressure ($p<0.01$ for all) and mean pulmonary artery pressure ($p<0.01$ for all). There were also strong correlations with the pulmonary vascular resistance and all four echocardiogram indices. Interestingly, there was a correlation between these indices and exercise capacity, as measured by 6-minute walk distance ($p<0.01$ for all groups). There was strong correlation between $\text{VE}/\text{V}_{\text{CO}_2}$ and haemodynamic indices, PVR ($p<0.01$), cardiac index ($p=0.01$), pulmonary vascular resistance ($p<0.01$) and with 6MWD ($p<0.01$) but less good with mPAP ($p=0.02$). VO_2 correlated less well with haemodynamic indices, other than mPAP ($p=0.02$) but did correlate with mixed venous saturations ($p<0.01$) and 6MWD ($p<0.01$).

Index	TRPG r-value (p-value) n=36	PVAccT r-value (p-value) n=38	Systolic LVEI r-value (p-value) n=50	Diastolic LVEI r-value (p-value) n=50	VE/VCO 2 r-value (p-value) n=40	VO2/kg r-value (p-value) n=40
RAP (mmHg)	0.5 (<0.01)	-0.38 (0.02)	0.3 (0.04)	0.48 (<0.01)	0.26 (0.1)	-0.07 (0.65)
EDP (mmHg)	0.47 (<0.01)	-0.3 (0.04)	0.37 (<0.01)	0.39 (<0.01)	0.31 (0.04)	-0.18 (0.26)
mPAP (mmHg)	0.76 (<0.01)	-0.59 (<0.01)	0.39 (<0.01)	0.72 (<0.01)	0.63 (<0.01)	-0.37 (0.02)
PAWP (mmHg)	-0.12 (0.45)	0.08 (0.64)	0.04 (0.81)	0.01 (0.95)	0.39 (0.05)	0.1 (0.5)
CO (mmHg)	-0.45 (<0.01)	0.45 (<0.01)	-0.15 (0.31)	-0.16 (0.26)	0.49 (<0.01)	0.23 (0.16)
CI (L/min/ m ²)	-0.37 (0.02)	0.37 (0.02)	-0.08 (0.58)	-0.18 (0.21)	0.37 (0.01)	0.12 (0.47)
PVR (Wu)	-0.51 (<0.01)	0.76 (<0.01)	0.31 (0.02)	0.56 (<0.01)	0.72 (<0.01)	0.37 (0.02)
SvO2 (%)	-0.52 (<0.01)	-0.52 (<0.01)	-0.27 (0.06)	-0.44 (<0.01)	-0.59 (<0.01)	0.47 (<0.01)
NT- proBNP (pg/ml)	0.61 (<0.01)	-0.19 (0.34)	-0.12 (0.46)	0.42 (<0.01)	0.33 (0.04)	-0.32 (0.04)
6 MWT (m)	-0.74 (<0.01)	0.65 (<0.01)	-0.54 (<0.01)	-0.54 (<0.01)	0.64 (<0.01)	0.41 (<0.01)

Table 10. Correlation between Invasive Haemodynamic Indices, exercise capacity and biomarker levels and Echocardiogram Measurements

SD - standard deviation; TRPG - Tricuspid Regurgitant Pressure Gradient; PV AccT - Pulmonary Valve Acceleration Time; LVEI - Left Ventricular Eccentricity Index; RAP - Right Atrial Pressure; EDP - End Diastolic Pressure; mPAP - mean Pulmonary Artery Pressure; PAWP - Pulmonary Artery Wedge Pressure; CO - Cardiac Output; CI - Cardiac Index; BSA - Body Surface area; PVR - Pulmonary Vascular Resistance; SvO2 - Mixed venous saturations; NT-proBNP - N-Terminal Pro Natriuretic Peptide; 6MDT - 6-minute walk test distance

3.4 Discussion

In this study, I evaluated the non-invasive assessment of patients in the detection of pulmonary vascular disease using echocardiogram and cardiopulmonary exercise testing. The LVEI has been shown to be abnormally high in those with chronic thromboembolic pulmonary hypertension and can be used as a further index to detect this disease, which is of particular interest because, to my knowledge, this has not previously been demonstrated. In addition, the peak $\dot{V}O_2$, $\dot{V}E/\dot{V}CO_2$ and oxygen pulse have also been shown to be significantly different between those with and without pulmonary hypertension. These facts demonstrate the importance of the multimodal non-invasive assessment of patients with symptomatic chronic thromboembolic disease which could potentially be used in lieu of invasive assessment.

3.4.1 Detection of pulmonary hypertension

I demonstrated differences in novel geometric indices between patients with chronic thromboembolic pulmonary hypertension compared with control subjects. The eccentricity index, measured in both end-systole and end-diastole, was significantly higher in those with CTEPH. The established indices of increased tricuspid regurgitation pressure and reduced pulmonary valve acceleration time were also seen, adding confidence that these findings were genuine(98). This can be explained by an increase in right ventricular afterload. This leads to an increase in the pressure which needs to be overcome by the right ventricle to facilitate pulmonary perfusion. There is also consequent tricuspid regurgitation. This increase in pressure also leads to a reduction in flow velocity through the pulmonary valve, leading to reduced pulmonary valve acceleration time. Over time, with maladaptation of the RV, there is dilatation of the ventricle. This leads to dilatation of the tricuspid valve annulus, further worsening the tricuspid valve regurgitation.

The progressive change over time leads to further dysfunction of the RV and ventricular dyssynchrony. In those with normal pulmonary artery pressures, the RV and LV contract and relax simultaneously. However, in pulmonary hypertension there is loss of this synchronous movement. The RV undergoes diastole later than the LV, meaning that at the end of diastole for the LV, the pressure in the RV exceeds that of the LV, causing the septum to shift towards the left side, contrary to what occurs in those with healthy pulmonary vasculature. This study shows that the eccentricity index, as measured by echocardiogram, can quantify the septal shift. This relationship with established indices used to measure pressure suggest a causal link between increasing pressure and increasing eccentricity index, which was originally hypothesised. The correlation between the LVEI and mPAP supports this. As echocardiography remains the main screening tool for detecting pulmonary hypertension, it shows that these measurements could be used in clinical practice in to detect patients who may benefit from invasive investigations, particularly in those where TRPG is not measurable.

Furthermore, I have demonstrated the use of CPET in the detection of pulmonary hypertension in those with chronic pulmonary vascular obstruction. In this cohort, I have shown that the peak VO_2 , VE/VCO_2 and oxygen pulse can be used to differentiate between those with and without pulmonary hypertension in those with a central distribution of pulmonary vascular obstruction. This can be explained by the increased dead space ventilation seen with progressive pulmonary vascular occlusion seen in those with CTEPH. The oxygen pulse correlates well with stroke volume(186). In those with CTEPH there is right ventricular dysfunction and dilatation with increased afterload, leading to a reduction in stroke volume, which can be seen in the low oxygen pulse during CPET.

The differences in haemodynamic indices between groups with and without pulmonary hypertension was demonstrated, which is to be expected, but lends confidence to the validity of the novel findings. There was a significantly higher BMI in the control group, with no difference in cardiac output. As such, cardiac index may be a more reliable variable than cardiac output, and it is seen to be significantly higher in the control subject group. The pulmonary vascular resistance and the NT-proBNP levels of the CTEPH groups were higher in the

severe group, suggesting that this cohort have advanced disease. However, this is not reflected in the functional capacity, as measured by the 6-minute walk distance. These findings may be explained by the presence of thromboembolism within the pulmonary vasculature, limiting blood flow, leading to increased pressure within the pulmonary vasculature right sided cardiac chambers. The lack of difference in the 6-minute walk distance may be explained by a selection bias. The patients included in the study were patients who were able to undergo all investigations, including cardiopulmonary exercise test. To glean meaningful information from a CPET, the patient must have a performance status that is compatible with exercising for up to twelve minutes against resistance.

3.4.2 Subgroup Analysis

Given the findings seen between those with and without resting pulmonary hypertension, the investigations in the subgroups of those with normal pulmonary vasculature, chronic thromboembolic pulmonary disease (CTEPD), proximal CTEPH and those with distal CTEPH were evaluated to assess for the use of these investigations in evaluating where patients may be in the spectrum of thrombotic pulmonary vascular disease.

3.4.2.1 Baseline variables

Although there were significant differences between the groups for several of the indices measured in right heart catheterisation, there were only a few that could detect a signal that they could be used to detect the different diseases. The mean pulmonary artery pressure was at the upper limited of normal in the CTEPD category and was higher in those with proximal CTEPH. This is to be expected given the disease definitions. There was a progressive decline in cardiac output between groups from normal in those without pulmonary vascular obstruction to progressively more abnormal those with distal obstruction. Although there were variations in body mass index between groups, similar effects are seen for cardiac index (which corrects for body surface area). There is also a progressive rise in pulmonary vascular resistance between the groups, as might be expected. Indeed, as the amount of pulmonary vascular occlusion increases in these cohorts, there is an associated rise in resistance. Again, the pulmonary vascular resistance is near the upper limit of normal in those with

CTEPD but there were no significant differences between those with proximal versus distal occlusion. Mixed venous saturations also show a significant decline across the four subgroups, which reflects the reduced cardiac output with increased extraction of oxygen in peripheral muscles.

3.4.2.2 Echocardiogram

The eccentricity index was of value in discrimination between those with CTEPD and proximal CTEPH. The TRPG showed significant differences, but in up to 30% of patients it is not possible to measure this. PVAcCT has not been shown to be a reliable predictor in discriminating between CTEPD and proximal CTEPH in this population. However, LVEI in systole and diastole were significantly different. This suggests it can be used as a further index in determining whether a patient requires further investigation and adds to the justification of the risks of invasive measurements in those where it is high. This is in keeping with other studies that have used the septal angle, a similar measurement, in the detection of CTEPH using CT(187) and MRI(9).

As might be expected established echocardiographic indices, including TRPG and PVAcCT, show progressive change across the thrombotic vascular disease spectrum as more of the pulmonary vasculature is occluded.

3.4.3 Correlations

Echocardiography is the main screening tool for pulmonary hypertension, is widely available and is an inexpensive tool. As such, the majority of patients are referred to the pulmonary vascular service based on the changes seen on echocardiogram. I assessed how well-established indices (tricuspid regurgitation and pulmonary valve acceleration time) and novel indices including eccentricity index in systole and diastole, correlated with the gold standard right heart catheter indices, biomarkers, and exercise tolerance.

The eccentricity index can be used to detect the presence of pulmonary hypertension. It has been demonstrated that the eccentricity indices correlated well with the pressure measurements, pulmonary vascular resistance, and exercise capacity, using 6MWD. The diastolic eccentricity index also correlated with NT-proBNP. The TRPG and PVAccT showed good correlation with the invasive pressure-related indices. This study demonstrated that in pulmonary hypertension these were robust measurements reflecting a high probability of the presence of disease. Notably, there is a correlation of left ventricular eccentricity index measured in systole and diastole with the mean pulmonary artery pressure. This adds confidence to its use in detection of disease and adds justification to further evaluate patients with suspected pulmonary hypertension with other non-invasive and invasive investigations.

Using CPET indices, VE/VCO₂ showed good correlation with pulmonary haemodynamics, NT-proBNP, mixed venous saturations and, as might be expected, exercise tolerance measured by 6MWD. Peak VO₂ showed no correlation with invasive measurements, other than mean pulmonary artery pressure but did correlate well with NT-proBNP, 6MWD and mixed venous saturations. This demonstrates the benefits of using CPET in conjunction with other non-invasive investigations in the evaluation of a patient having underlying chronic pulmonary arterial occlusion.

3.4.4 Comparison to other studies

This data demonstrates that a high eccentricity index is predictive of CTEPH, both in systole and diastole. The eccentricity index was first described in a pulmonary hypertension cohort in 1985 (154) and, more recently, has been shown to be predictive of the presence of pulmonary hypertension IPAH in a paediatric population (183). The echocardiography data from this analysis supports these studies and is in agreement with *Howard et al.* (144) who recommend that this should be reported formally in an echocardiogram when performed to look for the presence of pulmonary hypertension, which is not routine practice in our institution. The echocardiography data also supports the well-established indices of tricuspid regurgitant pressure gradient and pulmonary valve acceleration time being used to guide the clinician as to the presence of pulmonary hypertension (141, 144), which supports the validity of these findings ar.

3.4.5 Strengths and weaknesses

This cohort of patients underwent comprehensive and concurrent cardiopulmonary investigations. Their diagnoses were secure and were reviewed by two distinct national multidisciplinary meetings at the Scottish Pulmonary Vascular Unit and the National thromboendarterectomy centre, based in Royal Papworth Hospital in Cambridge. All investigations and analyses were performed by experts in their field, thereby minimising the chance of confounding diagnostic errors.

Despite these strengths, there were limitations to this study. This was a retrospective study, and the investigations were performed as part of clinical care, rather than under trial conditions. Therefore, while the patients represent a 'real world' cohort there was some missing data, such as the CPET results in those with distal CTEPH. In addition, arterial blood gas results were missing from the majority of the CPETs, limiting the assessment of dead-space ventilation (V_D/V_T). The patients for this study were selected because of their full data set. Whilst this was done in a consecutive way, this will incur some bias as the patients were required to be of a sufficient functional class such that meaningful data can be gleaned from their CPET. Patients with more limitation, and therefore likely to have more severe disease, would not be able to perform CPET, thereby excluding them from the study. However, it is those with milder disease that can be detected early and stand to benefit from therapy that we wish to detect abnormalities in.

The clinical impact of the eccentricity index using echocardiography could be limited by interobserver variability. The quality of echocardiographic images can be compromised by body habitus and positioning, thereby limiting the conclusions that can be drawn from it. However, the main use of echocardiogram is to detect abnormality, which then prompts further investigation, rather than to necessarily quantify severity of illness. Therefore, it is hoped that having another index that can be applied will aid in the detection of pulmonary vascular disease.

3.5 Conclusions

This study has shown that a high LVEI in systole and diastole can be used to detect the presence of CTEPH. Whilst there are limitations of echocardiography in the detection of pulmonary vascular disease, LVEI can be used as a further index in the evaluation of a patient with suspected pulmonary hypertension, particularly in those where TRPG cannot be measured. CPET remains a very useful non-invasive investigation for the detection of pulmonary vascular disease and quantification of exercise limitation. Multi-modality investigation remains the optimal approach in the diagnosis and risk assessment of these patients. These findings, in relation to echocardiographic assessment of LVEI should be further evaluated in large prospective studies of patients with suspected or confirmed pulmonary vascular disease. This is supported by the ESC/ERS guideline approach in CTEPH and ESC/ERS guidelines, which both recommend an initial echocardiographic assessment and an assessment of lung perfusion in the respective diagnoses.

4 Assessing Cardiac Geometry, using cardiac Magnetic Resonance Imaging, in the Diagnosis of Chronic Thromboembolic Pulmonary Vascular Disease

4.1 Introduction

4.1.1 Background

Pulmonary hypertension is a progressive disease, associated with a poor prognosis at 5 years and a high associated symptom burden(188). The disorder may be idiopathic or complicate a number of medical conditions, including connective tissue disease and the majority of cardiovascular and respiratory diseases. It may also be the result of occlusive pulmonary emboli, in the form of Chronic Thromboembolic pulmonary hypertension (CTEPH), classed as Group IV in the 2018 Nice classification of pulmonary hypertension(64). CTEPH is defined by a mean pulmonary arterial pressure above 20mmHg and a pulmonary capillary wedge pressure of ≤ 15 mmg, as measured by right heart catheterization, along with at least one persistent perfusion defect seen on imaging (V/Q scanning or pulmonary angiography) after 3 months of anticoagulation (3).

The reason that some people develop CTEPH, and others do not, is unclear. The presence of acute thrombus induces an inflammatory response within the vessel lumen. This organizes the thrombus, before spontaneously lysing it. Over time, there is usually complete resolution of the thrombus, restoring normal blood flow. However, in some cases, the clot is not completely lysed and leads to organisation of this material into webs or bands which obstruct blood flow, leading to increased pulmonary vascular resistance and increased pulmonary artery pressure(165).

As mentioned above and in Chapter 4, the reasons why patients go on to develop CTEPH is not fully understood and have been previously described in Chapter 4. CTEPH can cause remodelling of the small pulmonary vasculature, where there is intimal thickening, intimal fibrosis, fibromuscular proliferation and remodelling of the small vessels down to the arterioles and venule levels(174). One theory is that endothelial dysfunction is caused through the increased vessel sheer stress from redirected blood flow into vessels that are not obstructed by thrombus.

Clinically, CTEPH leads to exercise intolerance and right heart failure can ensue, causing premature death(177). Early in the disease, the right ventricle (RV) hypertrophies to compensate for increased afterload. This adaptive increase in the thickness of the wall reduces stress on the RV and can maintain effective function for some time. However, it is unable to do this long-term, particularly during exercise. The thrombotic remodelling process usually progresses with time, increasing RV afterload. This then leads to maladaptive changes to the RV with hypertrophy, dilatation, reduced contractile force and increased myocardial fibrosis all contributing to failing RV function. The ventricle then enters a cycle of progressive dysfunction because of, increased oxygen demand, reduced cardiac output leading to reduced perfusion and eventual ventricular failure(189).

The management of CTEPH has been described previously (178): there is a potential cure for chronic thromboembolic pulmonary hypertension in the form of surgery. Removal of the thrombotic material from the central pulmonary vessels, known as pulmonary thromboendarterectomy, can substantially improve blood flow leading to cure in some cases. Even in those who are not considered to be cured, this procedure is associated with marked improvements in pulmonary haemodynamics, significant symptomatic improvement and greater survival (178). This surgery is, however, very invasive and carries its own risks. For those who do not wish to undertake the surgical risks, or for those in whom the thromboembolism distribution is more distal, balloon pulmonary angioplasty (BPA) is an alternative mechanical solution. For BPA, a catheter is passed percutaneously into the pulmonary vasculature. Contrast is injected and obstructive thrombus identified using fluoroscopy. Similar to coronary angioplasty, inflation of a balloon at the distal tip of the catheter allows relief of the obstruction, allowing blood to flow with less resistance.

Chronic thromboembolic pulmonary disease (CTEPD) is a complication following acute pulmonary embolus and is characterized by chronic vascular obstruction and exercise intolerance, without evidence of pulmonary hypertension at rest. These patients can have a functional limitation when tested with cardiopulmonary exercise testing(177, 179) (CPET) (180) and successful treatment with PEA has been performed(181).

Cardiopulmonary exercise testing can be used to accurately quantify their exercise tolerance and assesses patients' respiratory and cardiovascular capacity. I used the indices of low peak VO_2 and high VE/VCO_2 to assess the level of functional limitation. The peak VO_2 is the maximum amount of oxygen that can be taken up by the tissues, and defines the cardiorespiratory performance, and is usually decreased in those with significant pulmonary vascular disease. VE/VCO_2 is the ratio of minute ventilation to production of carbon dioxide. This ratio increases when there is increased ventilation/perfusion mismatching, such as dead space ventilation, which is seen in pulmonary vascular disease, and specifically in thrombotic pulmonary vascular disease. It is of both diagnostic and prognostic value.

For patients to benefit from these well-established treatments, an accurate diagnosis is required. As described in Chapter 4, echocardiography remains the main screening investigation for pulmonary hypertension, mainly because it is inexpensive, widely available, and convenient to perform. Tricuspid regurgitation is used to estimate right ventricular systolic pressure but can over or underestimate pressure and is not present in up to 30% of patients(182). In addition, the reproducibility of echocardiography is variable, especially in those with pulmonary hypertension. *Sato et al.* demonstrated that there was a positive predictive value of 64.3% in estimation of the TAPSE in those with precapillary pulmonary hypertension when using echocardiography compared to cardiac magnetic resonance imaging (CMR), compared to 73.3% in those without pulmonary hypertension(190). The gold standard diagnostic investigation remains right heart catheterization (RHC)(53), in conjunction with a number of imaging modalities, namely computer tomography pulmonary angiography (CTPA) and CMR. RHC is an invasive investigation, which carries some associated risks and discomfort for patients. Ideally there would be an accurate non-invasive investigation, which would reliably provide the diagnosis without exposing patients to such risk.

There has been increasing use of CMR for the investigation and management of pulmonary arterial hypertension in recent years. This partly reflects increased availability, improved acquisition times and ease of use(7). CMR has several advantages over echocardiography, including in the assessment of LV and RV mass, volume, and ejection fraction, and is currently recognised as the gold

standard for assessment of the RV(8). CMR measurements are more reproducible than echocardiogram, making this a more attractive investigation to use as part of research studies(8).

Although CMR is valuable and reproducible for measuring chamber volumes, there is no reliable way of measuring pressure within the right ventricle. However, there are several ways that CMR may indicate the presence of increased RV and pulmonary artery pressure. Increased pulmonary vascular resistance can be detected via the observation of low flow within the main pulmonary artery, as seen on velocity-encoded CMR, when images are taken perpendicular to the pulmonary artery, immediately distal to the pulmonary valve(191). The main pulmonary arteries become enlarged in pulmonary hypertension because of pressure and volume overload. In idiopathic pulmonary arterial hypertension (IPAH), fibrous remodelling of the vascular wall leads to reduced distensibility of the PA, calculated as: $(PA \text{ maximum area} - PA \text{ minimum area}) / PA \text{ minimum area}$ (192). Pulmonary artery distensibility has been extensively researched using MRI imaging in various forms of PH. *Sanz et al* demonstrated that reduced pulmonary artery distensibility is reduced in those with exercise induced pulmonary hypertension and therefore is a sensitive measure for the early presence of disease(193). A reduction in pulmonary artery area change, a similar measurement, has also been shown to be a sensitive diagnostic tool in pulmonary hypertension and can predict clinical outcome(194).

In addition to the pulmonary artery, there is abnormal movement of the interventricular septum. At end-systole, there is shift of the septum from right to left, signifying pressure overload in the RV compared to the LV. The eccentricity index (EI) quantifies this septal flattening, and has the potential to indirectly indicate the pressure within the RV(154). This is defined as the ratio of the length of two perpendicular minor-axis diameters, one of which is bisected and is perpendicular to the interventricular septum (Figure 16). This measurement is obtained at end-systole and end-diastole(154). This has recently been validated for use in paediatric patients with pulmonary hypertension and in adults with IPAH(183). However, this has not been previously assessed in patients with chronic thromboembolic disease or CTEPH using either echocardiogram or CMR. The septal angle has been used in large populations to develop a regression equations to predict the presence or absence of PH in populations of patients with suspected PH including those with CTEPH using CMR (9, 10) and CTPA(195), showing promise for the use of interventricular shift in detection of disease.

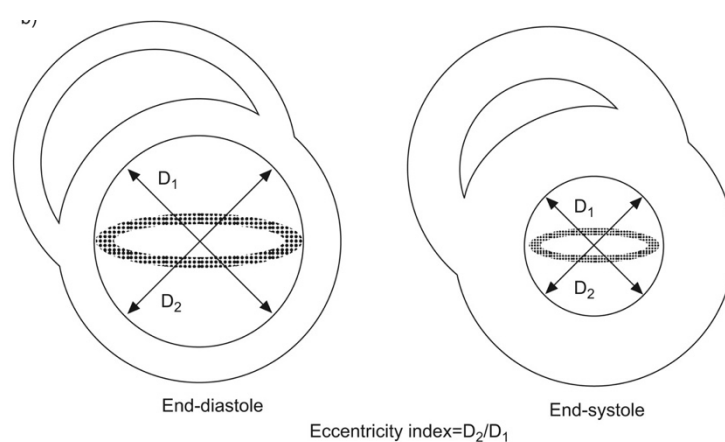


Figure 16. Pictorial description of how to measure the eccentricity index in diastole and systole(183).

4.1.2 Aims

It is hypothesised that systolic and diastolic eccentricity index is abnormal in those with CTEPH and is normal in those without resting pulmonary hypertension, even in the presence of thrombotic pulmonary vascular disease. Given that validated treatments thus far are based on the pre-2018 definition of pulmonary hypertension, I have used that definition (mPAP \geq 25mmHg, \geq 3 Wu and pulmonary artery wedge pressure of $<$ 15mmHg) for the patients in this study.

I aimed to:

- To evaluate differences between the eccentricity index in patients with and without pulmonary hypertension at rest, using CMR.
- To evaluate if systolic and diastolic eccentricity index is normal in those without resting pulmonary hypertension, even in the presence of CTEPD.
- To determine if distensibility of the main pulmonary arteries is reduced in both CTEPH and CTEPD compared to those without thrombotic pulmonary vascular disease.
- To measure peak blood flow within the pulmonary artery and calculate if this is lower in CTEPH and CTEPD than in controls.

4.2 Methods

Patients were identified from the electronic database in the Scottish Pulmonary Vascular Unit, based at the Golden Jubilee National Hospital, Glasgow. Thirty patients diagnosed with CTEPH since 2014 were identified (20 with proximal disease and 10 with distal disease), as only patients from this time onwards had CMR available for analysis. Direct comparison with 20 patients without resting pulmonary hypertension was made: 10 of these patients had chronic thromboembolic disease while the other 10 were patients had neither pulmonary hypertension nor thromboembolic disease. These were a group of patients who had been investigated in the SPVU and found at right heart catheter to have no evidence of pulmonary hypertension. The investigations were obtained contemporaneously.

Comparison of data from right heart catheter and CMR across groups was performed to assess for any differences that might allow me to predict the presence, or absence, of thrombotic vascular disease using non-invasive methods.

Finally, correlation of non-invasive measurements with right heart catheterisation indices was assessed to measure performance against well-defined diagnostic and prognostic investigations.

4.2.1 Cardiopulmonary exercise testing

Cardiopulmonary exercise testing was performed using an incremental cycle ergometer. The ramp rate was chosen by the physiologist, based on the participants' self-reported fitness, with the aim of exercising for 8-12 minutes.

4.2.2 Cardiac magnetic resonance imaging

CMR imaging was performed in the supine position on a 1.5-T magnetic resonance imaging scanner (Sonata Magnetom, Siemens, Erlangen, Germany) using an 8-channel cardiac coil. Short axis cine images were acquired using electrographic gating multislice balance steady state free precession sequence (20 frames per cardiac cycle, 8mm slice thickness, matrix 256x256; BW, 125kHz/pixel; TR/TE, 3.7/). Main pulmonary artery flow curve is captured using velocity-encoded CMR (VE-CMR), perpendicular to the pulmonary artery and performed during breath hold.

4.2.2.1 CMR analysis

RV and LV volumes was determined by automatic tracing endocardial borders of short axis stack obtained during breath-hold using. Images were analysed using the Circle Vascular Imaging (version 5.11 Calgary, Canada) with the observer blinded to the patients' clinical information. All borders were manually checked and corrected as needed.

I measured the eccentricity index at end systole and end diastole in the left and right ventricles at mid-ventricular level - defined as the level of the papillary muscles. The LV eccentricity index is defined as the ratio of the length of the two-perpendicular minor-axis diameters, one of which is bisected and perpendicular to the interventricular septum. As the LV is circular, this would be expected to be 1.0(154).

Main pulmonary artery distensibility will be determined from lumen area measurements at the moment of maximal flow and the moment of isovolumetric contraction to calculate $(PA \text{ maximum area} - PA \text{ minimum area}) / PA \text{ minimum area}$. Flow curves will be developed using the VE-CMR images obtained perpendicular to the pulmonary artery during breath hold.

4.2.3 Right heart catheterisation

All patients had undergone RHC within 4 days of CMR. The right heart catheters have all taken place at the Golden Jubilee National Hospital with an 8F Swan-Ganz, introduced using the Seldinger technique through the internal jugular or femoral vein. Hemodynamic parameters including the right atrial pressure, right ventricular pressure and pulmonary artery pressure and pulmonary artery wedge pressure were all taken at rest. Cardiac output was measured using the thermodilution method and PVR calculated after the procedure.

4.2.4 Statistical analysis

Data was stored on NHS password secure encrypted computers and will be analysed using Microsoft Excel and Graph Pad Prism version 9 (San Diego, CA, USA)

Students t-test or Mann-Whitney U test were employed depending on the distribution of the data. ANOVA was used to assess for differences between subgroups. Correlation analysis will be performed by Spearman analysis. Receiver Operator Curves will be used to identify clinically relevant thresholds that can be used to identify the presence of chronic thromboembolic pulmonary vascular disease. Bland Altman plots will be used to describe the agreements between investigations.

4.3 Results

50 patients were recruited to the study, including twenty patients with no pulmonary hypertension at rest and thirty with pulmonary hypertension, as shown in Figure 17. In the group with no pulmonary hypertension, ten had normal pulmonary vasculature and ten had chronic thromboembolic disease. In the group with pulmonary hypertension, twenty had central distribution of thromboembolic material and ten had distal distribution, as agreed by the multidisciplinary team at the Scottish Pulmonary Vascular Unity and the UK National Thromboendarterectomy Unit at Papworth Hospital, Cambridge.

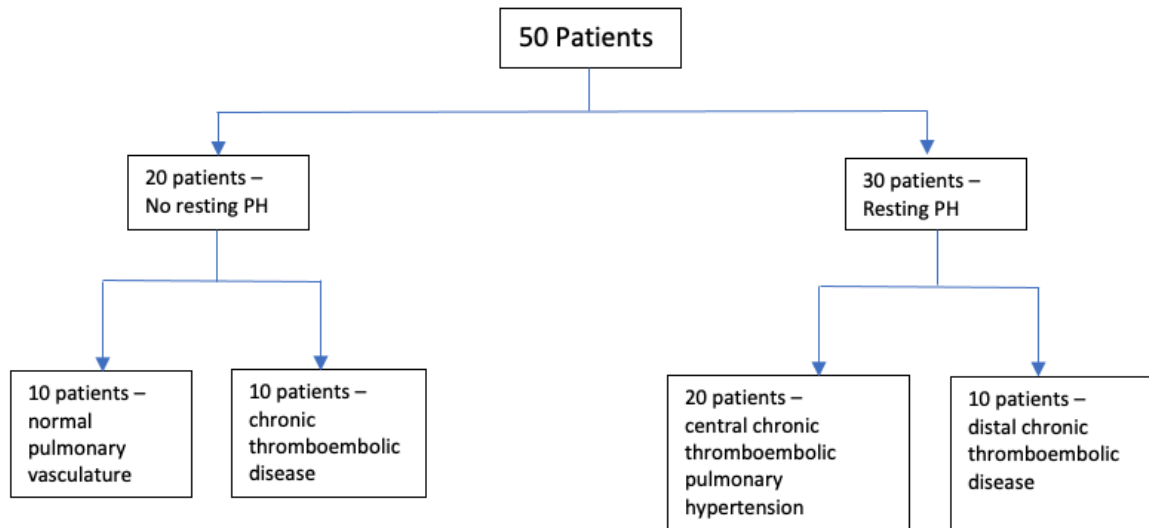


Figure 17. Patient recruitment to study.

The baseline variables between those with and without resting pulmonary hypertension are provided in Table 11. As expected, there were significant differences in haemodynamics between the groups, but there were no differences in age and sex between groups. A proportion of the CMR images have been assessed by a second reviewer, with minimal interobserver variability (R=0.9).

4.3.1 Assessing those with pulmonary hypertension

4.3.1.1 Baseline variables

In Table 11 I have shown the baseline variables of all patients, split between those with pulmonary hypertension at rest and those without. I have shown that there are no differences in age and sex ($p=0.79$ and $p=0.36$, respectively) between groups and that there are the expected differences in right heart catheter indices between groups, in keeping with pre-capillary pulmonary hypertension in those with CTEPH. The BMI is higher in the non-PH group. Of note, atrial pressure was significantly higher in patients with CTEPH compared to those without PH (6.0 ± 3.9 mmHg vs 3.2 ± 2.3 mmHg; $p=0.01$), which reflects RV dysfunction. There is a significantly higher end diastolic pressure in CTEPH (8.8 ± 4.3 mmHg vs 5.3 ± 2.6 mmHg; $p=0.01$), along with a higher mean pulmonary artery pressure (40.2 ± 11.4 mmHg vs 17 ± 4.4 mmHg $p=0.01$). The pulmonary artery wedge pressures are normal in both groups, with no significant differences between the groups, in keeping with pre-capillary disease in CTEPH. NT-proBNP was significantly higher in patients with CTEPH (1004 ± 1291 pg/ml vs 184 ± 155 pg/ml, $p=0.01$) but there was no significant difference in exercise capacity between groups.

Index	Non-PH, n=20 Mean (SD)	CTEPH, n=30 Mean (SD)	P-Value ⁺
Age (Years)	53.9 (17.5)	52.2 (15.9)	0.73
Sex (M)	8	16	0.36
BMI (kg/m ²)	32.3 (6.0)	28.4 (5.6)	0.03
RAP (mmHg)	3.2 (2.3)	6.0 (3.9)	<0.01
RVEDP (mmHg)	5.3 (2.6)	8.8 (4.3)	<0.01
mPAP (mmHg)	17 (4.4)	40.2 (11.4)	<0.01
PAWP (mmHg)	8.3 (3.4)	7.5 (3.6)	0.46
CO (L/min)	5.1 (1.1)	4.1 (0.9)	<0.01
CI (CO/BSA)	2.5 (0.6)	2.1 (0.4)	<0.01
PVR (wu)	1.9 (1.2)	8.5 (4.7)	<0.01
SvO ₂ (%)	73.1 (4.2)	63.5 (6.8)	<0.01
NT-proBNP (pg/ml)	184 (155)	1004 (1291)	0.01
6MWT distance (m)	407 (115)	389 (95)	0.55

Table 11. Baseline Variables between those with and without pulmonary hypertension.

⁺Unpaired T-test

BMI - Body Mass Index; RAP - Right Atrial Pressure; RVEDP - Right Ventricular End Diastolic Pressure; mPAP - mean Pulmonary Artery Pressure; PAWP - Pulmonary Artery Wedge Pressure; CO - Cardiac Output; CI - Cardiac Index; BSA - Body Surface Area; PVR - Pulmonary Vascular Resistance; Wu - Wood Units - SvO₂ - Mixed venous saturations.

4.3.1.2 Cardiopulmonary exercise testing

Mean CPET values for the two groups are in Table 12. There was no significant difference in the peak VO₂ between groups but there was a significantly higher VE/VCO₂ (49.6 ±11.5 vs 34.3 ±6.9; p=<0.01) in CTEPH.

	Non-PH, n=20 Mean (SD)	CTEPH, n=30 Mean (SD)	p-value ⁺
Peak VO ₂ ml/kg/min	16 (5.1)	13 (3.8)	0.13
V _E /V _{CO2}	34.3 (6.9)	49.6 (11.5)	<0.01

Table 12. Baseline Cardiopulmonary exercise tests between those with and without resting pulmonary hypertension

⁺Mann Whitney U test

4.3.1.3 Cardiac magnetic resonance imaging

CMR changes between those with pulmonary hypertension and those without have been assessed and are found in Table 13. There is a significantly lower left ventricular ejection fraction in the CTEPH group (57.7% ±10.6 vs 62.4% ±6.5; p=0.02) and a lower stroke volume (65.9mls vs 84.7mls; p 0.03). The right ventricular function is significantly worse in CTEPH, as might be expected. The RV has a higher end diastolic volume (184.8 ±22.6mls vs 163.1 ±18.7mls; p 0.04) and a lower ejection fraction (40.1% ±10.6 vs 55.6% ±10.4; p=0.01), in keeping with RV dysfunction. In addition, the systolic and diastolic eccentricity index are higher in CTEPH (1.3 ± 0.5 vs 1.0 ±0.01, p=<0.01: 1.2 ±0.2 vs 0.98 ±0.01, p=<0.01, respectively), the pulmonary artery distensibility is significantly reduced in CTEPH (0.13 ±0.1 cm² vs 0.46 ±0.23 cm²; p=0.01) but no significant differences are seen in peak blood flow.

Index	Non-PH, n=20 Mean (SD)	CTEPH, n=30 Mean (SD)	P-Value ⁺
Heart rate (bpm)	66 (9)	73 (16)	0.03
LVEDV (mls)	153 (35.2)	129 (39.1)	0.07
LVESV (mls)	58 (19.7)	56.2 (23.3)	0.66
LVEF (%)	62.4 (6.5)	57.7 (10.6)	0.02
SV (mls)	84.7 (22.6)	65.9 (18.7)	0.03
CO (L/min)	5.5 (1.2)	5.1 (1.2)	0.26
RVEDV (mls)	163.1 (55.9)	184.8 (49.7)	0.04
RVESV (mls)	75.8 (46.1)	112.9 (38)	<0.01
RVEF (%)	55.6 (10.4)	40.1 (10.6)	<0.01
Distensibility (cm ²)	0.46 (0.23)	0.13 (0.1)	<0.01
Systolic LVEI	1.0 (0.01)	1.3 (0.5)	<0.01
Diastolic LVEI	0.98 (0.01)	1.22 (0.2)	<0.01
Peak Blood Flow (mls/s)	386.1 (60)	365.1 (104)	0.23

Table 13. CMR indices in patients with chronic thromboembolic pulmonary hypertension versus those without

Bpm - beats per minute; *mls* - millilitres; *LVEF* = Left Ventricular Ejection Fraction, *LVEDV* = Left Ventricular End Diastolic Volume, *SV* = Stroke Volume, *CO* = Cardiac Output, *LV Mass* = Left ventricular Mass, *RVEF* = Right Ventricular Ejection Fraction, *RV EDV* = Right Ventricular Ejection Fraction, *RV EDV* = Right Ventricular End Diastolic Volume, *RV ESV* = Right Ventricular End Systolic Volume; *LVEI* - Left Ventricular Eccentricity Index

Given the novel cardiac indices were significantly different between those with pulmonary hypertension and those without, clinically relevant thresholds that could be used by clinicians to identify the presence of CTEPH were ascertained by Receiver Operator Curves (Figure 18). The threshold of the systolic LVEI for the detection of pulmonary hypertension is 1.1 (AUC=0.84, sensitivity 0.8, specificity 0.9), for diastolic LVEI is also 1.1 but is more specific (AUC=0.94,

sensitivity 0.8, specificity 0.9). The threshold for pulmonary artery distensibility is 0.28 (AUC=0.95, sensitivity 0.9, specificity 0.8). I found no relevant thresholds for peak blood flow.

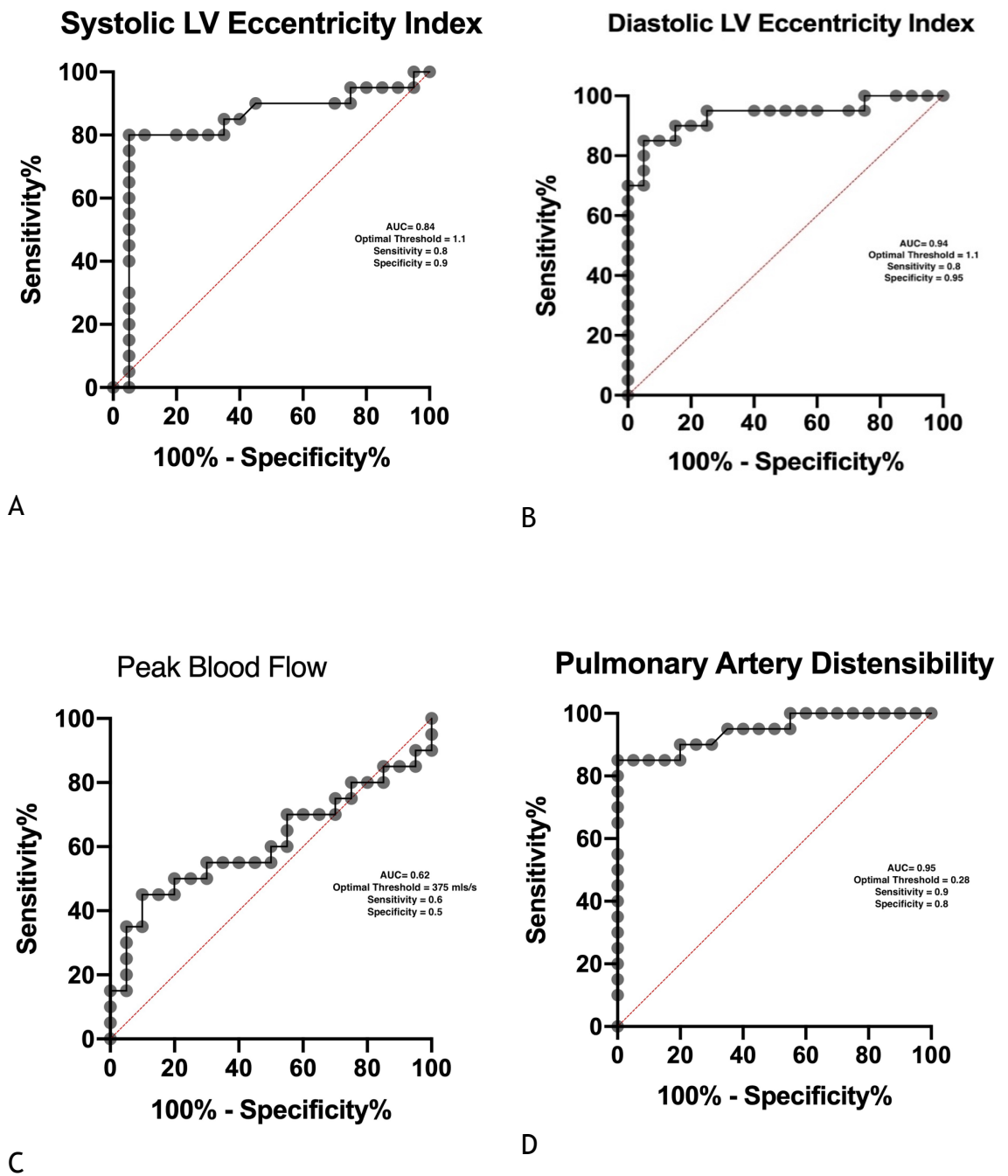


Figure 18. Receiver Operator Curves for thresholds of novel MRI indices

As can be seen in Figure 18, the systolic and diastolic eccentricity index and pulmonary artery distensibility have clear clinically relevant thresholds for detection of pulmonary hypertension. I combined these using the thresholds to assess for improved the diagnostic success for CTEPH (Figure 19). Whilst there is a significant difference between the groups, there is no improvement when combining the indices compared to using them independently.

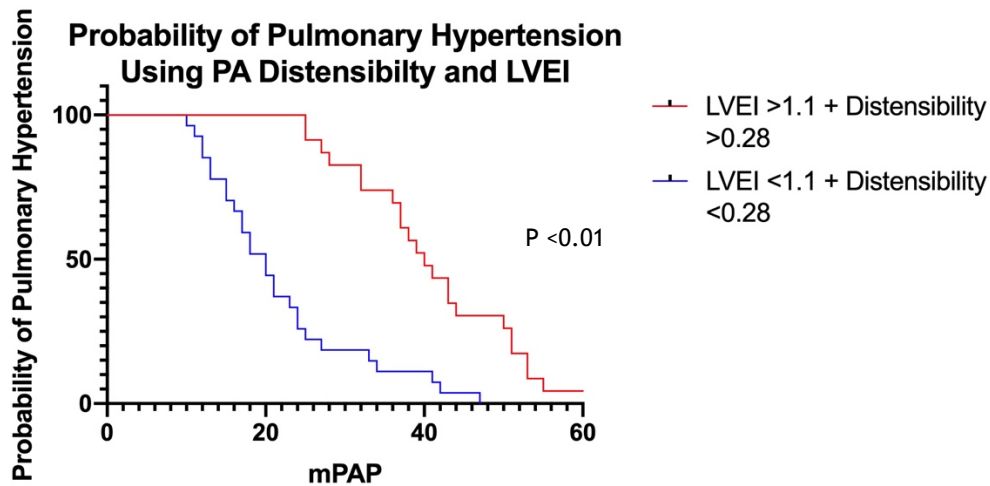


Figure 19. Sensitivity of pulmonary hypertension detection using combined systolic and diastolic LVEI with pulmonary artery distensibility.

4.3.2 Subgroups of chronic thromboembolic pulmonary vascular disease

4.3.2.1 Baseline variables

Table 14 shows the distribution of the variables across all four subgroups, using analysis of variance (ANOVA) to look for significant differences. The findings represent what might be expected in groups across the thrombotic vascular disease spectrum. There is a progressive rise in the mean pulmonary artery pressure ($p < 0.01$) and pulmonary vascular resistance ($p < 0.01$) and a reduction in the cardiac index ($p < 0.01$) and mixed venous saturations ($p < 0.01$).

Index	Normal Mean (SD) n=10	CTED Mean (SD) n=10	Proximal CTEPH Mean (SD) n=20	Distal CTEPH Mean (SD) n=10	P-Value ⁺
Age (Years)	46 (18.9)	61.8 (12.2)	51.9 (16.2)	65.7 (9.3)	0.01
BMI (kg/m ²)	30.4 (5)	34.1 (6.5)	28.5 (5.7)	29.7 (4.3)	0.08
RAP (mmHg)	3.4 (2.8)	2.9 (1.9)	6.3 (3.9)	5.6 (4.1)	0.04
EDP (mmHg)	6.2 (2.8)	4.3 (2.2)	8.9 (4.4)	8.7 (4.4)	0.01
mPAP (mmHg)	14.1 (3.4)	19.9 (3.1)	41.1 (13.5)	38.3 (4.4)	<0.001
PAWP (mmHg)	7.8 (3.0)	8.7 (3.9)	7.4 (3.4)	7.7 (4.1)	0.82
CO (mmHg)	5.6 (1.1)	4.5 (0.8)	4.3 (0.9)	3.9 (0.8)	<0.001
CI (CO/BSA)	2.9 (0.6)	2.2 (0.2)	2.2 (0.4)	2.0 (0.4)	<0.001
PVR (Wu)	1.2 (0.9)	2.5(1.1)	8.6 (4.5)	8.3 (2.7)	<0.001
SvO ₂ (%)	74.7 (5.1)	71.5 (2.2)	64.45 (6.7)	61.6 (7.0)	<0.001
NT-proBNP (pg/ml)	198 (162)	173 (157)	987 (1296)	1037 (1349)	0.09
6 MWT (m)	431 (129)	383 (101)	416 (100)	310 (127)	0.07

Table 14. ANOVA of the haemodynamic values of across all groups
SD - Standard Deviation; BMI - Body Mass Index; mmHg - millimetres of mercury; RAP - Right Atrial Pressure; EDP - End Diastolic Pressure; mPAP - mean Pulmonary Artery Pressure; PAWP - Pulmonary Artery Wedge Pressure; CO - Cardiac Output; CI - Cardiac Index; BSA - Body Surface area; PVR - Pulmonary Vascular Resistance; SvO₂ - Mixed venous saturations; NT-proBNP - N-Terminal Pro Natriuretic Peptide; 6MDT - 6-minute walk test distance

4.3.2.2 Cardiopulmonary exercise testing

I have demonstrated significant changes in cardiopulmonary exercise testing. Those with distal CTEPH in our population were unable to perform cardiopulmonary exercise testing due to physical limitations, and, as such there are no data available for this group. I have displayed data for the other three groups. Between groups, there was a progressive decline in the peak VO₂ (p=0.02) and a progressive rise in the V_E/V_{CO2} (p<0.01), showing that those with CTEPH have greater dead-space ventilation.

	Normal	CTED	Proximal CTEPH	p-value ⁺
VO ₂ ml/kg/min	17.7 (5.3)	14.4 (4.7)	12.8 (3.8)	0.02
V _E /V _{CO2}	31.7 (5.2)	36.9 (7.7)	49.67 (11.81)	<0.001

Table 15. Baseline Cardiopulmonary exercise testing between subgroups of thrombotic pulmonary vascular disease

⁺ANOVA

4.3.2.3 Cardiac magnetic resonance imaging

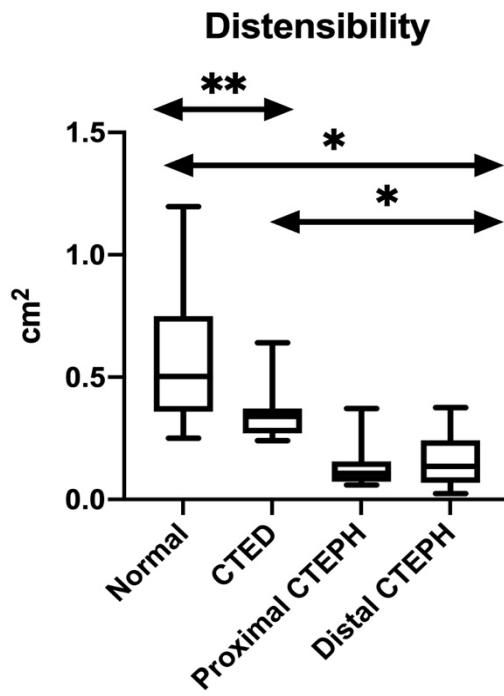
The CMR indices of the subgroups of thrombotic pulmonary vascular disease are shown (Table 16). Of note, there is a progressive decline in the RV ejection fraction (p<0.01), in keeping with RV dysfunction.

Index	Normal n=10 Mean (SD)	CTED n=10 Mean (SD)	Proximal CTEPH, n=20 Mean (SD)	Distal CTEPH, n=10 Mean (SD)	P- Value ⁺
Heart rate (bpm)	73 (5)	59 (7)	78 (11)	70 (12)	0.002
LVEDV (mls)	146.8 (34.8)	158.3 (36.6)	132.5 (37.9)	125.4 (37.3)	0.17
LVESV (mls)	56.5 (25.4)	59.5 (12.9)	53.5 (23)	56.9 (22.8)	0.91
LVEF (%)	62.5 (8.8)	62.3 (3.5)	57.3 (8.9)	55 (9.5)	0.10
SV (mls)	80.9 (14.6)	88.3(28.9)	65.2 (21.8)	67.3 (10.9)	0.02
CO (L/min)	5.8 (1)	5.2 (1.3)	5.4 (1.4)	4.5 (0.6)	0.11
RVEDV (mls)	171.1 (70.2)	155 (39)	184.1 (43.9)	192.6 (47.9)	0.34
RVESV (mls)	86.8 (62)	64.9 (19.7)	110.7 (42.3)	112.6 (34.4)	0.03
RVEF (%)	52.9 (12.6)	58.3 (7.2)	40.3 (12.7)	40 (5)	<0.01

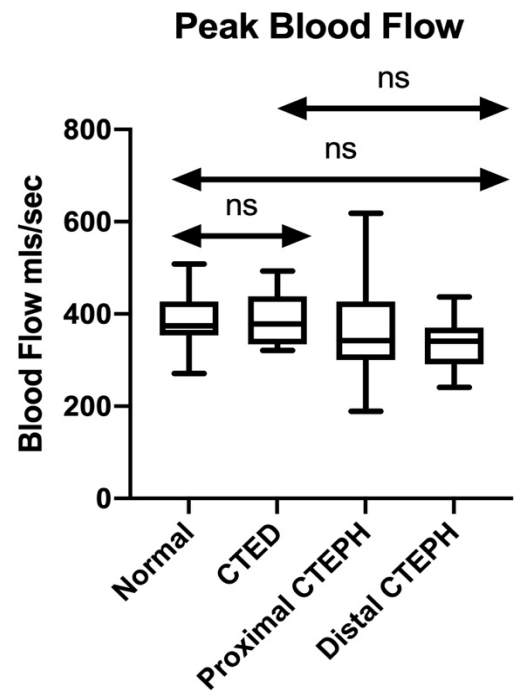
Table 16. Baseline CMR indices between subgroups of thrombotic pulmonary vascular disease
⁺ANOVA

Bpm - beats per minute; mls - millilitres; LVEF = Left Ventricular Ejection Fraction, LVEDV = Left Ventricular End Diastolic Volume, SV = Stroke Volume, CO = Cardiac Output, LV Mass = Left ventricular Mass, RVEF = Right Ventricular Ejection Fraction, RV EDV = Right Ventricular Ejection Fraction, RV EDV = Right Ventricular End Diastolic Volume, RV ESV = Right Ventricular End Systolic Volume

Given the differences seen in the CTEPH group compared to the non-PH group, the novel geometric cardiac indices were plotted for the four subgroups to assess for any ways of differentiating them, which could be used in clinical practice (Figure 20).



A



B

C

D

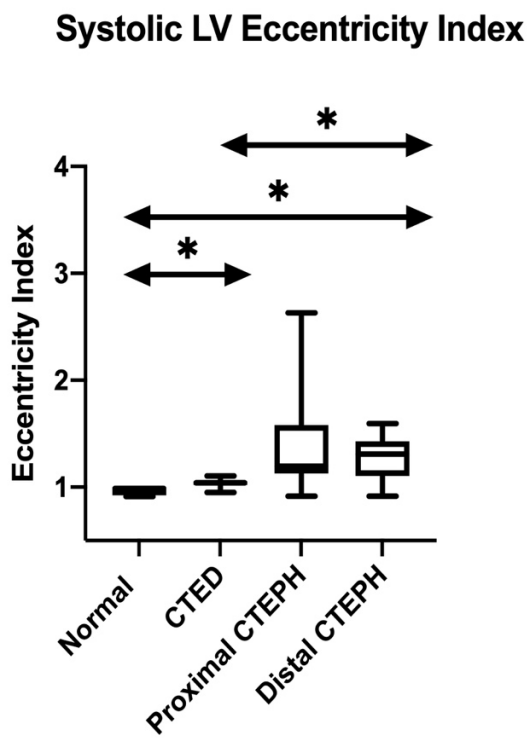


Figure 20. Novel MRI indices in no pulmonary vascular obstruction, CTEPD, proximal and distal CTEPH

P-value = ANOVA
 * = <math><0.01</math> ** = <math><0.05</math>

A - Pulmonary Artery Distensibility, B - Peak Blood Flow in the Pulmonary Artery

C - Systolic Left Ventricular Eccentricity Index, D - Diastolic Left Ventricular Eccentricity Index

4.3.3 Normal pulmonary vasculature versus CTEPD

Patients without pulmonary hypertension were divided into two groups - those without evidence of pulmonary vascular obstruction on CT and V/Q imaging (normal controls), and those with residual radiological proven thromboembolic disease. The differences in baseline variables and novel CMR indices were evaluated (Table 17). There were no significant differences between age and sex. Although the mean pulmonary artery pressures and pulmonary vascular resistance were within the normal range for both groups, mPAP (19.9 ± 3.1 vs 14.1 ± 3.4 mmHg; $p < 0.01$) and pulmonary vascular resistance (2.5 ± 1.1 vs 1.2 ± 0.9 WU; $p = 0.01$) were higher in the CTEPD group, in keeping with pulmonary vascular occlusions. In addition, there was a significantly lower pulmonary artery distensibility ($0.35 \pm 0.1 \text{ cm}^2$ vs $0.57 \pm 0.4 \text{ cm}^2$; $p = 0.03$) and a significantly higher LVEI in systole (1.03 ± 0.04 vs 0.97 ± 0.04 ; $p < 0.01$) and diastole (1.02 ± 0.05 vs 0.96 ± 0.03 ; $p = 0.02$) in the CTEPD group compared to normal but no significant difference in peak blood flow between these groups. Threshold analysis for identifying the presence of CTEPD using systolic and diastolic LVEI is 1.0 and pulmonary artery distensibility is 0.37 cm^2 .

Index	Normal (n=10) Mean (SD)	CTEPD (n=10) Mean (SD)	P-Value ⁺
Age (Years)	46 (18.9)	62 (12.2)	0.04
Sex (Male)	4	4	0.65
BMI (kg/m ²)	30.4 (5)	34.1 (6.5)	0.17
RAP (mmHg)	3.4 (2.8)	2.9 (1.9)	0.64
mPAP (mmHg)	14.1 (3.4)	19.9 (3.1)	<0.01
PAWP (mmHg)	7.8 (3)	8.7 (3.9)	0.57
CO (mmHg)	5.6 (1.1)	4.5 (0.8)	0.02
CI (L/min/m ²)	2.9 (0.6)	2.2 (0.25)	<0.01
PVR (Wu)	1.2 (0.9)	2.5 (1.1)	0.01
SvO ₂ (%)	74.7 (5.1)	71.5 (2.2)	0.09
Distensibility	0.57 (0.3)	0.35 (0.1)	0.03
Systolic LVEI	0.97 (0.04)	1.03 (0.04)	<0.01
Diastolic LVEI	0.96 (0.03)	1.02 (0.05)	0.02
Peak Blood Flow (mls/s)	384.3 (64)	387.8 (59.3)	0.97

*Table 17. Differences between patients with normal pulmonary vasculature and CTEPD group
⁺Unpaired T-Test performed for normal distributed variables, Mann Whitney U performed for others
BMI - Body Mass Index; RAP - Right Atrial Pressure; EDP - End Diastolic Pressure; mPAP - mean Pulmonary Artery Pressure; PAWP - Pulmonary Artery Wedge Pressure; CO - Cardiac Output; CI - Cardiac Index; PVR - Pulmonary Vascular Resistance; SvO₂ - Mixed venous saturations; cm² - centimetre squared; LVEI - Left Ventricular Eccentricity Index; mls/s - millilitres per second*

4.3.4 Correlations between CMR Indices and established markers of pulmonary hypertension severity

In pulmonary hypertension, there are a number of indices, both physiological and haemodynamic, that have proven to correlate well with survival(53). In the absence of being able to directly correlate the efficacy of these MRI indices with survival in this study, I assessed for a correlation between these well-established indices with our novel CMR indices (Table 18). The eccentricity indices correlated well with right heart catheter measurements and exercise capacity. The distensibility correlated well with NT-proBNP ($p<0.02$). Despite peak blood flow not being useful in the detection of CTEPH, there was a correlation with pulmonary vascular resistance ($p<0.01$) and mean pulmonary artery pressure ($p<0.02$). There was good correlation for all MRI indices and VO_2 and with the systolic LVEI and V_E/V_{CO_2} ($p<0.01$).

Index	Systolic LVEI*	Diastolic LVEI*	Distensibility*	Peak Blood Flow*
	r-value (p-value)	r-value (p-value)	r-value (p-value)	r-value (p-value)
RAP (mmHg)	0.32 (0.02)	0.32 (0.02)	-0.11 (0.43)	-0.07 (0.61)
EDP (mmHg)	0.31 (0.02)	0.36 (<0.01)	-0.08 (0.59)	-0.12 (0.41)
mPAP (mmHg)	0.74 (<0.01)	0.75 (<0.01)	-0.27 (0.06)	0.33 (0.02)
CI (CO/BSA)	-0.43 (<0.01)	-0.41 (<0.01)	-0.09 (0.53)	0.33 (0.02)
PVR (Wu)	0.72 (<0.01)	0.72 (<0.01)	-0.21 (0.14)	-0.40 (<0.01)
SvO2 (%)	-0.65 (<0.01)	-0.68 (<0.01)	0.15 (0.3)	0.61 (<0.01)
NT-proBNP (pg/ml)	0.34 (0.03)	0.28 (0.08)	-0.38 (0.02)	-0.04 (0.83)
6MWT (m)	-0.71 (0.01)	-0.78 (<0.01)	0.77 (<0.01)	0.18 (0.29)
VO ₂ ml/kg/min	0.7 (<0.01)	0.9 (<0.01)	0.9 (<0.01)	-0.6 (<0.01)
V _E /V _{CO2}	0.4 (<0.01)	0.2 (0.2)	-0.04 (0.9)	-0.3 (0.05)

Table 18. Correlation of prognostic indices with novel geometric cardiac MRI indices.

*Spearman Correlation

RAP - Right Atrial Pressure; EDP - End Diastolic Pressure; mPAP - mean Pulmonary Artery Pressure; PAWP - Pulmonary Artery Wedge Pressure; CO - Cardiac Output; CI - Cardiac Index; BSA - Body Surface area; PVR - Pulmonary Vascular Resistance; SvO₂ - Mixed venous saturations; NT-proBNP - N-Terminal Pro Natriuretic Peptide; 6MDT - 6-minute walk test distance

4.3.5 Comparing cardiac magnetic resonance imaging with echocardiography

Although CMR is increasingly used to assess cardiac function, its use is not ubiquitous. Echocardiography remains the main screening tool for pulmonary hypertension and is both inexpensive and more widely available. As such, I aimed to correlate the assessment of the eccentricity index using echocardiography and CMR, which can be seen in the Bland Altman Plots in Figure 21. There is a good correlation between the diastolic LVEI measured by echocardiogram and CMR, but a low correlation between the systolic LVEI.

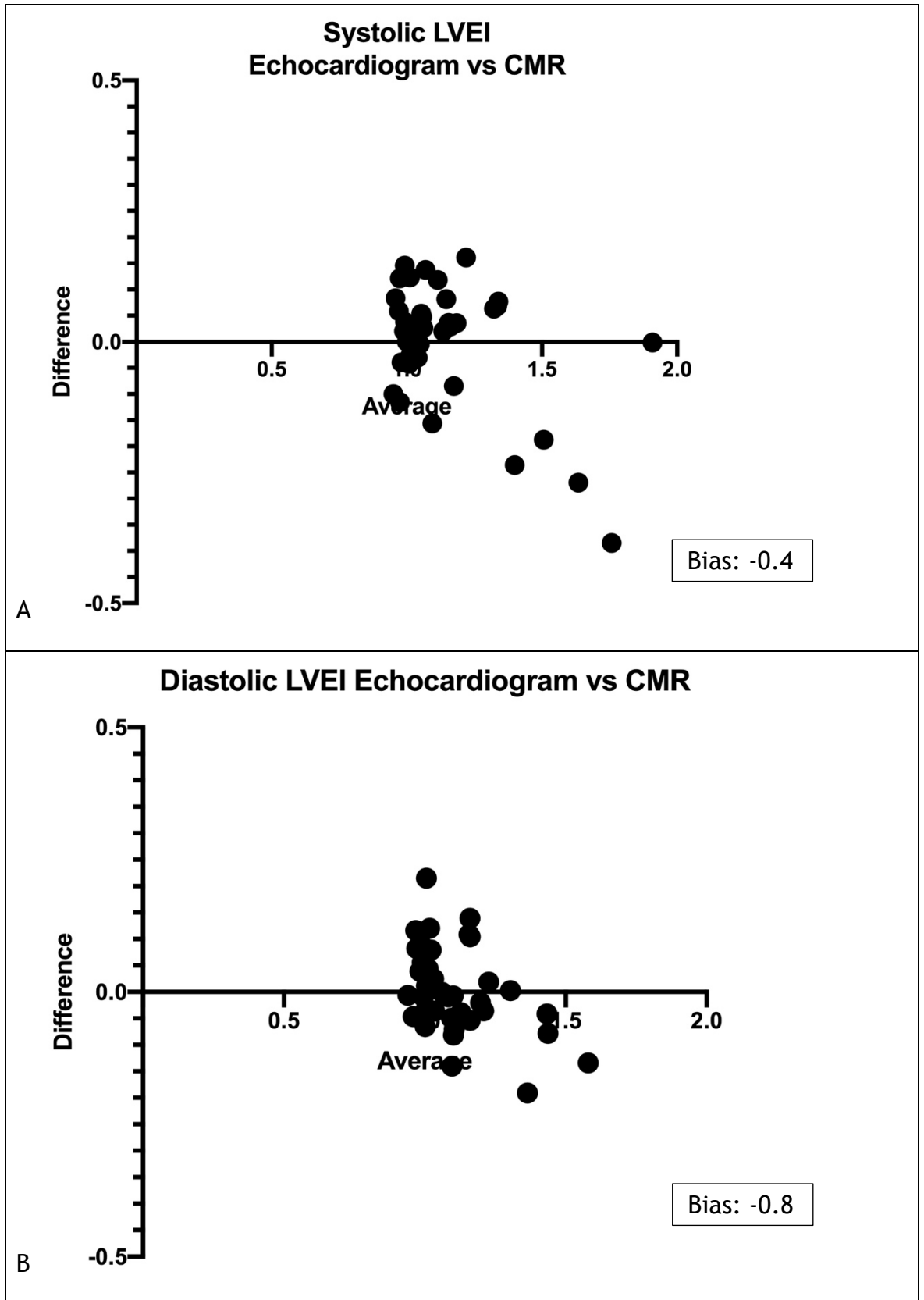


Figure 21. Bland-Altman Comparison of Echocardiogram and CMR when measuring Systolic (A) and Diastolic (B) LV Eccentricity Index.

4.4 Discussion

In this retrospective cohort study of patients, I have demonstrated three important findings. Firstly, that elevated EI, both in systole and diastole, and reduced pulmonary artery distensibility are predictive of the presence of pulmonary hypertension in CTEPH. Secondly, both EI and pulmonary artery distensibility could discriminate between the normal, CTEPD and CTEPH population. Finally, both systolic and diastolic EI correlate with clinical markers of outcome.

4.4.1 Analysis of pulmonary hypertension compared to controls

4.4.1.1 Baseline demographic variables

I have demonstrated differences in novel geometric indices between patients with chronic thromboembolic pulmonary hypertension compared with control subjects. The differences in the haemodynamic indices are demonstrated, which is to be expected, but lends confidence to the validity of the data. The pulmonary vascular resistance and the NT-proBNP levels of the CTEPH groups are markedly raised, suggesting that this cohort have advanced disease. However, this is not reflected in the functional capacity, as measured by the 6-minute walk distance. These findings are explained by the presence of thromboembolism within the pulmonary vasculature, limiting blood flow, leading to increased pressure within the pulmonary vasculature right sided cardiac chambers. The lack of difference in the 6-minute walk distance may be explained by a selection bias. The patients included in the study were patients who were able to undergo all investigations, including cardiopulmonary exercise test. To glean meaningful information from a CPET, the patient must have a performance status that is compatible with exercising for up to twelve minutes against resistance. This is usually assessed initially by performing a 6-minute walk distance test and, if patients have very low walk distance, they do not undergo CPET. Therefore, by default, those who have done a CPET will have 6MWD reflective of functional class III or above.

4.4.1.2 Cardiac magnetic resonance imaging

When comparing the cardiac MRI indices between those with pulmonary hypertension and those without. As expected, resting heart rate of those with CTEPH was significantly higher than it was in patients without PH. Patients with pulmonary hypertension have a fixed stroke volume and to improve cardiac output, they must increase their resting heart rate. There was a trend for mean left ventricular volumes to be lower in patients with CTEPH, but this did not meet statistical significance. This can be explained, at least in part, by the fluid and pressure overloaded right ventricle, compressing the interventricular septum towards the left side. The mean right ventricle ejection fraction is also significantly reduced in those with pulmonary hypertension, suggesting there is maladaptation of the right ventricle with reduced systolic function.

Whilst there are clear differences in the volumes of the cardiac chambers between the groups, for the individual patient, it is not always easy to detect the changes in early or mild disease. As such, it is useful to have more indices that may be reflective of patients in these positions. Therefore, I examined the utility of the eccentricity index measured at end systole and end diastole. This measurement helps to quantify the shift of the interventricular septum, as is seen in pulmonary hypertension. Previous studies have shown that systolic and diastolic eccentricity are increased in patients with CTEPH. *Swift et al* demonstrated in a study from ASPIRE in 2012 that a systolic EI of 1.6 and diastolic EI of 1.3 in 59 patients was diagnostic of pulmonary hypertension in those with CTEPH. The eccentricity index is significantly increased in those with CTEPH in both of these cardiac phases, which suggests the septum is shifted towards the left side, leading to a reduction in the left ventricular volume. Although this has previously been demonstrated in CTEPH using CMR(196), this is the first time it has been investigated in relation to functional limitation, measured by CPET. Pulmonary artery distensibility is seen to be significantly reduced in those with CTEPH, compared to those without resting pulmonary hypertension. This can be explained because in those patients with CTEPH, there is dilatation of the pulmonary artery such that the connective tissues are stretched to their maximal capacity in order to accommodate the increased volume. Over time, the pressure rises within the vessel as there is no further accommodation possible. In the healthy lung, the distensibility of the pulmonary artery allows the reduction in the variability of pressure during systole and diastole, such that there is a more constant blood flow through the vessel. In CTEPH, this mechanism appears to be lost due to the increased vessel volumes and there is little difference between the volume of the vessel during systole and diastole. This has been demonstrated to be significantly different between those with CTEPH and those without and shows promise for use in the non-invasive detection of pulmonary hypertension using CMR. Although ROC curves were used in order to detect thresholds that would detect disease, this would ideally be trialled in a test population in order to validate this finding.

Peak blood flow was also analysed as part of the study as it has shown promise when used to detect the presence of pulmonary arterial hypertension(197). I have shown a numerically lower mean value in those with pulmonary hypertension, but this did not meet statistical significance when assessing the peak blood flow between those with and those without pulmonary hypertension. This may be because the presence of thrombus within pulmonary vessels causes occlusion proximally, meaning that the peak blood flow velocity overall was reduced in those with CTEPH. However, often immediately after an area of stenosis, there is post stenotic dilatation of the vessel, which will alter the dynamics of the blood flow and therefore reduce the reliability of this measurement in occlusive pulmonary vascular disease. This is different to the pathology seen in Group 1 pulmonary hypertension, where there is progressive narrowing in the whole vessel, leading to an overall reduction in peak blood flow.

4.4.2 Comparing the subgroups of pulmonary vascular disease

Given the findings seen between those with and without resting pulmonary hypertension, I evaluated the differences between subgroups of those with normal pulmonary vasculature, chronic thromboembolic pulmonary disease (CTEPD), proximal CTEPH and those with distal CTEPH. I made these further assessments in order to understand whether they have utility in evaluating the point at which the patient lies on the spectrum of thrombotic pulmonary vascular disease.

4.4.2.1 Baseline variables

Although there were significant differences across the groups for a number of the indices measured in right heart catheterisation, there are only a few that could lend a signal that they could be used to detect the different diseases. I have demonstrated that the mean pulmonary artery pressure was at the upper limit of normal in the CTEPD category and was higher in those with proximal CTEPH. This is to be expected given the disease definitions. The cardiac output showed a progressive decline from normal in those without pulmonary vascular obstruction to those with distal obstruction. There are variations in body mass index, but taking into account body surface area, a decline is also seen in

cardiac index. There is also a progressive rise in pulmonary vascular resistance, as might be expected as the amount of pulmonary vascular occlusion increases in these cohorts, there is a rise in resistance. Again, the pulmonary vascular resistance is nearing the upper limit of normal in those with CTEPD but there were no significant differences between those with proximal occlusion versus those with distal disease. Mixed venous saturations also show a significant decline across the four subgroups, which would reflect the reduction in cardiac output, meaning that oxygen extraction from muscle is increased.

4.4.2.2 Cardiac magnetic resonance Imaging

I have shown a significant difference in stroke volume with those in the CTEPH group having lower values. This may, in part, be due to the compression of the left ventricle by the dilated right ventricle, leading to poorer left ventricular filling. Those in the CTEPH groups had larger right ventricular end-diastolic volume and the left ventricular end-diastolic volumes are lower. As described in the Frank-Starling mechanism, a more poorly filled left ventricle will lead to a lower stroke volume. The larger right ventricular volumes and significantly lower right ventricular ejection fraction in the CTEPH group demonstrates the maladaptation of the right ventricle, with reduced systolic function in response to chronically increased afterload.

Interestingly, although there are some significant differences in the volumetric measurements in the RV, there are more significant changes seen in the pressure related indices, such as the LV eccentricity index in systole and diastole. The lower LV volumes and higher RV volumes in those with proximal and distal CTEPH are not significantly different enough to confidently identify where a patient lies on the disease spectrum. However, incorporating the eccentricity index may lend some more confidence to the clinician that there is the presence of chronic thromboembolic disease, or signs of pulmonary hypertension. I have shown significant differences between normal groups and those with CTEPD. Similarly, I have shown significant differences between those with CTEPD and CTEPH.

In addition, I have shown that there is reduced pulmonary artery distensibility in those with CTEPD compared to normal patients, helping the clinician identify those with thrombotic disease, even in the absence of pulmonary hypertension. This difference can be explained by the thrombotic exclusion distally, leading to the pulmonary artery stretching to accommodate the blood volume during the cardiac cycle. This is thought to be one of the first phases in adaptation to chronically raised pressure and is clearly demonstrated here even in the absence of pulmonary hypertension. In addition, there is a further reduction in pulmonary artery distensibility in those with CTEPH, but no difference between those with proximal or distal disease. Initially, these pressure-related indices could be used to help guide the clinician in identifying those who require invasive investigations. More work is required to establish the reliability of these indices for routine clinical use, but they have promise for use in identifying the presence of disease. I have, however, not demonstrated any clear relationship of peak blood flow velocity in the thrombotic disease spectrum: there was no observed role for its use in identifying pulmonary hypertension from normal pressure, or in identifying any subgroup. It is possible this is related to thrombus distribution in these conditions, and so more work is required to establish if there is a role for this parameter in helping to identify those with CTEPD or CTEPH.

4.4.3 Correlating CMR findings with echocardiogram and CPET

Although echocardiography is more widely available, CMR is recognised as the gold standard for evaluation of cardiac function in pulmonary hypertension and, specifically, right ventricular function. There is less interobserver variation and CMR is more reliable for measurement of function. However, it is more expensive, time consuming and less available. Quality images depend largely on breath holding, which can be challenging in patients with pulmonary hypertension.

Perhaps unsurprisingly, given the overall relationship between echocardiogram and CMR eccentricity index measurements seen in the Bland-Altman plots in Figure 21, similar findings are observed when looking at correlations between CMR eccentricity index with invasive haemodynamic indices, exercise tolerance and NT-proBNP. I have shown that, although the distensibility of the main pulmonary artery is reduced in pulmonary hypertension and could be a useful tool in the detection of the disease, I have not demonstrated a good correlation between this with haemodynamic measurements. I have not shown a relationship between peak blood flow and these indices. However, given the small sample sizes, further, larger, studies should be performed to further assess these.

To further assess the correlation of CMR indices with exercise tolerance, the measurements from CPET were assessed. The 6MWD is a submaximal test, in that patients will not be expected to reach their maximal heart rate capacity during the investigation and can be influenced by several external factors, such as musculoskeletal issues, or increased BMI, which can be negated using a cycle ergometer. The novel CMR indices of the eccentricity indices and pulmonary artery distensibility have shown good correlation with the cardiopulmonary exercise tests. The peak blood flow did not show any correlation with the cardiopulmonary exercise testing values in this study.

4.4.4 Strengths and weaknesses

Age and sex matched patients across the spectrum of thrombotic pulmonary vascular obstruction have been included in this study. The comprehensive investigations performed have all been contemporaneous and the diagnoses agreed by two expert multidisciplinary meetings, namely the Scottish Pulmonary Vascular Unit and the National thromboendarterectomy centre for the UK, based in Royal Papworth Hospital in Cambridge. The investigations have all been performed by experts in their fields, reducing the chance of potential errors.

Despite the strengths of the study, there are recognised weaknesses. Firstly, the study is retrospective. As such, there are some data missing, such as cardiopulmonary exercise tests in those with distal CTEPH. Secondly, there are some data points missing from the investigations that I would have liked to assess more closely, such as the ratio of dead-space over tidal volume (V_D/V_T). However, arterial blood gas samples were not always obtained during CPET and, as such, this could not be assessed or calculated retrospectively. Finally, assessing the use of these findings for the impact on longer-term outcomes for those who are unable to have surgical intervention would be of use, but long term follow up data are required for this. The patients selected for this study were included because of their full complement of data from investigations, and in particular those with proximal CTEPH who had CPET. This will incur some level of bias in the selection because these patients have to be of a sufficient functional class to perform a CPET and therefore, by default, the most functionally limited have not be included. However, the detection of early subtle disease is perhaps more important than that of significant end stage pulmonary vascular thrombotic disease.

4.4.5 Implications for current practice

The assessment of the right ventricle is central to the investigation of clinically relevant thrombotic pulmonary vascular disease. The quantitative evaluation of the RV is challenging due to the shape of the chamber and the RV wall mass is much less than that of the LV. There are often areas of poorly defined trabeculae in the RV, making volume measurements challenging. Whilst echocardiography is the most widely available, safe, and inexpensive method of evaluating cardiac function, there are some limitations which make assessment difficult. In those with large body habitus, or chest wall deformities, achieving good views of the RV can be challenging. As such, images of the RV free wall can be poor, which introduces a subjective assessment by using regional parameters to estimate RV function. In addition, tricuspid regurgitation is required for the assessment of PA pressure by echocardiography and is not present in 30% of the population. Meanwhile, imaging the LV is more reliable than the RV using both echocardiogram and CMR. The well-defined endocardial borders serve to reduce the challenges when measuring volumes. The LV muscular volume is six-fold that

of the RV, making identification of borders easier. As such, measuring the LV eccentricity index if there is suspicion of pulmonary vascular disease should be performed and reported as routine, in addition to the other indices, if they are present.

Although CMR carries its own challenges because of cost, availability, time taken to perform the imaging and local expertise in its interpretation, CMR imaging overcomes some of the challenges posed by echocardiography. The free wall and endocardial borders are well defined, making volume measurements more reliable and reproducible than that seen on echocardiograms, and minimises the subjective element to their interpretation. Accurate RV ejection fraction can be measured, which may give an indication to raised pulmonary artery pressure. In the absence of measurements that can be used to estimate pressure, measuring the eccentricity index in systole and diastole, and the pulmonary artery distensibility, may provide a sensitive indication as to the presence of pulmonary hypertension in those with thrombotic pulmonary vascular disease.

4.5 Conclusions

In this retrospective cohort study of patients, I have demonstrated the following:

- an elevated eccentricity index, both in systole and diastole, and a lower pulmonary artery distensibility is associated with the presence of pulmonary hypertension in patients who suspected of having CTEPH.
- A raised LVEI (>1.1) has a high sensitivity and specificity of determining patients with the presence of PH on CMR and that both EI and pulmonary artery distensibility can differentiate between the normal and CTEPH population.
- Further work is required to establish these findings in a prospective manner and to assess the benefits of using these investigations to predict long term outcomes.

5 The Effect of Exercise Rehabilitation on Cardiac Function in Precapillary Pulmonary Hypertension, as Measured by Cardiac Magnetic Resonance Imaging

5.1 Background

5.1.1 Precapillary pulmonary hypertension

Precapillary pulmonary hypertension describes pulmonary hypertension due to pulmonary vascular remodelling. This incorporates group I, group III and group IV of the most recent classification of pulmonary hypertension(64). This diagnosis requires mPAP of $>20\text{mmHg}$, pulmonary vascular resistance of $>3\text{Wu}$ and a PAWP of $<15\text{mmHg}$ as measured by right heart catheter. Post-capillary disease is caused by group II which is a consequence of left heart. Group V disease can be pre- or post- capillary. As such, an accurate wedge pressure is essential to avoid erroneous classification of the disease. As described by the WHO, there are a number of causes of pulmonary hypertension. Clinicians must consider all possible comorbidities in a patient to conclude the correct diagnosis, which will then dictate the treatments. There are several treatments available to patients with precapillary pulmonary hypertension, indeed there is a potential cure available to those with central chronic thromboembolic pulmonary hypertension, but should the treatments be offered to those with an erroneous diagnosis, there is potential for harm.

5.1.2 Treatment of Precapillary pulmonary hypertension

Currently, the main treatment options for pulmonary hypertension are pharmacological. The choice of medical therapy depends on risk stratification at the time of baseline assessment and in response to therapy already administered. The European Respiratory Society and European Society of Cardiology guidelines use a multiparametric assessment in order to stratify a patient into low- intermediate- or high-risk groups for 1-year mortality. This strategy includes clinical indices, functional and exercise capacity, right ventricular function and haemodynamic indices to quantify risk(53).

Determinants of prognosis ^a (estimated 1-year mortality)	Low risk <5%	Intermediate risk 5–10%	High risk >10%
Clinical signs of right heart failure	Absent	Absent	Present
Progression of symptoms	No	Slow	Rapid
Syncope	No	Occasional syncope ^b	Repeated syncope ^c
WHO functional class	I, II	III	IV
6MWD	>440 m	165–440 m	<165 m
Cardiopulmonary exercise testing	Peak $\dot{V}O_2$ >15 ml/min/kg (>65% pred.) VE/ $\dot{V}CO_2$ slope <36	Peak $\dot{V}O_2$ 11–15 ml/min/kg (35–65% pred.) VE/ $\dot{V}CO_2$ slope 36–44.9	Peak $\dot{V}O_2$ <11 ml/min/kg (<35% pred.) VE/ $\dot{V}CO_2$ slope ≥45
NT-proBNP plasma levels	BNP <50 ng/l NT-proBNP <300 ng/l	BNP 50–300 ng/l NT-proBNP 300–1400 ng/l	BNP >300 ng/l NT-proBNP >1400 ng/l
Imaging (echocardiography, CMR imaging)	RA area <18 cm ² No pericardial effusion	RA area 18–26 cm ² No or minimal, pericardial effusion	RA area >26 cm ² pericardial effusion
Haemodynamics	RAP <8 mmHg CI ≥2.5 l/min/m ² SvO ₂ >65%	RAP 8–14 mmHg CI 2.0–2.4 l/min/m ² SvO ₂ 60–65%	RAP >14 mmHg CI <2.0 l/min/m ² SvO ₂ <60%

Figure 22. European Society of Cardiology Risk Stratification of Pulmonary Arterial Hypertension (53)

The three pathways of treatment of precapillary pulmonary hypertension have previously been covered in this thesis, namely nitric oxide, endothelin receptor antagonists and prostanoids are the main groups of pulmonary vasodilators. For those in low or intermediate risk groups, dual oral therapy, with a phosphodiesterase inhibitor targeting the nitric oxide pathway and an endothelin receptor antagonist, have been shown to improve exercise capacity, quality of life and prolong time to clinical deterioration(198). Prostanoids are reserved for those patients presenting with a high risk for 1-year mortality, used in combination with the other two pathways. The prostanoids have been shown to improve pulmonary haemodynamic indices by reducing pulmonary vascular resistance(199), improve exercise capacity(200, 201) and quality of life (202). However, side effects and difficulties in administering prostanoid therapy have limited their more common use in precapillary disease. In addition, there is no evidence for improved outcomes in up front triple therapy with oral prostanoid therapy.

As pharmacological therapies are becoming more available, there is also a drive to develop non-pharmacological therapies that can be used in conjunction with medical therapies.

5.1.3 Exercise Rehabilitation in Cardiorespiratory Disease

Exercise rehabilitation has long been recognised to be an effective treatment for those with left sided heart disease(203). It has been shown to be a safe intervention and to exercise capacity and symptom burden in patients with chronic left sided ventricular dysfunction. There have been multiple trials in this area effects(204) and, more recently, *Heran et al. (205)* demonstrated that in those with coronary artery disease, exercise rehabilitation appears to reduce the risk of hospital admissions in the short term (<12 months) and reduces over all cardiovascular mortality. However, there was no evidence of a reduction in ischaemic events, or requirement for cardiac intervention in the form of coronary artery bypass grafting or percutaneous coronary angiogram in those who underwent cardiac rehabilitation compared to standard medical care(205).

In addition, exercise rehabilitation in those with left ventricular dysfunction has been shown to improve left heart function. *Giannuzzi et al. (206)* demonstrated improvements in the left ventricular ejection fraction in a multicentre study assessing the long-term effects of left ventricular remodelling in those with heart failure, in addition to the improvements in exercise tolerance and quality of life. Furthermore, *Cicek et al. (207)* assessed a cohort of sedentary patients who underwent a period of exercise rehabilitation and demonstrated improvements in left ventricular diastolic function, with no other medical interventions. This shows that exercise rehabilitation has potential benefits in those with normal and abnormal baseline function. Moderate intensity exercise has also been shown to alter pathways leading to myocardial fibrosis in those with diabetes, which may play a part in improving cardiac function(208).

Exercise rehabilitation has also been shown to have benefits for those with chronic pulmonary conditions. In those with Chronic Obstructive Pulmonary Disease (COPD), in a Cochrane review of 65 randomised clinical trials by *McCarthy et al*, it was shown to improve quality of life and exercise capacity(209). There was a 40 m improvement in walk distance and an 8% improvement in quality of life, using a 100-point scale. This is now a recommended intervention for all patients who are functionally limited by COPD or who have recently been hospitalized as a result. There have also been improvements seen in patient with bronchiectasis, suggesting that those with Medical Research Council Grade dyspnoea ≥ 2 , defined as those breathless when

walking fast on flat ground or walking up a slight incline, stand to gain similar benefits from rehabilitation compared to those with COPD in terms of quality of life and exercise tolerance(210).

Given the associated improvements in patients with cardiorespiratory disease, there have been studies assessing the benefits of exercise rehabilitation in patients with pulmonary arterial hypertension. It had been postulated that these patients were at risk of sudden cardiac death and had been advised against exercise rehabilitation(211, 212). Thus, several early trials were performed to ensure the safety of this intervention(138, 153).

5.1.4 Exercise rehabilitation in Pulmonary Hypertension

The early exercise trials in pulmonary hypertension demonstrated the safety and feasibility of rehabilitation in this disease. *Mereles et al* demonstrated the safety of the intervention and showed an improvement in quality of life and exercise capacity in a group of thirteen patients(138). *De Man et al (213)* demonstrated and improvement in exercise capacity and in quadricep muscle function in twelve patients with IPAH.

Larger studies have been performed and have replicated these findings of improved exercise tolerance and quality of life(153). The mechanism by which these outcomes are achieved is likely to be multifactorial. Firstly, there is improvement in peripheral muscle function, as demonstrated by *de Man et al (213)* who found increased capillarisation of muscle fibres and oxidated enzyme activity of the type I fibres. Secondly, exercise training appears to improve pulmonary haemodynamics and pulmonary blood flow. *Ley et al (214)* demonstrated and improvement in pulmonary perfusion in twenty patients with precapillary pulmonary hypertension and *Ehlken et al (215)* observed improvement in mean pulmonary artery pressure and pulmonary vascular resistance in addition to replicating the findings of other studies in terms of improvement in quality of life and exercise capacity.

Whilst these studies have demonstrated positive effects of rehabilitation in pulmonary hypertension, there is little available data on the changes in cardiac function that occur in response to training. It has been considered that the main cardiac influence on exercise intolerance is right ventricular dysfunction.

However, there is also little data on the function of the left ventricle in this disease. The aim of this study is to determine the pattern and magnitude of change in cardiac function, as assessed by CMR analysis, in patients with precapillary PH participating in a controlled trial of exercise training.

5.1.5 Aims

- To assess for change in 6MWD in response to exercise
- To determine if there is a change in quality of life measured by the Emphasis 10 questionnaire(139) in response to exercise
- To assess for a change in resting RV ejection fraction measured by CMR at 15 weeks. Detailed CMR analysis was a secondary outcome measure.

5.2 Methods

Ethical approval for the study was granted by the West of Scotland Research Ethics Committee 4 (15/WS/0197), NCT02961023. Between February 2016 and July 2018, patients with precapillary pulmonary hypertension attending the Scottish Pulmonary Vascular unit were recruited to a controlled trial of exercise training. The active intervention was a training programme developed in Heidelberg, specifically designed for patients with pulmonary hypertension, which includes aerobic and resistance training and respiratory muscle training (138). The programme is of high frequency (several daily sessions) but of low intensity (moderate workload targets) and was delivered in two phases. In the first phase, patients underwent three weeks of supervised residential exercise training in small groups or individually. Patients then returned home, where they underwent a further 12 weeks of remotely supervised exercise. Exercise programmes were individualised to the patient, principally by using targets of heart rate achieved and perceived Borg core for breathlessness (111) with exercise intensity increasing if the subject improved.

5.2.1 Study Design

The cohort of patients was divided into two arms, treatment, and control. Both arms of the trial are shown in Figure 23. In the treatment group, patients were entered immediately into the exercise programme, and were assessed before and after the training programme. In the control group, patients received standard medical therapy only for fifteen weeks, before being entered into the exercise programme. These patients were assessed at three time points namely on enrolment, immediately prior to and after exercise training.

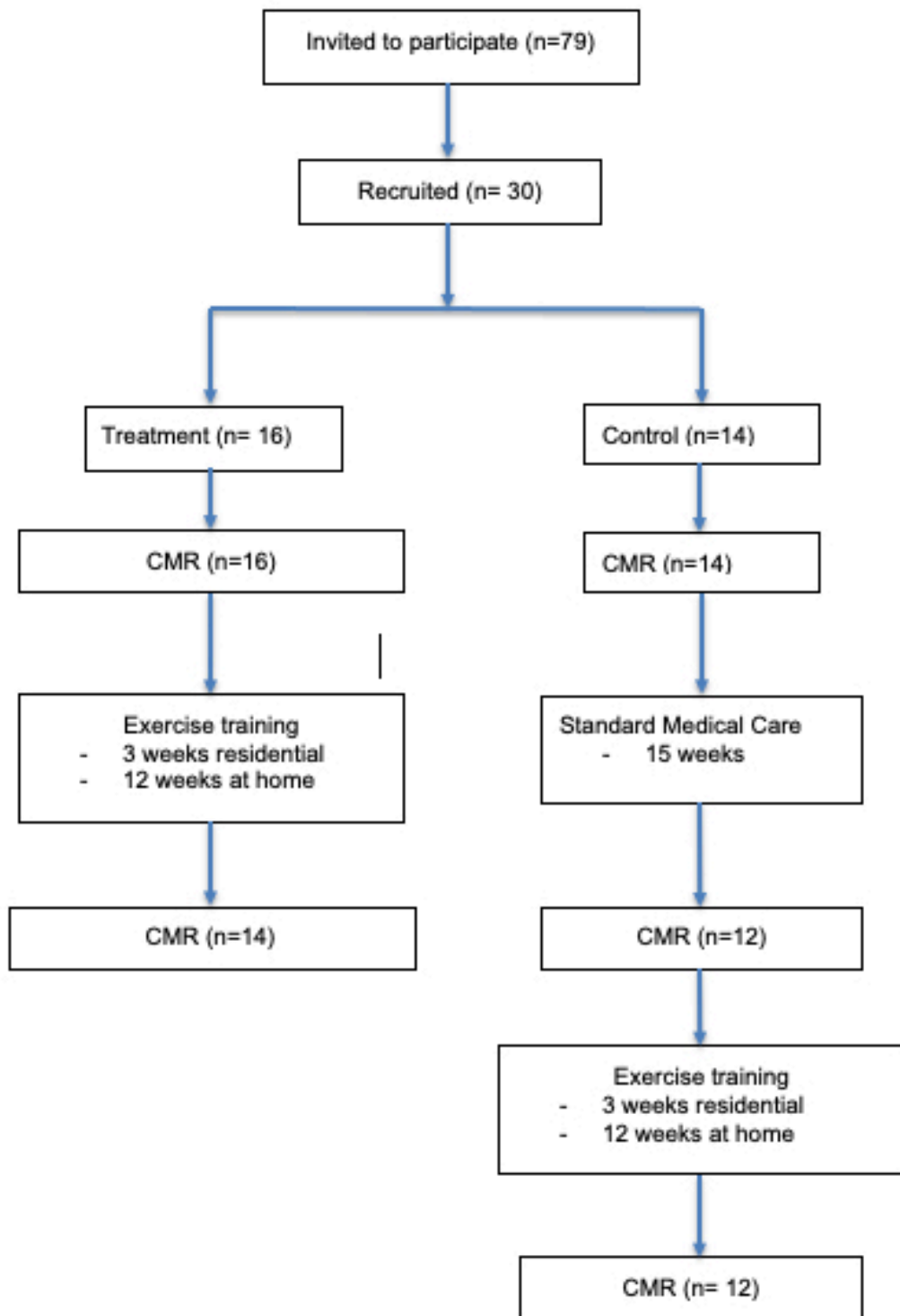


Figure 23. Exercise Trial Recruitment

5.2.2 Inclusion Criteria

The study population included patients who have been diagnosed with pre-capillary pulmonary hypertension, as defined as a mean pulmonary artery pressure ≥ 25 mmHg, pulmonary vascular resistance of ≥ 3 Wu and a pulmonary

artery wedge pressure of <15mmHg. All participants were over the age of 18 classed as World Health Organisation functional class (WHO-FC) II-III and stable on optimal disease targeted therapy for ≥ 3 months. Those who were excluded were pregnant patients, those who had features of decompensated pulmonary hypertension, such as exercise induced syncope and those with significant peripheral vascular disease, neurological or musculoskeletal comorbidity.

CMR imaging was performed in the supine position on a 1.5-T magnetic resonance imaging scanner (Sonata Magnetom, Siemens, Erlangen, Germany) using an 8-channel cardiac coil. Short axis cine images were acquired using electrographic gating multislice balance steady state free precession sequence (20 frames per cardiac cycle, 8mm slice thickness, matrix 256x256; BW, 125kHz/pixel; TR/TE, 3.7/1.6ms). Short-axis stack of images were acquired covering apex to the base.

5.2.3 Imaging Technique

Images were analysed using the Circle Vascular Imaging (version 5.11 Calgary, Canada) with the observer blinded to the patients' clinical information. All borders were manually checked and corrected as needed. RV and LV volumes were determined by automatic tracing epicardial, and endocardial borders of short axis stack obtained during breath-hold. Measurements were taken at end systole and end diastole. End-systole was deemed to be the image with smallest cavity size. End-diastole was defined as the largest cavity volume. From this, right ventricular end diastolic volume (RVEDV), right ventricular end systolic volume (RVESV), RV Ejection Fraction (RVEF), left ventricular End Diastolic Volume (LVEDV), left ventricular end systolic volume LVESV, LV ejection fraction (LVEF) and the ventricular masses were calculated. For the calculation of the ventricular masses, the interventricular septum was deemed to be part of the left ventricle. Stroke volume and cardiac output were calculated using the flow across the pulmonary valve throughout systole using velocity encoded CMR images.

T1 maps were used to further characterise the cardiac tissue. It measures the longitudinal relaxation time of a tissue, which is how long it takes the protons of the specified area to re-equilibrate their spins after being excited by an

electromagnetic pulse. It can be used to assess the interstitial spaces related to increases in myocardial fibrosis or oedema. Normal myocardial T1 values were taken as between 900 and 1100 milliseconds. It can be increased in conditions where there is increased fibrotic change or extracellular protein deposits, such as in cardiac amyloid and reduced where there is fatty infiltration of the ventricles, as is seen post myocardial infarction affecting the LV. In this study, global T1 values were taken for the whole left ventricle. The ventricle was then divided into six segments, with 3 areas (anterior, middle, and posterior) highlighted in the interventricular septum and 3 areas in the left ventricular free wall. A mean of these three values were taken for the septum and the free wall. These values were compared before and after exercise as a representation of changes in cardiac fibrosis in response to exercise.

5.2.4 Tissue Tracking

3-Dimensional tissue tracking was used to evaluate the myocardial motion and deformation and provide a non-invasive assess the mechanics of the left ventricle. Using this method, global longitudinal, circumferential and radial strain pre and post exercise training, can be assessed, the former of which have been shown to be robust and reproducible measurements in clinical practice(150). This technique can detect early changes in ejection fraction. Strain is a measure of the compressibility of the myocardium. The strain is expressed as a fractional change in the size of the ventricle. Where there is a shortening, the figure is expressed in a negative value and a lengthening expressed as a positive value(151). Longitudinal strain reflects a change in length, so in systole there is shortening, representing a negative change. Circumferential strain reflects a change in length along the circumferential axis of the LV when viewing the heart in the short axis. There is a shortening in systole, representing a negative figure. Radial strain represents a change in thickness of the myocardium, which increases in systole, leading to a positive value(151, 152).

5.2.5 Quality of Life Assessment

Quality of life was assessed using the emPHasis-10 questionnaire, which has been designed specifically for use in pulmonary hypertension (Figure 24). This has

been developed using qualitative research that assesses the physical, emotional, and psychological perception of symptoms. It consists of 10 questions, each graded on a six-point semantic differential scale (0-5), which has contrasting adjectives at each end. The maximum overall score is 50. It has been validated with related patient outcome measures including the Hospital Anxiety and Depression questionnaire and the Dyspnoea-12 score.

emPHasis10 NHS/Hospital number:

Name: Date of birth:

This questionnaire is designed to determine how pulmonary hypertension (PH) affects your life. Please answer every question by placing a tick over the ONE NUMBER that best describes your recent experience of living with PH.

For each item below, place a tick (✓) in the box that best describes your experience.

I am not frustrated by my breathlessness	0 1 2 3 4 5	I am very frustrated by my breathlessness
Being breathless never interrupts my conversations	0 1 2 3 4 5	Being breathless always interrupts my conversations
I do not need to rest during the day	0 1 2 3 4 5	I always need to rest during the day
I do not feel exhausted	0 1 2 3 4 5	I always feel exhausted
I have lots of energy	0 1 2 3 4 5	I have no energy at all
When I walk up one flight of stairs I am not breathless	0 1 2 3 4 5	When I walk up one flight of stairs I am very breathless
I am confident out in public places/crowds despite my PH	0 1 2 3 4 5	I am not confident at all in public places/crowds because of my PH
PH does not control my life	0 1 2 3 4 5	PH completely controls my life
I am independent	0 1 2 3 4 5	I am completely dependent
I never feel like a burden	0 1 2 3 4 5	I always feel like a burden

Total: Date:

phaUK MANCHESTER BOA The University of Manchester

Copyright © 2010 phaUK. Date of publication October 2012 002

Figure 24. Emphasis 10 Questionnaire

5.2.6 Data Analysis

Data are presented as mean +/- standard deviation. The null hypothesis was that there would be no change improvement in exercise capacity following training. To reject this, power calculation suggested a sample size of 10 patients in each

group was required if the means of the distribution with equal SDs of 56m differed by at least 74m(153) with a type I error of 0.05 and 80% power. In order to account for potential dropouts, 30 patients were enrolled. Baseline characteristics were compared by Mann Whitney U testing. For comparison of categorical variables, chi-squared test was performed. Analysis of the primary outcome measures comparing exercise training and control arms was carried out using the Mann-Whitney U test.

For the secondary outcome measures, CMR results were compared pre and post exercise using the paired T-test. Stroke volume and Cardiac outputs presented have been calculated by flow methods. To explore further the variable effect of exercise training amongst patients, the group were split into those who responded to exercise training and those who did not. Response was defined as a >30m improvement in walk distance(140). Cardiac function between responders and non-responders were compared using the unpaired T-test.

5.3 Results

The recruitment target of 30 patients was achieved after inviting 79 eligible patients to take part either by letter or person-to-person contact. Twenty-six of thirty recruited patients completed the protocol and had CMR pre and post exercise training (see Figure 1). Of the four patients who did not undergo CMR one patient underwent lung transplantation (on waiting list prior to trial entry), one patient dropped out in the control phase and two dropped out in the treatment phase.

5.3.1 Baseline Characteristics

Nineteen of 26 patients were female with average age of 53 years. Baseline characteristics, subtype of precapillary pulmonary hypertension and drug therapies can be found in Table 19. All patients were on dual or triple therapy in view of their risk stratification when assessed and managed as part of clinical care and were all on stable therapy for at least 3 months prior to enrolment. There were no significant differences in baseline characteristics or drug therapies between the groups.

Variable	Study Population Mean (SD)	Treatment Mean (SD)	Control Mean (SD)	p-value*
Age (years)	52 (11)	54 (10)	48(12)	0.2
Sex (M)	27% (8/30)	25% (4/16)	21% (3/14)	0.54
BMI (kg/m ²)	30 (7)	31 (8)	28 (7)	0.19
6MWD (m)	422	413 (101)	427 (91)	0.56
DLCO (% pred)	55 (21)	53 (24)	59 (15)	0.57
RAP (mmHg)	7.9 (5.5)	8.9 (5.4)	6.8 (5.5)	0.18
mPAP (mmHg)	51 (11)	51 (10)	51 (12)	0.78
PAWP (mmHg)	6.4 (3.2)	6 (3)	6.8 (3.6)	0.56
CO (L/min)	4.2 (1.6)	4 (1.8)	4.4 (1.5)	0.2
SvO ₂ (%)	65	62 (12)	68 (11)	0.21
Log NTproBNP	2.3 (0.6)	2.4 (0.5)	2.3 (0.4)	0.37
EMPHASIS-10	26 (14)	28 (6)	24 (7)	0.23
Drug therapy				
Triple Therapy	43% (13/30)	56% (9/16)	29% (4/14)	0.73
Dual Oral Therapy	57% (17/30)	44% (7/16)	71% (10/14)	0.12
Diagnosis				
IPAH	67% (20/30)	69% (11/16)	64% (9/14)	
CTD-PAH	20% (6/30)	19% (3/16)	22% (3/14)	

POPH	3% (1/30)	6% (1/16)	0	
CHD-PAH	3% (1/30)	6% (1/16)	0	
Heritable	3% (1/30)	0%	7% (1/14)	
CTEPH	3% (1/30)	0%	7% (1/14)	

Table 19. Baseline characteristics, treatment, and pulmonary hypertension subtype.

*p-value is for treatment control comparison using Mann Whitney U Test.

BMI – body mass index; 6MWD – six-minute walk distance; DLCO – diffusing capacity for carbon monoxide; RAP – Right Atrial Pressure; mPAP – mean Pulmonary Artery Pressure; PAWP – Pulmonary Artery Wedge Pressure; CO – Cardiac Output; SvO₂ – mixed venous oxygen saturations, NTproBNP – N-terminal prohormone of brain natriuretic peptide. IPAH – idiopathic pulmonary arterial hypertension; CTD-PAH –pulmonary arterial hypertension related to connective tissue disease; POPH – portopulmonary hypertension; CHD-PAH –pulmonary arterial hypertension related to congenital heart disease; CTEPH – chronic thromboembolic pulmonary hypertension.

Results of primary outcome measures can be seen in Table 20. There was significant improvement in both 6MWD and quality of life after exercise training (32m ±49 vs 5m ±16; p=0.04) but no significant change was seen in RVEF on this analysis.

	Exercise Intervention (SD)	Control (SD)	P-Value*
Delta 6MWD (Group A) (n 14)	32m (49)	5m (16)	0.045
Delta 6MWD (Groups A and B) (n 25)	35m (47)	5m (16)	0.04
EMPHASIS -10 (Group A) (n 12)	-6.7 (14)	2.1 (4)	0.07
EMPHASIS -10 (Groups A and B) (n 22)	-5.2 (11)	2.1 (4)	0.02
RVEF (Group A) (n 14) (%)	-2.35 (9.92)	-1.13 (11.2)	0.75
RVEF (Groups A and B) (n 26) (%)	-1.4 (9.11)	-1.13 (11.2)	0.83

Table 20. Change in primary outcome measures in control phase versus exercise training phase.

Results for each variable are given firstly for the subjects initially allocated to the training arm without a control period (Group A) and then for this group combined with those who received training after a control period (Group B)

* Mann Whitney U Test.

6MWD – 6 Minute Walk Distance; RVEF – Right Ventricular Ejection Fraction

5.3.2 Effect of Training on Cardiac Function

Table 21 shows CMR indices before and after exercise training. The resting cardiac output ($5.9\text{L}/\text{min} \pm 1.7$ increased to $6.3\text{L}/\text{min} \pm 1.7$; $p=0.03$) and stroke volume ($75.4\text{ml} \pm 23.1$ increased to $80.9\text{ml} \pm 22.8$; $p<0.01$) after training. There were no significant changes in right heart function. No significant changes were seen in the strain analysis.

	Pre rehabilitation (SD)	Post rehabilitation (SD)	P-value*
LVEF (%)	62.5 (10.9)	64.2 (11.4)	0.14
LV EDV (ml)	112.1 (36.3)	124.5 (35.7)	0.56
SV (ml)	75.4 (23.1)	80.9 (22.8)	<0.01
CO (L/min)	5.9 (1.7)	6.3 (1.7)	0.03
LV Mass (g)	88.5 (19.0)	90.4 (19.5)	0.26
RVEF (%)	44.3 (12.9)	47.5 (13.3)	0.09
RV EDV (ml)	183.2 (57.8)	178.7 (61.7)	0.70
RV ESV (ml)	107.1 (55.1)	99.0 (58.7)	0.12
RV SV/ESV	1.5 (0.9)	1.3 (0.9)	0.09
HR	78 (21)	79 (21)	0.2
Native T1 values (milliseconds)	1023 (84)	1018 (71)	0.4
Global Longitudinal Strain (%)	-11.8 (5.2)	-12.6 (5)	0.3
Global Circumferential Strain (%)	-18.3 (4.4)	-19.3 (4.2)	0.2
Global Radial Strain (%)	37.5 (16)	36 (11.7)	0.8

Table 21. Changes to cardiac indices before and after training (n=26).

*Paired T Test. LVEF = Left Ventricular Ejection Fraction, LVEDV = Left Ventricular End Diastolic Volume, SV = Stroke Volume, CO = Cardiac Output, LV Mass = Left ventricular Mass, RVEF = Right Ventricular Ejection Fraction, RV EDV = Right Ventricular Ejection Fraction, RV EDV = Right Ventricular End Diastolic Volume, RV ESV = Right Ventricular End Systolic Volume, RV SV/ESV = Ratio of right ventricular Stroke volume to Right ventricular End Systolic Volume, HR = Heart Rate

The group was then split into responders and non-responders. 16/26 patients were classed as responders because their walk distance improved by more than 30 metres after training(140). Changes in resting cardiac function between those who responded and those who did not were compared. The results can be found in Table 22. In those who responded, there was a significant increase in LVEF ($62.5\% \pm 10.9$ vs $64.2\% \pm 11.4$, $p=0.03$) (Figure 2). No significant improvements in RV function, or any changes in heart rate were demonstrated.

5.3.3 Cardiac Strain

	Responders (SD)	Non-responders (SD)	P-value ⁺
Δ LVEF (%)	5.1(7.5)	-1.9 (5.9)	0.03
Δ LV EDV (ml)	2.8(13.7)	-0.69 (10.5)	0.52
Δ SV (ml)	5.6 (6.6)	2.6 (3.4)	0.23
Δ CO (L/min)	0.6 (0.9)	0.1 (0.9)	0.09
Δ LV Mass (g)	2.9(14.4)	2.8 (8.1)	0.99
Δ RVEF (%)	3(9.3)	0.97 (8)	0.61
Δ RV EDV (ml)	-3.4 (24.8)	-2.9 (10.3)	0.95
Δ RV ESV (ml)	-6.5(19.7)	-3 (17.9)	0.67
Δ (RV) SV/ESV	-0.18 (0.6)	-0.08 (0.4)	0.69
Δ Native T1 values (milliseconds)	9 (51)	6.6 (46)	0.89
Δ Global Longitudinal Strain (%)	2.3 (4.9)	-1.5 (5.1)	0.07
Δ Global Circumferential Strain (%)	0.4 (3)	1 (3.8)	0.64
Δ Global Radial Strain (%)	-2 (11.5)	2.4 (12.6)	0.37

Table 22. Comparison of change in cardiac indices between responders and non-responders to training. ⁺Mann Whitney U. LVEF = Left Ventricular Ejection Fraction, LVEDV = Left Ventricular End Diastolic Volume, SV = Stroke Volume, CO = Cardiac Output, LV Mass = Left ventricular Mass, RVEF = Right Ventricular Ejection Fraction, RV EDV = Right Ventricular End Diastolic Volume, RV ESV = Right Ventricular End Systolic Volume, RV SV/ESV = Ratio of Stroke volume to End Systolic Volume all from Right Ventricle.

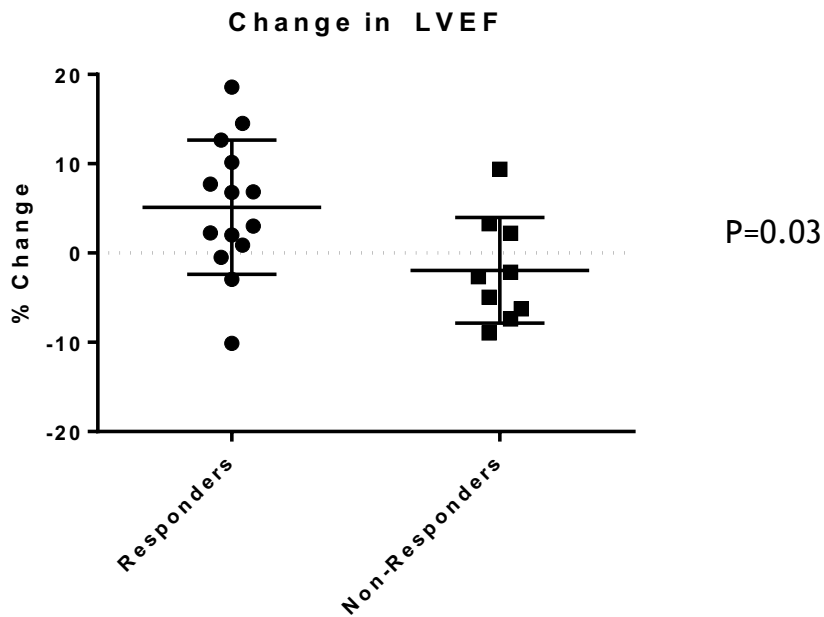


Figure 25. Changes in Left ventricular ejection function (LVEF) between responders to training and non-responders.

5.3.4 T1 Mapping

To further assess the changes in the LV, changes in native T1 mapping between the septal wall and the free wall pre- and post-exercise were calculated, shown in Table 23. There was no improvement in the whole cohort in the T1 mapping of the interventricular septum or the free wall. However, in those who responded to rehabilitation with clinically significant increase in exercise tolerance, there was a reduction in T1 mapping time of the interventricular septum (1061 ± 82 to 1027 ± 56 ; $p=0.04$)

	Interventricular Septum			Left Ventricular Free Wall		
	Pre-Exercise Mean (SD)	Post-Exercise Mean (SD)	P-value*	Pre-Exercise Mean (SD)	Post-Exercise Mean (SD)	P-value*
All Patients	1060 (89)	1055 (70)	0.38	975 (102)	965 (94)	0.75
Responders	1061 (82)	1027 (56)	0.04	962 (100)	960 (83)	0.38
Non-responders	1073 (94)	1110 (65)	0.3	972 (102)	965 (94)	0.78

Table 23. T1 Value Comparison Pre versus Post exercise in all patients, those who responded to rehabilitation as determined by 6-minute walk test and those who did not

*Wilcoxon Rank Test

5.4 Discussion

This study has demonstrated positive effects of an exercise training programme for patients with pulmonary hypertension. This exercise training programme was associated with improvement in 6MWD (with a group mean change above the minimally clinical significant difference(140)) and improved quality of life, measured by Emphasis-10. The improvement in exercise tolerance and quality of life is similar to that seen in patients undergoing cardiac rehabilitation and pulmonary rehabilitation. This is supported by *Chen et al* (216), who demonstrated a 41m improvement in 6-minute walk distance in those undergoing a home based cardiac rehabilitation in those with chronic heart failure. Not only was there an increase, but the minimal clinical significant difference for 6 minute walk distance in pulmonary arterial hypertension was achieved(140). This quality of life improvement was beyond the minimally important distance, according to a study evaluating the use of the Emphasis-10 in patients with PAH(217). Whilst this represents a very positive result for the individual patient, the Emphasis-10 score has been shown to correlate with survival(218). As such, long term follow-up of the exercise studies required so assess the survival benefits in pulmonary arterial hypertension.

This study demonstrates a statistically significant improvement in resting stroke volume and cardiac output after exercise training. However, *van Wolfe Ren SA et al* performed a study using anchor-based methods and detected a minimally important difference of 10ml in the stroke volume and 8 to 12ml for distribution-based anchors(219), which this study does not meet. Therefore, although improvement was detected, it could be argued this is not clinically significant. When further dividing the groups into 'responders' and 'non-responders' to training, defined as those who improved their 6-MWD by the clinically significant difference (30 metres), it was seen that left ventricular ejection fraction significantly improved at rest with no significant changes in the right ventricular variables. It has been postulated that the main cardiac reason for exercise intolerance in pulmonary arterial hypertension is related to RV dysfunction. With exertion, cardiac output increases to meet the systemic oxygen demands. The pulmonary circulation is unable to dilate or recruit more blood vessels to accommodate this change, leading to an increase in pulmonary artery pressure and RV afterload. This then prevents the increased stroke volume and cardiac output necessary to maintain a normal exercise capacity. In addition, over time, there is a dilatation of the RV, causing the interventricular septum to shift to the left side. This then impairs the diastolic function of the left ventricle, further limited the cardiac response to exercise(220). Given that there were not any significant changes in the RV after exercise, but did see an increase in exercise capacity, it suggests there are other potential causes of exercise intolerance.

The benefit from exercise training in PH is likely to involve multiple systems, the data from this study suggest that changes in cardiac function, specifically that of the left ventricle, could contribute to the improvement in exercise capacity. With exercise-induced breathlessness, patients also tend to be sedentary and have significant peripheral muscle deconditioning, which also reduces the workload experienced by the left ventricle(221). This can lead to atrophy and a relatively low-normal ejection fraction. This study data suggests that exercise training in pulmonary hypertension appears to improve left ventricular function when measured by LVEF but only in those subjects who manifested a positive training response (222). In patients following acute myocardial infarction, exercise rehabilitation has been shown to improve the contractility of the LV by improving the handling of intracellular calcium, which increases the isometric tension development of the myocyte(223). The association between training response and LVEF suggests that improvement in LV contractility is one of the mechanisms by which exercise training improves function in PH. To my knowledge, this has not previously been demonstrated in PH.

3-dimensional strain analysis was used to assess the compressibility of the left ventricle, to try further explaining the improvement in quality of life and exercise capacity. There were no improvements in the radial, circumferential and longitudinal strain, suggesting that the compressibility of the left ventricle is not significantly changed by exercise rehabilitation and is unlikely to contribute in a noteworthy way to the improvements seen in pulmonary arterial hypertension.

Given the improvement seen in the LV ejection fraction, and the suggestion that exercise training of the left ventricle is the main cardiac effect of exercise rehabilitation, changes within the substrate of the LV were assessed. This was done by evaluating any changes in the native T1 mapping in the heart. Both global T1 values and regional T1 values were calculated, dividing the LV in two regions: the septal wall and the free wall. Overall, there were no differences in the cohort pre and post exercise. However, when dividing the patients into those who respond to exercise and those who do not, there was a significant reduction in the native T1 values towards the normal values. The myocardial characteristics were different in a way that could reflect differences in myocardial oedema or fibrosis burden. Exercise has been shown to reduce cardiac fibrosis in a cohort of patients with diabetes mellitus(147). In pulmonary hypertension there is cardiac remodelling, both adaptive and maladaptive, which are both mediated by the myofibroblast. It is proposed that exercise training leads to adaptive remodelling, and thus a reduction in the interventricular septal fibrosis.

5.5 Study Limitations

There are limitations to this study. Although the centre in this study has the mandate to investigate and manage all patients in Scotland with PH, this is a relatively small single centre study. The aetiology of precapillary PH in the recruited patients was heterogeneous. The severity of PH varied amongst participants and medical treatments were not standardised. The size of the treatment effect seen was less than the value estimated from earlier studies that were used in the power calculation. This rendered the study at risk of being underpowered although a significant change was seen in the primary outcome measures.

5.6 Conclusions

This prospective trial has demonstrated that an exercise training programme improves exercise capacity and quality of life in precapillary pulmonary hypertension. Whilst the mechanism of this is likely to be multifactorial, it has been shown that there is a training effect on the heart, as shown by improved cardiac output and stroke volumes. By further assessing those who responded to exercise, it is hypothesised that this improvement is related to improved left heart contractility. To the best of my knowledge, this has not previously been demonstrated. Further studies are required to further validate these findings.

6 Pulmonary Thromboembolism in Hospitalised Patients with COVID-19

6.1 Introduction

In late 2019, The World Health Organisation was informed of a cluster of patients presenting with a rapidly progressive and fatal pneumonia in Wuhan City, Hubei Province, China. Within fourteen days, the causative agent was identified from viral genetic sequencing as a novel coronavirus, known as Severe Acute Respiratory Syndrome Coronavirus 2 (SARS-CoV-2). The syndrome caused by SARS-CoV-2, which consists mainly of upper respiratory coryzal symptoms and pneumonitis, was named COVID-19. With continued movement of people from Wuhan City around the world, the virus spread rapidly and was declared a global pandemic on 11th March 2020. The source of the virus has yet to be firmly established but the scientific agreement is that it is of animal origin and was transmitted to humans. It is thought that there was an intermediate host between the animal of origin and the human(224). Novel coronaviruses are identified but only a few have led to severe clinical disease in recent years, such as the epidemics of SARS-CoV in the Far East and Middle Eastern Respiratory Syndrome caused by MERS-CoV.

6.1.1 Coronaviruses

“Coronavirus” was devised in 1968 to describe the viruses seen under the electron microscope that have a crown- like, or “corona”, morphology, as seen in Figure 26. They are coated with spike proteins, which are central to receptor recognition and the cell membrane fusion process. The M-proteins on the viral surface serve to facilitate virus assembly and ensuring the virus assumes the correct shape. They are a diverse family of enveloped viruses that contain a single-strand, positive-sense RNA genome of varying length, usually between 26 - 32 kilobases. They are divided into three groups: group I contains the animal pathogens, which can cause feline and human respiratory syndromes; group II includes pathogens of veterinary significance, infecting horses and pigs leading to a variety of disease, and group III includes viruses that affect avian subjects.(225) They require a host to survive and replicate, and are found in

livestock and avian species, along with humans. As a group they infect the host using the spike protein to enter the cell entry receptors, such as the human aminopeptidase and angiotensin-converting enzyme 2. It is the distribution of these receptors on tissue that determines the infectivity of the virus. Once attached to the receptor, there is a change in the shape of the protein, leading to fusion of the viral and cell membranes, mediating the release of nucleocapsid into the cell. The coronavirus then replicates to produce full-length copies of the mRNA strand that are then incorporated into the newly formed virus(226). This mechanism involves a transcription mechanism that is not fully understood but is thought to be regulated by transcription-regulated sequences that are present in the RNA. Over time there are faults in the genetic replication process, which lead to mutations, or a change in the virus' genome. Those with a survival advantage, such as easier transmission, are allowed to replicate and quickly become the dominant strain within an environment. The 'wild-type' refers to the original strain and all mutations are relative to this. SARS-CoV-2 is a 19.9kb RNA beta-coronavirus, which has strong similarity to the genetic sequences of bat origin, although it is thought that pangolins, turtles, or snakes may have been the intermediate host that lead to human infection. It has a 79.5% and 51% sequence overlap with SARS-CoV and MERS-CoV, respectively(227).

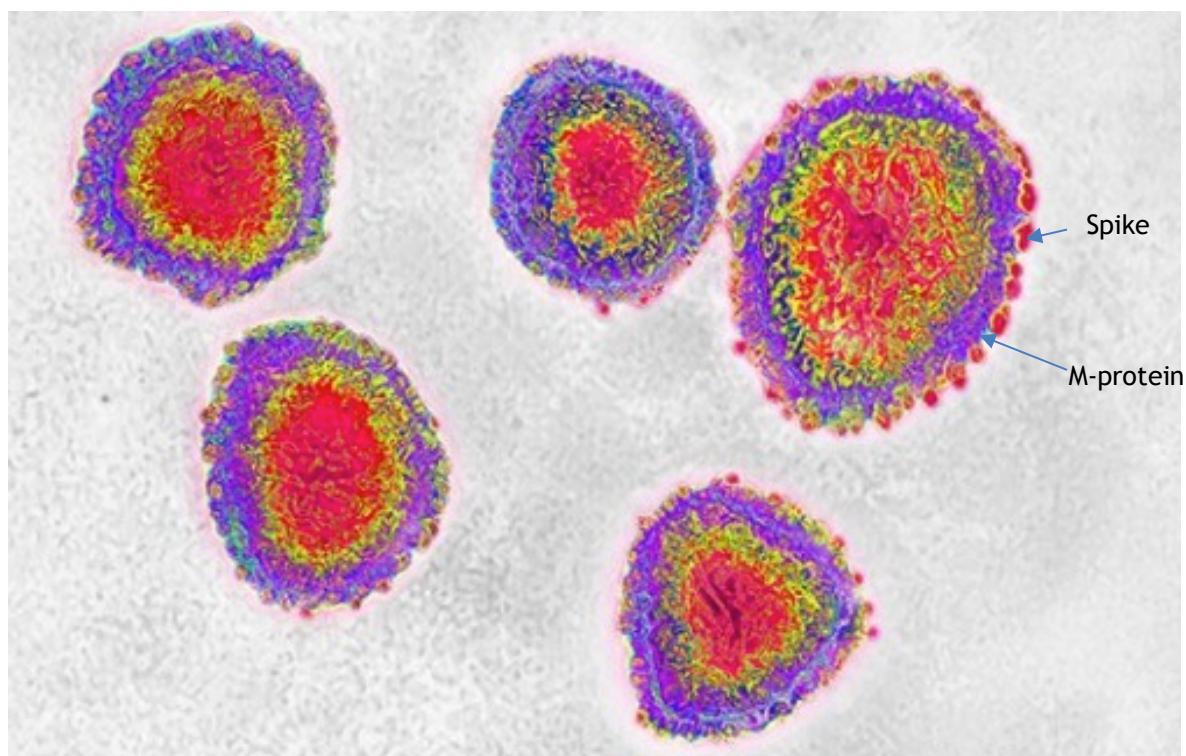


Figure 26. Electron Microscopy of Coronavirus(228)

Transmission of SARS-CoV-2 can occur via direct and indirect methods. Direct methods include droplet human-to-human transmission, which is usually droplets of respiratory origin that are projected into the environment via speaking, coughing, or sneezing. It is thought the droplets rarely travel more than six feet and, although usually only remain in the air for a short period of time, can persist for up to three hours(229). Transmission can also occur if a subject's hands are contaminated with the virus and subsequently come into contact with the mucous membranes of the eyes, nose, or mouth. Transmission between those without symptoms has also been recognised. Viral shedding from the respiratory system has been shown to continue for up to 13 days after symptoms have resolved, but viral shedding in stool has been seen to continue for 33 days(230), and can shed from a body beyond the time of death.

There have been hypothesised methods of transmission between animals and humans, along with several potential intermediate hosts identified but the exact mechanism of how this happens is not fully understood(231, 232). As has been demonstrated by the rapid global spread of SARS-CoV-2, the virus is highly contagious, and the methods of transmission are more complex than other coronavirus pandemics previously observed.

6.1.2 COVID-19 clinical syndrome

The incubation period of the wild-type virus is between 0-14 days, but most commonly the presentation occurred after 5-6 days. In those first identified as having Covid-19, the clinical syndrome observed was variable, between asymptomatic and severe respiratory illness, leading to death. It is estimated that 1 in 3 of those infected were asymptomatic. It is not known why some people who harbour infection exhibit symptoms and some do not. Those that do, however, display symptoms of loss of taste or smell, cough, and fever. Other less common symptoms include shortness of breath, myalgia, and headache. Gastrointestinal symptoms have been observed but, again, are less common. In the elderly population however many non-specific symptoms including delirium could be caused by Covid infection.

For those with wild-type disease exhibiting symptoms, it was seen that 40% have mild symptoms, defined as those who have symptoms but can care for themselves in their own environment, 40% have moderate symptoms, defined as being able to cope in their own environment but are dependent on others and 15% have severe symptoms that merit inpatient hospitalisation with oxygen support. The remaining 5% were observed to have critical illness, defined as those with severe respiratory failure, adult respiratory distress syndrome and multi-organ failure(233, 234). The risk of developing severe and critical illness was seen to increase in older males with underlying health conditions, such as obesity and systemic hypertension. Infants and children were observed to be less likely to develop severe disease.

6.1.3 Thrombosis

In addition to the lung parenchymal changes observed in COVID-19, a coagulopathy was also seen. This might be expected as part of the systemic illness presentation, as is seen in severe septic shock. However, during the first wave, anecdotal evidence suggested that there was increased incidence of venous and arterial thrombosis in those with mild or moderate disease. The coagulation abnormalities appeared to mimic other haematological conditions including disseminated intravascular coagulation (DIC) and thrombotic microangiopathy and are linked to higher mortality(135, 157). During this same time period, COVID-19 was noted increase the risk of thrombotic complications in the intensive care unit, with the incidence being as high as 30%(136), which is higher than is seen in other bacterial or viral pneumoniae(136, 235).

It has been suggested that in the early phase of infection with SARS CoV-2, there is a widespread endothelitis, affecting multiple organs(236). This is supported by the viral inclusion bodies being found within major organs out with the lung, such as the gastrointestinal tract. These inclusion bodies induce apoptosis, which in turn leads to infiltration of inflammatory cells and complement activation, causing microvascular thrombosis. There is further creation of tissue factor and induction of the clotting cascade, leading to presence of more thrombin, and thus fibrin(237). In addition, there is reduction in fibrinolytic pathways, which leads to rapid thrombus creation. The inflammatory process

also causes high levels of plasminogen activator inhibitor, further inhibiting natural thrombolysis and creating an environment where thrombus can propagate(238).

Furthermore, neutrophil extracellular traps have been seen in the autopsy samples of those who have died with Covid-19(239). These traps consist mainly of loose DNA and histones and are a protective mechanism to capture and immobilise invading organisms(239). However, they can also activate the pro-thrombotic pathways, which leads to further thrombus production and propagation(240).

6.1.4 Treatments

SARS-CoV-2 targets the angiotensin-converting-enzyme 2 receptor in respiratory epithelium to activate the protein for invasion and replication. This infective process triggers an inflammatory response which, in post-mortem analysis, has shown necrotic changes along with macrophage infiltration. As is seen in a number of critical illnesses, there is activation of pro-inflammatory T cells and a reduction in the regulatory T cells, which has led to clinicians using immunosuppressant medications for therapy. It was established early in the pandemic that, in addition to supportive therapies such as oxygen, systemic steroid therapy was effective in reducing mortality because of COVID-19 and all-cause mortality at 28 days(241). It remains the mainstay of treatment for those hospitalised with COVID-19.

Cytokine release syndrome (CRS) has been a recognised complication of Covid-19. This is caused by a severe acute inflammatory response to SARS-CoV-2 and can lead to tissue damage and death. This process is largely driven by interleukin-6(242). Tocilizumab, an interleukin-6 inhibitor, has been shown to be effective in those with pneumonia and severe inflammatory response, minimising the impact of CRS by binding to the soluble IL-6 receptor. It led to improvements in lung function in 91% of those enrolled in the trials and resulted in a shorter hospital stay(243). There are ongoing trials assessing the benefit of neutralising antibodies for the treatment of COVID-19, for example the BLAZE-1 trial for the assessment of Bamlanivimab.

In addition to treating the parenchymal disease, it was recognised there was a need to investigate the issues of haematological dysfunction. During the first wave it was unclear if the observed thrombotic episodes were predominantly microvascular or macrovascular. Perhaps more importantly was the question of whether these thrombotic episodes should be treated early and aggressively to minimise their severity. Low-molecular weight heparin (LMWH) was the preferred method of anticoagulation, but there was little evidence on what dose to use and how frequently it should be administered. Most clinicians adopted an individual risk assessment for patients (basis of risk versus benefit analysis), often after a thrombotic event had occurred. The question of thromboprophylaxis in active Covid infection remained during the early waves.

6.1.5 Assessment in Covid-19

Establishing the diagnosis of COVID-19 in the early waves was difficult, as testing was limited due to limitation of availability real time polymerase chain reaction (PCR) testing. Therefore, reliance on other forms of diagnostic testing emerged. Chest x-ray or thoracic computed tomography (CT) (244) have been used widely to clarify the diagnosis where there is dubiety and allows the detection and evaluation of sequelae SARS-CoV-2 infection. The established radiological appearances of Covid pneumonitis are now recognised(158). Where there were typical radiological appearances of Covid-19, but PCR testing was negative or not available, this was used as a diagnostic investigation that would dictate treatment options. When there was a lack of data on the mechanism of disease spread, care had to be taken to limit the contact with suspected cases so diagnostic investigations may not have been as thorough as with a community acquired bacterial infection. In addition, patients may well have been too unwell to transfer from clinical areas to the radiology department for three-dimensional imaging, meaning that two dimensional CXR was the best diagnostic test available to clinicians. As a result of these factors, establishing a secure diagnosis could, at times, be challenging.

At the time of writing, there was little data available on the incidence of thrombosis or comorbidity related to the development of thrombosis in hospitalised patients with COVID-19, particularly in patients managed outside critical care. Most evidence thus far have been limited to single or few hospital centres. Retrospectively, I measured the incidence of pulmonary embolus in all patients with COVID-19 admitted to hospitals in the whole of Scotland in critical care and ward environments.

6.1.6 Aims

It is hypothesised that Covid-19 increases the risk of pulmonary thromboembolism in hospitalised patients, which can affect their clinical outcomes. I aimed:

- To establish the incidence of pulmonary thromboembolism in this national Cohort of hospitalized patients with Covid-19.
- To determine if the risk of pulmonary thromboembolism remains in patients managed out with critical care.
- To assess if right heart strain increased the risk of death or requiring critical care support.
- To detect if there is any signal towards comorbidities that increase the risk of critical care admission or death.

6.2 Methods

The study was approved by The Public Benefits and Privacy Panel for Health and Social Care in Scotland and allowed access to data of these patients. All patients in Scotland between 23rd March 2020 and 31st May 2020 who underwent a computer tomography pulmonary angiogram (CTPA) were identified using the Scottish National Picture Archiving and Communications System (PACS), which archives all radiological imaging procedures performed in all public hospitals in Scotland. This captured all patients during the ‘first wave’ of the COVID-19 pandemic, where the wild-type virus was the predominant strain in the community. Patients who were diagnosed with pulmonary embolism were identified and cross-referenced with the Scottish Care Information (Sci-Store) database, which allowed assessment of whether a Covid-19 PCR had been performed, its result and allowed access to biomarkers, including haematological and biochemical investigations.

6.2.1 Patient recruitment

Patients included in the study had to have a positive RT-PCR test results for SARS-CoV-2 up to 30 days (mean 9.5 days) before their CTPA or within fourteen days afterwards. If no RT-PCR test had been performed, or if it was negative, patients were deemed to have COVID-19 clinical syndrome if they had classical lung parenchymal changes, as described by the British Society of Thoracic Radiology(158). As previously described, establishing a secure diagnosis where there was limited access to testing was challenging. Clinically, a pragmatic approach was taken when evaluating the clinical picture in conjunction with diagnostic investigations. However, to lend confidence to our cohort for the purposes of this study, patients who did not have a RT-PCR positive swab and with ‘probable’ or ‘indeterminate’ radiographic features of COVID-19 were excluded due to potential diagnostic uncertainty. The outline of the study is presented in Figure 27.

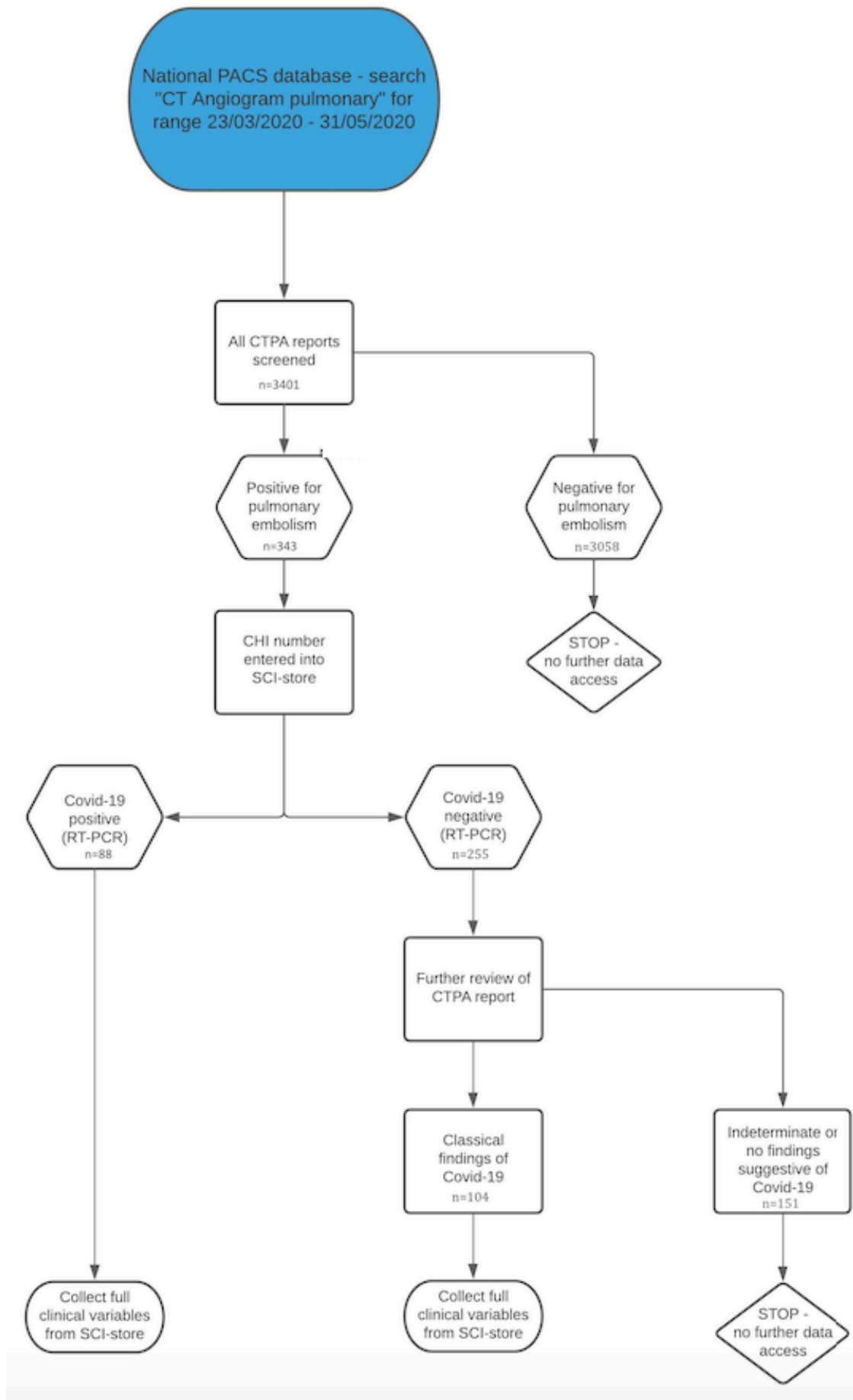


Figure 27. Consort diagram of patients included in study

Demographic data, the level of patient care (level 1 [ward-level] care or critical care) and comorbidities were gathered from the SCI Store database. Biomarker data and risk factors for PTE were also collected. D-dimer had been noted to be very high in the intensive care population with Covid-19(245), which perhaps reflected the activation of the thrombotic cascade seen in the widespread endothelitis in Covid-19 and I aimed to assess if this was higher than in controls. C-Reactive Protein, neutrophil count, lymphocyte count and lactate area all used in the risk stratification of sepsis, and these were compared with controls. Right heart strain was considered to be present in patients who had serum troponin greater than the local reference limit or had radiological evidence of right ventricular (RV) dilatation (right ventricular: left ventricular ratio [RV:LV] diameter >1), in agreement with the European Society of Cardiology guidelines. Medical records from the primary care physician were used to identify the presence of comorbidity. The SCI store includes documents from primary care with the past medical history coded for reference.

The Scottish Government published the data on the incidence of COVID-19 in hospitalised patients between 23rd March and 31st May 2020 online(160). These were the denominator for the calculation of the incidence of PTE in hospitalised patients with COVID-19 and used to calculate how many patients from the overall hospitalised COVID-19 population developed pulmonary thromboembolism.

6.2.2 Control Cohort

202 patients diagnosed with pulmonary embolus between 11th July 2011 and 4th December 2018 were used as a control to examine for differences between biomarkers in those with and without COVID-19 disease. These patients were a heterogenous group of hospitalised patients with provoked and unprovoked pulmonary embolus followed up in the outpatient clinic when this facility was in its infancy, and therefore includes only a small proportion of those diagnosed with pulmonary thromboembolism during that time. However, it was felt to be a representative population of hospitalised patients with pulmonary embolism to allow a comparison. Patients in this group with troponin, above the local reference range, or have RV:LV ratio >1 were identified as having right heart

strain. In addition, data were gathered from previously published studies on the incidence of pulmonary embolus in hospitalised patients(161) and those with pneumococcal pneumonia from a cohort in Taiwan(162). In this study, they compared the incidence of venous thromboembolism in 18 928 patients with pneumococcal pneumonia to an age and sex-matched cohort of 75 712 patients without pneumonia. They demonstrated a 1.97-fold increase in the risk of pulmonary thromboembolism in the pneumococcal cohort. This was then used as a comparison to the current COVID-19 population.

6.2.3 Statistical analysis

Incidence of pulmonary thromboembolism percentage was calculated using the total number of hospitalized COVID-19 patients during the described time period divided by the number of patients with evidence of COVID-19 and a positive CTPA for pulmonary thromboembolism. Binary logistic regression was used to establish if the presence of comorbidity, increasing age or sex leads to an increased risk of a composite endpoint of critical care admission or death. Survival was calculated using Cox Proportionate Hazard Regression in those patients with right heart strain, those in intensive care and in males. Comorbidities were then assessed in the population managed in level 1 care areas and grouping together all those managed in critical care, levels 2 and 3 to identify if the risk of PTE was high both in ward-based environments and in critical care. Chi Squared was used to look for increased frequency of PTE in the critical care groups compared with the ward-based patients. Mann Whitney U test was used to look for any significant differences between non-parametric data in the biomarker groups. Multivariate analysis was used to adjust for age and sex when comparing the presences of right heart strain in the control versus Covid-19 group. Statistical analysis was completed using IBM SPSS Statistics Version 27 and GraphPad Prism version 8. A p-value of <0.05 was taken to be statistically significant.

6.3 Results

Between 23 March 2020 and 31 May 2020, 3401 CTPAs were screened using the Scottish National PACS system. 192 were identified as positive for PTE with either co-existing RT-PCR evidence of COVID-19 (n=104) or classical radiological changes consistent with COVID-19 (n=88).

During this time, 5195 patients were admitted to National Health Service hospitals with COVID-19 in Scotland.

6.3.1 Incidence of PTE in Patients Admitted to Hospital with COVID-19

This incidence of PTE in all patients admitted to Scottish hospitals with COVID-19 was 3.7%. This is significantly higher than the 1% incidence of PTE documented in hospitalised patients (ward based and critical care) in Scotland prior to the COVID-19 epidemic(246) ($p < 0.01$). Of 5195 patients admitted to hospital with COVID-19, 475 were admitted to critical care, in whom the incidence of radiologically confirmed PTE was 6% (n=29). This was also higher than the 2.6-3.5% seen in other intensive care units, where patients were admitted with a wide range of medical and surgical pathologies, prior to the COVID-19 pandemic(247, 248).

The remaining 4720 patients were managed in level 1 care, in whom the incidence of radiologically proven PTE was 3.5% (n=163). 1807 (34%) hospitalised patients with COVID-19 died, 43 (22%) of whom had radiologically confirmed PTE.

Table 24 demonstrates the demographics of COVID-19 patients with PTE and historical control patients. I did not have access to reliable medical records around the length of stay, requirement for critical care or BMI for those in the control group and, as such, these factors have not been included.

Baseline Demographic	COVID-19 (n=192)	Control (n=202) Mean (SD)	p-value
Age in years	60.2 (14.1)	59 (16)	0.57 ⁺
Gender, Male (%)	64.5	46	<0.01 ⁺⁺
Right Heart Strain (%)	27	31	0.61 ⁺⁺
Median Length of hospital stay until PE diagnosis in days (IQR)	1 (9)		
Median Length of time between positive RT PCR and PE (days)	8 (14)		
BMI (kg/m ²)	30.2 (8.3)		
ITU patients (%)	15		
RT-PCR swab positive (%)	54		

Table 24 Demographics of Population

⁺Wilcoxon signed rank test. ⁺⁺CHI squared.

Values listed are Mean (SD) unless otherwise stated

BMI - Body Mass index. RT-PCR = Real Time Polymerase Chain Reaction

6.3.2 The effects of comorbidities on the risk of death or likelihood of requiring critical care

All CTPA images and image reports were accessible. 81% of the patient's primary care records were accessed, which provided information on comorbidities. Not all patients had biomarkers analysed but in the patients who did, all were accessible. The numbers of patients included are presented in the data tables (see below). Obesity (BMI >30kg/m²), systemic hypertension, malignancy or cardiovascular disease (including ischaemic heart disease, cardiomyopathy, peripheral vascular disease) were not associated with the outcome of critical care or death (Table 25Error! Reference source not found.).

Comorbidity	Number of patients with comorbidities (n=155)	Odds Ratio	95% CI
Body Mass Index >30kg/m ²	47	0.99	0.94-1.04
Systemic Hypertension	15	0.97	0.41-2.33
Malignancy [^]	31	1.05	0.22-5.2
Cardiovascular Disease ^{^^}	19	0.80	0.20-3.13
Diabetes Mellitus	31	0.45	0.14-1.44

Table 25. The Effects of Comorbidities on the Likelihood of admission to Critical Care or Mortality

⁺ Binary Logistic Regression

[^] Either current or previous solid organ malignancy coded on primary care records

^{^^} History of ischaemic heart disease or left ventricular systolic dysfunction coded on primary care records

Univariate analysis for comorbidities was performed and is seen in Table 26. I did not demonstrate any significance in the comorbidities contributing to ICU admission or death. Differences in the comorbidities between the ward-based patients and critical care are found in Table 27. No difference was seen between the groups.

Comorbidity	Odds Ratio	Confidence interval	P-Value
Obesity	0.72	0.32 - 1.2	0.38
Systemic Hypertension	1.01	0.31 - 3.1	0.99
Diabetes	1.11	0.35 - 3.32	0.86
Cardiovascular disease	1.07	0.25 - 3.86	0.92
Inflammatory diseases	0.61	0.03 - 4.44	0.67
Malignancy	0.61	0.09 - 2.63	0.55

Table 26. Univariate analysis of comorbidities in those with COVID-19

Comorbidities	All patients n=192 (%)	Patients in Critical care n=29 (%)	Patients in Level 1 care n=163 (%)	P-value**
Systemic Hypertension	36 (19)	4 (13)	32 (20)	0.62
Malignancy	15 (8)	1 (3)	14 (7)	0.25
Diabetes Mellitus	31 (16)	3 (10)	28 (15)	0.54
Cardiovascular Disease	19 (10)	1 (3)	18 (11)	0.55

Table 27 Comorbidities of Critical Care patients and those in Level 1 Care

6.3.3 Survival with pulmonary thromboembolism

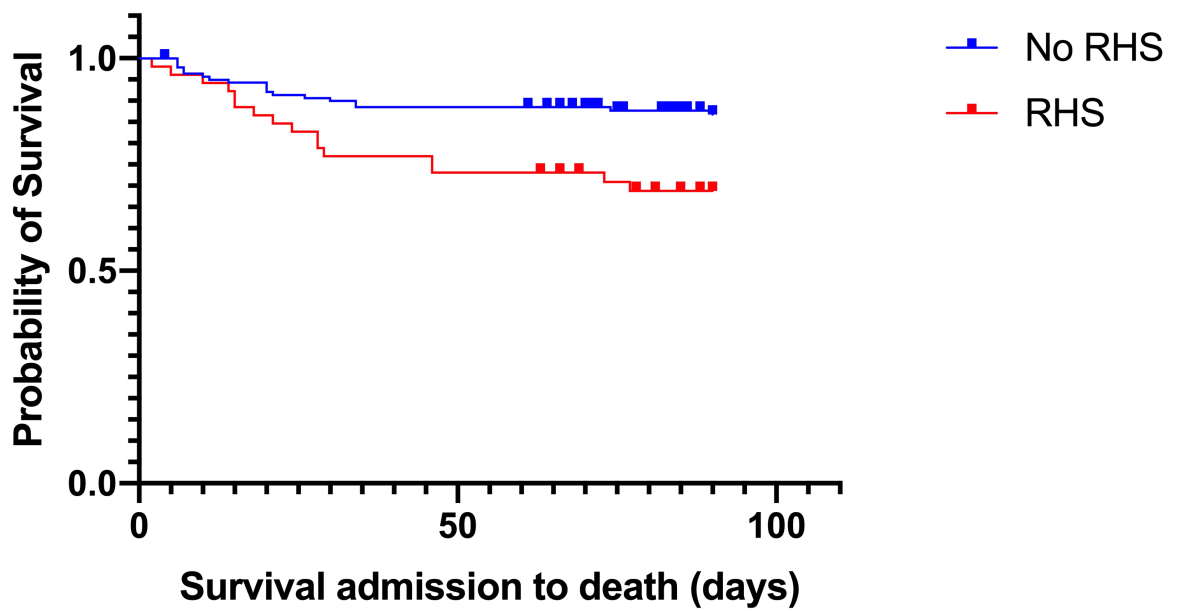
30-day survival was evaluated due to its use in other risk stratification criteria, such as the Pulmonary Embolus Severity Index(249) and was observed to be significantly worse in those with right heart strain and those requiring critical care. I adjusted for age and sex when comparing the outcomes of right heart strain and there were no differences between the COVID-19 group (p=0.6) and the control group (p=0.1) (Table 28). This was also seen in survival to 90 days as shown in Figure 28.

Patient status	% Survival to 30 days N (%)	Patient Status	% Survival to 30 days N (%)	Odds Ratio⁺	95% CI
Right heart strain (n=52)	25 (48)	No Right Heart Strain (n=140)	128 (91)	4.12	2.24-7.55
Critical Care (n=29)	15 (55)	Level 1 Care (n=163)	146 (89)	1.75	0.86-3.57
Male (n=124)	91 (73)	Female (n=68)	46 (67)	1.78	0.88-3.62

Table 28. 30-day Survival from admission with Pulmonary Thromboembolism

⁺ Cox Proportional Hazard Regression

Right Heart Strain Survival to 90 days



	Number at risk		
	0 Days	30 days	60 days
—	140	126	123
—	52	41	40

Figure 28. Kaplan Meier curve of 90-day survival in those with right heart strain. $p=0.01$.

Patients in critical care were more likely to have right heart strain: 55% of the patients with PTE in critical care had right heart strain (one diagnosed using troponin only), compared to 21% of the ward-based patients with PTE (five of these patients had right heart strain diagnosed via troponin only).

6.3.4 Differences in biomarkers between COVID-19 and historical control patients

D-Dimer (4059 ± 5421 ng/ml vs 2874 ± 4905 ng/ml, $p=0.02$), troponin (310 ± 705 vs 140 ± 253 ng/L, $p=0.01$), neutrophil count (9.5 ± 3.9 vs $7.2 \pm 2.9 \times 10^9/L$, $p<0.01$), lactate (1.9 ± 1 vs 1.5 ± 0.8 mmol/L, $p<0.05$) and CRP (110 ± 99 vs 60 ± 65 mg/L, $p<0.01$) were significantly higher in those with COVID-19 compared to the historical control group while the lymphocyte count was reduced (1.1 ± 0.7 vs $1.8 \pm 0.8 \times 10^9/L$, $p<0.01$) (Figure 29).

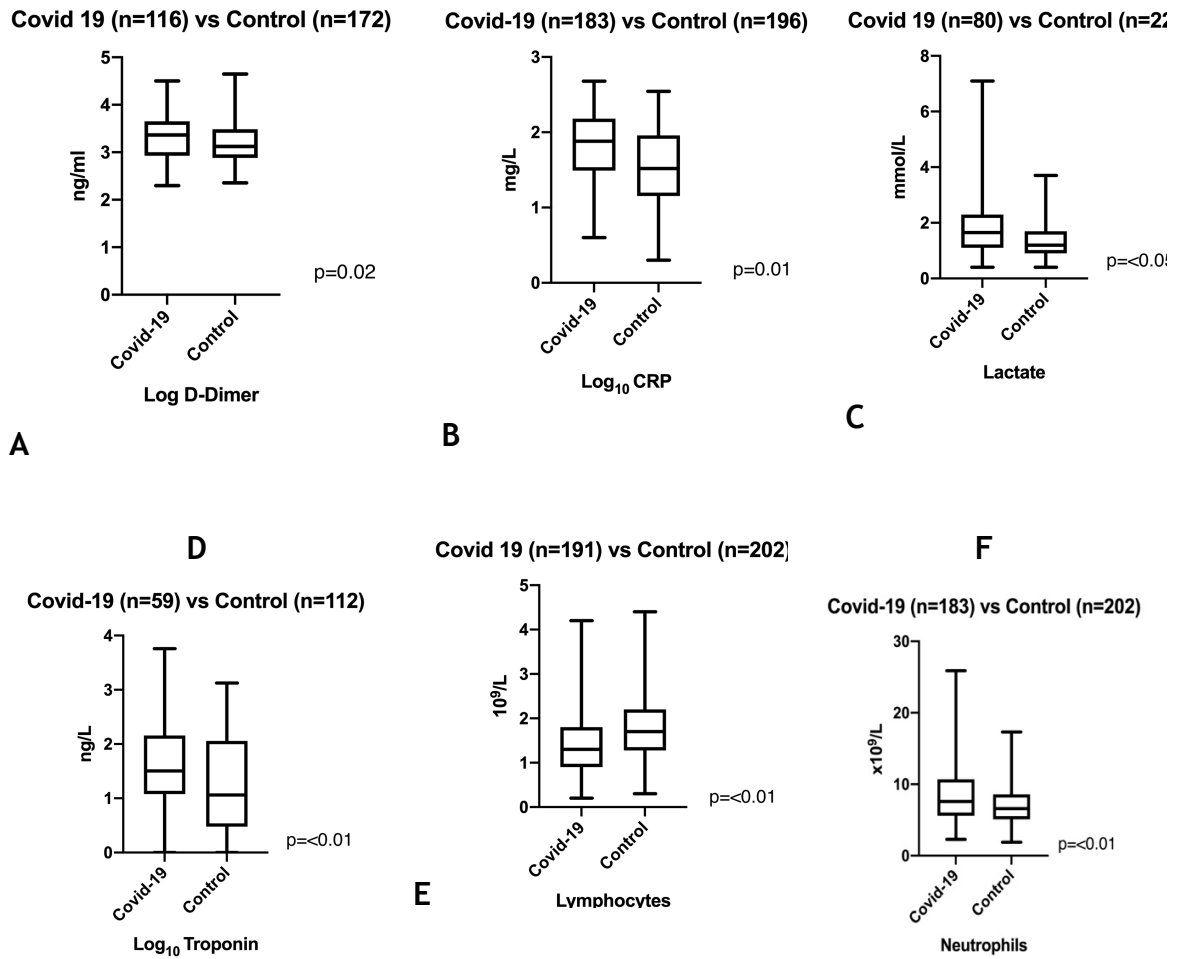


Figure 29. Comparison in biomarkers between those with COVID-19 and control group.

6.4 Discussion

There is now a large body of evidence published supporting that there is a substantially increased risk of pulmonary thromboembolism in patients hospitalized with COVID-19. However, many of these studies were single centre, and were published early in the first wave of the pandemic and were mainly focused on the patients managed in the critical care unit(136). At the time of publication, this was the first study to recognise this risk when assessing patients at a national level in both critical care and ward-level care as other previous studies had been single centre studies or had focussed only on those in intensive care (136, 250). Collection of accurate healthcare data in Scotland is made possible because of the Community Health Index (CHI) number. This is a unique identifier of individual patients using the Community Health Index (CHI) number, which is assigned to individuals at birth, or on registration with primary care if the patient has immigrated to Scotland. This CHI number was attained from the CTPA performed at the time of diagnosis and can be cross referenced with primary care health records to identify comorbidity. These are unique to this study. It has been established that 3.7% of all patients admitted to hospital during the 'first-wave' of the COVID-19 pandemic had a radiologically confirmed PTE. Previous studies in Scotland, by the Scottish Patient Safety Survey, have demonstrated that the incidence of PTE in hospitalized patients prior to the COVID-19 pandemic is 1% (246). Here, data is provided by Information Services Division and National Records of Scotland for access to the data on coding of VTE in hospitalized patients admitted in Scotland. The number of episodes is assessed annually, and this was done to assess the mortality associated with it and the financial impact on health services. In addition, the incidence of PTE in those hospitalized with COVID-19 is higher than previously seen in non-COVID-19 pneumonia, which has previously been reported to have an incidence of 1-2%(161, 162). My study supports other evidence that COVID-19 increases the risk of developing PTE in those managed in the critical care setting(136), who, in this cohort, have an incidence of 6% of developing PTE.

It is also notable that taking those managed in level 1 care alone, the incidence is 3.5% and this is in agreement with a smaller study in New York, USA(251). *Bilaloglu et al* assessed the incidence of all arterial and venous thrombosis over a shorter period and including only those RT-PCR positive for COVID-19. Here, they recruited 3334 consecutive adult admissions to a single centre and assessment for thrombotic events was done as part of clinical care, rather than a screening process. These included deep venous thromboembolism, pulmonary embolism ischaemic cerebrovascular accidents and myocardial infarction. They showed an incidence of any thrombotic event to be 10.6%, but an incidence of 3.2% of pulmonary embolism in their cohort. There are a number of advantages of our study. It includes a greater samples size, is national data and is specific for PTE. In addition it includes both those RT-PCR positive and those with classical radiological findings on radiological imaging, which is a more accurate representation of the population as false negative RT-PCR had been seen to be as high as 29% in the early stages of the pandemic(252). A criticism could be that the study did not only include those with positive RT-PCR. At the time of the first wave the access to PCR testing was not readily available and may not have been as accurate as currently available diagnostic tests. Therefore it was felt a more accurate representation would be to include patient with clinical and radiological features that corresponded to Covid-19 infection.

A higher incidence of PTE in men was shown, despite the higher incidence of COVID-19 in Scottish women (404 per 100,000 compared to 259 per 100,000)(160). This may be explained by a more severe form of COVID-19 seen in men, given that the incidence of requirement for critical care was also higher in men (17 per 100,000 in males vs 6.3 per 100,00 in females)(160). However, it remains possible that, irrespective of COVID-19 pneumonia severity, men are at higher risk of developing PTE than women (253). The influence of gender and severity of Covid-19 syndrome remains unclear.

A greater proportion of PTE-associated right heart strain in patients in intensive care compared to those in level 1 care is perhaps to be expected. This could be explained by those in critical care having a greater parenchymal inflammatory component in addition to the PTE, or, indeed, that those in critical care were likely to have had a higher clot burden leading to greater cardiac dysfunction. However, I have not evaluated the contribution of clot burden or parenchymal

changes in our cohort.

Using biomarkers to compare those with COVID-19 and those without, the higher C-Reactive Protein supports the theory that there is an inflammatory component to thrombogenesis. D-Dimer levels at presentation with PTE were noted to be significantly higher in the COVID-19 group compared the control group, which correspond with phenomenon seen in other studies (254). The lymphocyte count was significantly lower in the COVID-19 group. These findings are now well recognized to be associated with severe COVID-19 infection with the D-Dimer levels reflecting the increased systemic and pulmonary macro and microvascular thrombosis(255). Neutrophil count was also observed to be significantly higher in those with COVID-19, which may have contributed to the immune mediated thrombotic process(256). These findings are in keeping with the hypothesis that the thrombosis in Covid-19 is the result of a systemic inflammatory endothelitis, which triggers activation of the coagulation cascade.

Mean BMI of the COVID-19 cohort associated PTE was in the obese category and the majority of patients in the intensive care unit had a BMI of $> 25 \text{ kg/m}^2$. This is in keeping with other studies demonstrating that higher BMI is associated with increasing COVID-19 disease severity but obesity is also an independent risk factor for PTE(257). However, in this group, I did not detect an association between those overweight and an increased risk of admission to critical care or increased mortality. This could be due to a lack of power of this study to demonstrate this.

The median time from RT-PCR sample to presentation with PTE was 8 days and the median time from admission to PTE diagnosis was 1 day. This study includes patients who had initial SARS-CoV-2 testing performed in the community prior to admission, in addition to those who had had testing performed in hospital and serves to highlight that patients with COVID-19 who are managed in the community are also at risk of PTE. This serves to reinforce prompt consideration of optimal prophylactic anticoagulation of patients on admission to hospital with COVID-19 and to have a low threshold for early radiological assessment for PTE and treatment. Indeed, studies performed subsequent to this have demonstrated an additional benefit in actively screening for pulmonary embolism in Covid-19. *Korevaar et al* (258) evaluated the use of screening in 541 patients over a period of 3 months in a multi-centre trial, using D-Dimer as an initial screening tool,

with a threshold of 1.00mg/L. If above this, a CTPA was performed to assess for presence of PTE, and they showed an incidence of 5.8%.

I have shown a higher incidence of PTE in the critical care setting, which, at the time of study, support the guidance that these may benefit from higher doses of prophylactic low molecular weight heparin (259, 260). However, subsequent evidence supports the use of standard prophylaxis for patients with Covid-19. Patients with COVID-19 associated PTE managed in critical care were more likely to have right heart strain. It is possible that this reflects a higher clot burden in these patients, however, it is probably more likely to represent the combination of thrombus load, marked parenchymal lung changes and consequent hypoxia seen in severe COVID-19. *Gunay et al* (261) performed a single centre, prospective study evaluating the cardiac function in 51 patients with moderate or severe Covid-19 without pulmonary embolism or risk factors for cardiac dysfunction. They showed that there was evidence of subclinical right ventricular dysfunction in these patients, with a higher right ventricular end-diastolic and end-systolic area compared to healthy controls and a lower right ventricular fractional area change in those with Covid-19. This demonstrates that the parenchymal disease alone contributes to poorer cardiac function. *D'Andrea et al* (262) also evaluated a cohort of patients with Covid-19 to assess for the presence and impact of cardiac dysfunction. Using echocardiography, RV end-diastolic diameters were measured, and pulmonary artery pressures estimated in 115 patients, 26 of whom had a cardiac injury. The patients with cardiac injury were also noted to have a higher systemic inflammatory response, as measured by C-reactive protein, D-Dimer and on CT appearances of the parenchyma. Similar to my study, they demonstrated adverse survival outcomes in those with cardiac dysfunction. The multifactorial pathophysiology in the cohort I studied, who have parenchymal disease and pulmonary embolus, is likely to explain the significantly poorer survival observed in patients with right heart strain in this population.

A range of relevant comorbidities in patients with COVID-19 associated PTE were evaluated. Although the occurrence of comorbidities observed was probably lower than would be observed in non-COVID-19 critical care populations(245, 263, 264), I did not find any significant difference in the prevalence of comorbidity between patients managed in critical care versus ward care. The

numbers of patients in the critical care group are too limited to make a meaningful assessment of association between comorbidity and the risk of PTE in this group.

Despite this study having key strengths in its capture of robust, national data in patients cared for in all hospital settings, there are limitations. As is common in retrospective data analysis, there are some missing data, in particular for biomarker and comorbidity data, but it should be recognised that this was gathering of clinically indicated investigations, and, as such, they were not always performed uniformly in patients and were at the discretion of the treating physician. As such, there is a degree of heterogeneity in the investigations results available. Patients are diagnosed on the basis of RT-PCR positive testing for SARS-CoV-2 or, where this was not available, or was negative, on the basis of internationally agreed diagnostic radiological criteria for COVID-19(158). Whilst there is confidence of including these patients in our data because of international agreement for the classical appearances of COVID-19, there remains some diagnostic uncertainty in patients who do not have positive RT-PCR. With these diagnostic criteria, the study can conclude that the proportion of those with thrombosis is at least 3.7% but could potentially be higher. Although the gold standard diagnostic investigation for PTE is CTPA, it is conceivable that a number of critically unwell patients were too unstable for transfer for radiological investigation and were treated empirically for PTE. Furthermore, patients treated at ward level who were deemed too frail, palliative or had a contraindication to CTPA would not have received a formal investigation for PTE. The true incidence of COVID-19 associated PTE may therefore be even higher than is reported here. Efforts have been made to be rigorous in the assessment of patients with right heart strain using the European Society of Cardiology guidelines for the diagnostic criteria of right heart strain. However, troponin levels could be influenced by other effects of COVID-19 and not purely from the pulmonary embolus. These patients have a systemic illness, and it is acknowledged that there is no perfect way of assessing for right heart strain retrospectively. Patients assessed for peripheral deep vein thrombosis diagnosed by lower limb venous ultrasound were not studied in this cohort. Moreover, there was limited access to demographic data and details surrounding the management of the control group. For the Covid-19 group, primary care

records were used in order to gather details of comorbidities on individuals were used. These, too, may be imperfect and, as such, comorbidities could have been present but not included in our analysis. In addition, there was limited access to the comorbidities of the control group, and the same limitation applies to this group.

6.5 Limitations

Due to the retrospective nature of the study, there are missing data points for both demographic data, including BMI, and biomarkers. As such, all analysis was performed only for those with available complete data.

Whilst all CTPAs performed across Scotland during this time are included, some patients may have been too unwell to facilitate safe transfer for this to be performed and therefore would have been missed. In addition, some smaller, rural hospitals will not have had access to CTPA equal to that of urban-based university hospitals. As such, there may have been some patients not included in our study who did have underlying Covid-19 PTE. Furthermore, I have not included those who had lower limb doppler performed and had venous thromboembolism diagnosed by this measure.

6.6 Conclusions

At the time of analysis and dissemination, this study was the first to report national data informing the incidence, demographics, and comorbidities of patients with COVID-19 associated PTE. I have established that hospitalised patients with COVID-19 have a higher incidence of PTE than would be expected in the general hospitalised population, or those hospitalised with pneumonia and this risk is not confined to critical care. In the context of COVID-19, PTE may present later in the illness following initial diagnosis and it has been shown it can occur up to 14 days after the positive RT-PCR test. PTE should be actively considered in deteriorating patients with COVID-19 with a low threshold for radiological assessment and, at the very least, should receive appropriate thromboprophylaxis to reduce the risk of PTE.

7 Conclusions

This thesis has been a journey of pulmonary thromboembolic disease: I have assessed for the incidence and originating factors for acute pulmonary thromboembolic disease, evaluated novel diagnostic tools in order to detect disease non-invasively and assessed for effective treatments in patients with pre-capillary pulmonary hypertension that may be used as an adjunct in treatment of chronic thromboembolic pulmonary hypertension.

Whilst there are several recognised risk factors for developing acute pulmonary embolus, I have shown that there is an increased incidence of acute pulmonary embolism in those patients hospitalized with Covid-19, both in those who are managed in ward-based environment and the critical care unit. It is hypothesized that this is associated with the systemic small endothelial dysfunction that leads to the development of the acute illness, but at the time of writing, it is too soon to say whether there is a particularly high risk of developing CTEPH because of Covid-19 associated acute pulmonary embolus. To my knowledge, this was the first study to assess the national incidence of pulmonary embolus associated with Covid-19 and the first study to attempt to evaluate the incidence of pulmonary embolism in those hospitalized with Covid-19 outside the critical care unit. Whilst this is of interest, it also raises awareness for clinicians in looking for other causes of hypoxia and physiological decline in those with established Covid-19. Initially, this data contributed to local policy in increasing prophylactic anticoagulation of inpatients with Covid-19 to address the increased risk posed to these patients, however, subsequent work specifically performed to address this question has shown no benefit of higher dose anticoagulation.

There remain several unanswered questions on the long-term effects of Covid-19, and specifically the long-term effects of pulmonary embolism associated with it. Ongoing symptom burden of shortness of breath and functional limitation are likely to be multifactorial, but chronic thrombotic occlusion of the pulmonary vasculature, will need to be excluded. As such, there is a need for more accessible and reliable non-invasive investigations that will detect the presence of thrombotic pulmonary vascular disease. Using echocardiography, I have shown

that the left ventricular eccentricity index can be used to detect the presence of thrombotic pulmonary vascular disease. This is a novel finding, and to my knowledge, has never previously been reported in thrombotic pulmonary vascular disease. The standard indices, including tricuspid regurgitant pressure gradient is not present in a proportion of patients so this offers another bedside index that is easy to measure that will quantify the interventricular septal shift and lend confidence to the clinician in justifying the use of more detailed investigations into the right heart and the pulmonary vasculature.

Cardiopulmonary exercise testing has also been shown to be a very useful tool in the assessment of patients in who are breathless to identify if the origin of this is cardiac, respiratory, or muscular dysfunction and is able to quantify the degree of functional limitation. However, patients do need a degree of fitness and have a satisfactory musculoskeletal system in order to glean meaningful information and in those who are severely functionally impaired this maybe limited, therefore imaging tends to be the main focus initially.

Given the well-established limitations with echocardiography, I went on to further evaluate the use of cardiac magnetic resonance imaging. Magnetic resonance imaging is the gold standard investigation in evaluating cardiac function in pulmonary vascular disease. It is more costly, more labour intensive and less convenient for patients than echocardiography but the images are of better quality and image acquisition is not user dependent. Furthermore, it facilitates imaging of the main pulmonary vasculature and can be performed, with contrast, at the same time as a pulmonary angiogram, allowing complete visualisation of the pulmonary vascular tree. The left ventricular eccentricity index has not previously been evaluated using magnetic resonance imaging and nor has it previously been assessed in thrombotic pulmonary vascular disease. I have shown, to my knowledge, for the first time that an elevated left ventricular eccentricity index in systole and diastole is associated with the presence of pulmonary hypertension and, indeed, a lower pulmonary artery distensibility. I detected a threshold of >1.1 whereby there is a high degree of sensitivity and specificity for the presence of pulmonary hypertension. In addition, cardiac magnetic resonance imaging can be used to differentiate CTEPH from CTEPD without the risk of invasive investigations.

Traditionally the treatments of pulmonary vascular disease have been pharmacologically based and, in the case of thrombotic pulmonary vascular disease, based on mechanical solutions in the form of surgery or balloon pulmonary angioplasty. I have shown that exercise training can increase exercise capacity and improve quality of life in those with precapillary pulmonary hypertension. This is likely to be multifactorial, however using cardiac magnetic resonance imaging, I have shown that improvements in left heart contractility is a contributing factor, which is a novel finding. I did not show improvements in the right ventricular function, suggesting that improved exercise is not related to significantly improved pulmonary haemodynamics, therefore there is still a central role for the mechanical and pharmacological treatments to improve the pulmonary haemodynamics. The study was performed on a heterogenous group of patients with pre-capillary pulmonary hypertension, including those with CTEPH, but further work is required to ensure that those with specifically CTEPH do stand to benefit. It would also be of interest to assess the role of 'pre-habilitation', where those with CTEPH undergo an exercise training programme to look for improvements in quality of life and exercise tolerance before surgery or balloon pulmonary angioplasty and evaluate its use in improving post-procedural outcomes.

I believe that this thesis has contributed novel findings to the existing body of work in the causes of disease, the diagnosis, and the treatment of patients with thrombotic pulmonary vascular disease. There is much that is not yet understood in this condition but in the future, it is hoped that patients at risk of developing the disease can have access to investigations that lead to a timely diagnosis and effective therapies, thereby improving quality of life and improved survival.

8 Future Directions

This thesis has demonstrated novel findings in the causes of pulmonary thromboembolism, novel means of detecting the presence of disease and the effects of non-pharmacological therapies for treatment. The incidence of disease is increasing, and we do not yet know much about the long-term effects of thrombosis associated with Covid-19. Having access to non-invasive investigation is vital to the timely detection of disease.

However, there is still much to learn about thrombotic pulmonary vascular disease. The current treatment options carry significant risk to patients and the overall prognosis of CTEPH remains poor. Whilst current diagnostic tools can detect the presence of the disease, more work is required to detect the functional impact of thrombosis on an individual patient's haemodynamics and cardiac function leading to functional impairment. In assessing this, mechanical treatments (surgery and balloon pulmonary angioplasty) can be more focussed on areas of vasculature that are most severely affected.

I had intended to perform a study using perfusion mapping to assess for the presence of pulmonary vascular thrombosis in the hope of quantifying the functional impairment associated with thrombosis (see Appendix). In doing this, it may become easier to select which treatments a patient would benefit from. In the case of balloon pulmonary angioplasty where a number of treatment sessions are required, it may be that these could be reduced and more focussed on the areas having the greatest functional impact, thereby reducing risk to patients and reducing overall cost.

In addition to improved diagnostics in the evaluation of thrombotic pulmonary vascular disease, there is more to learn in the use of CMR in pulmonary vascular disease. Whilst it is the gold standard investigation for RV assessment and has significant benefits over echocardiography, there remains no way of accurately measuring pressure with CMR. 4D flow of blood through the pulmonary artery may yield some options in assessing for pulmonary arterial hypertension. I had intended to undertake a study to look at wall shear stress within the pulmonary vasculature using CMR. The shear stress may be another non-invasive tool that could be used in the detection of disease and response to therapy, but further studies are required to validate this as a tool that can be used in clinical practice.

9 Appendix

9.1 Study Design - Using Iodine Mapping in the diagnosis and assessment of function limitation in patients with chronic thromboembolic disease

This project was due to form the basis of this thesis. It was conceived in 2018, coinciding with the emerging use of iodine mapping in pulmonary vascular disease. There was a novel scanner purchased by the University of Glasgow and NHS Greater Glasgow and Clyde that could facilitate Iodine Mapping and, prior to this project, was exclusively used for neuroimaging. With this scanner available, we wanted to evaluate its use in patients with possible underlying chronic thromboembolic disease. The project was peer reviewed and assessed by the Research and Development team at NHS Greater Glasgow in Clyde during 2019. Ethical Approval for the study was granted in April 2020. However, around this time, there was the emergence and rapid spread of the SARS-CoV 2 virus associated clinical syndrome Covid-19. As such, I was not able to pursue this study beyond the point of patient recruitment and the study was abandoned. However, given the significant volume of work required to reach the stage of patient recruitment, and the learning experience this was for me, I felt it prudent to include it as part of my thesis in the form a study design.

9.2 Background

Acute pulmonary embolism is a common and potentially fatal condition. It affects 0.06% of the population annually (74), with the risk substantially increasing with age, and has a high incidence of recurrence. There is an in-hospital rate of death ranging from 6-15%. The presence of acute thrombus induces an acute inflammatory response within the lumen. This process organises the thrombus, before spontaneously lysing it. In the majority of cases there is full resolution of thrombus but, in some cases, the inflammatory and lysing process can lead to damage of the vascular endothelium (75). With heparin treatment, the spontaneous process of thrombus resolution allows the lumen of the vessel to become patent and the normal pattern of venous flow is re-established. With follow up imaging of patients treated for acute pulmonary embolus, there is approximately 50% reduction in thrombus burden at 4 weeks (76).

Treatment is usually administered for at least 12 weeks, but often be indefinite if there is a risk of thrombosis recurrence. Treatment depends on if there has been a provoking factor or not. Provoking factors include major surgery, prolonged immobilisation, hormonal contraception, or direct trauma. Treatment with anticoagulation is recommended if there is no identifiable provoking factor, or if there is a risk factor that will persist for the lifetime of the patients, such as a solid organ malignancy, a collagen vascular disease or thrombophilia condition. 3 months has been chosen for those with provoked PE because the risk of VTE in the first year is 1% and 0.5% in the years thereafter. The reason that lifelong anticoagulation is advised with no provoking factor is that the risk of recurrence in the first year is 10% and 5% per year thereafter(265). However, patients' bleeding risk need also be considered when advising lifelong anticoagulation.

Despite treatment, however, approximately half of patients have chronic pulmonary vascular abnormalities at follow up and the underlying cause of incomplete thrombus resolution is unknown. Larger, central thrombi are least likely to fully resolve. Pathology studies from patients who have had pulmonary endarterectomy for chronic thromboembolic pulmonary hypertension (CTEPH) have yielded a heterogeneous collection of thrombus material, consisting of fibrous plaques with signs of angiogenesis or atherosclerotic lesions containing cholesterol, macrophages, and T-lymphocytes(77, 78). The clinical significance of incomplete thrombus resolution is unknown as is not clear how many of these patients have resulting functional limitation(79).

CTEPH is the result of thrombus related persistent perfusion defects within the pulmonary vasculature, which leads to increased pulmonary vascular resistance and increased pulmonary arterial pressure. It most commonly occurs within 2 years of the index acute pulmonary embolus episode(266). It is defined by a mean pulmonary arterial pressure above 20mmHg and a pulmonary capillary wedge pressure of less than 15mmg, as measured by right heart catheterisation along with at least one persistent perfusion defect seen on imaging (V/Q scanning or pulmonary angiography) after 3 months of anticoagulation. CTEPH can cause remodelling of the small pulmonary vasculature, in addition to chronic stenosis of larger vessels. *Dorfmuller et al(267)* have shown that there is

eccentric intimal thickening in the distal muscular pulmonary arteries and concentric intimal thickening. This persists despite surgery and can lead to ongoing symptoms or pulmonary hypertension after intervention. Clinically, it leads to impaired exercise capacity and can proceed to right heart failure and premature death. The diagnosis and management of CTEPH is well validated(80).

However, there are limited studies on the effects of chronic thromboembolic pulmonary disease (CTEPD). This is most commonly seen as a complication following acute pulmonary embolus and is characterised by chronic vascular obstruction and exercise intolerance, without evidence of pulmonary hypertension at rest. It has been shown that these patients can have a functional limitation when tested with cardiopulmonary exercise testing(177, 179) (CPET) (180) and successful treatment with PEA has been performed(181). The exact cause of this functional limitation is not clear, but it has been hypothesised that there is altered gas exchange following acute pulmonary embolus. There may also be more of a haemodynamic effect of chronic pulmonary vascular occlusion that is not evident during right heart catheterisation. Pulmonary Vascular Resistance (PVR) is part of the diagnostic criteria for CTEPH. However, impedance of forward blood flow through the vasculature is not captured by the PVR and these values may be vastly different depending on the distribution of thrombus, rather than the volume of clot burden itself. It has been shown there is greater stress on the right ventricle in those with proximal thrombus compared to those with a more distal pattern(268). There are altered ventilation/perfusion ratios with increased dead space ventilation, hypoxaemia and hypocapnoea in acute pulmonary embolus and are thought to persist in patients with CTED(184). As a result, it is important to assess for the presence of thrombus in the central pulmonary arteries using CT scanning and for the presence of distal thrombus, currently performed using scintigraphy. This may be important in defining the haemodynamic effects of CTED, the effects this has on the right ventricle and on patients' symptoms(268).

Patients' symptoms often poorly correlate with underlying pathophysiology and the underlying cause of poor exercise tolerance is not clear. However, in view of the symptoms generally only being on exertion, perhaps taking resting measurements during investigations is an approach that could be modified by

assessing them both at rest and exertion(269). Patients with CTEPD showed similar ventilatory limitations as those patients with CTEPH along with dysfunctional pulmonary perfusion, as shown by abnormal ventilatory equivalents and anaerobic threshold (184) when measured by cardiopulmonary exercise testing (180). There is abnormal pulmonary artery compliance, as demonstrated by a steep mean pulmonary artery pressure/ cardiac output slope measured during exercise right heart catheterisation. Post operatively, the improvement in symptoms is associated with an improvement in the right ventricular/stroke volume relationship and improved ventilatory efficiency, suggesting that these are the two key sources of symptoms in CTED(269).

There are a number of investigations available to allow diagnosis of chronic thromboembolic disease. These are often used in combination, rather than individually, in evaluating symptoms. Ventilation-perfusion scintigraphy is the most sensitive widely available investigation for the detection of chronic thromboembolic disease, particularly when the disease has a more distal distribution(270). This involves the inhalation of radioisotope labelled aerosol, technetium 99, delivered via a non-rebreathe mask when the patient is supine, to assess ventilation. The small particles of the isotope can reach the distal areas of tracheobronchial ventilation. This reflects the regional ventilation of the lung. Technetium 99 macroaggregated albumin is then injected with the patient supine. The radionuclide particles are small enough to reach, and lodge, in the precapillary arterioles, reflecting distal pulmonary perfusion. The ventilation and perfusion images are then compared. Using the PIOPED criteria(271), the images can then be classed as low, intermediate or high probability for pulmonary embolus depending on the number of segmental or subsegmental mismatches between the images. Whilst this investigation is able to detect pulmonary vascular obstruction and has a high negative predictive value, there are a number of reasons why a V/Q may be indeterminate(272), such as atelectasis, or emphysema. This can have some adverse consequences of patients receiving therapeutic anticoagulation erroneously. Invasive pulmonary angiography can also be used to assess for pulmonary embolus. This involves the passing of a pulmonary angiogram catheter via a central vein directly into the main pulmonary arteries. Iodine based contrast is then injected under fluoroscopic guidance to each lobe of the lung. The distribution of the contrast

can be seen across several cardiac cycles and allows good visualisation of the central and distal perfusion. However, although this is a valuable tool at assessing perfusion, it comes with less of a radiation dose to a standard CT-pulmonary angiogram and does not provide any meaningful images of the lung parenchyma(273), in addition to carrying the risk of an invasive procedure(274).

CT-pulmonary angiogram is the most commonly used tool for assessing the pulmonary vasculature and is the gold standard investigation for excluding acute pulmonary embolus. There are various methods of performing these scans, but the most common is using a bolus tracking technique. The patient is positioned supine. There is a so-called scout scan performed initially, in order to facilitate the area that should be scanned. It should cover from apices to diaphragm in the caudocranial direction. There is a region of interest selected in the main pulmonary trunk, just inferior to the carina. A threshold of 100 Hounsfield units is placed on this area, which reflects the presence of iodine-based contrast. Once the 60mls of contrast is injected and reaches the pulmonary artery, the scanner detects this change in fluid density and triggers the scanning of the lungs, which is performed during inspiration. The images produced provide an anatomical display of perfusion of the lung and can identify the presence or absence of contrast filling in the proximal pulmonary arteries. The absence of filling is deemed to reflect the presence of thrombus. There are subtle ways of detecting the presence of acute or chronic thrombus, with the latter having a more laminated appearance. The bronchial arteries can also be visualised, which are hypertrophied in CTEPH. In addition to the pulmonary vascular appearances, the CTPA provides information on the lung parenchyma, which may show mosaicism in CTEPH, or the presences of pulmonary infarcts. The right heart can also be seen. Measuring the RV:LV can give an indication of the presence of pulmonary hypertension if the ratio is >1 .

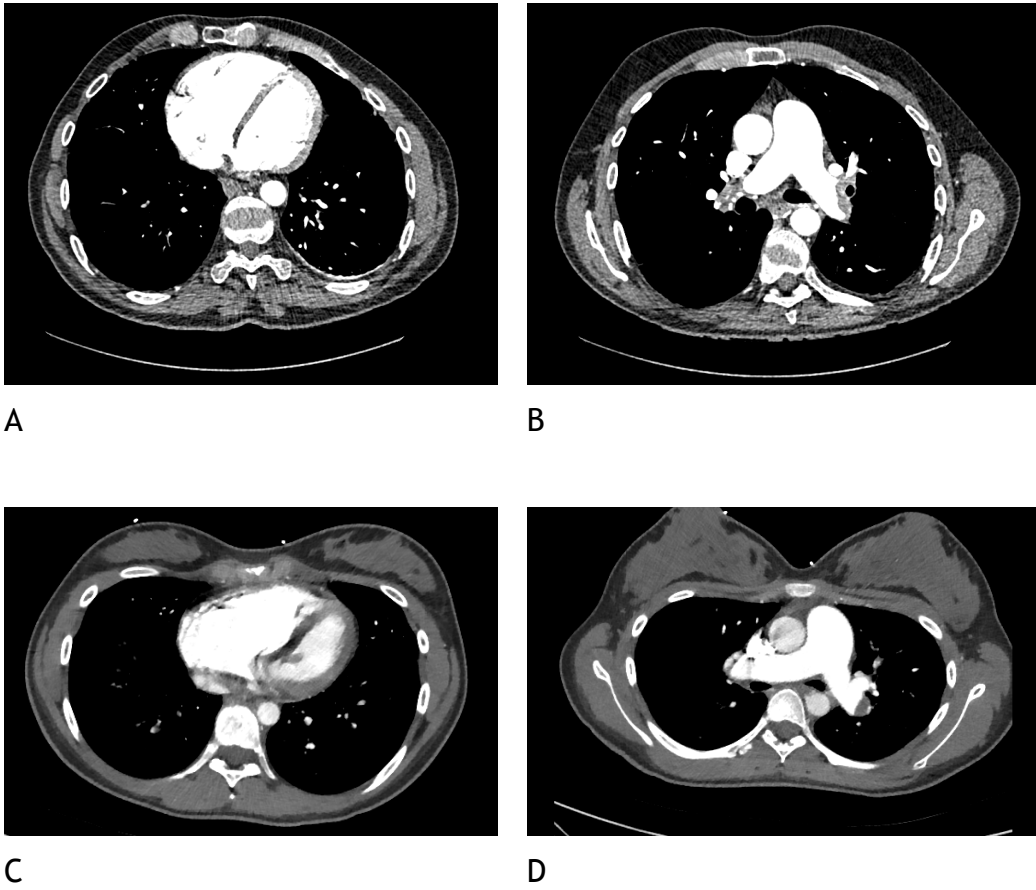


Figure 30. Images of Chronic and Acute Thrombus

A. Right heart dilatation (RV:LV >1) in chronic thromboembolic disease. B. Laminated chronic thrombus in the left pulmonary artery. C. Right heart dilatation in acute pulmonary embolus (RV:LV >1), showing septal deviation to the left ventricle. D. Acute thromboembolism in the left pulmonary artery obstructing blood flow to the left upper lobe.

Despite the information gleaned from a standard CTPA being diagnostic for the presence or absence of proximal thrombus, there is no meaningful way of assessing the functional impact of the thrombus on blood flow. Iodine mapping is a tool that has been around for many years but so far has had limited impact in day-to-day clinical practice, but has shown some promise when used to identify malignant or benign lesions in the lung and the liver(275). Iodine mapping of the pulmonary arterial system allows the visualisation of abnormalities in the blood flow map in the lung distal to the pulmonary embolus. It is used in conjunction with standard CTPA and has been shown to increase the sensitivity of PE detection(276). This can be performed using dual energy CTPA (DECT), or digital subtraction imaging, with comparable rates of detection using either of the techniques(277). The differences are that DECT requires hardware, which produces two different energy x-ray photon spectra, allowing the interrogation of materials with different attenuating properties at different energies. This allows images to be reconstructed in a form that removes substances of known composition, such as iodine-based contrast. The image subtraction is purely a software manipulation of the images and does not require the scanner to have extra hardware, therefore is more convenient to perform where there is only access to a standard scanner. In this technique, images are acquired pre-contrast and then subsequently subtracted from post-contrast images. A perfusion map is then created showing the distribution of the iodine contrast. The presence of iodine is a surrogate for blood flow. As such, the functional impact of thrombus present in the pulmonary artery can be demonstrated. However, it is not clear at what level of perfusion deficit patients will begin to develop symptoms.

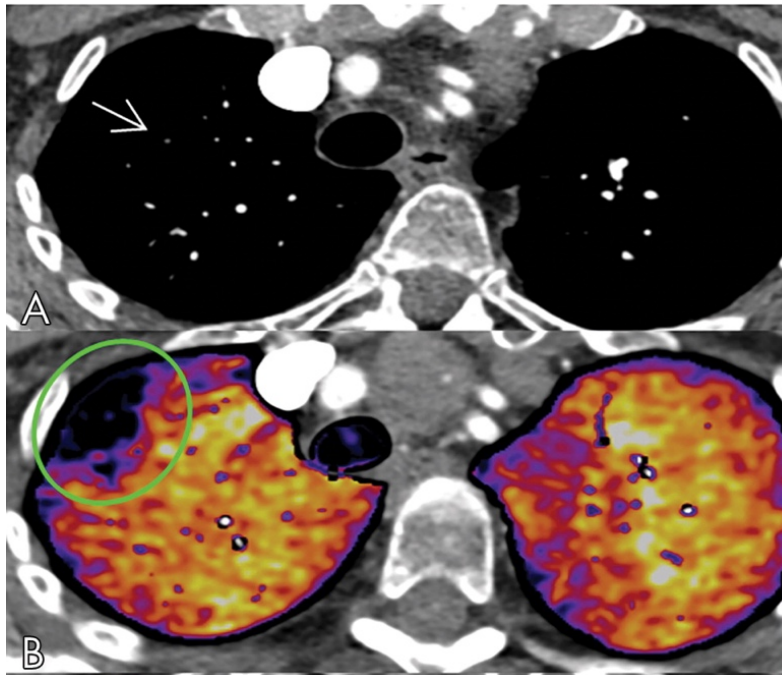


Figure 31. Comparison of standard CT angiography with image subtraction iodine mapping in detecting pulmonary embolus(278).

- A. Standard CT angiography showing reduced contrast enhancement in the right lower lobe in the presence of pulmonary thromboembolism.
 B. Subtraction imaging iodine Map demonstrating the functional impact of thrombus with wedge shaped perfusion defect in the right lower lobe.

The post-PE syndrome is a varied collection of symptoms, such as persistent dyspnoea and exercise intolerance, that can occur in patients after an acute pulmonary embolus(279). This doesn't necessarily reflect underlying pulmonary vascular dysfunction, although this is clearly possible. Other causes may lead to these symptoms include peripheral muscle deconditioning or cardiac dysfunction. The best way of assessing for, and quantifying, exercise intolerance in pulmonary vascular disease is using cardiopulmonary exercise testing. This can either be done in the form of a treadmill or a cycle ergometer. The latter is the most common and the one chosen to be used in this study because of its availability. A low peak VO_2 , Work rate, Oxygen pulse, end tidal CO_2 and exertional desaturation are all associated with the presence of pulmonary vascular disease. In addition, raised ventilatory equivalents (V_E/V_{CO_2}), dead space ventilation (V_D/V_T) and alveolar-arterial oxygen tension are suggestive(119).

Our study would aim to provide data on patients presenting with symptoms of chronic thromboembolic disease and assessing if the iodine map correlates with functional limitation, measured by CPET (low peak VO_2 , high V_D/V_T , high V_E/V_{CO_2}). We hypothesise that the pulmonary blood volume, as assessed by iodine mapping, will correlate with functional limitation and findings on CPET.

9.3 Study

9.3.1 Aims and Objectives

- To assess if adding iodine mapping to standard CTPA increases the sensitivity of CTEPD detection.
- To correlate the iodine map with functional limitation measured by CPET (low peak VO_2 , high V_D/V_T , high V_E/V_{CO_2}).
- We aim to compare the sensitivity of CTPA with V/Q scanning.

9.3.2 Study design

A prospective observational cross-sectional study is proposed to assess patients presenting with symptoms of chronic thromboembolic disease and correlate the iodine map with functional CPET findings and CT V/Q Scintigraphy. Whilst it is understood that not all patients who are symptomatic after an acute pulmonary embolus are so because of chronic thromboembolic disease, these investigations are likely to lead the clinician towards a definitive diagnosis, even if it is not chronic thromboembolism. As such, these investigations can, and usually are, performed as part of standard care.

9.3.3 Inclusion Criteria

- Aged 18 and above
- Able to give informed consent
- Previous acute pulmonary embolus
- Breathlessness suggestive of chronic thromboembolic disease after minimum of 3 months of anticoagulation.

9.3.4 Exclusion Criteria

- Unable to provide consent
- Pregnant patients or those breast feeding
- Those with renal dysfunction, eGFR <30
- Those with a prior documented intolerance to iodine contrast
- Those with isolated subsegmental pulmonary embolus
- Patients with severe left ventricular systolic dysfunction or valvular heart disease
- Patients with severe lung disease
- Patients unable to undertake a cardiopulmonary exercise test.

9.4 Methodology

The trial participants would be recruited from the post-pulmonary embolus outpatient clinic at the Victoria Hospital Glasgow, The Golden Jubilee Hospital and Gartnavel General Hospital. Patients will be referred there from secondary care following an episode of acute pulmonary embolus. If patients attending this clinic are no longer symptomatic of breathlessness, anticoagulation is recommended to stop. If this has been a single episode of thrombosis.

However, if patients are symptomatic, it is recommended that they continue anticoagulation therapy until further investigations are completed, so long as their risk of bleeding does not exceed that of further thrombosis. Patients will usually undergo a battery of investigations to try and ascertain the cause of their symptoms. The order in which they are performed often depends on the exact symptoms they have but also on their comorbidities. These investigations include echocardiogram, V/Q scintigraphy, CTPA and CPET. Performing the CTPA with a computer tomography scanner with image subtraction capabilities is proposed, which will allow an iodine map to be created. As before, this will be carried out in the Imaging Centre of Excellence, located at the Queen Elizabeth University Hospital.

9.4.1 Iodine Mapping

Iodine mapping can be performed using dual energy CTPA or digital subtraction CTPA. Using the latter does not require additional hardware and will be used in this study. The iodine map is a surrogate for pulmonary blood flow. The map demonstrates the local iodine concentration, reflecting the changes seen when there is interference in blood flow, for example in pulmonary embolus. This is achieved using digital image subtraction using T pulmonary angiography (*Toshiba/Canon Aquilion One Vision Edition*). The iodine map consists of a pre-contrast scan followed by a contrast enhanced scan using iodine-based contrast and taking images once the contrast reaches the pulmonary trunk. Both scans are done in the same scanner settings, except for a higher noise index used for the pre-contrast scan. The pre-contrast scan images are then subtracted from the post-contrast images, leaving a map of iodine contrast distribution. The map is then produced using a heat map, using relative contrast enhancement. The

area of highest contrast enhancement is deemed to be 100% contrast, usually seen in the main pulmonary artery, and all other levels of iodine enhancement in vasculature are compared to this.

Collimation 320 x 0,5 mm

Rotation time 275 ms

Tube potential 100 or 120 kV, dependent on patient size

Automatic exposure control Pre-contrast scan: noise index = 30 Postcontrast scan: noise index = 22,5

Scan range Whole lung

Image reconstruction Iterative, AIDR 3D strong, filter F09

Contrast injection 70 ml lobitridol 300 (Iomeron 300) at a 5 ml/s infusion rate, bolus tracking in the pulmonary trunk

9.4.1.1 Radiation Exposure

Radiation exposure is dependent on patient weight. The standard CTPA radiation dose, performed as part of the existing algorithm, is 5mSv - 10mSv. With this generation of CT scanner, the radiation exposure is expected to be the same or less than standard CTPA (280).

9.4.2 Postprocessing

The software used for processing is Sure Subtraction, Toshiba Medical Systems; FDA report K130960, that processes data as follows:

- Segmenting the lungs for processing
- Registering and correcting for changes in the location and volume of the pulmonary structures between pre and post contrast scans
- Subtracting the pre and post scans to create the iodine map
- Removing vessels and interpolating gaps
- Noise reduction filtering
- Super-imposed a colour coded iodine head map over the contrast enhanced area.

9.4.3 Interpretation

The quality of CTPA images is assessed to ensure adequate enhancement of pulmonary vessels and ensure there is minimal interference from artefact. Photon starvation in areas of the lungs will lead to inadequate enhancement. Distortion of images due to respiration will result in the contours of pre and post contrast scanning to be misaligned. As iodine mapping can only be used complementary to standard CTPA, these images must be assessed for the presence of thrombus and parenchymal abnormalities in the standard fashion by a qualified radiologist.

The heat map developed as part of the iodine map is based on a relative colour scale, from 0-100, with 100 being the areas of highest contrast. The scale be adjusted to account for differences individual patients, but for the majority of scans, no changes are required. Black areas on the map are set at 0 and reflect zero perfusion. The map needs to be interrogated in three directions. It is normal to expect an antero-posterior gradient. Irregular perfusion may be seen in a number of diseases, including both vascular and parenchymal disease. Assessing in multiple directions allows the differentiation of perfusion inhomogeneities due to vascular or broncho-pathologies to be appreciated. Multiplanar-reconstructions of 5-10mm are sufficient for initial interpretation because larger vascular or bronchial abnormalities tend to affect areas larger than the secondary lobule. For smaller areas, such as subsegmental pulmonary embolus, 1mm thick reconstructions are required.

Perfusion defects are taken in context of their location and shape within the lung. Perfusion defects that correlate to segments are likely to reflect vascular occlusion. More heterogenous appearances within the lung are most likely to reflect parenchymal abnormalities.

9.5 Follow-up

Following investigations as per the standard algorithm, patients will be followed up at the outpatient clinic. At that time their symptoms will be assessed for ongoing evidence of chronic thromboembolic disease. All patients will remain on anti-coagulation throughout the period of investigation, e.g., those with recurrent venous thromboembolic disease and those with active malignancy.

- Information will be collected from case notes from baseline investigations. These include
- Pre-diagnostic risk score, if done, e.g., Pulmonary Embolus Severity Index Score
- Haemodynamic status (heart rate, blood pressure, respiratory rate, temperature)
- Any oxygen supplements
- Renal function
- Troponin
- NTproBNP
- QOL
- Medication list
- Sex, Height, weight, and BMI
- Echocardiogram findings, if done as part of standard care
- Right Ventricle/Left ventricle ratio and main PA size, as measured on CT
- The above investigations are required as part of standard care.
- At follow up, results of the following will be assessed:
 - The above information
 - Echocardiogram
 - CTPA, including Iodine Map
 - V/Q Scintigraphy
 - Cardiopulmonary exercise testing
 - Pulmonary Function Tests including 6-minute walk test
 - NTproBNP

If above investigations suggest need for right heart catheter/pulmonary angiography as part of standard care to assess for the presence of pulmonary hypertension, data from this will be used. Again, all the above tests are acquired as part of standard clinical care at follow up, except from the iodine map.

9.6 Data Management

Data will be stored on NHS password secure encrypted computers and will be analysed using Microsoft Excel and IBM SPSS Statistics (IBM, NY, USA, Version 25).

9.7 Expected Outcomes

CTPA with iodine mapping will be more sensitive to detect the presence of chronic thromboembolic disease than using standard CTPA alone.

CTPA with iodine mapping will have similar sensitivity for the detection of distal pulmonary vascular occlusion as V/Q scintigraphy.

Cross sectional data on iodine mapping, as assessed by computer tomography, will correlate with functional limitation, as measured by CPET, in patients with suspected chronic thromboembolic disease.

DURATION OF PROJECT: The planned duration of this study is 24 months.

9.8 Power of Study

This is a pilot study. As far as we are aware, there are no previous studies correlating CPET with iodine mapping in chronic thromboembolic disease. Recruitment of 50 patients over the study period is planned, with the aim of recruiting 25 patients with chronic thromboembolic disease(281).

Data will be presented as mean \pm SD or median and IQR.

Correlation will be performed by Pearson or Spearman.

Students t-test or Mann-Whitney U test will also be employed depending on the distribution of the data.

9.9 Ethical Approval

This protocol was submitted to the West of Scotland Research Ethics Service 1 and was granted approval on the 15th April 2020 (REC ref 20/WS/0064), protocol Number (GsN19RM569).

1. Humbert M, Sitbon O, Chaouat A, Bertocchi M, Habib G, Gressin V, et al. Survival in patients with idiopathic, familial, and anorexigen-associated pulmonary arterial hypertension in the modern management era. *Circulation*. 2010;122(2):156-63.
2. Hoeper MM, Kramer T, Pan Z, Eichstaedt CA, Spiesshoefer J, Benjamin N, et al. Mortality in pulmonary arterial hypertension: prediction by the 2015 European pulmonary hypertension guidelines risk stratification model. *Eur Respir J*. 2017;50(2).
3. Galiè N, McLaughlin VV, Rubin LJ, Simonneau G. An overview of the 6th World Symposium on Pulmonary Hypertension. *Eur Respir J*. 2019;53(1).
4. Simonneau G, Robbins IM, Beghetti M, Channick RN, Delcroix M, Denton CP, et al. Updated clinical classification of pulmonary hypertension. *J Am Coll Cardiol*. 2009;54(1 Suppl):S43-54.
5. Humbert M, Guignabert C, Bonnet S, Dorfmüller P, Klinger JR, Nicolls MR, et al. Pathology and pathobiology of pulmonary hypertension: state of the art and research perspectives. *Eur Respir J*. 2019;53(1).
6. Gall H, Hoeper MM, Richter MJ, Cacheris W, Hinzmann B, Mayer E. An epidemiological analysis of the burden of chronic thromboembolic pulmonary hypertension in the USA, Europe and Japan. *Eur Respir Rev*. 2017;26(143).
7. Kramer CM, Barkhausen J, Bucciarelli-Ducci C, Flamm SD, Kim RJ, Nagel E. Standardized cardiovascular magnetic resonance imaging (CMR) protocols: 2020 update. *J Cardiovasc Magn Reson*. 2020;22(1):17.
8. McLure LE, Peacock AJ. Cardiac magnetic resonance imaging for the assessment of the heart and pulmonary circulation in pulmonary hypertension. *Eur Respir J*. 2009;33(6):1454-66.
9. Johns CS, Kiely DG, Rajaram S, Hill C, Thomas S, Karunasaagarar K, et al. Diagnosis of Pulmonary Hypertension with Cardiac MRI: Derivation and Validation of Regression Models. *Radiology*. 2019;290(1):61-8.
10. Whitfield AJ, Solanki R, Johns CS, Kiely D, Wild J, Swift AJ. MRI Prediction of Precapillary Pulmonary Hypertension according to the Sixth World Symposium on Pulmonary Hypertension. *Radiology*. 2020;294(2):482.
11. Alabed S, Alandejani F, Dwivedi K, Karunasaagarar K, Sharkey M, Garg P, et al. Validation of Artificial Intelligence Cardiac MRI Measurements: Relationship to Heart Catheterization and Mortality Prediction. *Radiology*. 2022;304(3):E56.
12. Kovacs G, Berghold A, Scheidl S, Olschewski H. Pulmonary arterial pressure during rest and exercise in healthy subjects: a systematic review. *Eur Respir J*. 2009;34(4):888-94.
13. Chaouat A, Naeije R, Weitzenblum E. Pulmonary hypertension in COPD. *Eur Respir J*. 2008;32(5):1371-85.
14. Chemla D, Lau EM, Papelier Y, Attal P, Hervé P. Pulmonary vascular resistance and compliance relationship in pulmonary hypertension. *Eur Respir J*. 2015;46(4):1178-89.
15. Pulmonary Arteries. *Asklepios Medical Atlas: Science Photo Library*; 2016.
16. McCullagh A, Rosenthal M, Wanner A, Hurtado A, Padley S, Bush A. The bronchial circulation--worth a closer look: a review of the relationship between the bronchial vasculature and airway inflammation. *Pediatr Pulmonol*. 2010;45(1):1-13.
17. Bruzzi JF, Rémy-Jardin M, Delhaye D, Teisseire A, Khalil C, Rémy J. Multi-detector row CT of hemoptysis. *Radiographics*. 2006;26(1):3-22.

18. PUMP KK. The bronchial arteries and their anastomoses in the human lung. *Dis Chest*. 1963;43:245-55.
19. AVIADO DM, DALY MD, LEE CY, SCHMIDT CF. The contribution of the bronchial circulation to the venous admixture in pulmonary venous blood. *J Physiol*. 1961;155:602-22.
20. Ley S, Kreitner KF, Morgenstern I, Thelen M, Kauczor HU. Bronchopulmonary shunts in patients with chronic thromboembolic pulmonary hypertension: evaluation with helical CT and MR imaging. *AJR Am J Roentgenol*. 2002;179(5):1209-15.
21. Remy-Jardin M, Duhamel A, Deken V, Bouaziz N, Dumont P, Remy J. Systemic collateral supply in patients with chronic thromboembolic and primary pulmonary hypertension: assessment with multi-detector row helical CT angiography. *Radiology*. 2005;235(1):274-81.
22. Endrys J, Hayat N, Cherian G. Comparison of bronchopulmonary collaterals and collateral blood flow in patients with chronic thromboembolic and primary pulmonary hypertension. *Heart*. 1997;78(2):171-6.
23. Enson Y. Pulmonary heart disease: relation of pulmonary hypertension to abnormal lung structure and function. *Bull N Y Acad Med*. 1977;53(6):551-66.
24. McCredie RM. The pulmonary capillary bed in various forms of pulmonary hypertension. *Circulation*. 1966;33(6):854-61.
25. Woodcock T. Plasma volume, tissue oedema, and the steady-state Starling principle. *BJA Education: BJA*; February 2017. p. 74-8.
26. Chamarthy MR, Kandathil A, Kalva SP. Pulmonary vascular pathophysiology. *Cardiovasc Diagn Ther*. 2018;8(3):208-13.
27. Ryan US, Ryan JW. Cell biology of pulmonary endothelium. *Circulation*. 1984;70(5 Pt 2):III46-62.
28. Hartsock A, Nelson WJ. Adherens and tight junctions: structure, function and connections to the actin cytoskeleton. *Biochim Biophys Acta*. 2008;1778(3):660-9.
29. Mehta D, Bhattacharya J, Matthay MA, Malik AB. Integrated control of lung fluid balance. *Am J Physiol Lung Cell Mol Physiol*. 2004;287(6):L1081-90.
30. Ryan US. Pulmonary endothelium: a dynamic interface. *Clin Invest Med*. 1986;9(2):124-32.
31. Cherian PP, Siller-Jackson AJ, Gu S, Wang X, Bonewald LF, Sprague E, et al. Mechanical strain opens connexin 43 hemichannels in osteocytes: a novel mechanism for the release of prostaglandin. *Mol Biol Cell*. 2005;16(7):3100-6.
32. Contreras JE, Sánchez HA, Eugenin EA, Speidel D, Theis M, Willecke K, et al. Metabolic inhibition induces opening of unapposed connexin 43 gap junction hemichannels and reduces gap junctional communication in cortical astrocytes in culture. *Proc Natl Acad Sci U S A*. 2002;99(1):495-500.
33. Lampe PD, Lau AF. The effects of connexin phosphorylation on gap junctional communication. *Int J Biochem Cell Biol*. 2004;36(7):1171-86.
34. Cowan DB, Jones M, Garcia LM, Noria S, del Nido PJ, McGowan FX. Hypoxia and stretch regulate intercellular communication in vascular smooth muscle cells through reactive oxygen species formation. *Arterioscler Thromb Vasc Biol*. 2003;23(10):1754-60.
35. Huertas A, Guignabert C, Barberà JA, Bärtsch P, Bhattacharya J, Bhattacharya S, et al. Pulmonary vascular endothelium: the orchestra conductor in respiratory diseases: Highlights from basic research to therapy. *Eur Respir J*. 2018;51(4).

36. Siemerink MJ, Klaassen I, Van Noorden CJ, Schlingemann RO. Endothelial tip cells in ocular angiogenesis: potential target for anti-angiogenesis therapy. *J Histochem Cytochem*. 2013;61(2):101-15.
37. Betz C, Lenard A, Belting HG, Affolter M. Cell behaviors and dynamics during angiogenesis. *Development*. 2016;143(13):2249-60.
38. Suresh K, Shimoda LA. Lung Circulation. *Compr Physiol*. 2016;6(2):897-943.
39. Brudin LH, Rhodes CG, Valind SO, Jones T, Hughes JM. Interrelationships between regional blood flow, blood volume, and ventilation in supine humans. *J Appl Physiol* (1985). 1994;76(3):1205-10.
40. Galvin I, Drummond GB, Nirmalan M. Distribution of blood flow and ventilation in the lung: gravity is not the only factor. *Br J Anaesth*. 2007;98(4):420-8.
41. Lumb AB, Horncastle E. Pharmacology and Physiology for Anesthesia. In: Hemmings HC, Egan TD, editors. Second ed: Elsevier 2019. p. 586-612.
42. Dell'Italia LJ. The right ventricle: anatomy, physiology, and clinical importance. *Curr Probl Cardiol*. 1991;16(10):653-720.
43. Ho SY, Nihoyannopoulos P. Anatomy, echocardiography, and normal right ventricular dimensions. *Heart*. 2006;92 Suppl 1:i2-13.
44. Bharati S, McAllister HA, Tatoes CJ, Miller RA, Weinberg M, Bucheleres HG, et al. Anatomic variations in underdeveloped right ventricle related to tricuspid atresia and stenosis. *J Thorac Cardiovasc Surg*. 1976;72(3):383-400.
45. Farb A, Burke AP, Virmani R. Anatomy and pathology of the right ventricle (including acquired tricuspid and pulmonic valve disease). *Cardiol Clin*. 1992;10(1):1-21.
46. Stubbs H, MacLellan A, Lua S, Dormand H, Church C. The right ventricle under pressure: Anatomy and imaging in sickness and health. *J Anat*. 2022.
47. Kovács A, Lakatos B, Tokodi M, Merkely B. Right ventricular mechanical pattern in health and disease: beyond longitudinal shortening. *Heart Fail Rev*. 2019;24(4):511-20.
48. Bleeker GB, Steendijk P, Holman ER, Yu CM, Breithardt OA, Kaandorp TA, et al. Assessing right ventricular function: the role of echocardiography and complementary technologies. *Heart*. 2006;92 Suppl 1:i19-26.
49. Woods RH. A Few Applications of a Physical Theorem to Membranes in the Human Body in a State of Tension. *J Anat Physiol*. 1892;26(Pt 3):362-70.
50. Dell'Italia LJ. Mechanism of postextrasystolic potentiation in the right ventricle. *Am J Cardiol*. 1990;65(11):736-41.
51. Holubarsch C, Ruf T, Goldstein DJ, Ashton RC, Nickl W, Pieske B, et al. Existence of the Frank-Starling mechanism in the failing human heart. Investigations on the organ, tissue, and sarcomere levels. *Circulation*. 1996;94(4):683-9.
52. MacNee W. Pathophysiology of cor pulmonale in chronic obstructive pulmonary disease. Part One. *Am J Respir Crit Care Med*. 1994;150(3):833-52.
53. Galiè N, Humbert M, Vachiery JL, Gibbs S, Lang I, Torbicki A, et al. [2015 ESC/ERS Guidelines for the diagnosis and treatment of pulmonary hypertension]. *Kardiol Pol*. 2015;73(12):1127-206.
54. Vonk-Noordegraaf A, Westerhof N. Describing right ventricular function. *Eur Respir J*. 2013;41(6):1419-23.
55. de Man FS, Handoko ML, van Ballegoij JJ, Schalij I, Bogaards SJ, Postmus PE, et al. Bisoprolol delays progression towards right heart failure in experimental pulmonary hypertension. *Circ Heart Fail*. 2012;5(1):97-105.

56. Monge García MI, Santos A. Understanding ventriculo-arterial coupling. *Ann Transl Med.* 2020;8(12):795.
57. Kremer N, Rako Z, Douschan P, Gall H, Ghofrani HA, Grimminger F, et al. Unmasking right ventricular-arterial uncoupling during fluid challenge in pulmonary hypertension. *J Heart Lung Transplant.* 2022;41(3):345-55.
58. Farrer-Brown G. Vascular pattern of myocardium of right ventricle of human heart. *Br Heart J.* 1968;30(5):679-86.
59. Geerts L, Bovendeerd P, Nicolay K, Arts T. Characterization of the normal cardiac myofiber field in goat measured with MR-diffusion tensor imaging. *Am J Physiol Heart Circ Physiol.* 2002;283(1):H139-45.
60. Greenbaum RA, Ho SY, Gibson DG, Becker AE, Anderson RH. Left ventricular fibre architecture in man. *Br Heart J.* 1981;45(3):248-63.
61. Young AA, Imai H, Chang CN, Axel L. Two-dimensional left ventricular deformation during systole using magnetic resonance imaging with spatial modulation of magnetization. *Circulation.* 1994;89(2):740-52.
62. Santamore WP, Dell'Italia LJ. Ventricular interdependence: significant left ventricular contributions to right ventricular systolic function. *Prog Cardiovasc Dis.* 1998;40(4):289-308.
63. Hoffman D, Sisto D, Frater RW, Nikolic SD. Left-to-right ventricular interaction with a noncontracting right ventricle. *J Thorac Cardiovasc Surg.* 1994;107(6):1496-502.
64. Simonneau G, Montani D, Celermajer DS, Denton CP, Gatzoulis MA, Krowka M, et al. Haemodynamic definitions and updated clinical classification of pulmonary hypertension. *Eur Respir J.* 2019;53(1).
65. Tuder RM, Archer SL, Dorfmueller P, Erzurum SC, Guignabert C, Michelakis E, et al. Relevant issues in the pathology and pathobiology of pulmonary hypertension. *J Am Coll Cardiol.* 2013;62(25 Suppl):D4-12.
66. Budhiraja R, Tuder RM, Hassoun PM. Endothelial dysfunction in pulmonary hypertension. *Circulation.* 2004;109(2):159-65.
67. Giaid A, Saleh D. Reduced expression of endothelial nitric oxide synthase in the lungs of patients with pulmonary hypertension. *N Engl J Med.* 1995;333(4):214-21.
68. Tzoumas N, Farrah TE, Dhaun N, Webb DJ. Established and emerging therapeutic uses of PDE type 5 inhibitors in cardiovascular disease. *Br J Pharmacol.* 2020;177(24):5467-88.
69. Christman BW, McPherson CD, Newman JH, King GA, Bernard GR, Groves BM, et al. An imbalance between the excretion of thromboxane and prostacyclin metabolites in pulmonary hypertension. *N Engl J Med.* 1992;327(2):70-5.
70. Tuder RM, Cool CD, Geraci MW, Wang J, Abman SH, Wright L, et al. Prostacyclin synthase expression is decreased in lungs from patients with severe pulmonary hypertension. *Am J Respir Crit Care Med.* 1999;159(6):1925-32.
71. Tabima DM, Frizzell S, Gladwin MT. Reactive oxygen and nitrogen species in pulmonary hypertension. *Free Radic Biol Med.* 2012;52(9):1970-86.
72. Giaid A, Yanagisawa M, Langleben D, Michel RP, Levy R, Shennib H, et al. Expression of endothelin-1 in the lungs of patients with pulmonary hypertension. *N Engl J Med.* 1993;328(24):1732-9.
73. Cervantes J, Rojas G. Virchow's Legacy: deep vein thrombosis and pulmonary embolism. *World J Surg.* 2005;29 Suppl 1:S30-4.
74. Andersson T, Söderberg S. Incidence of acute pulmonary embolism, related comorbidities and survival; analysis of a Swedish national cohort. *BMC Cardiovasc Disord.* 2017;17(1):155.

75. Wagenvoort CA. Pathology of pulmonary thromboembolism. *Chest*. 1995;107(1 Suppl):10S-7S.
76. Hao Q, Dong BR, Yue J, Wu T, Liu GJ. Thrombolytic therapy for pulmonary embolism. *Cochrane Database Syst Rev*. 2015(9):CD004437.
77. Bernard J, Yi ES. Pulmonary thromboendarterectomy: a clinicopathologic study of 200 consecutive pulmonary thromboendarterectomy cases in one institution. *Hum Pathol*. 2007;38(6):871-7.
78. Arbustini E, Morbini P, D'Armini AM, Repetto A, Minzioni G, Piovella F, et al. Plaque composition in plexogenic and thromboembolic pulmonary hypertension: the critical role of thrombotic material in pultaceous core formation. *Heart*. 2002;88(2):177-82.
79. Delcroix M, Kerr K, Fedullo P. Chronic Thromboembolic Pulmonary Hypertension. *Epidemiology and Risk Factors*. *Ann Am Thorac Soc*. 2016;13 Suppl 3:S201-6.
80. Jenkins D, Madani M, Fadel E, D'Armini AM, Mayer E. Pulmonary endarterectomy in the management of chronic thromboembolic pulmonary hypertension. *Eur Respir Rev*. 2017;26(143).
81. Lang I, Meyer BC, Ogo T, Matsubara H, Kurzyna M, Ghofrani HA, et al. Balloon pulmonary angioplasty in chronic thromboembolic pulmonary hypertension. *Eur Respir Rev*. 2017;26(143).
82. Valerio L, Mavromanoli AC, Barco S, Abele C, Becker D, Bruch L, et al. Chronic thromboembolic pulmonary hypertension and impairment after pulmonary embolism: the FOCUS study. *Eur Heart J*. 2022;43(36):3387-98.
83. Durrington C, Hurdman JA, Elliot CA, Maclean R, Van Veen J, Sacccullo G, et al. Systematic pulmonary embolism follow-up increases diagnostic rates of chronic thromboembolic pulmonary hypertension and identifies less severe disease: results from the ASPIRE Registry. *Eur Respir J*. 2024.
84. Rich S. Right ventricular adaptation and maladaptation in chronic pulmonary arterial hypertension. *Cardiol Clin*. 2012;30(2):257-69.
85. Vonk-Noordegraaf A, Haddad F, Chin KM, Forfia PR, Kawut SM, Lumens J, et al. Right heart adaptation to pulmonary arterial hypertension: physiology and pathobiology. *J Am Coll Cardiol*. 2013;62(25 Suppl):D22-33.
86. Badagliacca R, Poscia R, Pezzuto B, Papa S, Pesce F, Manzi G, et al. Right ventricular concentric hypertrophy and clinical worsening in idiopathic pulmonary arterial hypertension. *J Heart Lung Transplant*. 2016;35(11):1321-9.
87. Goh ZM, Alabed S, Shahin Y, Rothman AMK, Garg P, Lawrie A, et al. Right Ventricular Adaptation Assessed Using Cardiac Magnetic Resonance Predicts Survival in Pulmonary Arterial Hypertension. *JACC Cardiovasc Imaging*. 2021;14(6):1271-2.
88. Watts JA, Marchick MR, Kline JA. Right ventricular heart failure from pulmonary embolism: key distinctions from chronic pulmonary hypertension. *J Card Fail*. 2010;16(3):250-9.
89. Helderma F, Mauritz GJ, Andringa KE, Vonk-Noordegraaf A, Marcus JT. Early onset of retrograde flow in the main pulmonary artery is a characteristic of pulmonary arterial hypertension. *J Magn Reson Imaging*. 2011;33(6):1362-8.
90. Vonk Noordegraaf A, Galiè N. The role of the right ventricle in pulmonary arterial hypertension. *Eur Respir Rev*. 2011;20(122):243-53.
91. Naeije R, Manes A. The right ventricle in pulmonary arterial hypertension. *Eur Respir Rev*. 2014;23(134):476-87.
92. Feigenbaum H. Echocardiographic evaluation of left ventricular function: beyond ejection fraction. *J Cardiol*. 2006;48(4):175-82.

93. Burgess MI, Mogulkoc N, Bright-Thomas RJ, Bishop P, Egan JJ, Ray SG. Comparison of echocardiographic markers of right ventricular function in determining prognosis in chronic pulmonary disease. *J Am Soc Echocardiogr.* 2002;15(6):633-9.
94. Kaul S, Tei C, Hopkins JM, Shah PM. Assessment of right ventricular function using two-dimensional echocardiography. *Am Heart J.* 1984;107(3):526-31.
95. D'Alto M, Romeo E, Argiento P, D'Andrea A, Vanderpool R, Correra A, et al. Accuracy and precision of echocardiography versus right heart catheterization for the assessment of pulmonary hypertension. *Int J Cardiol.* 2013;168(4):4058-62.
96. Magnino C, Omedè P, Avenatti E, Presutti D, Iannaccone A, Chiarlo M, et al. Inaccuracy of Right Atrial Pressure Estimates Through Inferior Vena Cava Indices. *Am J Cardiol.* 2017;120(9):1667-73.
97. Bax S, Bredy C, Kempny A, Dimopoulos K, Devaraj A, Walsh S, et al. A stepwise composite echocardiographic score predicts severe pulmonary hypertension in patients with interstitial lung disease. *ERJ Open Res.* 2018;4(2).
98. Parasuraman S, Walker S, Loudon BL, Gollop ND, Wilson AM, Lowery C, et al. Assessment of pulmonary artery pressure by echocardiography-A comprehensive review. *Int J Cardiol Heart Vasc.* 2016;12:45-51.
99. Roeleveld RJ, Marcus JT, Faes TJ, Gan TJ, Boonstra A, Postmus PE, et al. Interventricular septal configuration at mr imaging and pulmonary arterial pressure in pulmonary hypertension. *Radiology.* 2005;234(3):710-7.
100. Alabed S, Shahin Y, Garg P, Alandejani F, Johns CS, Lewis RA, et al. Cardiac-MRI Predicts Clinical Worsening and Mortality in Pulmonary Arterial Hypertension: A Systematic Review and Meta-Analysis. *JACC Cardiovasc Imaging.* 2021;14(5):931-42.
101. Goerne H, Batra K, Rajiah P. Imaging of pulmonary hypertension: an update. *Cardiovasc Diagn Ther.* 2018;8(3):279-96.
102. Lewis RA, Johns CS, Cogliano M, Capener D, Tubman E, Elliot CA, et al. Identification of Cardiac Magnetic Resonance Imaging Thresholds for Risk Stratification in Pulmonary Arterial Hypertension. *Am J Respir Crit Care Med.* 2020;201(4):458-68.
103. van Wolferen SA, Marcus JT, Boonstra A, Marques KM, Bronzwaer JG, Spreeuwenberg MD, et al. Prognostic value of right ventricular mass, volume, and function in idiopathic pulmonary arterial hypertension. *Eur Heart J.* 2007;28(10):1250-7.
104. Sanz J, Kuschnir P, Rius T, Salguero R, Sulica R, Einstein AJ, et al. Pulmonary arterial hypertension: noninvasive detection with phase-contrast MR imaging. *Radiology.* 2007;243(1):70-9.
105. Saggarr R, Sitbon O. Hemodynamics in pulmonary arterial hypertension: current and future perspectives. *Am J Cardiol.* 2012;110(6 Suppl):9S-15S.
106. Hoeper MM, Bogaard HJ, Condliffe R, Frantz R, Khanna D, Kurzyna M, et al. Definitions and diagnosis of pulmonary hypertension. *J Am Coll Cardiol.* 2013;62(25 Suppl):D42-50.
107. Robbins IM, Hemnes AR, Pugh ME, Brittain EL, Zhao DX, Piana RN, et al. High prevalence of occult pulmonary venous hypertension revealed by fluid challenge in pulmonary hypertension. *Circ Heart Fail.* 2014;7(1):116-22.
108. Demir R, Küçükoğlu MS. Six-minute walk test in pulmonary arterial hypertension. *Anatol J Cardiol.* 2015;15(3):249-54.

109. Gaine S, Simonneau G. The need to move from 6-minute walk distance to outcome trials in pulmonary arterial hypertension. *Eur Respir Rev*. 2013;22(130):487-94.
110. Laboratories ACoPSfCPF. ATS statement: guidelines for the six-minute walk test. *Am J Respir Crit Care Med*. 2002;166(1):111-7.
111. Borg GA. Psychophysical bases of perceived exertion. *Med Sci Sports Exerc*. 1982;14(5):377-81.
112. Lador F, Bringard A, Bengueddache S, Ferretti G, Bendjelid K, Soccacal PM, et al. Kinetics of Cardiac Output at the Onset of Exercise in Precapillary Pulmonary Hypertension. *Biomed Res Int*. 2016;2016:6050193.
113. Held M, Grün M, Holl R, Hübner G, Kaiser R, Karl S, et al. Cardiopulmonary exercise testing to detect chronic thromboembolic pulmonary hypertension in patients with normal echocardiography. *Respiration*. 2014;87(5):379-87.
114. Held M, Pfeuffer-Jovic E, Wilkens H, Güder G, Küsters F, Schäfers HJ, et al. Frequency and characterization of CTEPH and CTEPD according to the mPAP threshold > 20 mm Hg: Retrospective analysis from data of a prospective PE aftercare program. *Respir Med*. 2023;210:107177.
115. Velez-Roa S, Ciarka A, Najem B, Vachier JL, Naeije R, van de Borne P. Increased sympathetic nerve activity in pulmonary artery hypertension. *Circulation*. 2004;110(10):1308-12.
116. Farina S, Bruno N, Agalbato C, Contini M, Cassandro R, Elia D, et al. Physiological insights of exercise hyperventilation in arterial and chronic thromboembolic pulmonary hypertension. *Int J Cardiol*. 2018;259:178-82.
117. Dempsey JA, Smith CA. Pathophysiology of human ventilatory control. *Eur Respir J*. 2014;44(2):495-512.
118. Potus F, Malenfant S, Graydon C, Mainguy V, Tremblay È, Breuils-Bonnet S, et al. Impaired angiogenesis and peripheral muscle microcirculation loss contribute to exercise intolerance in pulmonary arterial hypertension. *Am J Respir Crit Care Med*. 2014;190(3):318-28.
119. Farina S, Correale M, Bruno N, Paolillo S, Salvioni E, Badagliacca R, et al. The role of cardiopulmonary exercise tests in pulmonary arterial hypertension. *Eur Respir Rev*. 2018;27(148).
120. Wensel R, Opitz CF, Anker SD, Winkler J, Höffken G, Kleber FX, et al. Assessment of survival in patients with primary pulmonary hypertension: importance of cardiopulmonary exercise testing. *Circulation*. 2002;106(3):319-24.
121. Degani-Costa LH, Nery LE, Rodrigues MT, Gimenes AC, Ferreira EV, Ota-Arakaki JS, et al. Does oxygen pulse trajectory during incremental exercise discriminate impaired oxygen delivery from poor muscle oxygen utilisation? *ERJ Open Res*. 2019;5(2).
122. Groepenhoff H, Vonk-Noordegraaf A, van de Veerdonk MC, Boonstra A, Westerhof N, Bogaard HJ. Prognostic relevance of changes in exercise test variables in pulmonary arterial hypertension. *PLoS One*. 2013;8(9):e72013.
123. Potter LR. Natriuretic peptide metabolism, clearance and degradation. *FEBS J*. 2011;278(11):1808-17.
124. Leuchte HH, El Nounou M, Tuerpe JC, Hartmann B, Baumgartner RA, Vogeser M, et al. N-terminal pro-brain natriuretic peptide and renal insufficiency as predictors of mortality in pulmonary hypertension. *Chest*. 2007;131(2):402-9.
125. Semenov AG, Katrukha AG. Analytical Issues with Natriuretic Peptides - has this been Overly Simplified? *EJIFCC*. 2016;27(3):189-207.

126. Williams MH, Handler CE, Akram R, Smith CJ, Das C, Smee J, et al. Role of N-terminal brain natriuretic peptide (N-TproBNP) in scleroderma-associated pulmonary arterial hypertension. *Eur Heart J*. 2006;27(12):1485-94.
127. Fenster BE, Lasalvia L, Schroeder JD, Smyser J, Silveira LJ, Buckner JK, et al. Cystatin C: a potential biomarker for pulmonary arterial hypertension. *Respirology*. 2014;19(4):583-9.
128. Berger A. Magnetic resonance imaging. *BMJ*. 2002;324(7328):35.
129. Huisman TA. Tumor-like lesions of the brain. *Cancer Imaging*. 2009;9 Spec No A:S10-3.
130. Abouzeid CM, Shah T, Johri A, Weinsaft JW, Kim J. Multimodality Imaging of the Right Ventricle. *Curr Treat Options Cardiovasc Med*. 2017;19(11):82.
131. Gatehouse PD, Rolf MP, Graves MJ, Hofman MB, Totman J, Werner B, et al. Flow measurement by cardiovascular magnetic resonance: a multi-centre multi-vendor study of background phase offset errors that can compromise the accuracy of derived regurgitant or shunt flow measurements. *J Cardiovasc Magn Reson*. 2010;12:5.
132. Nayak KS, Nielsen JF, Bernstein MA, Markl M, D Gatehouse P, M Botnar R, et al. Cardiovascular magnetic resonance phase contrast imaging. *J Cardiovasc Magn Reson*. 2015;17:71.
133. Pedrizzetti G, Claus P, Kilner PJ, Nagel E. Principles of cardiovascular magnetic resonance feature tracking and echocardiographic speckle tracking for informed clinical use. *J Cardiovasc Magn Reson*. 2016;18(1):51.
134. Morens DM, Breman JG, Calisher CH, Doherty PC, Hahn BH, Keusch GT, et al. The Origin of COVID-19 and Why It Matters. *Am J Trop Med Hyg*. 2020;103(3):955-9.
135. Tang N, Li D, Wang X, Sun Z. Abnormal coagulation parameters are associated with poor prognosis in patients with novel coronavirus pneumonia. *J Thromb Haemost*. 2020;18(4):844-7.
136. Klok FA, Kruip MJHA, van der Meer NJM, Arbous MS, Gommers DAMP, Kant KM, et al. Incidence of thrombotic complications in critically ill ICU patients with COVID-19. *Thromb Res*. 2020.
137. Association WM. World Medical Association Declaration of Helsinki: ethical principles for medical research involving human subjects. *JAMA*. 2013;310(20):2191-4.
138. Mereles D, Ehlken N, Kreuzer S, Ghofrani S, Hoeper MM, Halank M, et al. Exercise and respiratory training improve exercise capacity and quality of life in patients with severe chronic pulmonary hypertension. *Circulation*. 2006;114(14):1482-9.
139. Yorke J, Corris P, Gaine S, Gibbs JS, Kiely DG, Harries C, et al. emPHasis-10: development of a health-related quality of life measure in pulmonary hypertension. *Eur Respir J*. 2014;43(4):1106-13.
140. Mathai SC, Puhan MA, Lam D, Wise RA. The minimal important difference in the 6-minute walk test for patients with pulmonary arterial hypertension. *Am J Respir Crit Care Med*. 2012;186(5):428-33.
141. Augustine DX, Coates-Bradshaw LD, Willis J, Harkness A, Ring L, Grapsa J, et al. Echocardiographic assessment of pulmonary hypertension: a guideline protocol from the British Society of Echocardiography. *Echo Res Pract*. 2018;5(3):G11-G24.
142. Keramida K, Lazaros G, Nihoyannopoulos P. Right ventricular involvement in hypertrophic cardiomyopathy: Patterns and implications. *Hellenic J Cardiol*. 2020;61(1):3-8.

143. CardioServ. Echocardiogram Accreditation
<https://www.cardioserv.net/how-to-estimate-right-atrial-pressure/> [
144. Howard LS, Grapsa J, Dawson D, Bellamy M, Chambers JB, Masani ND, et al. Echocardiographic assessment of pulmonary hypertension: standard operating procedure. *Eur Respir Rev.* 2012;21(125):239-48.
145. Bai W, Sinclair M, Tarroni G, Oktay O, Rajchl M, Vaillant G, et al. Automated cardiovascular magnetic resonance image analysis with fully convolutional networks. *J Cardiovasc Magn Reson.* 2018;20(1):65.
146. Bertelsen L, Svendsen JH, Køber L, Haugan K, Højberg S, Thomsen C, et al. Flow measurement at the aortic root - impact of location of through-plane phase contrast velocity mapping. *J Cardiovasc Magn Reson.* 2016;18(1):55.
147. Kyselovič J, Leddy JJ. Cardiac Fibrosis: The Beneficial Effects of Exercise in Cardiac Fibrosis. *Adv Exp Med Biol.* 2017;999:257-68.
148. Taylor AJ, Salerno M, Dharmakumar R, Jerosch-Herold M. T1 Mapping: Basic Techniques and Clinical Applications. *JACC Cardiovasc Imaging.* 2016;9(1):67-81.
149. Haaf P, Garg P, Messroghli DR, Broadbent DA, Greenwood JP, Plein S. Cardiac T1 Mapping and Extracellular Volume (ECV) in clinical practice: a comprehensive review. *J Cardiovasc Magn Reson.* 2016;18(1):89.
150. Claus P, Omar AMS, Pedrizzetti G, Sengupta PP, Nagel E. Tissue Tracking Technology for Assessing Cardiac Mechanics: Principles, Normal Values, and Clinical Applications. *JACC Cardiovasc Imaging.* 2015;8(12):1444-60.
151. Johnson C, Kuyt K, Oxborough D, Stout M. Practical tips and tricks in measuring strain, strain rate and twist for the left and right ventricles. *Echo Res Pract.* 2019;6(3):R87-R98.
152. Augustine D, Lewandowski AJ, Lazdam M, Rai A, Francis J, Myerson S, et al. Global and regional left ventricular myocardial deformation measures by magnetic resonance feature tracking in healthy volunteers: comparison with tagging and relevance of gender. *J Cardiovasc Magn Reson.* 2013;15:8.
153. Grünig E, Lichtblau M, Ehlken N, Ghofrani HA, Reichenberger F, Staehler G, et al. Safety and efficacy of exercise training in various forms of pulmonary hypertension. *Eur Respir J.* 2012;40(1):84-92.
154. Ryan T, Petrovic O, Dillon JC, Feigenbaum H, Conley MJ, Armstrong WF. An echocardiographic index for separation of right ventricular volume and pressure overload. *J Am Coll Cardiol.* 1985;5(4):918-27.
155. Wharton G, Steeds R, Allen J, Phillips H, Jones R, Kanagala P, et al. A minimum dataset for a standard adult transthoracic echocardiogram: a guideline protocol from the British Society of Echocardiography. *Echo Res Pract.* 2015;2(1):G9-G24.
156. Radtke T, Crook S, Kaltsakas G, Louvaris Z, Berton D, Urquhart DS, et al. ERS statement on standardisation of cardiopulmonary exercise testing in chronic lung diseases. *Eur Respir Rev.* 2019;28(154).
157. Malas MB, Naazie IN, Elsayed N, Mathlouthi A, Marmor R, Clary B. Thromboembolism risk of COVID-19 is high and associated with a higher risk of mortality: A systematic review and meta-analysis. *EClinicalMedicine.* 2020;29:100639.
158. Imaging BSoT. Thoracic Imaging in

COVID-19 Infection. Guidance for the Reporting Radiologist

British Society of Thoracic Imaging. 2020.

159. Konstantinides SV, Meyer G, Becattini C, Bueno H, Geersing GJ, Harjola VP, et al. 2019 ESC Guidelines for the diagnosis and management of acute pulmonary embolism developed in collaboration with the European Respiratory Society (ERS): The Task Force for the diagnosis and management of acute pulmonary embolism of the European Society of Cardiology (ESC). *Eur Respir J*. 2019.
160. Directorate CMO. Coronavirus (Covid-19): Daily data for Scotland. Scottish Government Publications: Coronavirus In Scotland, Health and Social Care; 2020.
161. Hunt BJ. Preventing hospital associated venous thromboembolism. *BMJ*. 2019;365:l4239.
162. Chen YG, Lin TY, Huang WY, Lin CL, Dai MS, Kao CH. Association between pneumococcal pneumonia and venous thromboembolism in hospitalized patients: A nationwide population-based study. *Respirology*. 2015;20(5):799-804.
163. Ende-Verhaar YM, Cannegieter SC, Vonk Noordegraaf A, Delcroix M, Pruszczyk P, Mairuhu AT, et al. Incidence of chronic thromboembolic pulmonary hypertension after acute pulmonary embolism: a contemporary view of the published literature. *Eur Respir J*. 2017;49(2).
164. Pepke-Zaba J, Delcroix M, Lang I, Mayer E, Jansa P, Ambroz D, et al. Chronic thromboembolic pulmonary hypertension (CTEPH): results from an international prospective registry. *Circulation*. 2011;124(18):1973-81.
165. Banks DA, Pretorius GV, Kerr KM, Manecke GR. Pulmonary endarterectomy: part I. Pathophysiology, clinical manifestations, and diagnostic evaluation of chronic thromboembolic pulmonary hypertension. *Semin Cardiothorac Vasc Anesth*. 2014;18(4):319-30.
166. Frey MK, Alias S, Winter MP, Redwan B, Stübiger G, Panzenboeck A, et al. Splenectomy is modifying the vascular remodeling of thrombosis. *J Am Heart Assoc*. 2014;3(1):e000772.
167. Bonderman D, Wilkens H, Wakounig S, Schäfers HJ, Jansa P, Lindner J, et al. Risk factors for chronic thromboembolic pulmonary hypertension. *Eur Respir J*. 2009;33(2):325-31.
168. Karimi M, Cohan N. Cancer-associated thrombosis. *Open Cardiovasc Med J*. 2010;4:78-82.
169. Matthews DT, Hemnes AR. Current concepts in the pathogenesis of chronic thromboembolic pulmonary hypertension. *Pulm Circ*. 2016;6(2):145-54.
170. Wolf M, Boyer-Neumann C, Parent F, Eschwege V, Jaillet H, Meyer D, et al. Thrombotic risk factors in pulmonary hypertension. *Eur Respir J*. 2000;15(2):395-9.
171. Bonderman D, Turecek PL, Jakowitsch J, Weltermann A, Adlbrecht C, Schneider B, et al. High prevalence of elevated clotting factor VIII in chronic thromboembolic pulmonary hypertension. *Thromb Haemost*. 2003;90(3):372-6.
172. Marsh JJ, Chiles PG, Liang NC, Morris TA. Chronic thromboembolic pulmonary hypertension-associated dysfibrinogenemias exhibit disorganized fibrin structure. *Thromb Res*. 2013;132(6):729-34.
173. Remková A, Šimková I, Valkovičová T. Platelet abnormalities in chronic thromboembolic pulmonary hypertension. *Int J Clin Exp Med*. 2015;8(6):9700-7.
174. Galiè N, Kim NH. Pulmonary microvascular disease in chronic thromboembolic pulmonary hypertension. *Proc Am Thorac Soc*. 2006;3(7):571-6.
175. Walker CM, Rosado-de-Christenson ML, Martínez-Jiménez S, Kunin JR, Wible BC. Bronchial arteries: anatomy, function, hypertrophy, and anomalies. *Radiographics*. 2015;35(1):32-49.

176. Ghofrani HA, D'Armini AM, Grimminger F, Hoeper MM, Jansa P, Kim NH, et al. Riociguat for the treatment of chronic thromboembolic pulmonary hypertension. *N Engl J Med.* 2013;369(4):319-29.
177. Godinas L, Sattler C, Lau EM, Jaïs X, Taniguchi Y, Jevnikar M, et al. Dead-space ventilation is linked to exercise capacity and survival in distal chronic thromboembolic pulmonary hypertension. *J Heart Lung Transplant.* 2017;36(11):1234-42.
178. Pepke-Zaba J, Ghofrani HA, Hoeper MM. Medical management of chronic thromboembolic pulmonary hypertension. *Eur Respir Rev.* 2017;26(143).
179. McCabe C, Deboeck G, Harvey I, Ross RM, Gopalan D, Screaton N, et al. Inefficient exercise gas exchange identifies pulmonary hypertension in chronic thromboembolic obstruction following pulmonary embolism. *Thromb Res.* 2013;132(6):659-65.
180. Held M, Kolb P, Grün M, Jany B, Hübner G, Grgic A, et al. Functional Characterization of Patients with Chronic Thromboembolic Disease. *Respiration.* 2016;91(6):503-9.
181. Taboada D, Pepke-Zaba J, Jenkins DP, Berman M, Treacy CM, Cannon JE, et al. Outcome of pulmonary endarterectomy in symptomatic chronic thromboembolic disease. *Eur Respir J.* 2014;44(6):1635-45.
182. Antunes MJ, Rodríguez-Palomares J, Prendergast B, De Bonis M, Rosenhek R, Al-Attar N, et al. Management of tricuspid valve regurgitation: Position statement of the European Society of Cardiology Working Groups of Cardiovascular Surgery and Valvular Heart Disease. *Eur J Cardiothorac Surg.* 2017;52(6):1022-30.
183. Burkett DA, Patel SS, Mertens L, Friedberg MK, Ivy DD. Relationship Between Left Ventricular Geometry and Invasive Hemodynamics in Pediatric Pulmonary Hypertension. *Circ Cardiovasc Imaging.* 2020;13(5):e009825.
184. Weatherald J, Farina S, Bruno N, Laveneziana P. Cardiopulmonary Exercise Testing in Pulmonary Hypertension. *Ann Am Thorac Soc.* 2017;14(Supplement_1):S84-S92.
185. Johns CS, Rajaram S, Capener DA, Oram C, Elliot C, Condliffe R, et al. Non-invasive methods for estimating mPAP in COPD using cardiovascular magnetic resonance imaging. *Eur Radiol.* 2018;28(4):1438-48.
186. Deboeck G, Niset G, Lamotte M, Vachiéry JL, Naeije R. Exercise testing in pulmonary arterial hypertension and in chronic heart failure. *Eur Respir J.* 2004;23(5):747-51.
187. Tang Q, Liu M, Ma Z, Guo X, Kuang T, Yang Y. Non-invasive evaluation of hemodynamics in pulmonary hypertension by a Septal angle measured by computed tomography pulmonary angiography: Comparison with right-heart catheterization and association with N-terminal pro-B-type natriuretic peptide. *Exp Ther Med.* 2013;6(6):1350-8.
188. Thenappan T, Shah SJ, Rich S, Tian L, Archer SL, Gomberg-Maitland M. Survival in pulmonary arterial hypertension: a reappraisal of the NIH risk stratification equation. *Eur Respir J.* 2010;35(5):1079-87.
189. Liu J, Yang P, Tian H, Zhen K, McCabe C, Zhao L, et al. Right Ventricle Remodeling in Chronic Thromboembolic Pulmonary Hypertension. *J Transl Int Med.* 2022;10(2):125-33.
190. Sato T, Tsujino I, Ohira H, Oyama-Manabe N, Ito YM, Takashina C, et al. Accuracy of echocardiographic indices for serial monitoring of right ventricular systolic function in patients with precapillary pulmonary hypertension. *PLoS One.* 2017;12(11):e0187806.

191. Klok FA, Romeih S, Westenberg JJ, Kroft LJ, Huisman MV, de Roos A. Pulmonary flow profile and distensibility following acute pulmonary embolism. *J Cardiovasc Magn Reson.* 2011;13:14.
192. Rolf A, Rixe J, Kim WK, Guth S, Körlings N, Möllmann H, et al. Pulmonary vascular remodeling before and after pulmonary endarterectomy in patients with chronic thromboembolic pulmonary hypertension: a cardiac magnetic resonance study. *Int J Cardiovasc Imaging.* 2015;31(3):613-9.
193. Sanz J, Kariisa M, Dellegrottaglie S, Prat-González S, Garcia MJ, Fuster V, et al. Evaluation of pulmonary artery stiffness in pulmonary hypertension with cardiac magnetic resonance. *JACC Cardiovasc Imaging.* 2009;2(3):286-95.
194. Swift AJ, Rajaram S, Condliffe R, Capener D, Hurdman J, Elliot C, et al. Pulmonary artery relative area change detects mild elevations in pulmonary vascular resistance and predicts adverse outcome in pulmonary hypertension. *Invest Radiol.* 2012;47(10):571-7.
195. Swift AJ, Dwivedi K, Johns C, Garg P, Chin M, Currie BJ, et al. Diagnostic accuracy of CT pulmonary angiography in suspected pulmonary hypertension. *Eur Radiol.* 2020;30(9):4918-29.
196. Swift AJ, Rajaram S, Condliffe R, Capener D, Hurdman J, Elliot CA, et al. Diagnostic accuracy of cardiovascular magnetic resonance imaging of right ventricular morphology and function in the assessment of suspected pulmonary hypertension results from the ASPIRE registry. *J Cardiovasc Magn Reson.* 2012;14(1):40.
197. Gupta H, Ghimire G, Naeije R. The value of tools to assess pulmonary arterial hypertension. *Eur Respir Rev.* 2011;20(122):222-35.
198. Sitbon O, Sattler C, Bertoletti L, Savale L, Cottin V, Jaïs X, et al. Initial dual oral combination therapy in pulmonary arterial hypertension. *Eur Respir J.* 2016;47(6):1727-36.
199. Rubin LJ, Mendoza J, Hood M, McGoon M, Barst R, Williams WB, et al. Treatment of primary pulmonary hypertension with continuous intravenous prostacyclin (epoprostenol). Results of a randomized trial. *Ann Intern Med.* 1990;112(7):485-91.
200. Barst RJ, Rubin LJ, Long WA, McGoon MD, Rich S, Badesch DB, et al. A comparison of continuous intravenous epoprostenol (prostacyclin) with conventional therapy for primary pulmonary hypertension. *N Engl J Med.* 1996;334(5):296-301.
201. Simonneau G, Barst RJ, Galie N, Naeije R, Rich S, Bourge RC, et al. Continuous subcutaneous infusion of treprostinil, a prostacyclin analogue, in patients with pulmonary arterial hypertension: a double-blind, randomized, placebo-controlled trial. *Am J Respir Crit Care Med.* 2002;165(6):800-4.
202. McLaughlin VV, Benza RL, Rubin LJ, Channick RN, Voswinckel R, Tapson VF, et al. Addition of inhaled treprostinil to oral therapy for pulmonary arterial hypertension: a randomized controlled clinical trial. *J Am Coll Cardiol.* 2010;55(18):1915-22.
203. Coats AJ, Adamopoulos S, Meyer TE, Conway J, Sleight P. Effects of physical training in chronic heart failure. *Lancet.* 1990;335(8681):63-6.
204. Taylor RS, Long L, Mordi IR, Madsen MT, Davies EJ, Dalal H, et al. Exercise-Based Rehabilitation for Heart Failure: Cochrane Systematic Review, Meta-Analysis, and Trial Sequential Analysis. *JACC Heart Fail.* 2019;7(8):691-705.
205. Heran BS, Chen JM, Ebrahim S, Moxham T, Oldridge N, Rees K, et al. Exercise-based cardiac rehabilitation for coronary heart disease. *Cochrane Database Syst Rev.* 2011(7):CD001800.

206. Giannuzzi P, Temporelli PL, Corrà U, Tavazzi L, Group E-CS. Antiremodeling effect of long-term exercise training in patients with stable chronic heart failure: results of the Exercise in Left Ventricular Dysfunction and Chronic Heart Failure (ELVD-CHF) Trial. *Circulation*. 2003;108(5):554-9.
207. Cicek G, Imamoglu O, Gullu A, Celik O, Ozcan O, Gullu E, et al. The effect of exercises on left ventricular systolic and diastolic heart function in sedentary women: Step-aerobic vs core exercises. *J Exerc Sci Fit*. 2017;15(2):70-5.
208. Wang SQ, Li D, Yuan Y. Long-term moderate intensity exercise alleviates myocardial fibrosis in type 2 diabetic rats via inhibitions of oxidative stress and TGF- β 1/Smad pathway. *J Physiol Sci*. 2019;69(6):861-73.
209. McCarthy B, Casey D, Devane D, Murphy K, Murphy E, Lacasse Y. Pulmonary rehabilitation for chronic obstructive pulmonary disease. *Cochrane Database Syst Rev*. 2015(2):CD003793.
210. Patel S, Cole AD, Nolan CM, Barker RE, Jones SE, Kon S, et al. Pulmonary rehabilitation in bronchiectasis: a propensity-matched study. *Eur Respir J*. 2019;53(1).
211. Gaine SP, Rubin LJ. Primary pulmonary hypertension. *Lancet*. 1998;352(9129):719-25.
212. Desai SA, Channick RN. Exercise in patients with pulmonary arterial hypertension. *J Cardiopulm Rehabil Prev*. 2008;28(1):12-6.
213. de Man FS, Handoko ML, Groepenhoff H, van 't Hul AJ, Abbink J, Koppers RJ, et al. Effects of exercise training in patients with idiopathic pulmonary arterial hypertension. *Eur Respir J*. 2009;34(3):669-75.
214. Ley S, Fink C, Risse F, Ehlken N, Fischer C, Ley-Zaporozhan J, et al. Magnetic resonance imaging to assess the effect of exercise training on pulmonary perfusion and blood flow in patients with pulmonary hypertension. *Eur Radiol*. 2013;23(2):324-31.
215. Ehlken N, Lichtblau M, Klose H, Weidenhammer J, Fischer C, Nechwatal R, et al. Exercise training improves peak oxygen consumption and haemodynamics in patients with severe pulmonary arterial hypertension and inoperable chronic thrombo-embolic pulmonary hypertension: a prospective, randomized, controlled trial. *Eur Heart J*. 2016;37(1):35-44.
216. Chen YW, Wang CY, Lai YH, Liao YC, Wen YK, Chang ST, et al. Home-based cardiac rehabilitation improves quality of life, aerobic capacity, and readmission rates in patients with chronic heart failure. *Medicine (Baltimore)*. 2018;97(4):e9629.
217. Borgese M, Badesch D, Bull T, Chakinala M, DeMarco T, Feldman J, et al. EmPHasis-10 as a measure of health-related quality of life in pulmonary arterial hypertension: data from PHAR. *Eur Respir J*. 2021;57(2).
218. Favoccia C, Kempny A, Yorke J, Armstrong I, Price LC, McCabe C, et al. EmPHasis-10 score for the assessment of quality of life in various types of pulmonary hypertension and its relation to outcome. *Eur J Prev Cardiol*. 2019;26(12):1338-40.
219. van Wolferen SA, van de Veerdonk MC, Mauritz GJ, Jacobs W, Marcus JT, Marques KMJ, et al. Clinically significant change in stroke volume in pulmonary hypertension. *Chest*. 2011;139(5):1003-9.
220. Neder JA, Ramos RP, Ota-Arakaki JS, Hirai DM, D'Arsigny CL, O'Donnell D. Exercise intolerance in pulmonary arterial hypertension. The role of cardiopulmonary exercise testing. *Ann Am Thorac Soc*. 2015;12(4):604-12.
221. Arbab-Zadeh A, Dijk E, Prasad A, Fu Q, Torres P, Zhang R, et al. Effect of aging and physical activity on left ventricular compliance. *Circulation*. 2004;110(13):1799-805.

222. Goodman JM, Liu PP, Green HJ. Left ventricular adaptations following short-term endurance training. *J Appl Physiol* (1985). 2005;98(2):454-60.
223. Fernandes AA, Faria TeO, Ribeiro Júnior RF, Costa GP, Marchezini B, Silveira EA, et al. A single resistance exercise session improves myocardial contractility in spontaneously hypertensive rats. *Braz J Med Biol Res*. 2015;48(9):813-21.
224. Lu R, Zhao X, Li J, Niu P, Yang B, Wu H, et al. Genomic characterisation and epidemiology of 2019 novel coronavirus: implications for virus origins and receptor binding. *Lancet*. 2020;395(10224):565-74.
225. Weiss SR, Navas-Martin S. Coronavirus pathogenesis and the emerging pathogen severe acute respiratory syndrome coronavirus. *Microbiol Mol Biol Rev*. 2005;69(4):635-64.
226. V'kovski P, Kratzel A, Steiner S, Stalder H, Thiel V. Coronavirus biology and replication: implications for SARS-CoV-2. *Nat Rev Microbiol*. 2021;19(3):155-70.
227. Lotfi M, Hamblin MR, Rezaei N. COVID-19: Transmission, prevention, and potential therapeutic opportunities. *Clin Chim Acta*. 2020;508:254-66.
228. Cavallini J. The human coronavirus. *Science Photo Library*; 2020.
229. van Doremalen N, Bushmaker T, Morris DH, Holbrook MG, Gamble A, Williamson BN, et al. Aerosol and Surface Stability of SARS-CoV-2 as Compared with SARS-CoV-1. *N Engl J Med*. 2020;382(16):1564-7.
230. Gupta S, Parker J, Smits S, Underwood J, Dolwani S. Persistent viral shedding of SARS-CoV-2 in faeces - a rapid review. *Colorectal Dis*. 2020;22(6):611-20.
231. Peeri NC, Shrestha N, Rahman MS, Zaki R, Tan Z, Bibi S, et al. The SARS, MERS and novel coronavirus (COVID-19) epidemics, the newest and biggest global health threats: what lessons have we learned? *Int J Epidemiol*. 2020;49(3):717-26.
232. Shi J, Wen Z, Zhong G, Yang H, Wang C, Huang B, et al. Susceptibility of ferrets, cats, dogs, and other domesticated animals to SARS-coronavirus 2. *Science*. 2020;368(6494):1016-20.
233. Cheng VCC, Wong SC, Chen JHK, Yip CCY, Chuang VWM, Tsang OTY, et al. Escalating infection control response to the rapidly evolving epidemiology of the coronavirus disease 2019 (COVID-19) due to SARS-CoV-2 in Hong Kong. *Infect Control Hosp Epidemiol*. 2020;41(5):493-8.
234. Wu Z, McGoogan JM. Characteristics of and Important Lessons From the Coronavirus Disease 2019 (COVID-19) Outbreak in China: Summary of a Report of 72 314 Cases From the Chinese Center for Disease Control and Prevention. *JAMA*. 2020;323(13):1239-42.
235. Helms J, Severac F, Merdji H, Anglés-Cano E, Meziani F. Prothrombotic phenotype in COVID-19 severe patients. *Intensive Care Med*. 2020;46(7):1502-3.
236. Huertas A, Montani D, Savale L, Pichon J, Tu L, Parent F, et al. Endothelial cell dysfunction: a major player in SARS-CoV-2 infection (COVID-19)? *Eur Respir J*. 2020;56(1).
237. Varga Z, Flammer AJ, Steiger P, Haberecker M, Andermatt R, Zinkernagel AS, et al. Endothelial cell infection and endotheliitis in COVID-19. *Lancet*. 2020;395(10234):1417-8.
238. Panigada M, Bottino N, Tagliabue P, Grasselli G, Novembrino C, Chantarangkul V, et al. Hypercoagulability of COVID-19 patients in intensive care unit: A report of thromboelastography findings and other parameters of hemostasis. *J Thromb Haemost*. 2020;18(7):1738-42.

239. Zuo Y, Zuo M, Yalavarthi S, Gockman K, Madison JA, Shi H, et al. Neutrophil extracellular traps and thrombosis in COVID-19. *J Thromb Thrombolysis*. 2021;51(2):446-53.
240. Barnes BJ, Adrover JM, Baxter-Stoltzfus A, Borczuk A, Cools-Lartigue J, Crawford JM, et al. Targeting potential drivers of COVID-19: Neutrophil extracellular traps. *J Exp Med*. 2020;217(6).
241. Horby P, Lim WS, Emberson JR, Mafham M, Bell JL, Linsell L, et al. Dexamethasone in Hospitalized Patients with Covid-19. *N Engl J Med*. 2021;384(8):693-704.
242. Liu D, Zhang T, Wang Y, Xia L. Tocilizumab: The Key to Stop Coronavirus Disease 2019 (COVID-19)-Induced Cytokine Release Syndrome (CRS)? *Front Med (Lausanne)*. 2020;7:571597.
243. Luo L, Luo T, Du M, Mei H, Hu Y. Efficacy and safety of tocilizumab in hospitalized COVID-19 patients: A systematic review and meta-analysis. *J Infect*. 2022;84(3):418-67.
244. Long C, Xu H, Shen Q, Zhang X, Fan B, Wang C, et al. Diagnosis of the Coronavirus disease (COVID-19): rRT-PCR or CT? *Eur J Radiol*. 2020;126:108961.
245. Guan WJ, Ni ZY, Hu Y, Liang WH, Ou CQ, He JX, et al. Clinical Characteristics of Coronavirus Disease 2019 in China. *N Engl J Med*. 2020;382(18):1708-20.
246. The number of episodes in NHS Scotland with specified codes for Venous Thromboembolism. In: Scotland ISD, editor. Response to April 2015 Freedom of Information Request 2015.
247. Prichayudh S, Tumkosit M, Sriussadaporn S, Samorn P, Pak-art R, Kritayakirana K. Incidence and associated factors of deep vein thrombosis in Thai surgical ICU patients without chemoprophylaxis: one year study. *J Med Assoc Thai*. 2015;98(5):472-8.
248. Bahloul M, Chaari A, Kallel H, Abid L, Hamida CB, Dammak H, et al. Pulmonary embolism in intensive care unit: Predictive factors, clinical manifestations and outcome. *Ann Thorac Med*. 2010;5(2):97-103.
249. Jiménez D, Aujesky D, Moores L, Gómez V, Lobo JL, Uresandi F, et al. Simplification of the pulmonary embolism severity index for prognostication in patients with acute symptomatic pulmonary embolism. *Arch Intern Med*. 2010;170(15):1383-9.
250. Middeldorp S, Coppens M, van Haaps TF, Foppen M, Vlaar AP, Müller MCA, et al. Incidence of venous thromboembolism in hospitalized patients with COVID-19. *J Thromb Haemost*. 2020.
251. Bilaloglu S, Aphinyanaphongs Y, Jones S, Iturrate E, Hochman J, Berger JS. Thrombosis in Hospitalized Patients With COVID-19 in a New York City Health System. *JAMA*. 2020;324(8):799-801.
252. Woloshin S, Patel N, Kesselheim AS. False Negative Tests for SARS-CoV-2 Infection - Challenges and Implications. *N Engl J Med*. 2020;383(6):e38.
253. Robert-Ebadi H, Le Gal G, Carrier M, Couturaud F, Perrier A, Bounameaux H, et al. Differences in clinical presentation of pulmonary embolism in women and men. *J Thromb Haemost*. 2010;8(4):693-8.
254. Yu B, Li X, Chen J, Ouyang M, Zhang H, Zhao X, et al. Evaluation of variation in D-dimer levels among COVID-19 and bacterial pneumonia: a retrospective analysis. *J Thromb Thrombolysis*. 2020.
255. Tan L, Wang Q, Zhang D, Ding J, Huang Q, Tang YQ, et al. Correction: Lymphopenia predicts disease severity of COVID-19: a descriptive and predictive study. *Signal Transduct Target Ther*. 2020;5:61.

256. Brinkmann V, Reichard U, Goosmann C, Fauler B, Uhlemann Y, Weiss DS, et al. Neutrophil extracellular traps kill bacteria. *Science*. 2004;303(5663):1532-5.
257. Stein PD, Goldman J. Obesity and thromboembolic disease. *Clin Chest Med*. 2009;30(3):489-93, viii.
258. Korevaar DA, Aydemir I, Minnema MW, Azijli K, Beenen LF, Heijmans J, et al. Routine screening for pulmonary embolism in COVID-19 patients at the emergency department: impact of D-dimer testing followed by CTPA. *J Thromb Thrombolysis*. 2021;52(4):1068-73.
259. Dr C Bagot DBC, Dr C Church, Dr M Johnson. The Prevention and Management of Thromboembolism in Patients with Covid-19 Related Disease. Scottish Intercollegiate Guideline Network: Health Improvement Scotland; 2020.
260. Spyropoulos AC, Levy JH, Ageno W, Connors JM, Hunt BJ, Iba T, et al. Scientific and Standardization Committee communication: Clinical guidance on the diagnosis, prevention, and treatment of venous thromboembolism in hospitalized patients with COVID-19. *J Thromb Haemost*. 2020;18(8):1859-65.
261. Günay N, Demiröz Ö, Kahyaoğlu M, Başlılar Ş, Aydın M, Özer M, et al. The effect of moderate and severe COVID-19 pneumonia on short-term right ventricular functions: a prospective observational single pandemic center analysis. *Int J Cardiovasc Imaging*. 2021;37(6):1883-90.
262. D'Andrea A, Scarafile R, Riegler L, Liccardo B, Crescibene F, Cocchia R, et al. Right Ventricular Function and Pulmonary Pressures as Independent Predictors of Survival in Patients With COVID-19 Pneumonia. *JACC Cardiovasc Imaging*. 2020;13(11):2467-8.
263. Ongel EA, Karakurt Z, Salturk C, Takir HB, Burunsuzoglu B, Kargin F, et al. How do COPD comorbidities affect ICU outcomes? *Int J Chron Obstruct Pulmon Dis*. 2014;9:1187-96.
264. Wang D, Hu B, Hu C, Zhu F, Liu X, Zhang J, et al. Clinical Characteristics of 138 Hospitalized Patients With 2019 Novel Coronavirus-Infected Pneumonia in Wuhan, China. *JAMA*. 2020.
265. Kearon C, Akl EA, Ornelas J, Blaivas A, Jimenez D, Bounameaux H, et al. Antithrombotic Therapy for VTE Disease: CHEST Guideline and Expert Panel Report. *Chest*. 2016;149(2):315-52.
266. Becattini C, Agnelli G, Pesavento R, Silingardi M, Poggio R, Taliani MR, et al. Incidence of chronic thromboembolic pulmonary hypertension after a first episode of pulmonary embolism. *Chest*. 2006;130(1):172-5.
267. Dorfmueller P, Günther S, Ghigna MR, Thomas de Montpréville V, Boulate D, Paul JF, et al. Microvascular disease in chronic thromboembolic pulmonary hypertension: a role for pulmonary veins and systemic vasculature. *Eur Respir J*. 2014;44(5):1275-88.
268. McCabe C, Dimopoulos K, Pitcher A, Orchard E, Price LC, Kempny A, et al. Chronic thromboembolic disease following pulmonary embolism: time for a fresh look at old clot. *Eur Respir J*. 2020;55(4).
269. van Kan C, van der Plas MN, Reesink HJ, van Steenwijk RP, Kloek JJ, Tepaske R, et al. Hemodynamic and ventilatory responses during exercise in chronic thromboembolic disease. *J Thorac Cardiovasc Surg*. 2016;152(3):763-71.
270. Tunariu N, Gibbs SJ, Win Z, Gin-Sing W, Graham A, Gishen P, et al. Ventilation-perfusion scintigraphy is more sensitive than multidetector CTPA in detecting chronic thromboembolic pulmonary disease as a treatable cause of pulmonary hypertension. *J Nucl Med*. 2007;48(5):680-4.

271. Tilyou S. PIOPED(Prospective Investigation in Pulmonary Embolism Diagnosis) study compares lung scans and pulmonary arteriography. *J Nucl Med.* 1989;30(3):279-80.
272. Metter D, Tulchinsky M, Freeman LM. Current Status of Ventilation-Perfusion Scintigraphy for Suspected Pulmonary Embolism. *AJR Am J Roentgenol.* 2017;208(3):489-94.
273. Smith-Bindman R, Lipson J, Marcus R, Kim KP, Mahesh M, Gould R, et al. Radiation dose associated with common computed tomography examinations and the associated lifetime attributable risk of cancer. *Arch Intern Med.* 2009;169(22):2078-86.
274. Zuckerman WA, Turner ME, Kerstein J, Torres A, Vincent JA, Krishnan U, et al. Safety of cardiac catheterization at a center specializing in the care of patients with pulmonary arterial hypertension. *Pulm Circ.* 2013;3(4):831-9.
275. Zhang LJ, Yang GF, Wu SY, Xu J, Lu GM, Schoepf UJ. Dual-energy CT imaging of thoracic malignancies. *Cancer Imaging.* 2013;13:81-91.
276. Weidman EK, Plodkowski AJ, Halpenny DF, Hayes SA, Perez-Johnston R, Zheng J, et al. Dual-Energy CT Angiography for Detection of Pulmonary Emboli: Incremental Benefit of Iodine Maps. *Radiology.* 2018;289(2):546-53.
277. Grob D, Smit E, Oostveen LJ, Snoeren MM, Prokop M, Schaefer-Prokop CM, et al. Image Quality of Iodine Maps for Pulmonary Embolism: A Comparison of Subtraction CT and Dual-Energy CT. *AJR Am J Roentgenol.* 2019:1-7.
278. Grob D, Smit E, Prince J, Kist J, Stöger L, Geurts B, et al. Iodine Maps from Subtraction CT or Dual-Energy CT to Detect Pulmonary Emboli with CT Angiography: A Multiple-Observer Study. *Radiology.* 2019;292(1):197-205.
279. Pugliese SC, Kawut SM. The Post-Pulmonary Embolism Syndrome: Real or Ruse? *Ann Am Thorac Soc.* 2019;16(7):811-4.
280. Henzler T, Fink C, Schoenberg SO, Schoepf UJ. Dual-energy CT: radiation dose aspects. *AJR Am J Roentgenol.* 2012;199(5 Suppl):S16-25.
281. Klok FA, van der Hulle T, den Exter PL, Lankeit M, Huisman MV, Konstantinides S. The post-PE syndrome: a new concept for chronic complications of pulmonary embolism. *Blood Rev.* 2014;28(6):221-6.